



THE HONG KONG
POLYTECHNIC UNIVERSITY

香港理工大學

Pao Yue-kong Library

包玉剛圖書館

Copyright Undertaking

This thesis is protected by copyright, with all rights reserved.

By reading and using the thesis, the reader understands and agrees to the following terms:

1. The reader will abide by the rules and legal ordinances governing copyright regarding the use of the thesis.
2. The reader will use the thesis for the purpose of research or private study only and not for distribution or further reproduction or any other purpose.
3. The reader agrees to indemnify and hold the University harmless from and against any loss, damage, cost, liability or expenses arising from copyright infringement or unauthorized usage.

IMPORTANT

If you have reasons to believe that any materials in this thesis are deemed not suitable to be distributed in this form, or a copyright owner having difficulty with the material being included in our database, please contact lbsys@polyu.edu.hk providing details. The Library will look into your claim and consider taking remedial action upon receipt of the written requests.

**STRESS-MEMORY OF POLYMERIC MATERIALS AND
ITS APPLICATION IN SMART COMPRESSION
STOCKINGS**

NARAYANA HARISHKUMAR

PhD

The Hong Kong Polytechnic University

2018

The Hong Kong Polytechnic University

Institute of Textiles and Clothing

**Stress-Memory of Polymeric Materials and Its
Application in Smart Compression Stockings**

NARAYANA HARISHKUMAR

A thesis submitted in partial fulfillment of the requirements for the
degree of Doctor of Philosophy

November 2017

CERTIFICATE OF ORIGINALITY

I hereby declare that this thesis is my own work and that, to the best of my knowledge and belief, it reproduces no material previously published or written, nor material that has been accepted for the award of any other degree or diploma, except where due acknowledgement has been made in the text.

_____(Signed)

NARAYANA Harishkumar (Name of Student)

ABSTRACT

Shape memory polymers (SMPs) have been considered as an important class of stimuli-responsive smart polymers over past few decades due to their compelling behaviors. SMPs are not only limited to shape memory functions (i.e. fixity or recovery), instead other physical parameters such as stress, temperature, chrome can also be memorized and retrieved with an external stimulus such as temperature. Thus, these polymers could be regarded as memory polymers (MPs). MPs in the current context have both shape and stress memories. Similar to shape memory, stress-memory represents a newly discovered phenomenon where the stress in a polymeric material can be programmed, stored and retrieved reversibly upon an external heat stimulus. It can serve different smart functions in stress control. This innovative research project aims to exploit the memory potentials (stress/strain) in polymeric film, filaments/fibers, and textile fabric structures towards designing and investigating the smart medical compression stocking to manage the phlebological and lymphatic related chronic venous disorders such as varicose veins, venous ulcers, and venous stasis.

Most of the reported studies pertaining to stress in the MPs are basically related to shape recovery, namely, recovery force/stress to recover the original shape from the deformed shape caused mainly by the elasticity or viscous strain. But it is still a misconception. The response of the recovery stress is not stable over time due to presence of impure memory stress, viscous stress, and elastic stress components. Several examples can be found where MPs are used in sensors and actuators, however the presence of impeditive stress-strain components restrain the full potential of MPs. The present study aims to distinguish, quantify, and characterize the total stress-strain components in the polymer network and proposes unique programming methods to selectively eliminate the impeditive parts and

utilize the pure memory stress from the MP network, hence will expand the application potential of MPs. To further extend the potential domains of MP, the present research exploits the stress memory potential of MPs for designing smart stocking for functional compression management. So far, there exists several shortcomings in the current compression products such as stockings/bandages; 1) once applied on the limb with predetermined elastic force; there is no any further means to change the pressure externally, 2) lack of massage function for old or hospitalized immobile patients having limited calf muscle function, 3) selection of the stockings with improper size, 4) different classes of stockings to provide different levels of compression, 5) It is difficult to achieve the targeted pressure level and pressure drop over time is also a major concern due to the time dependence of the system behaviors. Hence, there is an imperious need of any smart material and textile structures with novel functions to address these problems with profound scientific approach.

To overcome the unsolved research gap, an impending approach in this research project has been drawn the attention to find a most suitable smart material i.e. stress-memory polymer. A novel stress-memory behavior has been discovered and optimized right from the polymeric film, filaments/fibers, and textile structures for designing multi-functional smart compression stockings. Herein, semi-crystalline polyurethanes based on poly(ϵ -caprolactone) diol (PCL-4000 g.mol⁻¹) and poly(1,6-hexamethylene adipate) diol (PHA-3000 g.mol⁻¹) as a soft segment, 4,4'-methylenediphenyl diisocyanate (MDI), and chain extender 1,4-butanediol (BDO) as hard segment have been synthesized to prepare the stress-memory polymers. A thermomechanical smart tensile stress-memory programming is newly proposed to eliminate the negative components (elastic and viscous stress/strain) to obtain the pure “memory stress” which is stable, cyclically repeatable/controllable without loss over time. This unique property is termed as “stress-memory” behavior and

the concept was enlightened with a novel “switch-spring-frame” model to elucidate the evolution of memory stress. The stress analysis in the MP film is investigated to unveil and quantify the total stress-strain components. A constitutive model based on phase transition approach has been used to predict and analyze the individual stress components during thermomechanical process. In contrast to earlier models, a new approach of using relaxed or memory modulus has been proposed to precisely predict stress components. The predicted results have significant agreement with experimental data. The further approach is to unveil and comprehend the stress-memory behavior especially at filament/fiber level which is prerequisite to design the smart stocking for the first time. MP is melt spun and produced filaments to investigate stress-memory behavior. The results have shown maximum memory stress compared to film and the underlying reason is unveiled by mechanical and structural characterizations. Stress-memory filaments were further integrated as a main load bearing element into optimized fleecy or mock inlay textile knitted structure to control the stress/interfacial pressure via external heat stimulus. Based on the interfacial pressure analysis, it is shown that the level of stress and massage effect in the stocking structure can be controlled via parameters such as textile structures and physical parameters including leg radius, deformation level, and temperature range. In addition, the massage effect was confirmed by Doppler ultrasound test to measure the change in venous blood flow. This is the summary of entire research work to advent the multi-functional compression stocking which unifies pressure gradient, massage effect, single size stocking, and selective pressure control for advanced level of compression therapy to overcome existing major shortcomings.

Scientific findings in semi-crystalline stress-memory polymeric materials may inspire people to re-examine existing materials such as elastomers/rubbers and develop novel structures and smart functions in soft materials, particularly polymers. Mechanisms

revealed in stress-memory behavior of polymers, their fibers and fabrics right through compression stockings would bridge the gap between fundamental study and practical applications. This study helps to shed insights for broadening applications of MPs to interdisciplinary areas such as artificial muscles, soft skins, massage devices and electronic sensors/actuators.

PUBLICATIONS AND CREDENTIALS

REFEREED JOURNAL PAPERS

1. **Narayana, H.**, Hu, J.L, Kumar, B., Shang, S., Han, J., Liu, P., Lin, T., Ji, F., and Zhu, Y. (2017). "Stress-memory polymeric filaments for advanced compression therapy." Journal of Materials Chemistry B 5(10): 1905-1916. (Impact Factor: 4.54, Q1)
2. Hu, J.L and **Narayana, H.** (2017). "Novel Behavior in Smart Polymeric Materials: Stress Memory and its Potential Applications. "Advances in Science & Technology" 97.
3. Hu J.L, **Narayana, H.** (2016). "Review of Memory Polymeric Fibers and Its Potential Applications." Advance Research in Textile Engineering 1(2): 1-7. (*Invited*)
4. Kumar, B., Hu, J.L., Pan, N., **Narayana, H.** (2016). "A Smart Orthopedic Compression Device based on a Polymeric Stress Memory Actuator." Materials and Design, 97, 222-229. (Impact Factor: 3.501, Q1)
5. **Narayana, H.**, Hu, J.L., Kumar, B., Shang, S. (2015). "Constituent Analysis of Stress Memory in Semi-Crystalline Polyurethane." Journal of Polymer Science Part B- Polymer Physics, 54(13): 941-947. (Impact Factor: 3.83, Q2)
6. Hu, J. L., Kumar, B., and **Narayana, H.** (2015). "Stress Memory Polymers." Journal of Polymer Science, Part B: Polymer Physics 53(13): 893-898. (Impact Factor: 3.83, Q2)
7. **Narayana, H.**, Hu, J.L., Kumar, B., Shang, S., Ying, M., and Young, J. R., Designing of Functional Memory Medical Stocking for Pressure Control and Massaging, "Materials Science and Engineering: C" (*Communicated, #: MSEC_2017_3347*)

BOOK CHAPTERS

1. **Narayana, H.**, Hu, J.L., Kumar., B, Memory Fibers, Handbook of Fibrous Materials Vol-1, Wiley-VCH Books, Boschstrasse, Weinheim, Germany. (*Accepted, Manuscript #: HFB-34220-019*)
2. Kumar, B., **Narayana, H.**, Hu, J.L., Fibers for Medical Compression, Handbook of Fibrous Materials Vol-2, Wiley-VCH Books, Boschstrasse, Weinheim, Germany. (*Communicated*)
3. Hu, J.L., Jahid, A., **Narayana, H.**, Venkatesan, H., Fundamentals of the Fibrous Materials, Handbook of Fibrous Materials Vol-1, Wiley-VCH Books, Boschstrasse, Weinheim, Germany. (*Accepted, Manuscript #: HFB-34220-001*)

PATENTS

1. Hu, J.L., Kumar, B., Jianping, H., Wu, Y., Zhao, Y, **Narayana, H.** (2015): For stress-memory polymer materials and intelligent pressure device., Filing Number: PRC 201510037396.1, Filing date: 2015/01/23.
2. HU, J.L., **Narayana, H.**, Kumar, B, Smart Stress-memory Fabric for Controlled Static and Dynamic Compression Applications, Filing Number: PRC 201711095848.7, Filing date: 2017/11/09.

INVITED LECTURES

1. Hu, J.L., Narayana, H. New Paradigm for Textile Materials: From Practicality to Sensitivity in Asian Textile Conference-13 (Deakin University, Technical Textiles and Nonwovens Association (TTNA), Geelong, Australia, Nov. 3-6, 2015)

2. Hu, J.L., Narayana, H., Memory Fibers in MRS Fall Meeting, Multifunctionality in Polymer-Based Materials, Gels, and Interfaces Symposium (Hynes Convention Center, Boston, Massachusetts, USA, Nov. 29-Dec. 4. 2015)

CONFERENCE PUBLICATIONS

1. **Narayana, H.**, Hu, J.L., Kumar, B., Shang, S. and Liu, P. ”*Study of Memory Polymeric Filaments and its Optimization for Smart Compression Stockings*”, The 14th Asian Textile conference (ATC-2017), June 28th to 30th , The Hong Kong Polytechnic University, Hong Kong.
2. **Narayana, H.**, Hu, J.L., Kumar, B., “*Stress Memory Filaments as Advanced Material for Smart Compression Management*”, The Fiber Society’s 2017 Spring Conference on *Next Generation Fibers for Smart Products*, May 17th – 19th, RWTH University, Aachen, Germany.
3. **Narayana, H.**, Hu, J.L., Kumar, B., Shang, S. “*Stress Memory Polymers: A Novel Approach towards Constituent Analysis and Implication in Smart Compression Stockings*”, The 20th Annual Conference of HKSTAM 2016, The 12th Shanghai-Hong Kong Forum on Mechanics and Its Application, April 9th, HKUST, Hong Kong.
4. Hu, J.L., **Narayana, H.**, “*Novel Behavior in Smart Polymeric Materials: Stress Memory and its Potential Applications*” in CIMTEC-2016, Symposium-H: “Electroactive Polymers and Shape Memory Polymers: Advances in Materials and Devices”, June 5-10, 2016, Perugia, Italy.
5. **Narayana, H.**, Hu, J.L., Kumar, B. “*Smart Compression Stockings: Implication of Novel Stress Memory Behavior using Smart Polymeric Material*” in Textile Summit-2016 organized by ITC, June 28-30th 2016, The Hong Kong Polytechnic University,

Hong Kong. (Partner universities: North Carolina State University, USA / University of Leeds, UK / Shinshu University, Japan).

ACADEMIC CREDENTIALS

1. **Outstanding Teaching Award** for getting best students' feedback (5 out of 5) (2017/August)
2. Excellent Academic Paper, **Excellence Award** for converting basic research into application stage in Textile Industry from "China Chemical Fiber Industry Association, Hengyi Fund" (2017)
3. 'Stress-memory Polymeric Filaments for Advanced Compression Therapy' was highlighted in the Royal Society of Chemistry (**RSC**) '**Chemistry World**' news, 24th Feb 2017. – [Stressed polymers give calf massages](#) (*Published in JMC-B [cover image](#)*)
4. **Best paper presentation award** - Textile Summit-2016 organized by ITC, The Hong Kong Polytechnic University, Hong Kong (June 28-30th 2016)
5. **Best student presentation award** - The 12th Shanghai-HK Forum on Mechanics and Its Application, Hong Kong University of Science and Technology, HK (9th April-2016). – [Published in the ITC news](#).

ACKNOWLEDGEMENTS

Firstly, I would like to express my sincere gratitude to my Chief Supervisor, **Professor JINLIAN HU** for giving me this great opportunity to pursue Ph.D. study. I am very much fortunate to do my Ph.D. at the World's first Shape Memory Textiles Centre founded by Professor HU. Her continuous support, encouragement, inspiration, patience, motivation, and immense knowledge during my studies was the instrumental to broaden my research expertise and to aim for impactful top-rank journal publications with commendable credits. Her great support created an opportunity for me to be bestowed with notable awards and recognitions mentioned in the previous section. I have acquainted both academic and industry related research expertise, research grant writing skills, and international collaboration opportunities by working under her with a great support. Her valuable suggestions and timely guidance helped me throughout my degree to write this thesis. I could have not imagined having a better guide and mentor for my Ph.D. study.

Besides my Chief Supervisor, I would like to extend my outspoken thanks to Co-supervisors, **Dr. Songmin Shang** (Associate Professor, ITC, PolyU) and **Dr. Bipin Kumar** (Assistant Professor, IITD, India) for their continuous support, encouragement, and motivation for conducting this research.

My sincere thanks to the Fang Brothers Knitting Pvt. Ltd for providing PhD scholarship, which helped me to accomplish my studies without any financial crisis.

I would like to thank my fellow doctoral students and lab mates worked in Prof. Hu's group over past 4 years. Heartfelt thanks to Dr. Yong Zhu, Dr. Fenglong Ji, Dr. You Wu, Mr. Jianping Han, Dr. Tan Lin, Dr. Xueling Xiao, Ms. Susanna Li, Dr. Cuili Zheng, Dr. Ruiqi Xie, Mr. Jianming Chen, and Dr. Suman Thakur for their help, which is an everlasting

memory. I also extend my thanks to other members who are not mentioned here. My special thanks to Dr. Liu Pengqing (Sichuan Univ. PRC) for helping in melt spinning, Dr. Prakash Vasudevan (Director, SITRA, India) for support in knitting, Dr. Michael Ying (HTI, PolyU) for helping in Ultrasound testing and analysis. My sincere thanks to Prof. K. Murugesh Babu for his continuous encouragement, motivation, and recommending me to pursue Ph.D. at ITC. I also thank Ms. Pavithra, O, for her kind help during my PhD application.

Wholehearted thanks to my parents, Mr. Narayana, A, Smt. Taravathi, brother, Mr. Prashanth Kumar, and Fiancée, Shruthi Shree for their invaluable spiritual support and encouragement given to pursue my Ph.D. overseas and in my life.

Many thanks to my friends for accepting nothing less than excellence from me. Hearty thanks to my roommates Dr. Babak Beygi, Dr. Nandeesha Veeranna, Mr. Harun Venkatesan, and friends, Mr. Kiran Kumar, Mr. Parth Shah, Ms. Tanuja S, Dr. Udayraj, Mr. Yuvraj, Mr. Virag R, Dr. Esterina, Dr. Akshay Raj, Ms. Bhamini, Ms. Anjana B, and Ms. Anushree, for their great help and moral support given during my studies in Hong Kong.

TABLE OF CONTENTS

CERTIFICATE OF ORIGINALITY	I
ABSTRACT.....	II
PUBLICATIONS AND CREDENTIALS.....	VI
ACKNOWLEDGEMENTS.....	X
TABLE OF CONTENTS.....	XII
LIST OF FIGURES	XVIII
LIST OF TABLES.....	XXVII
LIST OF ABBREVIATIONS AND SYMBOLS	XXVIII
CHAPTER 1: INTRODUCTION.....	1
1.1. Stress-strain Related Studies in MPs.....	3
1.2. Background of Compression Management	6
1.3. Studies on Interfacial Pressure of Compression Bandages	8
1.4. Studies on Smart Actuators for Compression Management	9
1.5. Problems Being Addressed	9
1.6. Motivation for the Research	12
1.7. Research objectives	14
1.8. Novelty and significance of the research project	15
1.9. Outline of the thesis.....	16
CHAPTER 2: LITERATURE REVIEW	19
2.1. Introduction to Shape Memory Materials	19
2.2. Introduction to Shape Memory Polymers (SMPs)	20
2.2.1. Molecular Mechanism of SMPs.....	21
2.2.2. Transition Types of SMPs	22
2.2.3. Shape Memory Effect in SMPs.....	22

2.2.4.	Evaluation of shape memory properties	24
2.2.5.	Shape memory or memory polymers?	25
2.3.	Memory Polymeric Fibers (MPFs).....	26
2.3.1.	Which fibers do have better performance, wet or melt spun?	28
2.3.2.	Effect of post spinning operations on MP fiber properties	30
2.3.3.	Recent advances in MP fibers.....	33
2.4.	Characterization Techniques for Memory Polymeric Materials	34
2.5.	Thermal-induced Memory Polymers in Textile Applications.....	35
2.5.1.	Fabrics made of memory materials.....	36
2.6.	Stress-Strain Related Studies in Memory Polymers.....	37
2.6.1.	A constitutive model approach in MPs.....	40
2.7.	Compression Therapy and Its Management	46
2.7.1.	Introduction.....	46
2.7.2.	Cardiovascular system and anatomy of veins in human body.....	47
2.7.3.	Chronic Venous Deficiency (CVD).....	49
2.7.4.	What choices of material do we have for compression?.....	51
2.7.5.	Studies on interfacial pressure of bandages/stockings.....	54
2.7.6.	Role of textiles in compression stockings.....	56
2.7.7.	Research on stress in MPs, modeling, and application in compression stocking	59
CHAPTER 3: EXPERIMENTAL WORK		62
3.1.	Materials and Equipment Utilized.....	63
3.2.	Preparation of Stress-Memory Polymer, Filaments/Fibers, and Fabrics.....	65
3.2.1.	Synthesis of semi-crystalline memory polymer (MP)	65
3.2.2.	Preparation of memory polymeric film.....	66

3.2.3.	Spinning of memory polymeric filaments (MPFs)	66
3.2.4.	Preparation of stocking fabrics using memory polymeric filaments	67
3.3.	Characterization Techniques	71
3.3.1.	Preconditioning for stress-memory polymeric material	71
3.3.2.	Stress-memory tensile programming test.....	72
3.3.3.	Differential scanning calorimetry (DSC) analysis.....	74
3.3.4.	Thermomechanical (TMA) analysis	74
3.3.5.	Characterization of memory polymeric film for constituent analysis	75
3.3.6.	Fourier Transform Infrared (FTIR) spectroscopy analysis	76
3.3.7.	Wide angle X-ray diffraction (WAXD) analysis	77
3.3.8.	Evaluation of shape memory properties	78
3.3.9.	Characterization of stress-memory filaments integrative stocking fabrics..	79
3.3.10.	Interfacial pressure measurement of the memory fabrics	81
3.3.11.	Doppler Ultrasound examination.....	84
CHAPTER 4: STRESS-MEMORY POLYMERS.....		85
4.1.	Introduction	86
4.2.	Results and Discussion.....	87
4.2.1.	Mechanism models of stress-memory process	90
4.2.2.	Stress-memory response with different constraint methods	93
4.2.3.	Stress-memory response with different initial strains at single constraint ..	96
4.3.	Application of Stress-Memory Concept.....	98
4.4.	Summary	103
CHAPTER 5: CONSTITUENT ANALYSIS OF STRESS-MEMORY IN SEMI- CRYSTALLINE POLYURETHANE.....		104
5.1.	Introduction	105

5.2.	Experimental Results.....	109
5.2.1.	Evolution of the recovery stress.....	109
5.2.2.	Free strain recovery.....	111
5.2.3.	Moduli at different temperature levels.....	112
5.2.4.	Evolution of thermal stress and strain.....	112
5.2.5.	Stress components during recovery	114
5.2.6.	Modelling results	117
5.3.	Application of Stress-Memory Analysis	122
5.3.1.	Theoretical and design considerations for the MP actuator.....	124
5.3.2.	Experimental and modeled results of memory actuator/bandage	125
5.3.3.	Limitations of the memory actuator/bandage	128
5.4.	Summary	129
CHAPTER 6: STRESS-MEMORY FILAMENTS FOR ADVANCED		
COMPRESSION THERAPY		131
6.1.	Introduction	132
6.2.	Experimental Results and Discussion of MP Film and Filaments	134
6.2.1.	Mechanical properties of MP filaments.....	134
6.2.2.	FTIR Analysis of Memory Polymeric Film and MPFs	135
6.2.3.	Thermal Properties of MP Film and MPFs.....	136
6.2.4.	Thermo-mechanical properties	138
6.2.5.	Stress-memory response in MP Film and Filament.....	140
6.2.6.	Evolution of memory stress (M.S) in Film and MPFs.....	142
6.3.	Potential application of stress-memory filaments	150
6.4.	Summary	153

CHAPTER 7: DESIGNING OF ADVANCED SMART MEDICAL STOCKING USING

STRESS-MEMORY FILAMENTS FOR PRESSURE CONTROL AND MASSAGING ... 155

7.1.	Introduction	156
7.2.	Major Key Issues and Approach to Solve	159
7.2.1.	Polymer optimization and its transition temperature	159
7.2.2.	Stress-memory and its relaxation optimization.....	159
7.2.3.	Memory filament preparation and stocking structure optimization.....	160
7.2.4.	Achieving the target level of static and dynamic pressure	161
7.2.5.	Relationship between pressure and stocking structural parameters.....	162
7.3.	Experimental Results and Discussion	164
7.3.1.	Structural properties of memory stocking fabrics.....	166
7.3.2.	Effect of fabric structure on stocking pressure	167
7.3.3.	Effect of physical parameters.....	170
7.3.4.	Controlling massage effect via stocking structure	173
7.3.5.	Ultrasound examination of blood flow	175
7.4.	Pressure model validation	177
7.5.	Summary	179

CHAPTER 8: CONCLUSIONS AND SUGGESTIONS FOR FUTURE WORK... 181

8.1.	Conclusions	182
8.1.1.	Discovery of stress-memory in semi-crystalline MP.....	182
8.1.2.	Quantitative stress-memory analysis & design of memory film actuator..	183
8.1.3.	Engineering and optimization of stress-memory filaments	184
8.1.4.	Designing of smart compression stockings for static and massage pressure	185
8.2.	Suggestions for future work	186

REFERENCES..... 189

LIST OF FIGURES

Figure 1.1: Stress-memory of semi-crystalline memory polymers.....	3
Figure 1.2: a) Shape memory programming process, b) Stress-strain components in MPs based on the literature, c) Our distinguishing approach based on stress-memory.....	4
Figure 1.3: SMP based bandage reported in the literature.....	5
Figure 1.4: Background of compression therapy. a) Types of chronic venous disorders. b) Schematic showing the venous function, (b ₁): Functioning of Normal vein; (b ₂ & b ₃): Damaged vein. c) Principle of compression therapy, (c ₁): Gradient pressure; (c ₂): Normalized vein function upon therapy.	6
Figure 1.5: Modes of existing compression therapy. a) Static compression, b) Dynamic compression, c) Required method of compression in smart stocking	8
Figure 1.6: Concept of interfacial pressure development. a) Schematic showing the tension development in the stocking. b) Laplace’s law for thin walled cylinder. P: Internal radial pressure; T: Tension/unit length; r: radius; L: length.	12
Figure 2.1: Plot depicting the sensitive change of smart materials in ambient temperature	19
Figure 2.2: The Overall architecture of SMPs [14].	21
Figure 2.3: Schematic representing the shape memory effect in SMPs	22
Figure 2.4: Molecular mechanism of the thermal-induced SME [87].	23
Figure 2.5: Scheme of thermo-mechanical cyclic test. a) Plot of stress with strain and temperature. b) Typical curve of stress vs strain. (T _l): Low temperature (T<T _{trans}); (T _h): High temperature; (ε _p): Plastic strain; (ε _u): Fixed strain; (ε _m): Programming strain; (ε _m - ε _u): Elastic strain; ε _r = (ε _m - ε _p).	24

Figure 2.6: (a) Comparison of elastic modulus between MPFs and various manmade fibers. (b) MPF showing 100% shape recovery. [94]27

Figure 2.7: Influence of Spinning methods on thermal and shape memory properties. (a) DSC thermographs of melt and wet spun MPFs. (b) XRD profiles of melt and wet spun MPFs. (c & d) Stress-strain curves of melt and wet spun MPFs. M: Melt, W: Wet. [95]..28

Figure 2.8: Schematic passage of MP filament through thermal setting process31

Figure 2.9: Influence of heat treatment on fiber properties. a) DSC thermograms. b) Effect on tenacity. c) effect on linear density. d) Effect on breaking elongation. e) Effect on stress relaxation. [96]32

Figure 2.10: Characterization techniques of memory polymers.34

Figure 2.11: Different forms of MPUs for textile applications35

Figure 2.12: Shape recovery of a fabric having SMA spring with temp = 50°C.36

Figure 2.13: (A) Shape recovery of MP composite woven uniformly and densely of MP yarn at 50°C with recovery time (a) 0 s, (b) 15 s, and (c) 30 s. (B) Shape memory recovery of MP composite loosely woven fabric with SMP yarn at 50°C with recovery time (a) 0 s, (b) 30 s and (c) 60 s.....37

Figure 2.14: Self-adaptability of MP based garments37

Figure 2.15: Scheme of programming. (a) Strain-induced crystallization. (b) Stress-induced crystallization.....39

Figure 2.16: Stress-strain components based on literature. (a) Thermo-mechanical testing of MPs. (b) Components of MPs based on the literature from few decades.39

Figure 2.17: Schematic diagram of the micromechanics foundation of the 3-D MP constitutive model.....41

Figure 2.18: (a) A schematic representation of the decomposition for the recovery stress of compression programmed SMP. (b) Simulation results showing all the components.44

Figure 2.19: Effect of thermal stress. (a) Tensile stretch programming (negative). (b) Compression programming (positive).	45
Figure 2.20: Venous system. (a) Schematic Illustration of fluid transport through venous system. (b) Venous return to heart through veins.	47
Figure 2.21: Major symptoms of CVD. (a) Varicose veins. (b) Venous oedema. (c) Venous leg ulcers.	50
Figure 2.22: Current methods of compression therapy. (a) Bandages. (b) Stockings. (c) Intermittent pneumatic compression devices (IPCs).	51
Figure 2.23: Dynamic compression profile	56
Figure 2.24: Stocking made of SMPU. (a) Fabric structure. (b) SMP fabric attached to commercial stocking.	58
Figure 2.25: Stocking structure. (a) Notation diagram. (b) Schematic diagram of the structure.....	58
Figure 2.26: Experimental and theoretical prediction results. (a) Pressure variation at different temperature level. (b) comparison with theoretical prediction. (c) Pressure measurement set up. (d) Pressure variation at different level of strains (T=40°C). [167].	60
Figure 3.1: Chemical structures of the raw materials	64
Figure 3.2: Scheme of stress memory filaments integration and structural details of the memory stocking.....	67
Figure 3.3: Scheme of memory fabric knit structures. a) Notation diagram, b) Schematic illustration of knit structures, c) Microscopic image of memory fabrics on technical back. M=Memory filament, N=Nylon filament, SMPF = Stress memory polymeric filament. .	70
Figure 3.4: Stress-strain profile during a thermo-mechanical programming cycle. (a-f: different steps of the cycle).....	71

Figure 3.5: Scheme of stress memory programming. a) Representation of tensile programming. b) Profile of stress-time (b₁) and stress-strain (b₂) during programming. L_i: Initial length; L_f: Final length; T: Temperature; T_{trans}: Transition temperature; T_{Pl}: Programming-low temperature; T_{Ph}: Programming-high temperature. ①: Total stress; ②: Viscous stress; ③: Memory stress. S₀ to S₅: step zero to step 5.73

Figure 3.6: Schematic showing stress-strain-temperature profile during programming. T_l: low temperature; T_h: high temperature; σ-R: stress recovery; ε-R: strain recovery; ε_{def}: total deformation or initial strain.75

Figure 3.7: Scheme of thermo-mechanical cyclic test. a) Plot of stress with strain and temperature. b) Typical curve of stress vs strain. (T_l): Low temperature (T < T_{trans}); (T_h): High temperature; (ε_p): Plastic strain; (ε_u): Fixed strain; (ε_m): Programming strain; (ε_m - ε_u): Elastic strain; ε_r = (ε_m - ε_p).78

Figure 3.8: Scheme of interfacial pressure measurement in the stockings81

Figure 3.9: Schematic of pressure control. a) Cross-section of cylinder and the stocking, b) Pressure-time and temperature-time profiles during pressure measurement.....83

Figure 3.10: Set up for venous blood flow measurement using Doppler Ultrasound.....84

Figure 4.1: Thermal induced stress-memory of polymers. (a) Programming, stress memory and memory stress. (a₁): Experimental results showing stress-time profiles in programming and memory processes; (a₂): A stress memory cycle with stress charging (Ch) and discharging (Di) stages. (b) Stress-strain and stress-time profiles during programming. ①: Total stress; ②: Viscoelastic stress; ③: Memory stress. S₀→S₁: heating the original relaxed specimen; S₁→S₂: stretching the specimen; S₂→S₃: relaxing the specimen; S₃→S₄: cooling/charging the specimen; S₄↔S₅: Stress memory process, charging-discharging...87

Figure 4.2: Thermal properties of stress-memory polymer. a) DSC thermogram, b) TMA curve at the temperature ramp: 3 °C/min88

Figure 4.3: Components of stress-memory polymer revealed in this work.....89

Figure 4.4: Mechanism models of a thermal-responsive MP in programming and stress-memory process. (a) Switch–matrix-netpoint unit cell model. (b) Crystal-coil-crosslink model. (c) Switch-spring-frame model. Single arrows from (1) to (3) represent programming process while double arrows from (3) to (5) for cyclic stress memory process. (1) Original length at relaxed state; (2) Stretched length at heating; (3) Charged state at cooling; (4) During transition around T_{trans} ; (5) Discharged state at heating.....90

Figure 4.5: Scheme of stress-memory programming tests.....93

Figure 4.6: Evolution of memory stress at different discharging temperatures. a) Memory stress-time profile. b) Memory stress-temperature profile94

Figure 4.7: Maximum memory stress discharged at constraint strain (C.S) equal to the initial strain (I.S), total constraint. a) Stress-time profile. b) Stress-strain profile.....95

Figure 4.8: MS_{max} programmed at different I.S but discharged at the same C.S.....97

Figure 4.9: Controllability of memory stress, a combined memory stress profile under different conditions, partial constraint. $t_1 \rightarrow t_6$: different time intervals; $T_1 \rightarrow T_3$: different temperature levels.98

Figure 4.10: Application of stress memory. a) stress memory programming of stocking for gradient pressure. b) Pressure measurement set up.99

Figure 4.11: Results showing the pressure gradient (difference in two cases with pressure knob placement)..... 100

Figure 4.12: Dynamic compression pressure. a) Pressure profile of the stocking for massage effect. b) Compression stocking with massage effect. C_1 to C_5 : Cycles. c) Cross section of stocking and the leg showing pressure change with memory stress..... 101

Figure 4.13: A generalized model of stress memory potential for applications 102

Figure 5.1: Stress-strain-temperature profile during programming. T_h : high temperature; T_l : low temperature; σ -R: stress recovery; ϵ -R: strain recovery; ϵ_{def} : total deformation or initial strain..... 108

Figure 5.2: Experimental results of stress-strain profile (Initial modulus: IM; Memory modulus: MM) ($\epsilon = 20\%$, $T_h = 60\text{ }^\circ\text{C}$) 108

Figure 5.3: Experimental results showing the stress-time profile during programming and recovery process. Di: Discharging or heating above the transition. 109

Figure 5.4: Evolution of stress with time and temperature. a) Variation of recovery stress over time ($T = 60\text{ }^\circ\text{C}$). b) Recovery stress at different temperature levels during discharging ($\epsilon_{def} = 20\%$). 110

Figure 5.5: Experimental results of the recovered strain (ϵ_r) under no constraint condition 111

Figure 5.6: Results of initial (IM) and memory modulus (MM) at different temperature levels ($\epsilon_{def} = 20\%$). 112

Figure 5.7: Evolution of the thermal strain and stress. a) Thermal strain in an unstretched MP upon heating under no constraint. b) Evolution of thermal stress in an unstretched MP upon cooling under constraint..... 113

Figure 5.8: Theoretical prediction of the frozen fraction. Model fitting of experimental frozen fraction data to get C_f value for the modulus prediction. 118

Figure 5.9: Prediction of MM and IM evolution at different temperature levels 119

Figure 5.10: Prediction of recovered stress using memory modulus (E_m)..... 119

Figure 5.11: Prediction of recovered stress using initial or total modulus (E_T)..... 120

Figure 5.12: Model prediction at different strain levels (10% and 50% strain). Same model parameters (obtained at 20% strain; Table 5.1) are used to plot the model curves for different strains.	121
Figure 5.13: Embodiment of the memory bandage. a) Schematic of the proto type, b) Arrangement of embedded electric heating wire, c) Top view, d) Photograph of the prototype	123
Figure 5.14: Experimental set-up for pressure measurement	124
Figure 5.15: a) Variation of surface temperature with time (5.5 V). b) Results of maximum surface temperature with applied voltage.	125
Figure 5.16: Experimental result of pressure variation over time.	127
Figure 5.17: Experimental and theoretical predicted results of pressure at different levels of temperature.	127
Figure 5.18: Dynamic compression using prototype (2.5 V; $\epsilon_{pre}=10\%$; Heating/cooling time = 900 s)	128
Figure 6.1: FTIR spectra of memory polymeric film and filaments at different programmed strain levels.	135
Figure 6.2: DSC thermograms of film (a) and filament (b).	137
Figure 6.3: Thermo-mechanical cyclic test curves of MP film (a) and filaments (b). Note: Curves plotted for single filament in (b).	139
Figure 6.4: Experimental results of stress-memory response in MPs. Stress-time profile of MP film (a), and filament (b). (a ₁ , b ₁) Programming process; (a ₂ , b ₂) Cyclic response of M.S; (a ₃ , b ₃) Time dependent behavior of M.S with heat stimulus.	140
Figure 6.5: Memory stress-temperature profile at 20% strain.	142
Figure 6.6: Memory stress-temperature profile at 40% strain.	143
Figure 6.7: Memory stress-temperature profile at 60% strain.	143

Figure 6.8: Memory stress-strain profile at constant temperature (60 °C)	144
Figure 6.9: Schematic representing the structural changes in film and melt spun filaments on strain.....	146
Figure 6.10: DSC thermograms (cooling curves) of film and filaments at 0% (a), 20% (b), 40% (c), and 60% strain (d).	147
Figure 6.11: WAXD profiles of MP film and filaments at different stress-memory programmed strains. (a) Diffraction profiles of un-stretched specimens. (b) Diffraction profiles at 20% strain. (c) Diffraction profiles at 40% strain. (d) Diffraction profiles at 60% strain.....	149
Figure 6.12: Integration of stress-memory filaments into textile knit structure	150
Figure 6.13: Schematic showing the baseline pressure during rest condition	151
Figure 6.14: Experimental results of MPFs integrative stocking. Pressure-time profile at different strain level	151
Figure 6.15: Experimental results of MPFs integrative stocking. Pressure-time profile showing massage effect	152
Figure 6.16: a) Schematic of MPFs integrative stocking structure and the effect of massage on human limb upon thermal stimulus. b) Plot showing the relationship between memory stress and the strain as a function of temperature.	153
Figure 7.1: The thermal transition in Memory Polymers (MPs).	159
Figure 7.2: Experimental results stress-memory cycles in filaments (Chapter 6).....	160
Figure 7.3: Schematic showing the integration of stress-memory filaments to fabric structure. M: Memory filament, N: Nylon filament.	160
Figure 7.4: Scheme of relationship between pressure and stocking particulars	162

Figure 7.5: Set up for interfacial pressure measurement. a) Cylinders with different circumferences. b) Cylinder with pressure sensor. c) Memory stocking. d) Pressure measurement. 165

Figure 7.6: Effect of loop length on pressure profile (Series 3A) 167

Figure 7.7: Effect of fabric structures on pressure profile (Series A – 2.5 mm loop length) 168

Figure 7.8: Pressure profile of series A vs series B (2.5 mm loop length) 169

Figure 7.9: Effect of cylinder circumference on pressure under same tension..... 171

Figure 7.10: Pressure v/s time at different temperature levels..... 172

Figure 7.11: Pressure and time profile at different strain levels 172

Figure 7.12: Controlling massage effect via stocking structures; (a) 2A, (b) 3A, (c) 4A. (Loop length: 2.5 mm) 174

Figure 7.13: Measurement of blood flow via doppler ultrasound scanning. a) Scanned image of popliteal vein carrying impure blood. b) Graphs showing the change in blood flow velocity..... 176

Figure 7.14: Blood flow velocity comparison at different testing phase 177

Figure 7.15: a) Memory stress in the filament at 53.40% strain with temperature level. b) Experimental and theoretical pressure results at different levels of temperature. 178

LIST OF TABLES

Table 2.1: Thermal properties of melt and wet spun MP fibers [95].....	29
Table 2.2: Physical properties of MP fibers.....	30
Table 2.3: The CEAP classification.....	51
Table 2.4: Compression-stocking class definitions (U.S. & European)	53
Table 3.1: Raw materials/chemicals used in the research project	63
Table 3.2: Major equipment used in the research project.....	63
Table 5.1: Values of model parameters	118
Table 5.2: Values of model parameters used for pressure prediction.....	126
Table 6.1: Mechanical properties of MP filament	135
Table 6.2: Thermal properties of MP film and filament.....	136
Table 6.3: Thermo-mechanical cyclic properties of film and filament	138
Table 6.4: Peak memory stress values of film and filament as a function of temperature	144
Table 6.5: Thermal properties of film and filaments at different programmed strain levels	148
Table 7.1: Structural properties of memory stocking fabrics	166
Table 7.2: Pressure model parameters	179

LIST OF ABBREVIATIONS AND SYMBOLS

%	Percentage
°C	Degree Centigrade
Å	Angstrom (10^{-10} Meter or 0.1 nanometer)
BDO	1,4-butanediol
C.S.	Constraint Strain
Ch	Charging
cm	Centimeter
cN	Centinewton
CVD	Chronic Venous Disorders
DC	Direct Current
Di	Discharging
DMA	Dynamic Mechanical Analysis
DMF	N,N-dimethyl Formamide
DSC	Differential Scanning Calorimetry
dtex	Deci tex (Weight in grams of 1000 meters of length)
DVT	Deep Vein Thrombosis
E	Young's Modulus
E_e	Modulus Related to Entropic Deformation
E_i	Modulus Related to Internal Energetic Deformation
Eq.	Equation
FTIR	Fourier Transform Infrared Spectroscopy
g.mol^{-1}	Gram Per Mole
GSM	Grams Per Square Meter

LIST OF ABBREVIATIONS AND SYMBOLS

Hz	Hertz
I.S.	Initial Strain
IM	Initial Modulus
IPC	Intermittent Pneumatic Compression
J.g ⁻¹	Joule Per Gram
kPa	Kilopascal
L_f	Final Length
L_i	Initial Length
MDI	4,4'- methylenediphenyl Diisocyanate
min	Minute
ml	Milliliter
mm	Millimeter
MM	Memory Modulus
mmHg	Millimeter of Mercury
Mn	Number Average Molecular Weight
mN	Milli Newton
MP	Memory Polymer
MPa	Megapascal
MPFs	Memory Polymeric Filaments
MPU	Memory Polyurethane
MS	Memory Stress
MS _{max}	Maximum Memory Stress
MS _{min}	Minimum Memory Stress
N	Newton
PCL	Poly(ϵ -Caprolactone) diol

PHA	Poly(1,6-hexamethylene adipate) diol
PRF	Pulse Repetition Frequency
R_f	Shape Fixity Ratio
RM	Relaxed Modulus
R_r	Shape Recovery Ratio
s	Seconds
SME	Shape Memory Effect
SMFs	Shape Memory Fibers
SMP	Shape Memory Polymer
SMPFs	Shape Memory Polymeric Fibers
SMPU	Shape Memory Polyurethane
T	Temperature
t	Time
T_g	Glass Transition Temperature
T_h	High Temperature
T_l	Low Temperature
T_m	Melting Transition Temperature
TMA	Thermal Mechanical Analyzer
T_{Ph}	Programming-high Temperature
T_{Pl}	Programming-low Temperature
T_{trans}	Transition Temperature
V	Volt
WAXD	Wide Angle X-Ray Diffraction
$\alpha (T)$	Thermal Expansion Coefficient
Δ	Delta

ΔH_c	Enthalpy of Cooling
ΔH_m	Enthalpy of Melting
ΔH_m^0	Melting Enthalpy of Soft Segment
ε	Strain
ε_{pre} , ε_{def}	Initial Deformation or Given Strain
$\varepsilon-R$	Strain Recovery
ε_s	Stored Strain
θ	Theta
σ	Stress
$\sigma-R$	Stress Recovery
Ω	Ohm
π	pi
φ_f	Frozen Fraction

CHAPTER 1: INTRODUCTION

Highlights

This Chapter mainly introduces the background of shape memory materials, stress-related studies in the memory polymer networks, background of compression therapy, compression modalities, and related materials research as an overview. The major shortcomings of the compression therapy and motivation for this research to implement the stress-memory potential into smart compression stockings is highlighted. Further to this, key research objectives, brief outline and structure of the thesis is presented.

Smart materials, structures and systems, responsive to an external stimulus, are adaptive to our human demands [1-9]. Among smart materials, polymers with shape memory are at the forefront of research leading to comprehensive publications and wide applications [10-15]. Shape memory polymers (SMPs) are one of the important class of stimuli-responsive smart materials over past few decades. It has been attracting and steering the research direction of scientific community right from its inception towards numerous applications due to their compelling novel behaviors [16-18]. They have inherent nature of recovering the permanent conformation from the temporarily fixed shape (Figure 1.2a) upon an external stimulus such as heat, light, moisture, and magnetic field [19-23]. SMPs usually are composed of thermodynamically immiscible soft (reversible phase) and hard segments with different thermal transition temperature ranges attributed to shape fixation and shape recovery [24-26]. Thermal-responsive SMPs have been widely used in textile applications [14, 27, 28], sensors and actuators [29], drug delivery systems [30], self-healable materials [31-33], vascular stents [34, 35], medical casts [36], orthodontics [37], artificial muscles [38], and other applications.

In this study, SMPs are extended to memory polymers (MPs) which have both stress and shape memories. In fact, some polymers can remember shape [39], stress (stress-memory) [40], chrome (chromic-memory) [41] and temperature (temperature-memory) [6]. In addition to shape memory, Miaudet et al. published a work on the temperature memory [6], which Xie, used for stepwise programming [42]. Recently stress-memory phenomenon in a semi-crystalline polyurethane has been discovered and which was motivated by this research direction [40]. The discovery of this unique behavior and its potential application is well organized and reported chapter wise in this dissertation. Similar to shape memory, stress memory is a phenomenon whereby the stress in a polymer can be programmed, stored and retrieved reversibly with an external stimulus such as temperature and electricity. The

stress can vary with heating and cooling cycles around the transition temperature in a thermal sensitive polymer. The stress memory in one repeating cycle includes charging (Ch) and discharging (Di) stages as shown in Figure 1.1. Charging is the process where a stress is being stored under cooling in the material just like storing electricity into a battery while discharging releases the stored stress upon heating. Stress-memory may be mistaken as recovery stress which has been studied quite extensively [43, 44]. This current reported research work helps to distinguish them with a scientific approach. Recovery stress, determining the recoverability to its permanent shape from deformed conditions, always exists in shape memory polymers, but there may be a small or negligible memory stress in certain cases if T_g is used as the transition [45].

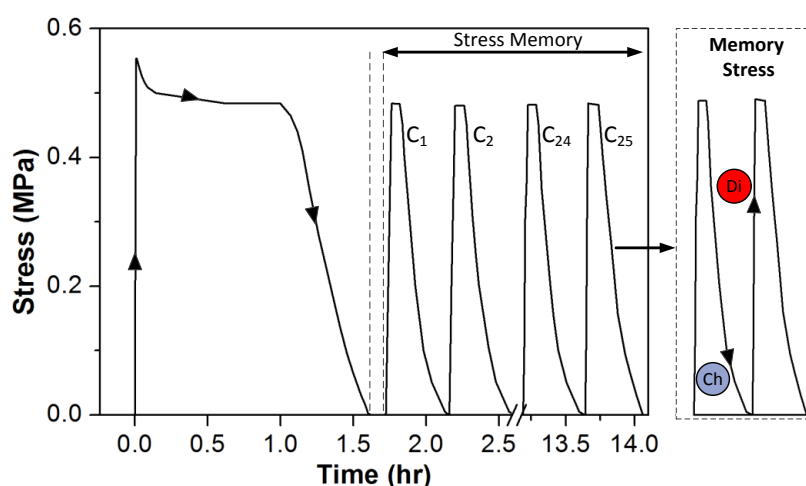


Figure 1.1: Stress-memory of semi-crystalline memory polymers

1.1. Stress-strain Related Studies in MPs

Figure 1.2 simplifies and outlines the shape memory programming and total and recovery stress components. The recovery stress (Figure 1.2a) contains multi-components including elastic and viscoelastic forces in addition to possible memory stress which is not dealt in the literature. It has been reported that the deformation components in MPs includes plasticity, viscoelasticity, and fixable or recoverable elasticity (Figure 1.2b). Most of the

reported literature states that, elasticity is the main driving force for shape recovery and impure recovery stress. Lin et al. have studied the shape memory behavior using viscoelastic model and stated that, the deformed/fixed polymer can recover its original shape by the *elastic force* of the hard segment [46].

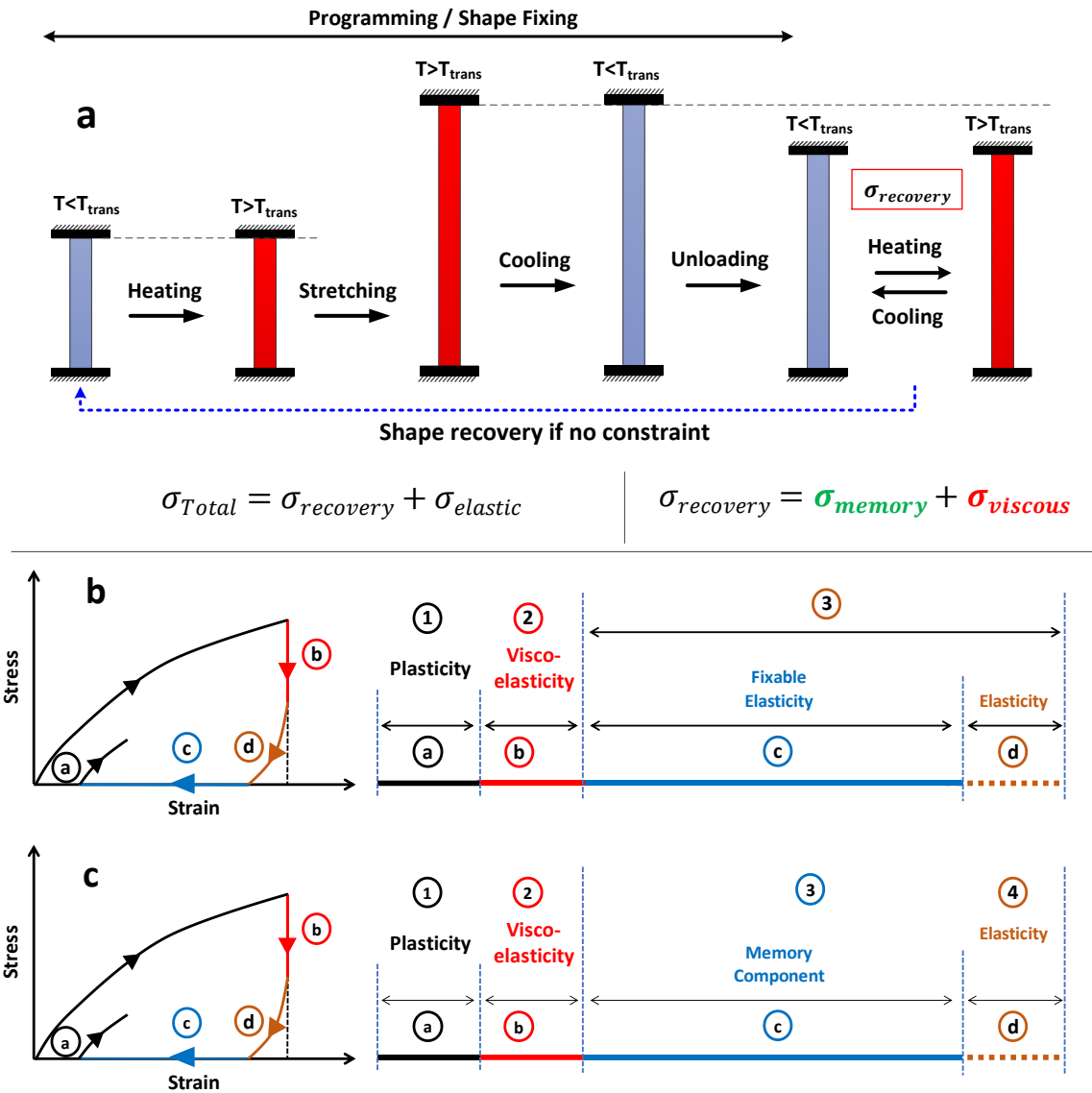


Figure 1.2: a) Shape memory programming process, b) Stress-strain components in MPs based on the literature, c) Our distinguishing approach based on stress-memory

Ivens et al. [47] have stated that, SMPs can exhibit a “spring back” effect (residual stress ~ elasticity) during cooling below transition temperature. Also, it has been discussed that, an important factor for shape memory effect is the stored *elastic energy* in the hard phase.

Even, Gall et al. have stated the same reason for the recovery of a deformed material [48]. Qi et al. [49] have investigated the underlying physical mechanisms and have stated that *viscous strain is the main driving force* for the shape recovery. Whereas, Wang et al. [44] have used phase transition based constitutive modeling approach and experimental method to classify the total stress-strain components. Their results also failed to predict the actual recovery stress due to presence of impure memory stress composed of viscous and elastic stress together.

This has been one of the major research gap to be covered to find the novel scientific approach for eliminating the impure or impeditive stress-strain components which affects the recovered stress in the MPs. A profound rationale, practice, and experimental investigations finally made a breakthrough to find the smart programming and discovered the stress-memory in MPs.

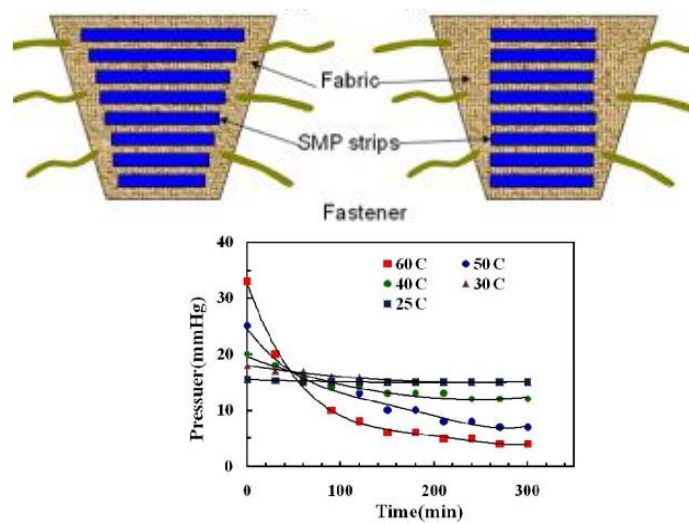


Figure 1.3: SMP based bandage reported in the literature [50]

Using this impure recovery stress Ahmad et al. [50] have attempted to use in compression related application (SMP film attached to fabric swatch as a compression system) and encountered pressure reduction over time (Figure 1.3). This is primarily because of the

presence of impeditive stress components and adds a limitation to use the MP for the applications needing stable and cyclic stress variation.

1.2. Background of Compression Management

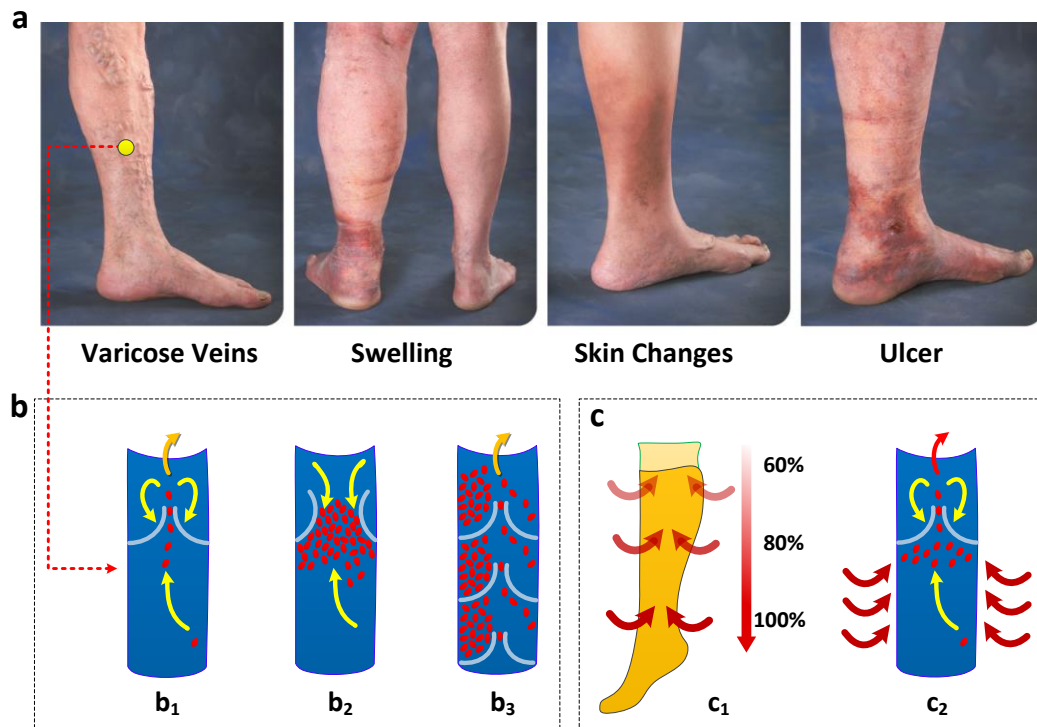


Figure 1.4: Background of compression therapy. a) Types of chronic venous disorders.

b) Schematic showing the venous function, (b₁): Functioning of Normal vein; (b₂ & b₃):

Damaged vein. c) Principle of compression therapy, (c₁): Gradient pressure; (c₂):

Normalized vein function upon therapy [55]

The newly discovered stress-memory concept from this research direction [40] in MPs can serve different functions in stress control with mainly contributive part (Memory stress) as a whole by eliminating the other impeditive parts and retaining only memory component (Figure 1.2c). This research work has been led to identify another individual modulus (relaxed or memory modulus) component [51] to predict and quantify the pure memory stress and other stress components in a semi-crystalline MP. If properly exploited, the pure contributive stable and cyclic memory stress could be obtained by stress memory

programming useful for precise designing a smart system to have controlled pressure for compression related applications. This can overcome number of problems in existing compression systems. In addition, it could be useful for applications such as sensors [52], mechanical engines, pressure garments, massage devices, and artificial muscles [53].

The recent discovery of stress-memory stems from the study and application of shape memory polymeric fibers to compression stockings [54] which are one of the most useful method for compression therapy. It is a very important healthcare and medical treatment for patients suffering from venous and lymphatic disorders including venous ulcers, lymphedema, varicose veins and deep vein thrombosis (DVT) (Figure 1.4a, b) [55]. The main principle of compression therapy is to apply certain level of pressure around the affected tissue on the limb to reduce the venous hypertension. The pressure gradient (Figure 1.4c₁) from “toe to knee” is required to improve the venous fluid returning to heart (Figure 1.4c₂). Apart from stocking, other devices include bandages (Figure 1.5a) and intermittent pneumatic compression (IPC) systems (Figure 1.5b) [56]. Many researchers have confirmed that the healing outcomes are better for the patients receiving compression treatment compared with no compression [57]. The research focus has been on comparing and evaluating the efficiency of different compression modalities including stockings, bandages and IPCs. Each of these devices holds its own significance for the treatment. Stocking is favoured for low pressure (< 50 mmHg) and allows easy application whereas a bandage is size independent and permits high pressure. IPC is primarily recommended for the patients with poor calf muscle function or limited ankle mobility. More than two modes (stocking and IPC) are also used to provide benefits of both static and dynamic compression leading to healing of venous ulcers and alleviates symptoms in patients with chronic venous insufficiency [58]. Additionally, a warming therapy in conjunction with compression

stocking is useful to increase blood flow and oxygen to the wound, and thus promote healing [59].

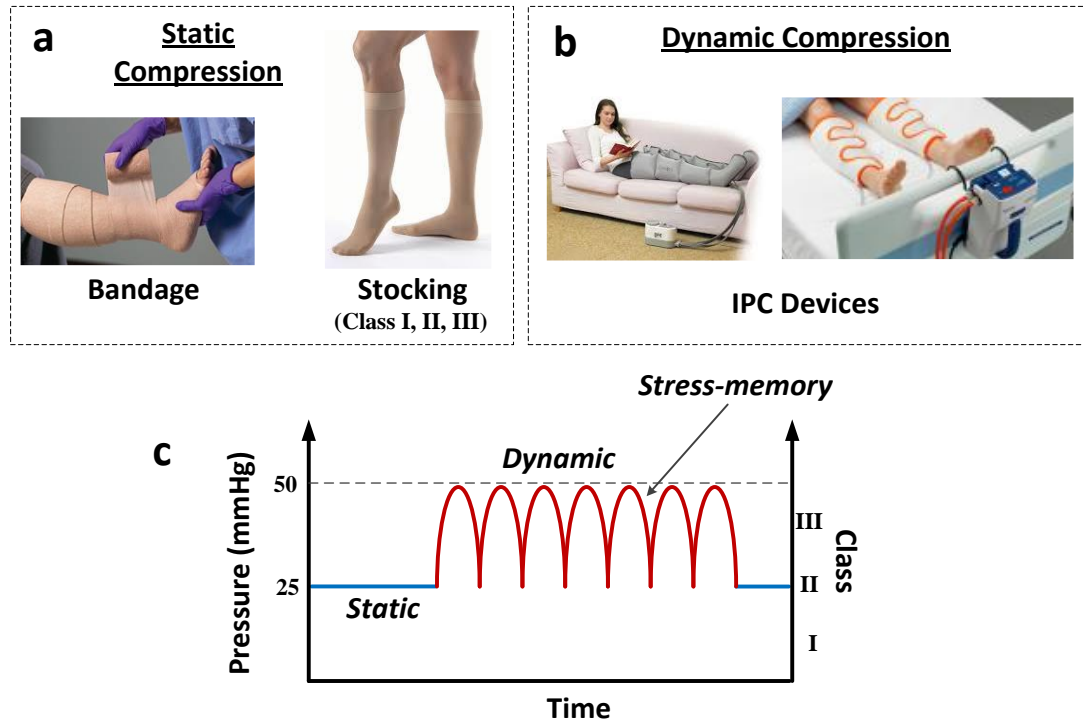


Figure 1.5: Modes of existing compression therapy. a) Static compression, b) Dynamic compression, c) Required method of compression in smart stocking (Source:

www.arjohuntleigh.us)

1.3. Studies on Interfacial Pressure of Compression Bandages

There has been a continuous effort to study pressure generated in the interface between the compression device and skin. Kumar et al. have identified and examined several influencing parameters on the interface pressure performance including bandage characteristics, limb geometry, application technique and physical activity [60]. They proposed a simple experimental technique to evaluate time-dependent performance of the bandage using fabric parameters, and modeled the pressure loss over time using stress relaxation parameters [61, 62]. They designed a prototype to examine the dynamic pressure variation of different bandages [63], and characterized the bandage performance during

movement or exercise of the limb without doing in-vivo pressure measurement [64]. They also studied different fibrous material and fabric structure on the pressure performance and found that the pressure drop is more for non-elastomeric polymers (cotton, viscose, PET, nylon, etc.; > 30% relaxation), as compared to elastomeric samples (polyurethane; < 10% relaxation) [65, 66]. In addition to study on bandage performance, they have also examined the comfort and compression properties of padding primarily used as sub-bandage layer in multi-layer compression system [67, 68].

1.4. Studies on Smart Actuators for Compression Management

Some researchers have made few attempts to use smart material that can be actuated to allow external pressure control. As an example, Munch-Fals et al. [69] and Pourazadi et al. [70] developed electro-active compression bandage systems using smart sensors and dielectric elastomers respectively to control pressure. However, these systems are bulky and non-porous and therefore lead to non-compliance. Moein et al. [71] proposed shape memory alloy based bandage but the fabric structure having alloy wires is rigid and not easily confirmable compare to textile yarns. Also, the actuating temperature is beyond 100 °C which is not convenient to put on legs for practical usage. Bauerfeind [72] proposed modified polyurethane threads having acid functional filler that can be actuated by human skin's pH, but the system has to be rinsed in alkaline solution before application, leads to complication and no added pressure control. Other inventions relate to wearable systems in bandages/stockings for monitoring pressure variation over time [73], which has no function to manage pressure on the leg.

1.5. Problems Being Addressed

It has been estimated that 2% of the general population in the world (age group: 18 to 64) is suffering from chronic venous ulcers [74]. This rate is further increased to 4% in people

over the age of 65. This has significant socioeconomic impact, costing 1% of total health care budgets in developed countries, for example in the USA, this costs \$2.5 billion to treat 6 million patients every year [74]. Both the incidence and cost are bound to increase in future due to changing lifestyle and growing aging population. Thus, there is a huge market in compression products for improving life quality of world population. On the other hand, from the above background number of inadequacies of conventional compression therapy approaches demonstrate a compelling demand for multi-functional stockings in terms of easy size fitting, static pressure, and dynamic (massage effect) pressure.

Current compression therapy has the following shortcomings:

1. Conventional compression products such as bandage and stockings are applied on affected limbs with predetermined compressive force with a given elasticity. Once it has wrapped over the limb, there is no any further any means to change or control the pressure level externally.
2. One of the common problem is difficult to achieve the targeted pressure level [75] due to various reasons including different leg attributes (shape or size) among patients and difference in materials (both stockings and legs), time and temperature dependence. Different class of stockings is to be used to achieve different pressure levels.
3. The selection of stockings with proper sizing and fitting has always been a challenge for both health practitioners and manufactures for better patient compliance and effective treatment [76].
4. With bandage application, there is always a need of trained personnel and the success is largely dependent on skill of the therapist [60].
5. For dynamic treatment (Figure 1.5b), the equipment like IPC is too expensive, noisy, bulky, and once attached requires immobility from the patients [58]. It is also not

breathable, uncomfortable and may not be efficient as it may not contact the skin surface evenly.

6. Except for IPC, other means are passive, meaning that they only provide a fixed level of initial pressure, which has no pressure control and are incapable of having massage effect and warming therapy required for elder and non-active patients to improve venous blood flow.
7. Stockings are repeatedly used in clinics due to high cost, which results in ineffective treatment as the reduced limb circumference leads to low strain and low pressure.
8. Stocking materials are viscoelastic in nature and their properties are time and temperature sensitive. Once the stockings are applied on limb with a given strain, developed strain will diminish gradually with time.
9. Even at a fixed temperature level, the modulus of the stocking material remains constant. Hence the relationship between the pressure and stocking size is not linear, revealing why it takes training and practice for a nurse to get even the initial pressure right.

The afore-mentioned challenges in compression products, particularly stocking may be solved if there is any possibility of *stress control in fabric materials*.

1. If smart polymeric filaments could offer choices with stress responsive to an external stimulus such as temperature. Also, if the filaments can increase the sufficient internal stress with increase in temperature stable for longer time with cyclic response.
2. Whose mechanical properties are sensitive enough to narrow range of temperature change and in the normal use temperature.

Among stimulus-responsive polymers, MPs have high relevance to our needs and have been solving many real-life problems in the areas of aerospace, biomedical, transport,

According to Laplace's law (Figure 1.6b), an internal radial pressure P exerted on the surface of skin is dependent on the internal stress developed in the tensioned stocking. If we can find a material whose internal stress can be easily adjusted in such a way that it can compensate the deviations of the pressure from the initially designated level, we can then sustain the desired pressure on the leg. In the quest for such materials with adjustable internal stress σ , polymeric materials are the logical choice for its widely known that their tensile modulus E , i.e., internal stress σ , can be altered if we control the temperature during operation. However, not all polymers can achieve this smart stocking function: after all, cotton and nylon used in current stockings are already polymers themselves. We need polymers with internal stress σ exceptionally sensitive to temperature change within a very narrow range and in the normal usable temperature.

Recently, a novel phenomenon of *stress-memory* in the segmented polyurethane has been discovered, according to which the internal stress in the memory polymer (MP) can be programmed, stored, and retrieved reversibly with an external thermal stimulus. Application of such MPs in the form of fibers/filaments could be potentially suitable for the development of smart compression stocking. As shown in Figure 1.6a, the circumferential tension in the stocking depends of strain and the leg radius. The smart fibers in the structure of stocking would allow controlling the internal stress using external stimulus, and thereby providing the freedom to adjust pressure level externally whenever needed.

1.7. Research objectives

The main objective of this research work is to study the novel stress-memory behavior in polymeric memory material for its application into smart compression stockings for functional compression management of phlebological and lymphatic medical disorders such as varicose veins, leg ulcers, and venous stasis.

1. To synthesize and optimize the semi-crystalline memory polyurethane (MP) and characterize its novel stress-memory behavior through distinct tensile programming conditions for obtaining its relationship with thermal, structural, and mechanical conditions.
2. To investigate, quantify and develop a constitutive model for the prediction of stress mechanics in the MP, and propose a unique methodology for extracting pure memory stress from MPs for its optimum cyclic performance without efficiency loss.
3. To engineer stress memory polymeric filaments through optimizing fiber spinning conditions and do a comparative analysis on the memory performance of both filaments and films.
4. To design smart compression stockings by integrating MP filaments into tubular fabrics through textile engineering, and study the response of structural and programming parameters on the interfacial pressure profile developed by the memory stocking.
5. To scientifically imply the stress-memory discovery into multi-functional smart medical compression stockings to achieve pressure gradient, controlled static and dynamic pressure (massage effect), size fitting, and selective pressure control.

1.8. Novelty and significance of the research project

1. Revealing the mechanisms in stress-memory behavior of polymers, their fibers and fabrics as well as compression stocking may lead to new science in soft materials, particularly polymers.
2. Scientific findings discovered in stress-memory polymer materials may inspire people to re-examine existing materials such as elastomers/rubbers and develop new materials which have novel structures and smart functions.
3. Theoretical approach of constitutive model developed for prediction of stress-memory behavior of polymeric materials will shed insights for broadening their applications requiring smart functions such as artificial muscles, soft skins, massage devices, and electronic sensors/actuators.
4. Techniques for measuring, programming, and analyzing memory stress for memory polymers, fibers, fabrics and compression stocking will set up new methods for polymeric materials research and applications.
5. Novel smart compression stockings will offer alternative treatment methods with added functions to medical chronic disorders.
6. Polymers and fibers developed here with stress-memory will make available new materials for applications requiring smart and soft functions related to forces.
7. The structures of fibers and textiles with optimal memory stress will enrich textile design for new applications in functional and smart devices.
8. The research outcome is very helpful in revolutionizing the compression therapy with stockings of multi-functionalities in single tubular size, easy application, and size fitting.

1.9. Outline of the thesis

This Thesis outlines the discovery of novel stress-memory behavior in a semi-crystalline memory polymer (MP) and its application in smart medical compression stockings. The stress-memory in the MP film, fiber/filament, and filament integrative textile fabric structure, and its relationship with thermal, structural, and mechanical properties have been studied both experimentally and analytically. The progressive approach towards designing the smart medical stocking using stress-memory potential is discussed chapter wise as follows.

Chapter 1: In this chapter, general background of shape memory polymers, stress-memory behavior, and the stress-strain components reported in the literature is discussed. The background of chronic disorders, compression therapy, available treatment modes, and the efficacy of different modalities are highlighted. The problems being addressed, motivation for this research direction, research objectives, and the novelty and significance of the work is presented.

Chapter 2: A comprehensive literature review on shape memory material, polymer, molecular mechanisms, studies on memory fibers, memory textiles, stress-strain related studies in MPs, constitutive model approach in MPs, and the research gap / drawbacks are highlighted. In addition, background of compression therapy, modalities, treatment update, and studies related to textiles, smart actuators for compression is presented.

Chapter 3: This chapter is mainly focused on comprehensively describing the experimental materials, methodologies followed, and characterization techniques involved in the entire research work. The experimental work is divided and explained as: 1) discovery of stress-memory phenomenon in thermal responsive semi-crystalline memory polymeric material (film), 2) constituent analysis of stress memory in semi-crystalline

polymeric material (film), 3) revelation of stress-memory behavior in memory polymeric filaments/fibers, 4) optimization of stress memory filaments/fibers integrative textile fabric structures for compression stockings, and its performance evaluation by pressure related study and Ultrasound blood flow measurement.

Chapter 4: A novel phenomenon of stress-memory is discovered in a Poly (ϵ -caprolactone) diol based semi-crystalline memory polyurethane and reported in this chapter. This concept is further enlightened by a switch-spring-frame model that would eliminate the limitation of existing models which overlooks the stimulus responsive nature of such polymers. The discovery being reported here is stemmed from a real case study into memory polymer fibers in compression stocking for chronic venous disorders. The concept of obtaining the pressure gradient and massage function is learned from the stress-memory testing and practically implemented via unique programming condition.

Chapter 5: In this chapter, the stress analysis in a semi-crystalline polyurethane is further investigated to unveil the total stress-strain components of the memory polymer. The evolution of stress under different temperature and strain levels is determined experimentally. A constitutive model based on phase transition and a novel memory modulus is further used to predict and characterize the individual stress components during the thermo-mechanical process. The predicted results are having significant agreement with the experimental data. Using this model, memory bandage has been designed based on the stress-memory film actuator and predicted the pressure test results for practical feasibility.

Chapter 6: For the first time, the novel stress memory behavior is revealed at melt spun filament/fiber level based on Poly(1,6-hexamethylene adipate) diol, semi-crystalline memory polyurethane in this chapter. The MP was synthesized and prepared film and melt spun filaments for the comparison. The evolution of memory stress is studied with

comprehensive thermal, mechanical, and structural characterizations. The stress-memory behavior is also realized in the filaments integrative smart compression stockings with pressure related studies.

Chapter 7: Based on the stress-memory investigation in the MP film and revelation at filament level, the next step is to design the stocking via textile structural optimization and it is well reported in this chapter. A pioneer approach is made to design and optimize the smart stocking structure by integrating the stress-memory filaments as a main load bearing element to control the internal stress. Six different textile knit structures were employed and investigated for pressure analysis and studied their effect together with physical parameters, leg radius, and programming conditions. An empirical relationship is derived and validated with experimental results, which provides the knowledge for how to control/manage the stocking pressure with structural modifications like never done before. In addition, the effect of massage function on venous blood flow is objectively measured by Doppler Ultrasound method.

Chapter 8: This chapter presents the conclusions and suggestions for the future work to further explore the potential of stress-memory polymeric material.

CHAPTER 2: LITERATURE REVIEW

2.1. Introduction to Shape Memory Materials

Shape memory materials (SMMs) are stimuli responsive smart materials which are given an intensified scientific and technological significance from both academia and industries in the past few decades. The term “shape-memory” was first proposed by Vernon in the year 1941 [77]. SMMs can undergo significant macroscopic deformation; can be programmed to one or many shapes and spontaneously recovered back to its permanent conformation upon exposure to an external stimulus such as heat [78], light [21], electricity, moisture, and magnetic field [19, 20, 22]. These smart materials are intrinsically sensitive to ambient temperature, to have the shape memory property; they should have the responsive range within a narrow range of temperature change (Figure 2.1). SMMs have been developed intensively in the past few decades [79, 80] and they include shape-memory alloys (SMAs), shape-memory ceramics, and shape-memory polymers.

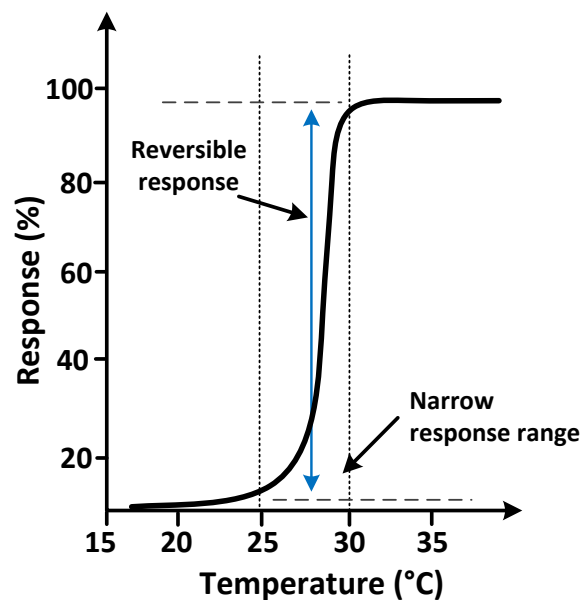


Figure 2.1: Plot depicting the sensitive change of smart materials in ambient temperature

2.2. Introduction to Shape Memory Polymers (SMPs)

Recently, the research focus in SMPs has been intensified both in fundamental studies and their application in multidisciplinary areas [14]. SMPs have drawn a significant attention from the researchers to serve into diversified applications from past few decades due to their advantages over alloys or ceramics. However, the importance of SMPs was not recognized till 1960s, when cross-linked polyethylene (PE) was used for making heat-shrinkable tubes and films [81]. SMPs were started to develop in the late 1980s, the acceleration in research began in the 1990s and making significant progress only in the recent past 5 to 10 years. The polymer network architectures with the applied processing and programming technology allow to tailor the properties of the SMPs and to control their shape memory behavior for vivid applications. SMPs can be crafted to several functions such as deployment, fixation, actuation, self-healing, and fitting [14]. SMPs have emerged into several interdisciplinary applications such as textiles, aerospace, biomedical, transport, construction, electronics, and consumer products. Scientific communities are much interested in discovering new phenomenon in the arena of shape memory polymers. SMPs having several advantages compared to SMAs [14], such as low density & low cost (SMP = 1.25 g/cc, NiTi SMA = 6.4 g/cc); easy processing with high quality and materials types (thin & ultrathin films and wires, foams with different porosities); extremely high recoverable strain than SMAs (100% to 95% in solids and foams respectively than 10% with SMAs); ease in tailoring of thermo-mechanical properties (by blending with different types of fillers or varying their compositions); wide shape recovery temperature from -20 °C to +150 °C; excellent chemical stability, biocompatibility/biodegradability; responsive to multiple stimuli and multi shape recovery ability.

2.2.1. Molecular Mechanism of SMPs

Most of the shape memory polymers are basically segmented structures and there are distinguishing molecular mechanisms for each segment. Hu et al., proposed an overall 3D SMP architecture based on the molecular mechanisms [27] as shown in Figure 2.2.

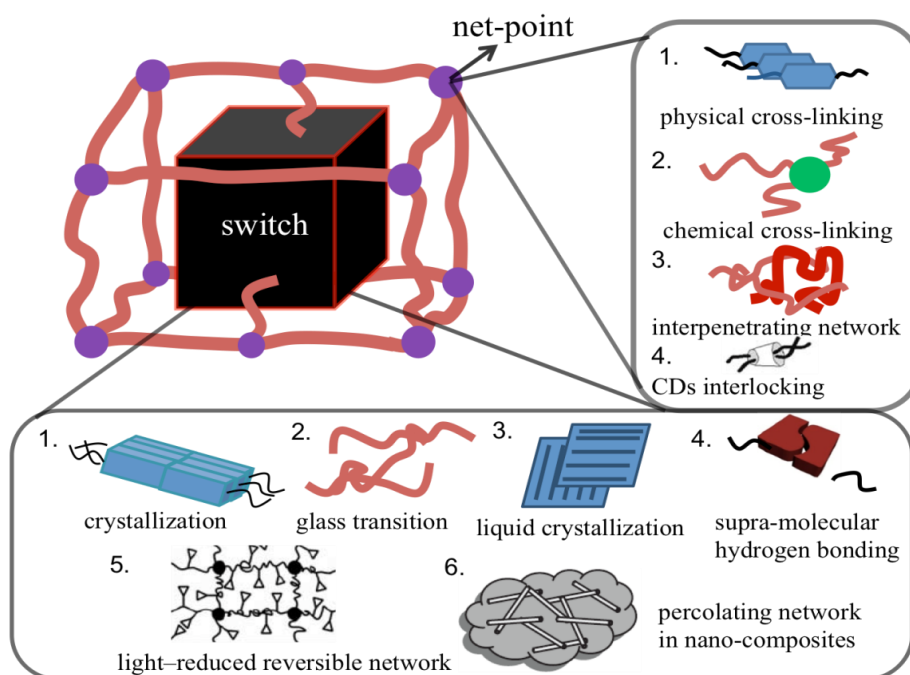


Figure 2.2: The Overall architecture of SMPs [14].

This schematic model can describe the structure of any type of SMP and it consists of both switch units and net-points. The net-points (hard segment) determine the permanent shape/configuration and can be made of either physical or chemical cross-links, with interpenetrated or interlocked supramolecular complex networks. The main driving force for strain/shape recovery in SMPs is the entropic elasticity of molecular chains/network in the switch unit. Basically, switch unit is the soft segment and responsible for shape fixation upon deformation and recovery upon certain external stimulus such as heat, light, and magnetic field. The switches such as amorphous, crystalline, and liquid crystalline phases, supramolecular entities, light-reversible coupling groups and newly utilized percolating

cellulose-whisker networks have served as soft segment in controlling the shape memory effect (SME) of SMPs.

2.2.2. Transition Types of SMPs

Transition is the temperature range of a polymeric system where the significant change in modulus and shape occur due to change in temperature. Basically, SMPs have glass (T_g) or melting (T_m) type of transition for the switch or soft segment. The inter molecular network chains of the soft segment in SMPs can be either crystalline or amorphous, therefore the T_{trans} can be either melting or glass type respectively [39, 82, 83]. If the $T_{trans} = T_m$, strain induced crystallization [84] occurs in the material upon deformation and cooling below the T_m . The shape recovery of the SMPs are prevented by the crystallites and until it is reheated above T_m [82]. Tobushi and Takahashi et al. [85, 86] stated that, if the $T_{trans} = T_g$, the Micro-Brownian motions of the polymeric network will be frozen and set into glassy state when cooled below T_g . The network will be in non-equilibrium state until it is reheated above T_g to activate the Micro-Brownian motions.

2.2.3. Shape Memory Effect in SMPs

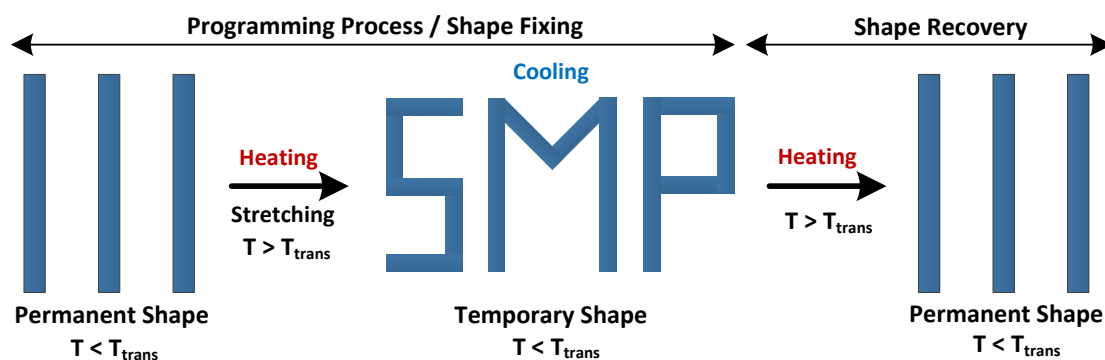


Figure 2.3: Schematic representing the shape memory effect in SMPs

Shape memory effect (SME) represents the capability of SMPs to memorize the original shape and allow the materials to recover the original shape from a temporarily deformed shape upon appropriate stimuli. Basically, SMPs are followed with two distinct features: fix ability and recoverability. Figure 2.3 shows the schematic representation of shape memory effect in SMPs. Fixability refers the ability of SMPs to maintain the deformed shape caused by certain stimuli from undeformed shape through a suitable programming process and it is termed as “shape fixing”. Recoverability refers to the ability of SMPs to recover their original undeformed shape from the temporarily deformed shape under the application of suitable stimuli and it is termed as “recoverability” (shape recovery). The SME in SMPs results from the unique structure and morphology of the polymeric system and influenced by the testing or programming conditions.

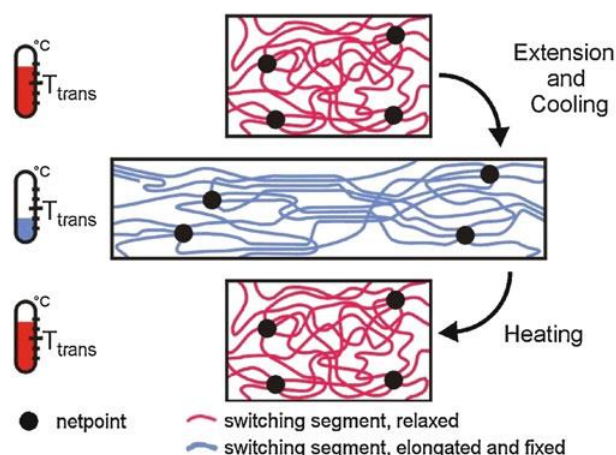


Figure 2.4: Molecular mechanism of the thermal-induced SME [87].

Figure 2.4 describes the molecular mechanism of the thermal-induced SME with melting type of transition for SMP. A significant change in mobility of the molecular chains can be seen below and above T_{trans} of switch segment, meanwhile, there is also a change in the modulus within a narrow range of temperature. The polymer system consists of hard segment (Net-points) and soft segment (switching segment) to enable the SME in SMPs. Net-points stabilizes the permanent shape or integrity of the polymer system and fixed by

the phase with highest thermal transition at T_{perm} . At the temperature below the transition range the switching segment molecular chains are rigid and mobility is limited. Whereas, the temperature above the transition range, the soft segment chains are flexible and in an amorphous state to enable the changes into a temporary shape. The SME in the SMPs can show on the basis of rubber elasticity even though the SMPs with no apparent network structure according to Liu et al [83]. When the polymer is deformed and cooled down quickly below T_{trans} , the effect of stress relaxation can be avoided and the elasticity can be preserved in the structure. Upon stimulus $>T_{trans}$, the stored elasticity can be recovered and triggers the permanent shape recovery.

2.2.4. Evaluation of shape memory properties

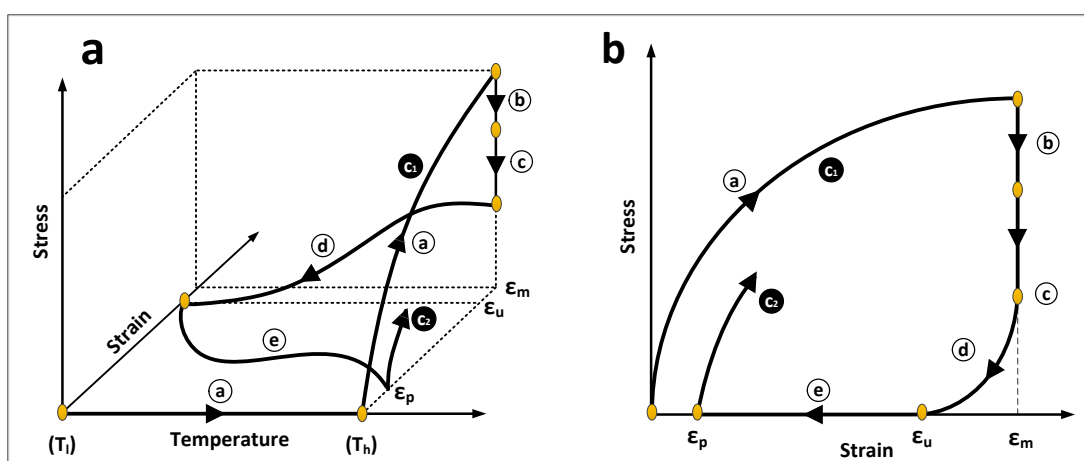


Figure 2.5: Scheme of thermo-mechanical cyclic test. a) Plot of stress with strain and temperature. b) Typical curve of stress vs strain. (T_l): Low temperature ($T < T_{trans}$); (T_h): High temperature; (ϵ_p): Plastic strain; (ϵ_u): Fixed strain; (ϵ_m): Programming strain; ($\epsilon_m - \epsilon_u$): Elastic strain; $\epsilon_r = (\epsilon_m - \epsilon_p)$.

The shape memory property of a SMP can be described by determining important quantities and they are shape/strain fixity and shape/strain recovery. Generally, shape memory properties of any polymeric materials are determined by a typical thermo-mechanical cyclic

tensile testing (Figure 2.5) using a tensile tester with a controlled heating chamber [39, 82, 85, 88]. The detailed methodology is shown as follows.

1) Step (a): Heating the specimen above the T_{trans} under zero strain condition. Programming to a desired strain level (ϵ_m) under constant strain rate (e.g 10 mm/min) at elevated temperature. 2) Step (b): Holding the specimen under constant strain at high temperature. 3) Step (c-d): Cooling ($T < T_{\text{trans}}$) and unloading the specimen under a constant rate to a strain level ϵ_u (ϵ_u can be achieved due to presence of elastic strain and hinders the complete shape fixation). 4) Step (e): Heating ($T > T_{\text{trans}}$) to achieve the shape recovery and to release the stored strain to ϵ_p . This is the one entire cycle (C_1). In the next step, another cycle (C_2) is carried out from step (a) to (e). Normally this procedure is repeated for five cycles and the last one is considered with the similar trend. The shape fixity and shape recovery can be expressed in %age as shown in Eq. (2.1) and Eq. (2.2) respectively.

$$\% \text{ shape fixity} = \frac{\epsilon_u}{\epsilon_m} \times 100 \quad (2.1)$$

$$\% \text{ shape recovery} = \frac{\epsilon_r}{\epsilon_m} \times 100 \quad (2.2)$$

2.2.5. Shape memory or memory polymers?

Shape memory polymers are considered as an important class of smart materials over past few decades due to their interesting behavior in changing or recovering shapes from the temporarily fixed configurations. They are tunable into one-way, two-way [89], and multi-shape memory [42] effect based on the polymer composition and molecular structure. Thus, the term ‘shape memory’ might have been used to identify these smart materials. Apart from shape, SMPs can also memorize other physical parameters such as stress (stress-memory) [40], temperature (temperature-memory) [90], chrome (chromic-memory) [41], and electricity (electrical-memory) [91]. Stress-memory refers to a phenomenon, where the stress in the material can be programmed, stored, and retrieved continuously for many

cycles upon a thermal stimulus. Lendlein et al. [90] explored temperature-memory effect in polymeric network with crystallizable controlling units. Temperature-memory creation procedure was enabled to program the material to recover the shape at different temperature levels. Wu et al. [41] developed a shape memory polyurethane with tetraphenylethylene units covalently connected to soft segments and found that the emission intensity (chrome) changes with shape change and recovery process. Whereas, Yuan et al. [91] introduced the electrical-memory effect in shape memory fibers loaded with carbon nanotubes/graphene flakes. They showed that, the composite fibers exhibit variations of electrical conductivity with an accurate memory while temperature changes to reach well defined maximum at a temperature equal to the temperature of programming. Based on the evidence of different other memory properties, SMPs could be termed as memory polymers (MPs) to acknowledge their versatile and unique behaviors.

2.3. Memory Polymeric Fibers (MPFs)

Fibers are fine substances with a high ratio of length to thickness and they can be produced with several polymer systems to exhibit interesting memory behaviors. Practically all polymerization methods can be followed to synthesize memory polymers (MPs). Polyurethane based MPs are segmented structure in which soft and hard segments are present in the same polymeric chain. Usually soft segment contains long chain macroglycol and hard segment possess low molecular weight chain extenders. Segmented polyurethanes are generally synthesized by pre-polymerization techniques, in which macroglycol reacts with diisocyanate to form soft segment and chain extender reacts with diisocyanate to provide hard segment. The critical/switch temperature of polyurethanes composed of two-phase heterogeneous structure is easily controllable and synthesized via bulk or solution polymerization techniques. Segmented polyurethane based MPFs are composed of thermodynamically immiscible fixed and reversible alternative phases and they can be spun

via melt, wet, reaction, dry, and electro spinning methods with tunable functionality for proper applications [78]. In general, fibers of cylindrical, hollow, nano, and electro active composite can be produced with variable diameters/linear densities with functional properties.

MPs have been investigated for few decades and spinning them into fibers and utilizing in the textile applications was first achieved by Hu et al. [92]. Their research team have developed MPU filaments (MPFs) via different spinning methods; dry, wet, melt, reaction, and electro spinning, using polyol as soft segment and small size polydiols/MDI as hard segment [78, 93]. For the first time, Hu et al have developed memory fibers via wet spinning in 2006 and investigated their mechanical, thermal, and shape memory properties. In addition, they have compared the difference between memory fibers and other man-made fibers (Figure 2.6a). Varying the ratio of hard segment content to soft segment could change the behavior of fibers, Zhu et al achieved complete shape recoverability in wet spun fibers (Figure 2.6b) [94].

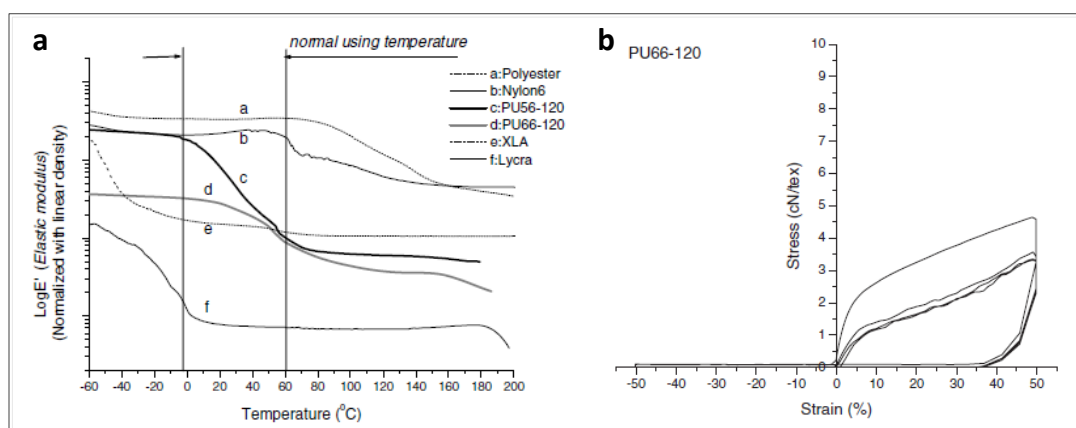


Figure 2.6: (a) Comparison of elastic modulus between MPFs and various manmade fibers. (b) MPF showing 100% shape recovery. [94]

Investigation of dynamic analysis revealed that difference between memory fibers and other man-made fibers in terms of decrease in the elastic modulus (E') in the normal apparel using temperature range. It can be seen from Figure 2.6a that, the decrease elastic modulus

in memory fibers PU56-120 and PU66-120 is very much significant in the normal using temperature range. Increasing the temperature above T_g , transforms glassy state into to rubbery region and this enabled to decrease the modulus. Lycra showed the decrease at -40°C and whereas other fibers showed between 100-105°C. Hence, memory fibers show the switch temperature in the normal using temperature to tune their memory behaviors, and it is advantageous to implicate for several applications. The plastic deformation or irreversible strain is most common in the film substrates, whereas thermal shrinkage occurs in the case of fibers. Zhu et al [94] claim that counteraction effect two opposite factors; irreversible strain and thermal shrinkage induces MP fibers to achieve complete shape recoverability as shown in the Figure 2.6b.

2.3.1. Which fibers do have better performance, wet or melt spun?

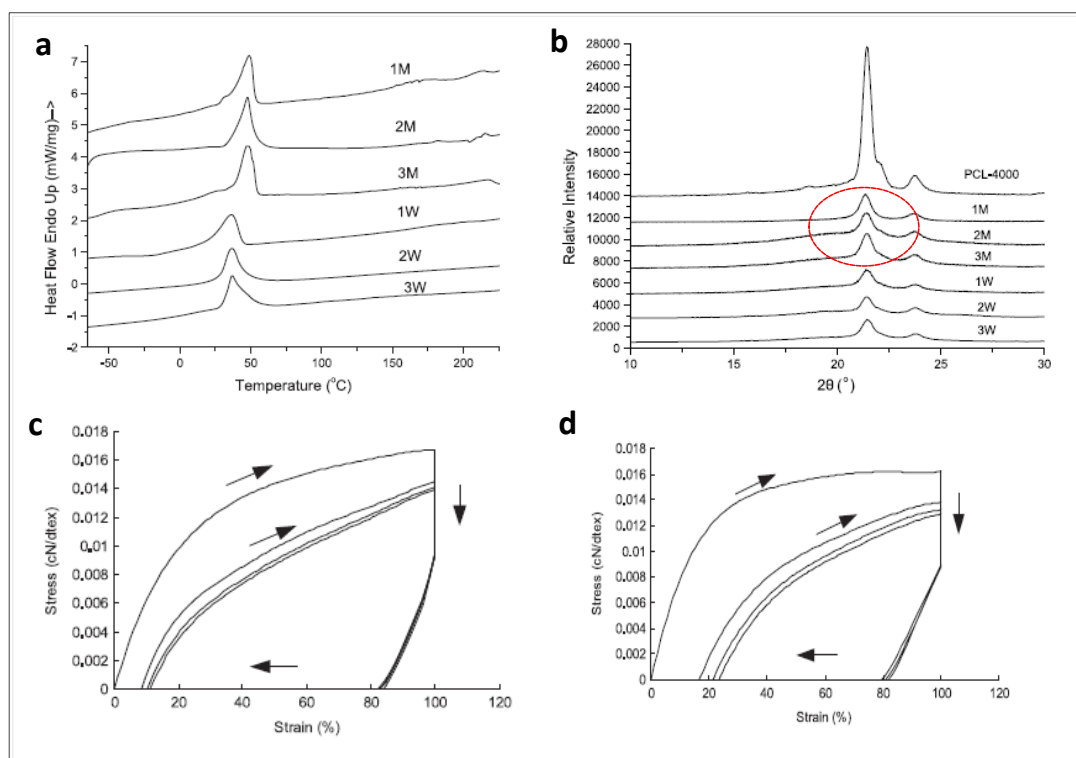


Figure 2.7: Influence of Spinning methods on thermal and shape memory properties. (a) DSC thermographs of melt and wet spun MPFs. (b) XRD profiles of melt and wet spun MPFs. (c & d) Stress-strain curves of melt and wet spun MPFs. M: Melt, W: Wet. [95]

Method of fiber spinning is very much crucial, and which thus decides the properties of fibers for adopting them into several applications. In line with this, Meng et al. [95] have investigated a comprehensive and extensive research to reveal the relationship between phase separation, thermal and mechanical properties and fibers spun with different spinning methods to unveil the underlying physics and property differences. Table 2.1 shows the thermal and mechanical properties of MP fibers spun by melt and wet spinning methods as a comparison. Melt spinning induces fibers to have higher crystallinity and melting transition of soft segment compared to wet spinning method (Table 2.1). It can also be seen that melt spun fibers have significant transition peaks for both soft segment (36-47°C) and hard segment (214°C) compared to no peaks in hard segment for wet spun fibers (Figure 2.7a). Higher crystallinity and larger melting enthalpy of melt spun fibers suggests that melt spinning induces perfect crystallinity and more ordered polymer packaging, significant rich hard segment phase in the fibers. The results of X-ray diffraction (XRD) profiles for fibers also shows that the crystalline peaks are significant and higher for melt spun fibers and this is in accordance with the Differential scanning calorimetry (DSC) traces (Figure 2.7b).

Table 2.1: Thermal properties of melt and wet spun MP fibers [95]

	Soft segment			Hard segment	
	T_m	ΔH	Crystallinity	T_m	ΔH
	(°C)	(J.g ⁻¹)	(%)	(°C)	(J.g ⁻¹)
1Melt spun	48.73	27.89	19.93	214.33	1.294
2Melt spun	47.67	28.46	20.17	214.94	1.305
3Melt spun	46.82	27.94	19.96	214.64	1.286
1Wet spun	36.23	22.8	16.29		
2Wet spun	36.62	22.82	16.3		
3Wet spun	36.98	22.78	16.27		

In addition, thermo-mechanical cyclic test results also have proven that melt spun fibers (shape fixity-86%, shape recovery-98%) could provide higher shape fixity and recovery ratios compared to wet spun (shape fixity-82%, shape recovery-95%) fibers (Figure 2.7c, 2.7d). The physical properties of MP fibers are shown tabulated in Table 2.2. Preparation of fibers using melt spinning does not include any type of solvent and it is also advantageous in terms of environmental and economy concerns. Henceforth, it is imperative to note that melt spinning could be chosen to produce MP fibers to have better performance to implicate them into vivid applications.

Table 2.2: Physical properties of MP fibers

SI No.	Particulars	
1	Tensile strength	> 0.9 cN/dtex
2	Elongation at break	350 to 500%
3	Initial Modulus	0.08 to 0.3 cN/dtex
4	Shape fixity ratio	80 to 100%
5	Shape recovery ratio	90 to 100%
6	Tunable switch temperature range	0 to 100°C
7	Diameter of electro spun fibers	50 to 700 nm

(Note: dtex- weight in grams of 10 Kms of fiber)

2.3.2. Effect of post spinning operations on MP fiber properties

MP fibers can be spun using different spinning methods. Spinning may induce some internal stress and structure deficiency in the fiber along its axis and this must be removed or nullified to enhance their performance properties. Post spinning operations such as heat treatment and drawing could help fiber to rearrange their molecular orientation and polymer

packaging at temperature above the transition of soft segment. The influence of post spinning operations on thermal, mechanical, and thermo-mechanical cyclic properties are discussed in this section.

2.3.2.1. *Effect of thermal setting or heat treatment*

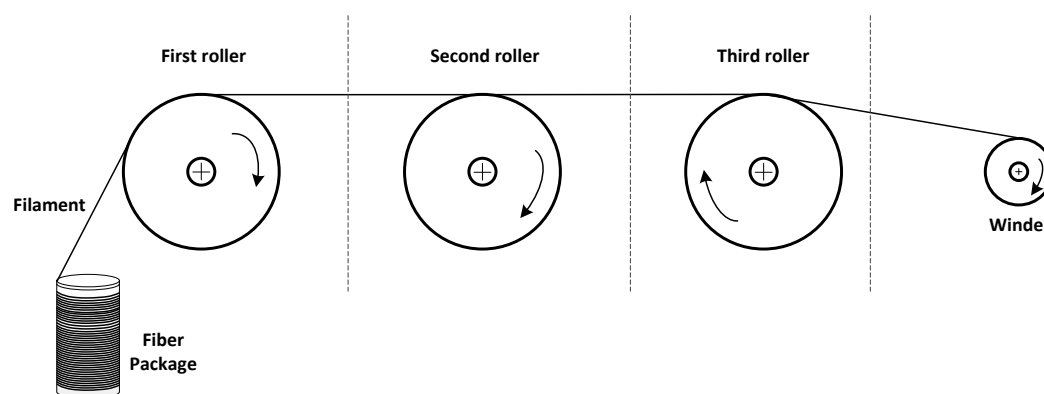


Figure 2.8: Schematic passage of MP filament through thermal setting process

Thermal setting or heat setting process is carried out at high temperature above the transition of soft segment in the fibers. A schematic of filament passage for roller heat setting is shown in Figure 2.8. Meng et al. have experimentally investigated and stated that thermal setting has a significant influence on the soft segment, thermal and mechanical properties [96]. In general, the transition temperature of soft segment ranges from 40 to 50 °C and hard segment with 200 to 240 °C. Heating the fibers above the soft segment transition, helps to increase the crystallinity and melting enthalpy by molecular reorientation with reduced entanglement in the molecular chains. As it can be seen from Figure 2.9a that, transition peak of soft segment is increasing with heat setting temperature and there is a significant peak for hard segment in the fiber treated at 125 °C. This suggests that the crystallinity of soft segment increases which is enabled by rotation of polymeric chains and ordered packaging. Heat treatment may repair the destroyed crystals during the spinning process to increase the crystallinity. Figure 2.9b shows the effect of heat treatment on the fiber tenacity, it can be noticed that at low temperature above the transition,

molecular disorientation occurs and thus yielding lower tenacity. Heat treatment at higher temperature improves the phase separation and hard segment stability which is visible in Figure 2.9b. Partial molecular disorientation at low temperature can also influence on the linear density by decreasing it, increasing the temperature can make the stable network and thus avoid further decrease in the linear density (Figure 2.9c).

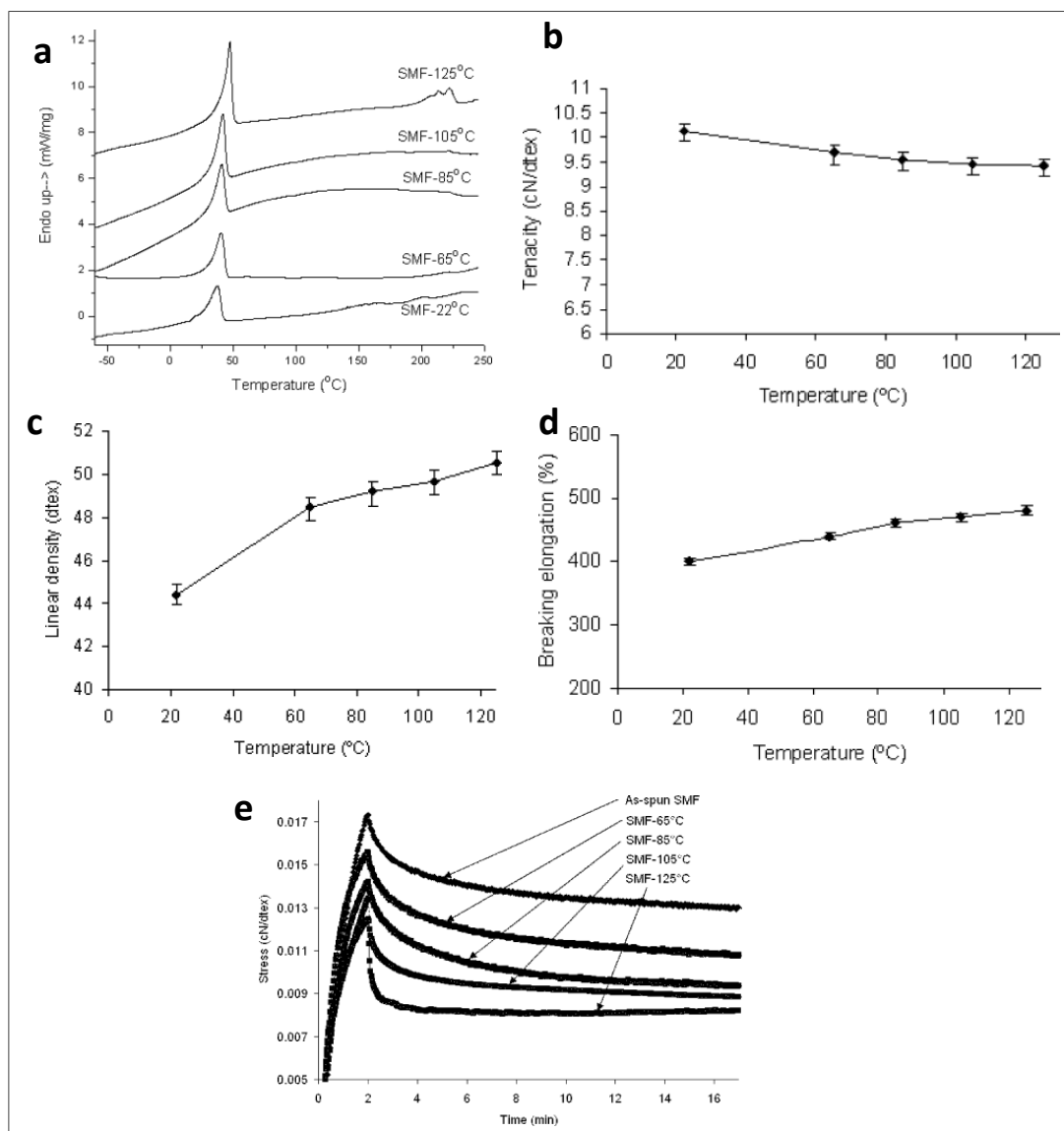


Figure 2.9: Influence of heat treatment on fiber properties. a) DSC thermograms. b) Effect on tenacity. c) effect on linear density. d) Effect on breaking elongation. e) Effect on stress relaxation. [96]

Apart from molecular disorientation, releasing the internal stress at high temperature can also increase the breaking elongation of the fiber (Figure 2.9d). If a fiber needs to be employed in an application which needs a long-time response, stress relaxation is the most important criteria to be considered. Increasing the heat treatment would cause the fiber to improve the phase separation and strong hydrogen bond with well-ordered hard segment network. High temperature treated fibers could show less decay in the stress and great stability over time (Figure 2.9e). Increasing in the crystallinity, phase separation, hydrogen bonding of hard segment would improve the shape fixity and shape recovery ratios as well. As we know, soft segment is responsible for shape fixation and hard segment stability for shape recovery during thermo-mechanical cyclic process [96].

2.3.2.2. Influence of drawing process

Drawing here refers to stretching or tensile deformation during the thermo-mechanical cyclic testing. Meng et al have studied the effect of both cold and thermal drawing on the shape memory effects for the wet spun fibers in comparison with commercial polyurethane fibers. Their experimental investigation reported that thermal drawn fibers could improve the shape fixation and shape recovery ratios as the soft segment crystallinity increases with hard segment stability and phase separation [97].

2.3.3. Recent advances in MP fibers

Researchers and industrial technocrats have been continuously working in the arena of MP fibers to scientifically apply them into vivid applications in multidisciplinary areas such as fiber supercapacitors, vibration damping structures, biomimetic fibrous scaffolds, fiber assembly for artificial muscles, and self-healing composites. Zhang et al. have fabricated a biodegradable Nano fibrous scaffolds with shape memory properties and implied into bone tissue engineering offering shape fixity and recovery ratios more than 90% [98].

Electrochemical performance of MP fiber based supercapacitors could offer an excellent stability suitable for shape programming and recovery [99, 100]. MP fibers possess higher toughness ($276\text{--}289\text{ MJ m}^{-3}$) compared to spider dragline silks (160 MJ m^{-3}) due to their excellent stretchability and having higher vibration damping capability [101, 102]. Two-way shape memory behaviour based MP fibers can be utilized in making hierarchically chiral structured artificial muscles [38]. The negative coefficient of thermal expansion of MP fibers is one order higher than those made of polyethylene fibers [103]. The great potential of memory fibers would further enable unveiling of untapped novel behaviors to prepare them as a futuristic smart material for broad horizon of applications to the mankind.

2.4. Characterization Techniques for Memory Polymeric Materials

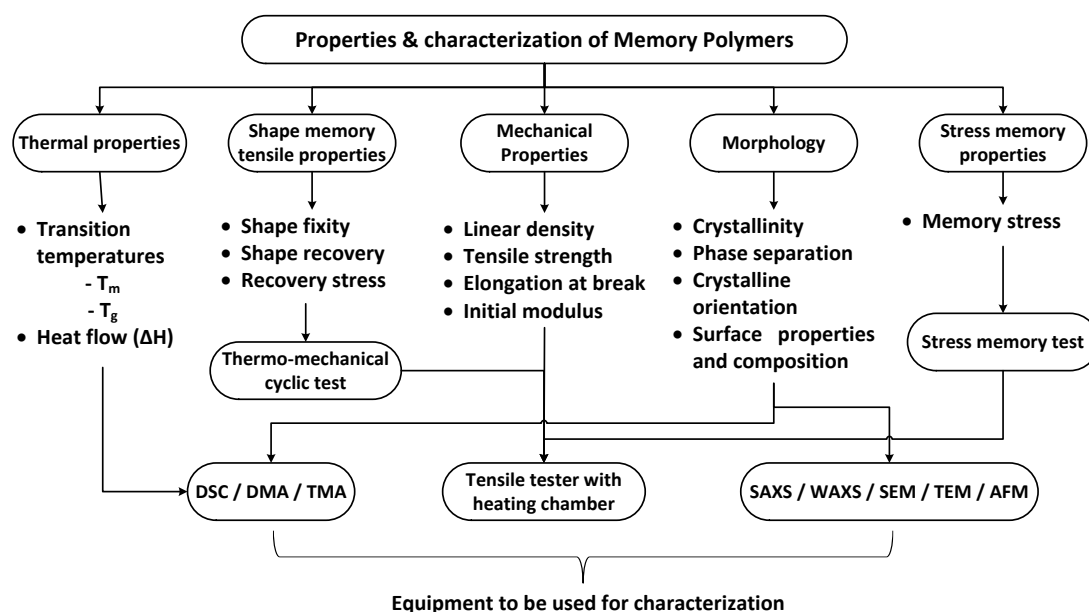


Figure 2.10: Characterization techniques of memory polymers.

Figure 2.10 shows the different techniques and equipment to be used to characterize the structural, physical properties and its relationship with the polymeric system. The techniques tabulated here is applicable for polymers in the form of bulk, film, filament, yarn, and foam.

2.5. Thermal-induced Memory Polymers in Textile Applications

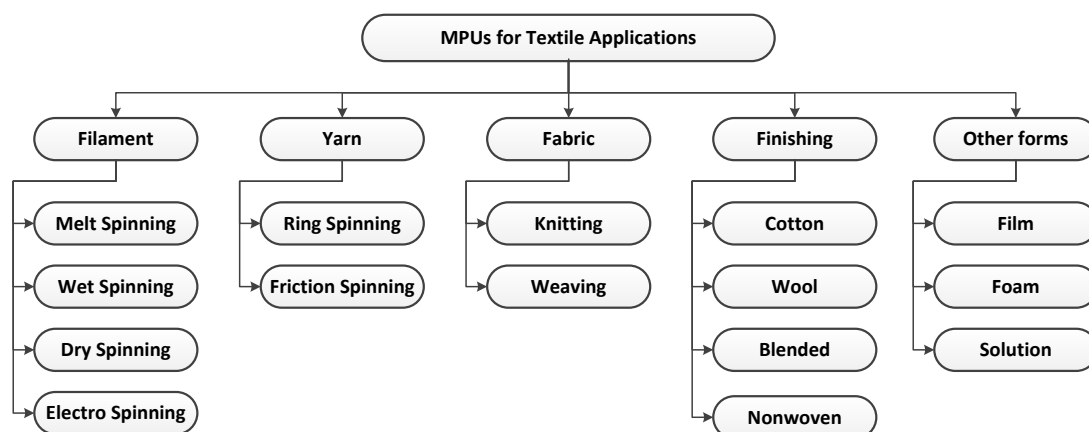


Figure 2.11: Different forms of MPUs for textile applications

MPUs are basically stimuli responsive smart polymers and they can be applied into textile materials to enhance their smart functions in 2 ways via finishing or built-in methods. Finishing method primarily involves *coating* or *laminating* techniques and built-in method includes the blending and spinning operations [27, 28, 104]. MPs can be applied on to textiles in different forms such as emulsion, solution, film, fiber, foam, and bulk forms under specific conditions. As shown in Figure 2.11, MP fibers can be prepared via spinning techniques and embedded into yarn by spinning to make flexible fabrics by knitting or weaving technique. Generally, MPs based on glass or melting transitions known as switches typically have a physical cross-linking structure, crystalline or amorphous hard phase, or chemical cross-linking structure and a low temperature transition to a crystalline or amorphous phase. Generally, in the original or permanent shape, the internal stress is either zero or significantly low. After the deformation, the applied stress will be stored in the cross-linking structure by cooling the transition. The deformed or temporary shape is fixed because of sharp increase in elastic modulus around the glass or melting transition temperature. The MP recovers its permanent shape upon heating the polymer above the

transition temperature, with the release of the internal stress stored by the cross-linked structure.

Major advantages of MPs in textile applications are, 1) the switching temp can be tailored even to set around body temperature, 2) superior processibility, 3) soft/tailorable mechanical properties, 4) high strain deformability and recoverability.

2.5.1. Fabrics made of memory materials

Stylios et al. have developed shape memory alloy (SMA) (0.2 mm diameter) integrated textile smart fabrics to achieve the SME effect (Figure 2.12). The aim was to develop the fabric to change aesthetic performance by changing the shape. *The achievable recovery strain is limited to about 6 to 8% [105].*

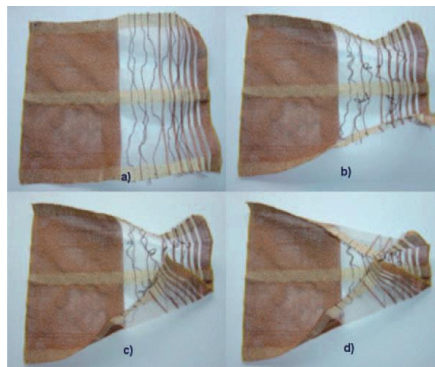


Figure 2.12: Shape recovery of a fabric having SMA spring with temp = 50°C [105].

Due to limitation of SMAs, Stylios et al. also showed a SME of fabric woven with Tg type of MP yarn having diameter of 0.4 mm. The recovery of the MP woven fabric showed a recovery at 50°C (Figure 2.13).

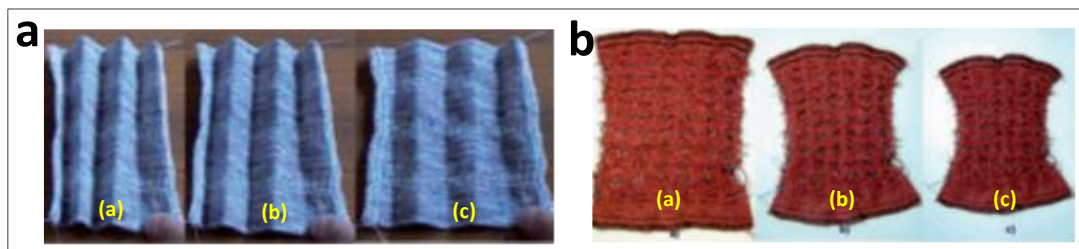


Figure 2.13: (A) Shape recovery of MP composite woven uniformly and densely of MP yarn at 50°C with recovery time (a) 0 s, (b) 15 s, and (c) 30 s. (B) Shape memory recovery of MP composite loosely woven fabric with SMP yarn at 50°C with recovery time (a) 0 s, (b) 30 s and (c) 60 s. [105]

Fabrics have been developed using MPFs using knitting and weaving methods by Hu et al [106]. These MPF based knitted garments are suitable to fit the wearer's body contour and it is shown relatively low vertical tension stress compared to elastic fibers (Figure 2.14). Biological properties such as cytotoxicity, hemolytic effects, and skin erythema have been investigated for SMPU fabrics with switching temperature around body temperature and showed negativity [107].

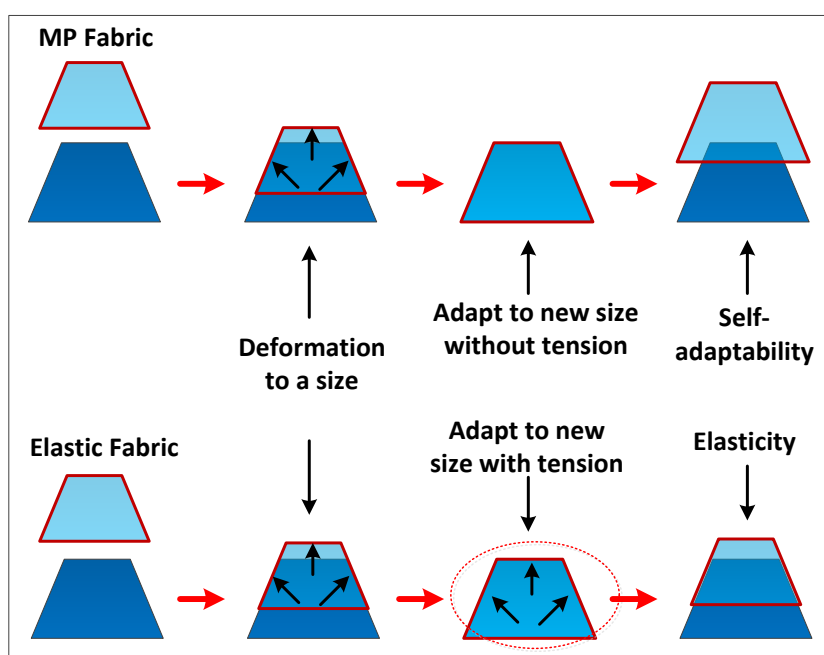


Figure 2.14: Self-adaptability of MP based garments [107]

2.6. Stress-Strain Related Studies in Memory Polymers

Most of the existing studies pertaining to stress in MPs are related to shape recovery, namely, recovery force/stress [47, 108, 109], which determines the recoverability of a fixed material to its original shape until a new concept of stress memory was reported in a recent

paper [110]. Recovery stress consists of both contributive and impeditive parts depending on the mode of programming process i.e compression or tensile [44]. The internal stress freezing can be achieved by normal shape fixing process in MPs at lower temperature ($T < T_{trans}$) in deformed state. Stress-strain characteristics of memory polymers are generally studied by their thermo-mechanical behaviors under specific conditions. Both stress and strain related studies must be given importance; stress response is very crucial rather than strain for several applications. Even though if a material can show 100% shape recoverability, the amount of stress imparted is more crucial. The evolution of recovery stress in such materials during strain recovery has been adopted in various applications such as shape memory orthodontic wires [37], medical casts [36], sutures [13], SMP McKibben artificial muscles [29], endovascular thrombectomy devices [111], and deployable orthopedic expandable stents [30].

Therefore, stress related studies are most significant to comprehend its unique behaviors to incorporate with applied and processing technologies into various practical applications. Understanding these stress related behaviors at different conditions is a very challenging task. In general, most of the stress related studies are followed by a typical thermo-mechanical cyclic test as a benchmark [82, 85]. The recovery stress can be normally determined by following strain-induced [82, 84, 112] or stress-induced crystallization [113, 114] methods for programming. The constant strain and stress is used for the fixation of the deformed strain in strain-induced and stress induced crystallization methods respectively (Figure 2.15). Additional deformation is given during cooling lead to storage of additional elastic strain under external load in stress-induced crystallization (stored strain is higher than the programmed strain). Constant strain with variable stress level is achieved during cyclic testing and no additional elastic strain is stored in strain-induced crystallization type of programming (programmed strain is higher than the stored strain).

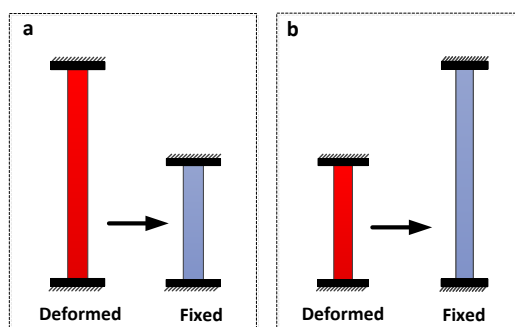


Figure 2.15: Scheme of programming. (a) Strain-induced crystallization. (b) Stress-induced crystallization.

Most of the available literatures have stated that, the entropic elastic energy is being stored in hard segments during programming and stress recovery process at higher strain level [46-48, 82, 87]. It has been reported in several stress related studies that, the deformation components in MPs includes plasticity, viscoelasticity, and elasticity (Figure 2.16).

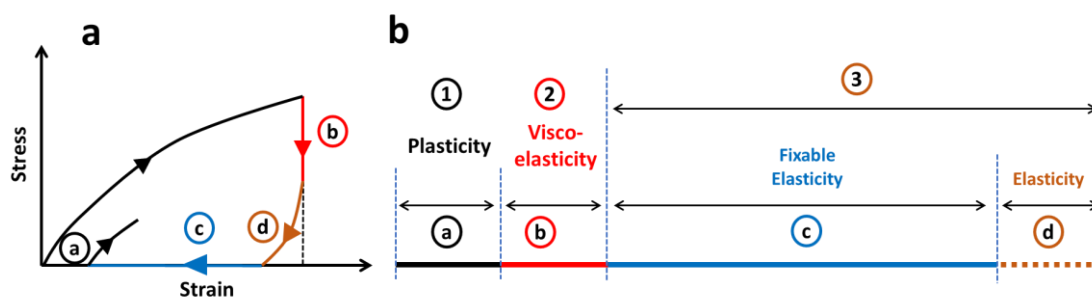


Figure 2.16: Stress-strain components based on literature. (a) Thermo-mechanical testing of MPs. (b) Components of MPs based on the literature from few decades.

Plasticity or irreversible strain in the material occurs due to permanent slippage of intermolecular chains in the polymeric system. The term visco-elasticity refers to “viscous and elastic behavior” of a material and this occurs generally at the intermediate region between below and above transition range of a polymeric material. Elasticity is a phenomenon, where the deformed shapes can return to its permanent conformation upon removing of external forces.

Lin et al. have studied the shape memory behavior using viscoelastic model and it is stated that, the deformation of MPs can be fixed by the hardened reversible phase (soft segment) which restricts the recovery of fixed phase (hard segment). The reversible phase can be softened by heating and the deformed/fixed polymer can recover its original shape by the *elastic force* of the fixed phase [46].

Ivens et al. [47] have stated that, fiber reinforced memory composites can exhibit a “spring back” effect during cooling below transition temperature. The peak stress was caused by the resistance to deformation in the cross-linked net points and in the switching segments of the material. A residual plateau stress can be traced for a prolonged period of time during cooling process after the stress relaxation and this is elasticity in the material. Also, it has been discussed that, an important factor for shape memory effect is the stored *elastic energy* in the hard phase. Even, Gall et al. have stated the same reason for the recovery of a deformed material [48].

Qi et al. [49] have investigated the underlying physical mechanisms during the shape memory behavior by a theoretical modeling approach using standard linear solid viscoelastic model. They have stated that *viscous strain is the main driving force* for the recovery of the MPs from the deformed state.

2.6.1. A constitutive model approach in MPs

Several constitutive models have been discovered to do the stress or strain analysis in the MPs. These models can be classified in to two main categories. The first approach is based on phase transition, where the polymer network is considered as active and frozen phases. The second approach is based on the thermoviscoelastic model [115, 116]. The phase transition model approach and its development is discussed here. Liu et al. [43] have systematically investigated the thermo-mechanical behavior of MPs from a macroscopic

view point during shape storage and recovery based on the thermodynamic concepts of entropy and internal energy. They have defined two kinds of C-C bonds, the ‘frozen bond’ and the ‘active bond’, to quantify the material state. The material state is basically known by the term ‘glassy’ ($T < T_{trans}$) and ‘rubbery’ ($T > T_{trans}$) in the specific temperature range. Figure 2.17 shows the schematic of 3-D MP model with the mixture of two extreme phases during thermos-mechanical cycle. The active phase is linked to rubbery state where the free conformational motion can potentially occur. The frozen phase is related to glassy behavior which does not allow any further conformational motion and only the stretching or small rotation of the polymer bonds occur. At a given temperature, the polymer matrix consists of both phases, and the frozen and active phases are predominant at lower temperature ($< T_{trans}$) and higher temperature ($> T_{trans}$) respectively.

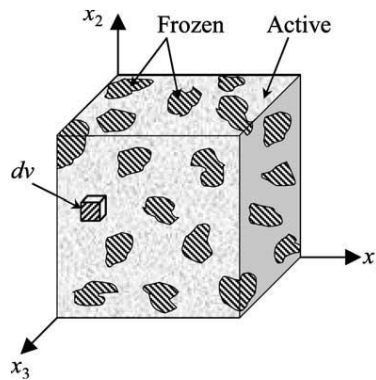


Figure 2.17: Schematic diagram of the micromechanics foundation of the 3-D MP constitutive model [43].

The shape memory behavior can be captured during thermo-mechanical cycle while the glass transition is embodied by changing the ratio of these two phases. The material is frozen gradually during cooling, and the ‘frozen fraction’ and the ‘active fraction’ can be defined as:

$$\varphi_f = \frac{V_{frz}}{V}, \quad \varphi_a = \frac{V_{act}}{V}, \quad \varphi_f + \varphi_a = 1 \quad (2.3)$$

Where, V = total volume of MP, V_{fz} = volume of the frozen phase, V_{act} = volume of the active phase. The total volume of the MP includes frozen and active volumes, in addition with the free-volume as well. The frozen fraction φ_f is considered as ‘physical’ internal state variable, which is related to the glass transition extent. So, from the Eq. 2.3, the active fraction is $\varphi_a = 1 - \varphi_f$. Under the conditions of slow strain rate and gradual rate of heating/cooling, φ_f and V_{fz} are totally depending on temperature (T):

$$\varphi_f = \varphi_f(T) \quad (2.4)$$

The fraction of the strain storage can be captured by $\varphi_f(T)$ as a function of temperature, if the material has been deformed at high temperature. An assumption has been made that, the corresponding stress (σ) in the two phases are equal:

$$\sigma = \varphi_f \sigma_f + (1 - \varphi_f) \sigma_a, \quad \sigma_f = \sigma_a = \sigma \quad (2.5)$$

So, the total strain (ϵ) will be:

$$\epsilon = \varphi_f \epsilon_f + (1 - \varphi_f) \epsilon_a \quad (2.6)$$

Where, ϵ_f and ϵ_a is strain in the frozen and active phase respectively. The further equations are obtained from the detailed derivations and assumptions made by Liu et al [43]. The strain storage during cooling depends on some variables ($\epsilon, \epsilon_s, T, \varphi_f$). The stored strain as a function of temperature, $\epsilon_s(T)$, describes the strain storage during cooling and it is a reversible process to release the strain during heating by decreasing the φ_f . ϵ_s is the internal variable and assumed to depend only on temperature and not affected by the current strain or stress during heating:

$$\epsilon_s = \epsilon_s(T). \quad (2.7)$$

The change of frozen fraction φ_f controls the strain releasing and storage. It is assumed that the rate of heating/cooling is constant and φ_f depends only on temperature and to characterize this, free strain recovery of a specimen is used. φ_f is the ratio of ϵ_s to ϵ_{pre} . The

retained uniaxial strain during recovery step is measured in the free strain recovery test and this corresponding to the change of stored strain (ϵ_s). If the thermal expansion does not affected by the initial strain, then the thermal strain can be subtracted from the total strain ϵ , and get a modified recovery strain ϵ^* . Thus, ratio of $\frac{\epsilon^*}{\epsilon_{\text{def}}}$ provides the φ_f as a function of temperature. A phenomenological function of T with variables, C_f and n is proposed and which can be obtained by fitting the strain ratio data, $\frac{\epsilon^*}{\epsilon_{\text{def}}}$:

$$\varphi_f(T) = 1 - \frac{1}{1 + C_f(T_h - T)^n} = \frac{\epsilon_s}{\epsilon_{\text{def}}} \quad (2.8)$$

The Young's modulus, E of the polymer is given as:

$$E(T) = \frac{1}{\frac{\varphi_f}{E_i} + \frac{1 - \varphi_f}{E_e}} \quad (2.9)$$

Where, E_i = modulus related to internal energetic deformation, E_e = modulus related to entropic deformation. Herein, E_i is considered as constant in the range of temperature. According to the rubber elasticity, the stress is a non-linear function upon large deformation range and it is linear stress function with smaller deformation ($\sim 10\%$), and E_e is a linear function of absolute temperature and becomes zero at 0 K:

$$E_i = \text{constant}, \quad E_e = 3NkT \quad (2.10)$$

Where, N is the cross-link density, k = Boltzmann's constant ($k = 1.38 \times 10^{-23}$ N m/K). The frozen fraction is depending on the temperature, Eq. (2.29). If the Young's modulus (E), at low (T_l) and high (T_h) temperature boundaries are known, then E_i , E_e , and E as a function of temperature can be obtained. The value of N can be calculated from the Eq. (2.10).

Wang et al. [44] used these equations to predict the recovery stress in a compression type programming and formulated its components including residual stress, memory stress, relaxed stress, and thermal stress (Figure 2.18a). However, the pure memory stress cannot be seen and predicted using their method and it can be observed that the recovery stress

does not remain stable but decreases over time (Figure 2.18b) [44] due to impure memory stress.

$$\sigma_r = \sigma_{\text{residual}} + \sigma_{\text{memorized}} + \sigma_{\text{thermal}} - \sigma_{\text{relaxed}} \quad (2.11)$$

Where, σ_r is recovery stress; σ_{residual} is the residual stress from the programming (i.e. elasticity); $\sigma_{\text{memorized}}$ is the memorized stress that can be achieved by firstly allowing free shape recovery of the specimen, and then pushing the specimen back to its constraint length. The stress produced by the external pushing load is equal to memorized stress; σ_{thermal} is the thermal stress it is due to thermal expansion of the specimen under high temperature. In fully constrained boundary condition, free expansion is not allowed and results in thermal stress; σ_{relaxed} is the relaxed stress due to stress relaxation effect under constrained condition.

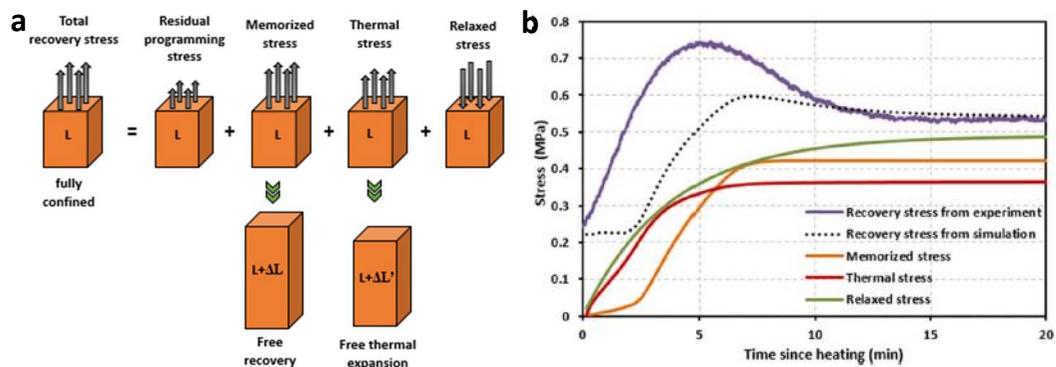


Figure 2.18: (a) A schematic representation of the decomposition for the recovery stress of compression programmed SMP. (b) Simulation results showing all the components [44].

Thermal stress could be positive or negative depending on the type of programming. It may reduce (in stretch programming) or increase (in compression programming) the recovery stress (Figure 2.19). It has been stated that, the total stress components are basically two types; contributive and impeditive parts. For compression programming, the contributive

part includes the memorized stress and thermal stress; and impeditive part consists of relaxed stress. For tensile stretch programming, memorized stress is contributive and relaxed stress is impeditive part.

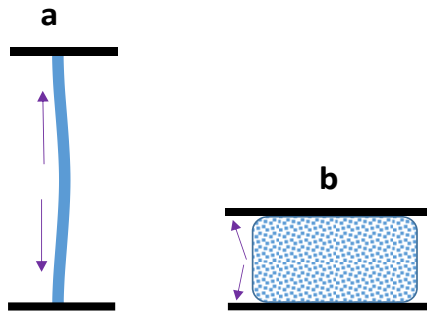


Figure 2.19: Effect of thermal stress. (a) Tensile stretch programming (negative). (b) Compression programming (positive).

In further to equations from Liu et al work, they have proposed below relations to predict the memorized stress and thermal stress.

$$\sigma_m = E(T) \cdot \varepsilon_r \cdot (1 - \varphi_f) \quad (2.12)$$

$$\sigma_t = \int_{T_l}^{T_h} E(T) \alpha(T) dT \quad (2.13)$$

Where, $\alpha(T)$ represents the thermal expansion coefficient of the specimen and T_l is the temperature used for cooling.

However, they have used the peak stress obtained during programming of specimen to calculate the modulus value for the prediction of stress components. Hence, the prediction of the recovery stress is not so well in agreement with the experimental data (Figure 2.20b). Also, the response of the recovery stress is not stable over time and the reason could be ascribed to presence of impure memory stress and viscous stress. A significant approach is very much necessary to eliminate the impeditive parts completely in order to get a pure memory stress which is to be used for a prolonged period of time needing for certain applications.

2.7. Compression Therapy and Its Management

2.7.1. Introduction

Chronic leg ulcer is defined as a defect in the skin below the level of knee persisting more than six weeks and shows no tendency to heal after three or more months. Gravity is the main reason why the chronic venous ulcer and related problems occur in the lower extremity of human body. Chronic ulceration induces a significant burden in terms of health and economy due to its higher rate of prevalence and chances of reoccurrence. It has been estimated that 2% of the general population in the world (age group: 18 to 64) is suffering from chronic venous ulcers [74, 117, 118]. This rate is further increased to 4% in people over the age of 65. Annually 0.6 million people are affected by lower extremity chronic ulcers in the United States. It has also been evaluated that 1 in 20 adults are prone to get attacked by venous ulceration in almost westernized countries [118]. This has significant socioeconomic impact, costing 1% of total health care budgets in developed countries, for example in the USA, this costs \$2.5 to 5 billion to treat 6 million patients every year [74, 117-119]. Both the incidence and cost are bound to increase in future due to changing lifestyle and growing aging population. It is expected that the intervention cost may escalate up to 71 million by 2030 year [118]. Thus, there is a huge market in compression products for improving life quality of world population.

Compression therapy is a corner stone in the conservative treatment of phlebological and lymphatic diseases such as varicose veins, venous leg ulceration, venous hypertension, venous oedema, venous stasis, deep vein thrombosis (DVTs), and other chronic venous disorders [60, 120]. The main principle of compression therapy is to apply the certain level of pressure around the affected tissue area on the limb to reduce the venous hypertension. This also helps to reduce the size of swollen limb, to keep the pressure gradient from “toe

to knee”, and improves the venous fluid return to heart. Compression therapy is in practice with usage of products such as compression bandages (elastic/inelastic), compression stockings, self-adjustable Velcro devices, and intermittent pneumatic compression (IPC) systems along with the stockings [56]. These products help to provide a graduated compression (pressure gradient) on the affected limb from toe to knee and ensure to return of venous to the heart. Graduated compression stockings [121] in combination with the IPC device is normally used to avoid the DVTs (Deep vein thrombosis) in immobile patients having limited calf muscle function, hospitalized for a prolonged period of time [122]. IPCs [123] and warming therapy [59] is also recommended to use in conjunction with the conventional products to improve the blood circulation and oxygen level around the affected area.

2.7.2. Cardiovascular system and anatomy of veins in human body

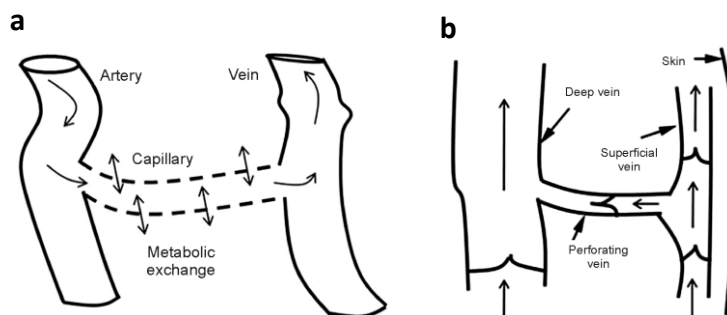


Figure 2.20: Venous system. (a) Schematic Illustration of fluid transport through venous system. (b) Venous return to heart through veins.

Human cardiovascular system is a closed blood circulatory system, in which the blood flows only in one direction. They are made of three type of blood vessels namely, arteries, veins, and capillaries around central organ called the heart. This central organ acts as a powerful pump to propel the fresh blood rich with nutrients to various tissues via arteries continuously. The impure blood with waste products returns to heart via unidirectional

venous system [124]. The oxygen, carbon dioxide, and other metabolite exchanges are take place through microscopic capillaries which acts as a bridge between arteries and veins (Figure 2.20a). The venous return depends on the pressure being developed in the veins [125, 126].

Basically, venous system is composed of deep veins, superficial veins, perforating veins and other complex network of veins to perform the venous return together. Deep veins are located at the central axis of the leg and surrounded by muscle and aponeurosis represents 90% of the total venous system. Superficial veins are the second largest network and located in the subcutaneous adipose layer, between the wall of skin and aponeurosis encasing muscles. These deep and superficial veins are connected together by perforated veins. It is very interesting that venous systems are embedded with venous valves which prevent the back flow of venous fluid during the transportation to the heart (Figure 2.20b). The efficacy of venous blood return to heart is largely dependent on the pressure inside the venous valves. The venous pressure is equal to the hydrostatic pressure produced by the height of the column of the blood between the right atrium and the measurement point at the ankle during sitting or standing position. In general, venous pressure is affected by gravity, body position, and limb movement. It ranges from 6.7 to 13.3 kPa (1 mmHg = 0.133 Pa); high pressure of 12 kPa in standing position, low pressure ranging from 0 to 1.3 kPa at supine position, and increase in pressure to 5.3 kPa during sitting position.

Gravity plays an opposite role in return of venous blood with pressure developed by the pumping system. Veins are passive and the pressure is just right to lift towards the heart but it relies on extra pressure and which is enhanced by the pumping systems namely, muscle pump, the distal calf (piston) pump, and the foot pump. Veins are made of thin muscle and elastic in nature. During walking, contraction of the muscles expels the blood into proximal collecting veins. The blood is drained from the superficial veins into the deep

veins during the relaxation of muscles or muscle pumps i.e. refilling the venous blood to subsequent ejection to heart. Upon dorsiflexion of the ankle, the calf muscle descends within the common fascia sheath and expels the blood in veins like a pump [60, 125]. Upon weight bearing on the foot, the veins are stretched and help to eject the venous blood. During pumping the venous blood forward, the valves get open and closed to prevent the back flow and it is termed as “reflux”.

2.7.3. Chronic Venous Deficiency (CVD)

Chronic venous deficiency is characterized by the delayed and disturbed return of venous blood to the heart. Chronic wounds probably occur due to poor cardiovascular system functioning in human body. The reasons ascribed to CVD could be improper foot or calf muscle pumping, aging of deep or superficial veins, limited mobility, and many other factors. Example of chronic wounds includes venous ulcers, leg ulcers, arterial ulcers, pressure ulcers and diabetic [60]. There are other numerous factors affecting CVD such as age, obesity and overweight, hereditary factors, limited mobility, working style, gender, deep vein thrombosis, exposure to heat, donning tight clothes, and diet.

Assessment of CVD: Excessive venous pressure or hypertension, dilation in vein’s diameter, and damaged vein wall leads to the development of varicose veins (Figure 2.21a). The main cause of leg oedema is due to malfunctioning of veins and incapable to push back the blood with excessive pressure leading to leakage into tissues (Figure 2.21b). Further progression of hypertension and pooling of blood within the surrounding muscle causes high pressure, lack of oxygen, food availability, and nutrients. Gradually deterioration of skin occurs and leads to leg ulceration (Figure 2.21c). The following symptoms for varicose veins: leg swelling, skin change, scaling, open sores; venous oedema: swelling at affected region; venous leg ulcers: itching, pain, swelling, hardened skin may occur. The

implications of CVD include, patients may experience a low quality of life (QOL) caused by continuous pain, clinical depression, discomfort, limited mobility, anxiety, social isolation, and economical burden due to expensive intervention [127-130].



Figure 2.21: Major symptoms of CVD. (a) Varicose veins. (b) Venous oedema. (c) Venous leg ulcers [131,132].

It is imperative that understanding the pathophysiology of chronic wounds improve the quality of patients unless knowing the underpinning root cause of the ulceration [131, 132]. For the benefit of an effective compression treatment, a meaningful and objective vascular assessment is mandatory [133-135]. There are few methods to rectify the actual source for the ulceration such as general assessment, physiological assessment, vascular assessment, routine investigations, and ulcer assessment. In order to know the actual arterial status of the affected limb, patients are screened for the Doppler Ultrasound and ABPI (ankle brachial pressure index) to be monitored; (ABPI = highest pressure at ankle / highest brachial pressure). For the precision diagnosis of venous problems, CEAP (Clinical-Etiology-Anatomy-Pathophysiology) classification was developed by an ad hoc committee of the American Venous Forum in 1994 [136]. This was adopted worldwide and being as the benchmark to provide the basis for scientific analysis of CVD. The CEAP classification [137, 138] is given below.

Table 2.3: The CEAP classification

C₀: No visible or palpable signs of venous disease	C₄: Changes in skin and subcutaneous tissue secondary to CVD
C₁: Reticular veins	C₅: Healed venous ulcer
C₂: Varicose veins	C₆: Active venous ulcer
C₃: Edema due to etiology	

2.7.4. What choices of material do we have for compression?

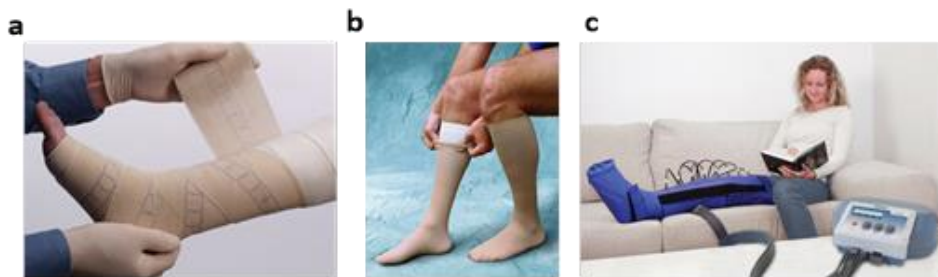


Figure 2.22: Current methods of compression therapy. (a) Bandages. (b) Stockings. (c) Intermittent pneumatic compression devices (IPCs) [121,139].

Compression therapy is the cornerstone in the treatment of lymphatic and chronic diseases. In general, compression is provided in the form of bandages or compression stockings (Figure 2.22a,b). For leg ulcers those do not respond well to these modalities, pneumatic compression devices or stockings in conjunction to this are used [121, 139]. Bandages and stockings deliver the compression in static and gradient manner from toe to knee. IPC devices are used to provide dynamic compression or massage effect (Figure 2.22c). Partsch [56] has recently reviewed the current modalities available for compression therapy and they are bandages, stockings, self-adjustable velcro devices [140, 141], compression pumps, and hybrid pump devices. Farah et al.[142] have comprehensively compiled the different modalities and treatment updates for leg ulcerations.

2.7.4.1. *Compression bandages*

Bandages are classified based upon their extensibility. Plaster/semi-rigid bandages are inelastic and provides pressure upon opposing the increase in leg volume [143, 144]. These bandages do not provide compression at rest due to inactive calf muscle and difficult to put on [145]. Short stretch bandages loose their pressure more than 50% within few hours and difficult to control externally. The pressure exerted by the elastic bandages is lesser than the inelastic bandages. Four layer or multilayer bandage system is complex to put on and also results in pressure loss over time. Both elastic and inelastic bandaging systems have been shown to be effective in achieving the ulcer healing rates of 40 to 70% in three months. However, there is no any evidence to prove that one type is better than other bandage type in healing the disease [55, 144]. All compression bandages are required to apply by the clinical therapist or personnel and success is largely depending on their skill.

2.7.4.2. *Compression stockings*

Compression stockings are considered as gold standard for the treatment of leg ulceration compared to bulky, non-compliance based bandages [146]. Compression stocking is preferred for low pressure range (< 50 mmHg), and allows easy application compared to multi-layer bandages which needs trained healthcare practitioners for wrapping [146]. Pressure can be achieved both in active and rest condition of a patient. As the stockings are made of textile knitted structures, gradient pressure can be achieved by tailoring the structure. Several factors such as amount of compression, type of knit structure, length can vary between stocking types.

Table 2.4: Compression-stocking class definitions (U.S. & European)

Class: Clinical Uses <i>(Class system is not used in U.S.)</i>	Pressure (mmHg)			
	UK	Germany	European	U.S.
A: Light compression	-	-	10-14	8-15
I: Minor varicose veins, functional venous insufficiency, mild oedema	14-17	18-21	15-21	16-20
II: Slight chronic venous insufficiency, mild/moderate oedema, surgery	18-24	25-32	25-32	20-30
III: Advanced chronic venous insufficiency, leg ulcers, severe oedema	25-35	34-46	34-46	30-40
IV: Very severe chronic venous insufficiency, very severe oedema	-	49-56	49-56	40-50

Basically, stockings are classified based on the degree of compression pressure and this varies between countries due to inconsistencies among testing devices (i.e. Instron, U.S., HATRA, British, and Hohenstein, European/German).

Hegarty et al. [147] have shown, different class of stockings will exert various pressure levels and it is a barrier for those are with different leg sizes. The difficulty for physicians is to prescribe the right stockings for desired pressure, due to standards varies from country to country. Stiffness of the stockings also plays an important role in increasing the pressure due to muscle activity compared to less stiffer stockings [148]. In addition, also it has been shown that using compression stockings (type II and III) improved the CFR (capillary filtration rate) than no compression (e.g. type I). Compression stockings shows several

advantages over bandages such as patients can easily put on or take off, they can maintain pressure level for longer time in contrast [145, 149]. Further to this, stockings may need to be taken off during night time if the pressure exerts more than 30 mmHg, skin allergies may cause due to this [150].

2.7.4.3. Intermittent pneumatic compression (IPC) devices

In general, IPC devices may be used for leg ulcers those do not respond well with the bandages or stockings. Also noncompliant patients due to less usage time of this device[151]. Basically an IPC device consists of air bladders that inflates and deflates periodically. Single chamber can be used for a uniform compression or a multiple chambers to achieve gradient pressure at different regions of the leg [58]. Studies based on intermittent compression systems have been reported that, when these IPCs used in place of bandages or stockings in terms of ulcer healing rate, no significant difference was found. It is unclear whether to use instead of bandages/stockings [123]. Also it has been revealed that apart from no significant difference, patients comfortability was improved [152]. Kakkos et al. [153] have hypothesized that venous stasis may occur during IPC usage due to deflation period of air filled chambers. Kendall healthcare has created an IPC that can detect changes in venous volume. If the leg volume changes, the bladder pressure also changes accordingly. Another custom sensors based IPC product developed by Hegarty et al. [154], can detect the changes in the leg volume, but not sensitive enough to measure blood flow velocity. The major hurdle to use these systems is patient needs to be immobile for several hours, bulky, noisy, and expensive [58, 147].

2.7.5. Studies on interfacial pressure of bandages/stockings

There has been a continuous effort to study pressure generated in the interface between the compression device and skin. Kumar et al. have identified and examined several

influencing parameters on the interface pressure performance including bandage characteristics, limb geometry, application technique and physical activity [60]. They proposed a simple experimental technique to evaluate time-dependent performance of the bandage using fabric parameters, and modeled the pressure loss over time using stress relaxation parameters [61, 62]. They designed a prototype to examine the dynamic pressure variation of different bandages [63], and characterized the bandage performance during movement or exercise of the limb without doing in-vivo pressure measurement [64]. They also studied different fibrous material and fabric structure on the pressure performance and found that the pressure drop is more for non-elastomeric polymers (cotton, viscose, PET, nylon, etc.; > 30% relaxation), as compared to elastomeric samples (polyurethane; < 10% relaxation) [65, 66]. In addition to study on bandage performance, they have also examined the comfort and compression properties of padding primarily used as sub-bandage layer in multi-layer compression system [67, 68]. Kumar et al. have utilized the SMPU filaments to make the circular knitted stockings in conjunction with nylon. It is shown that the pressure sustenance using SMPU filaments is very good and the pressure can be modulated externally by means of simple heating unlike replacement of conventional ones [155, 156]. The pressure study allows evaluating a compression device performance which is instrumental for designing custom-made compression garments to deliver a specific pressure [157]. Modeling approaches include the application of Laplace's law in determining the amount of pressure generated at the interface that depends primarily on the fabric tension and limb radius [158]. Graduated compression stockings are normally used for ensuring the positive blood flow from ankle up to heart [56]. For effective treatments, different classes of stockings are provided for light (14-17 mmHg), medium (18-24 mmHg) and strong (25-35 mmHg) levels of compression depending on the severity of the disease [146].

2.7.5.1. *Dynamic compression study*

The magnitude of pressure, inflation/deflation cycle times and total treatment time of the pneumatic compression devices (PCDs) is found to be critical [58]. A pressure dose of 40-50 mmHg has been found efficient in limb volumetric reduction (69 ml) and also comfortable to patients. Although a high pressure (60 mmHg) results in more volumetric reduction (100 ml), it is reported to cause pain and discomfort in treatment [159]. Results suggested that significant reduction in edema occurs irrespective of cyclic times (30-180s) (Figure 2.23) [58], however an inflation time of over 50s is recommended to generate effective tissue fluid pressures and provide enough time for creating tissue fluid flow [160].

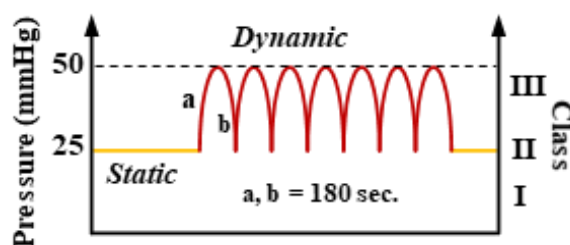


Figure 2.23: Dynamic compression profile

2.7.6. **Role of textiles in compression stockings**

Revolutionary Path of Medical Compression Stockings: In 1948, William Brown from England was the first man who was able to manufacture a stocking out of rubber threads. These stockings were uncomfortable to wear due to direct contact of rubber threads to skin surface. The actual use of medical compression stockings (MECS) were started in reality after the invention of Jonathan Spark, who developed rubber threads covered with cotton (core spun yarn). With a progressive development, ultrafine latex threads were started to use since 1960. Stockings were started to develop elastic yarns as inlay yarns and this was accepted by German standard and was not accepted by British standard. However, there

were good indications of comfort and durability. MECS were produced using following 3 types of methods.

1. *Double faced flatbed knitted with inlay yarns*: In this case, the form of the stockings was achieved by varying the number of needles on the flatbed knitting machines.
2. *Single faced, circular knitted MECS*: In this case, seamless circular stockings were knitted with inlaid and knitted elastic yarns. The only possibility of changing the form of the stockings is by varying the tightness of the courses and the tension of knitted yarns.
3. *Single or double faced knitted without inlay yarns*: This is similar to other two cases but only difference is knitted structure was without inlaid yarns.

Because of the different leg circumferences, flat bed knitting method was using to make customized MECS due to precision of maintaining the size of stockings up to 0.5 cm by varying the number of needles in each course. Whereas using circular knitting, the only possibility is to change the tension of input yarns to suit the form of stockings [145].

The most common materials for compression therapy are textiles. Different textile fibers (nylon, PET, cotton, elastane, etc.) and fabric structural characteristics have significant effects on the pressure distributions on the skin by a compression stocking [161]. Liu et al. have developed graduated compression stockings (ankle to thigh) using plain weft knitted fabric structures. Three fundamental stitches say plain, tuck, and miss stitches were employed in different patterns to study the effects of material properties on skin pressure. The resultant stockings were having pressure levels of light, mild, moderate, and strong. Tensile and shearing properties have significantly influenced the pressure performance [161]. Incorporating more elastomeric content and creating tighter construction helps to provide a more homogeneous pressure distribution and sustenance during the course of treatment [162].

Onkaraiah, P. [163] has attempted to integrate the SMPU filaments into stockings made of Nylon as a ground structure. 4 floats and 1 tuck pattern is used to imitate the inlay structure (Figure 2.24). She had attached the fabric piece made of SMPU filaments at ankle and bow region of the commercial stockings to compare the pressure magnitude at ankle and pressure along the leg on human subjects. The results indicated that circumferential pressure variation, wrinkling at the ankle bow in stockings was lesser compared to commercial ones.



Figure 2.24: Stocking made of SMPU. (a) Fabric structure. (b) SMP fabric attached to commercial stocking [163].

Chattopadhyay et al. have studied the effect of linear density of inlay yarns and input yarn (spandex) tension to optimize stocking structure for the pressure generation (Figure 2.25) [164, 165].

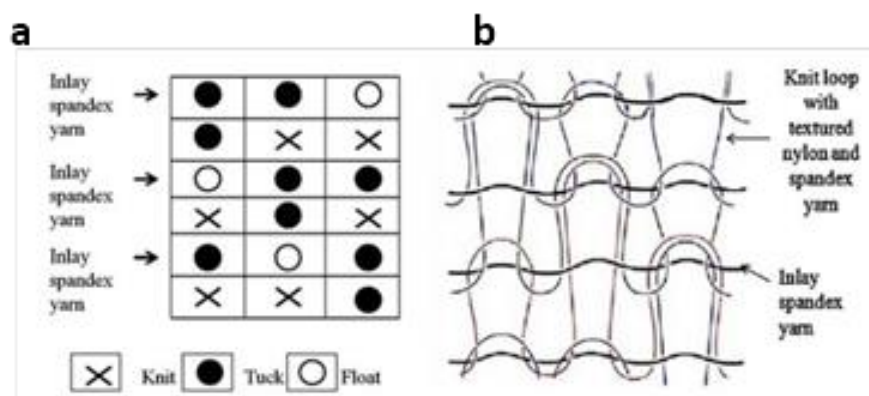


Figure 2.25: Stocking structure. (a) Notation diagram. (b) Schematic diagram of the structure [164, 165].

However, this structure is *not actual inlay* structure according to the notation diagram shown above. They have shown that, the tension development in the fabric in course wise direction was dependent on the inlay yarn properties. Increased linear density was resulted in increase in tension. Dias et al., [166] have invented customized production of pressure garments quickly and accurately by defining the shape characteristics of the body extremity and specifying knitting pattern. Such garments have the problem of loosening their elasticity due to continuous wear with *no extra benefits of massaging* for elderly or inactive patients.

2.7.7. Research on stress in MPs, modeling, and application in compression stocking

Most existing studies on stress in MPs are related to shape recovery, namely, the force required to recover a fixed shape when tested under a constrained strain [108, 109]. In these publications, stress memory was not a real concern and may be considered obliquely to have been measured as the recovery stress. Using this recovery stress, Ahmad et al [50] attempted to make compression-related applications which underwent a significant stress reduction over time (>50%). It has been well discussed in the Chapter 1 (Introduction).

Kumar et al. [167] have developed the stocking with blend yarns consists of Nylon and SMPU and studied relationship of pressure with the temperature. They have developed a model based on the rubber elasticity theory to predict the change in pressure of stockings as a function of temperature. The experimental results have proven that extra pressure of up to 50% can be modulated in stockings in a wrapped condition with change in temperature (Figure 2.26d). Following are the equations proposed to determine the interfacial pressure of a stocking.

$$\Delta\sigma = b\Delta T \quad (2.14)$$

$$\Delta P = \frac{w\Delta\sigma}{r} = \frac{wb\Delta T}{r} \quad (2.15)$$

Where, σ is the stress, b is constant, T is temperature, P is pressure, r is radius of leg, and w is the thickness of the stocking.

Once the stocking is applied on the leg, for a given radius i.e. strain (b), corresponding stress σ will be generated hence the P will be applied on the leg: the system is in equilibrium. If a stress dropping $\Delta\sigma$ occurs and to compensate that, temperature can be increased ΔT accordingly. By using the relationship in Eq. 9, material selection can be easily done to get the right pressure in the stocking.

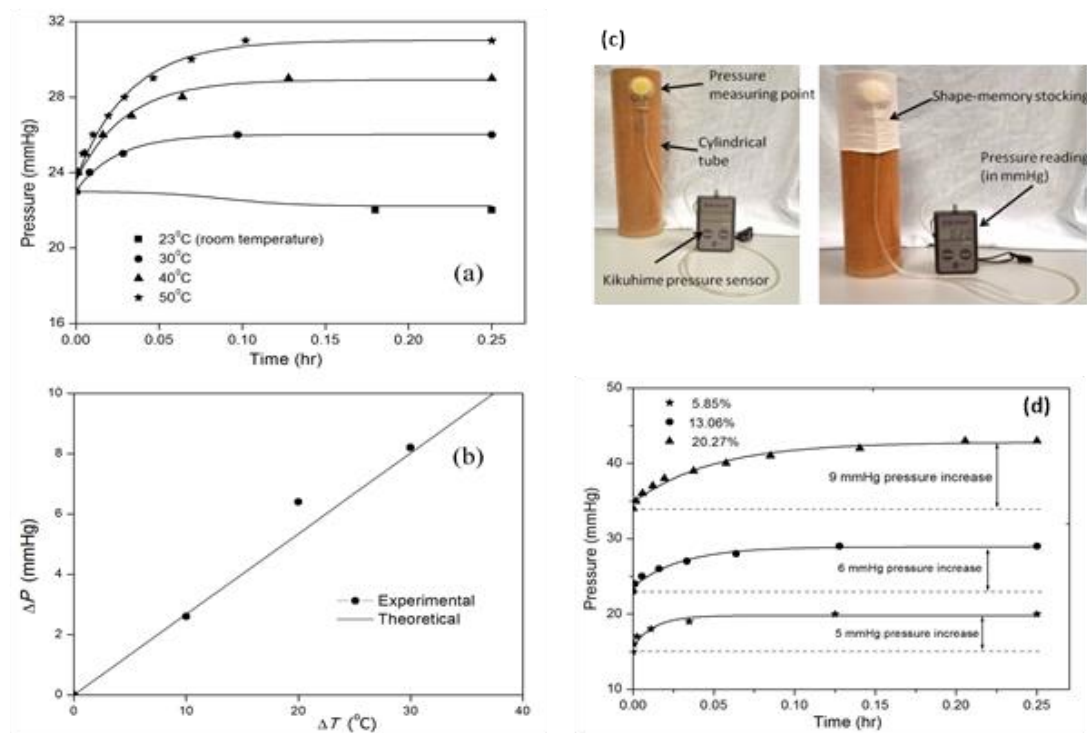


Figure 2.26: Experimental and theoretical prediction results. (a) Pressure variation at different temperature level. (b) comparison with theoretical prediction. (c) Pressure measurement set up. (d) Pressure variation at different level of strains ($T=40^{\circ}\text{C}$). [167]

However, the pressure gets stabilized over time with initial reduction in the pressure and the reason due to presence of Nylon filament in the stocking structure and its stress relaxation.

In this project, based on the literature gap, a novel stress-memory behavior in the semi-crystalline polyurethane has been discovered and scientifically utilized the potential to implement towards designing the smart compression stockings for advanced compression therapy.

CHAPTER 3: EXPERIMENTAL WORK

Highlights

This chapter is mainly focused on comprehensively describing the experimental materials, methodologies followed, and characterization techniques involved in the entire research work completed. The experimental work is divided and explained as: 1) discovery of stress-memory phenomenon in thermal responsive semi-crystalline memory polymeric material (film), 2) constituent analysis of stress-memory in semi-crystalline polymeric material (film), 3) revelation of stress-memory behavior in memory polymeric filaments/fibers, 4) optimization of stress-memory filaments/fibers integrative textile fabric structures for compression stockings, and its performance evaluation by pressure related study and Ultrasound blood flow measurement.

3.1. Materials and Equipment Utilized

The raw materials used for this research project and equipment for characterization/testing are summarized and tabulated in the Table 3.1. and Table 3.2 respectively.

Table 3.1: Raw materials/chemicals used in the research project

Raw Material / Chemicals	Abbreviations / Notes	Supplier
Poly(ϵ -caprolactone) diol	PCL, ($M_n = 4000 \text{ g.mol}^{-1}$)	Daicel Chemical Industries Ltd., Japan
Poly(1,6-hexamethylene adipate) diol	PHA ($M_n = 3000 \text{ g.mol}^{-1}$)	UBE industries, Japan
4,4'-methylenediphenyl diisocyanate	MDI	Aldrich Chemical Company, USA
1,4-butanediol	BDO	Acros Organics
N,N'-dimethylformamide	DMF (HPLC Grade)	Aldrich Chemical Company, USA

Table 3.2: Major equipment used in the research project

Equipment Name/Abbreviation	Supplier
Instron-5566 (with heating chamber)	Instron Corporation, USA
Melt Spinning Machine	Sichuan University, China
Differential Scanning Calorimetry/DSC	Perkin-Elmer Inc. USA
Fourier Transform Infrared Spectroscopy-2000/FT-IR	Perkin-Elmer Inc. USA
X-ray Diffractometer/XRD	Rigaku SmartLab, Japan

Dynamic Mechanical Analyser/DMA	Perkin-Elmer Inc. USA
Vacuum Oven	Sheldon Manufacturing, Inc.
Circular Knitting Machine (Model: CC4-MED)	MERZ, Germany
Kikuhime ^{TR} Compression Pressure Sensor	MediGROUP, Australia
Doppler Ultrasound	Esaote MyLab TM Six, Genoa, Italy
Leica Classic Stereomicroscopy (Model: M165C)	Leica Microsystems

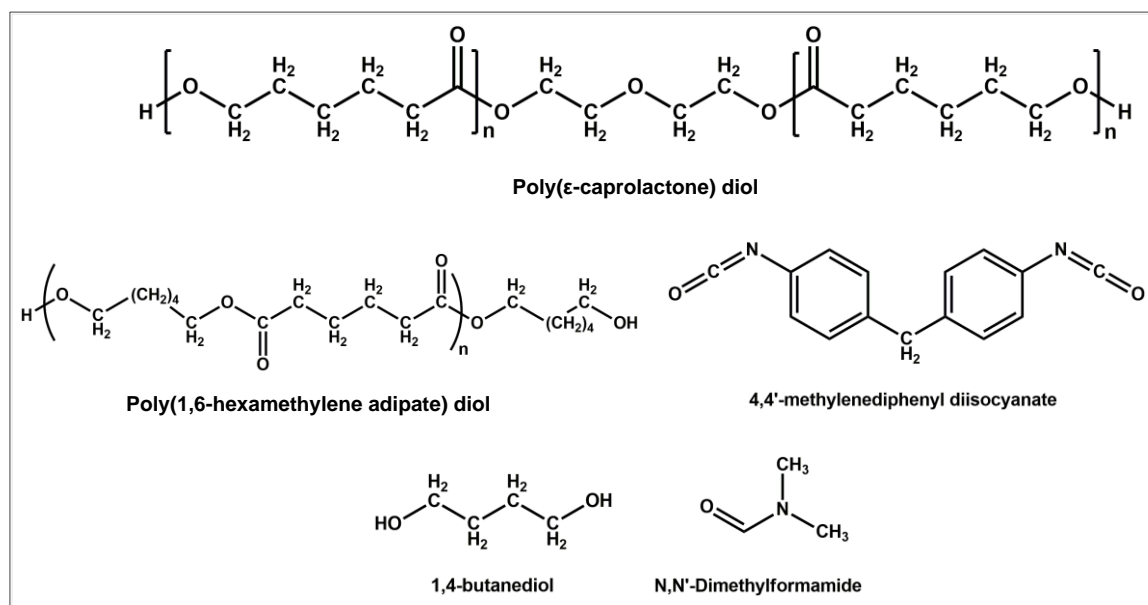


Figure 3.1: Chemical structures of the raw materials

3.2. Preparation of Stress-Memory Polymer, Filaments/Fibers, and Fabrics

3.2.1. Synthesis of semi-crystalline memory polymer (MP)

The synthesis of semi-crystalline memory polymer has been carried out using two types of macroglycol (soft segment/reversible phase) to prepare two different memory polymers and the materials used for the hard segment (fixed phase) are same. The macroglycols are: 1) Poly(ϵ -caprolactone) diols of molecular weight of 4000 g.mol⁻¹ (hereafter called PCL-4000), and 2) Poly(1,6-hexamethylene adipate) diol having molecular weight of 3000 g.mol⁻¹ (here after called PHA-3000). 4,4'- methylenediphenyl diisocyanate (MDI), and chain extender 1,4-butanediol (BDO) are used as a fixed phase (hard-segments). All experimental glass apparatus was dried in an oven at 400°C for 8 hrs prior to synthesis. PCL-4000 / PHA-3000 were degassed at a temperature of 80 °C under pressure of 0.1–0.2 kPa for 12 h prior to be used. The MDI (pure-grade) was used for the synthesis without any additional process. BDO was treated by 4 Å molecular sieves to ensure no moisture content before the synthesis. Memory polymer was prepared by using the bulk pre-polymerization method where, PCL-4000 or PHA-3000 and MDI kept for reaction at 80 °C around two to three hours. After completing the step formation of pre-polymer, BDO was added as a chain extender and stirred using mechanical stirrer for 5 minutes to accomplish the reaction. The ratio (weighted ratio) of hard segment to (MDI+BDO) to soft segment was 28/72 for MP with PCL-4000 and 28.5/71.5 for MP with PHA-3000. All the reactions were performed under the nitrogen environment and the temperature of less than 90 °C was maintained. The synthesized pre-polymer was casted into a pre-heated (100 °C) polytetrafluoroethylene (PTFE) mould. The resultant polyurethane sheet with thickness ~3.0 mm was obtained. The pre-polymer mould was kept in the vacuum oven for a period

of 24 h at a temperature of 100 °C. The casted MP sheets were crushed and extruded using a single-screw extruder followed by pelletizer to get the chips for melt spinning as a raw material. MP chips was dried for 24 hrs at 100 °C under vacuum condition to ensure the moisture level to be less than 100 ppm (parts per million) [40].

3.2.2. Preparation of memory polymeric film

A solvent N,N'-dimethylformamide (DMF) was used for the MP film preparation. The DMF was initially dried using 4 Å molecular sieves. The MP chips were poured in the DMF and the mixture was stirred for 6 to 8 hrs using magnetic stirrer until the entire polymer chips got dissolved in the DMF solvent. The weighted ratio of MP chips and solvent was at 1:9. The MP film was obtained by casting the MP solution into a rectangular Teflon mold (size: 20 × 20 cm) and drying in an oven at 80 °C for 24h. To eliminate the thermal history and residual solvent, the film was further dried at 100 °C in a vacuum oven under 10 mmHg. The thickness of the films prepared was in the range of 0.4 to 0.5 mm. The film was cut into strips of 1 cm width for performing stress memory tests [40, 168].

3.2.3. Spinning of memory polymeric filaments (MPFs)

Polymeric molds were crushed and converted into pieces having smaller size. The crushed material was then used to get the polymer ribbon using single screw extruder having five different temperature zones (zone1:125 °C, zone 2: 180 °C, zone 3: 190 °C, zone 4: 192 °C, zone 5: 194 °C) and used as raw material for melt spinning (Sichuan University, Chengdu, China). Polymer chips were stored overnight in a vacuum oven at 60 °C temperature and pressure of 0.08 MPa to ensure moisture residual less than 100 ppm. The MPFs were spun by melt spinning method using a single screw extruder (20 mm) with protected nitrogen environment. The

temperature levels of 120 °C, 180 °C, 202 °C, 202 °C were maintained at first, second, third, and fourth zones respectively. Constant temperature of 202°C was controlled at different sections including the extruder head, spinning pack, melt pipe, and pump. The temperature of laminar air was 22 °C. The pressure level of 4.55 MPa at extruder head and 22 MPa at spin pack was controlled. The spinneret was composed of 18 holes each of 0.4 mm in diameter and the filter dimensions of the spinneret was 600 mazes/square inch. The speed of 475 mtrs/min at winder and 15 m/min at overfeed was maintained. The linear density of the obtained filament was 150 denier (Weight in grams of 9000 meters of length) [93, 169].

3.2.4. Preparation of stocking fabrics using memory polymeric filaments

All the stocking fabrics were produced on MERZ (Model number - CC4-MED) medical compression stocking weft knitting machine. The machine cylinder diameter was 4.75 inches with 360 needles and 24 gauge (24 needles/inch). The machine was anchored with 4 types of yarn input devices and each of 9 yarn feeders and 3 furnishers for elastic yarn feeding. As the MP filaments to be in a relaxed state, fleecy knit structure was used to insert as an inlay yarn (Figure 3.2).

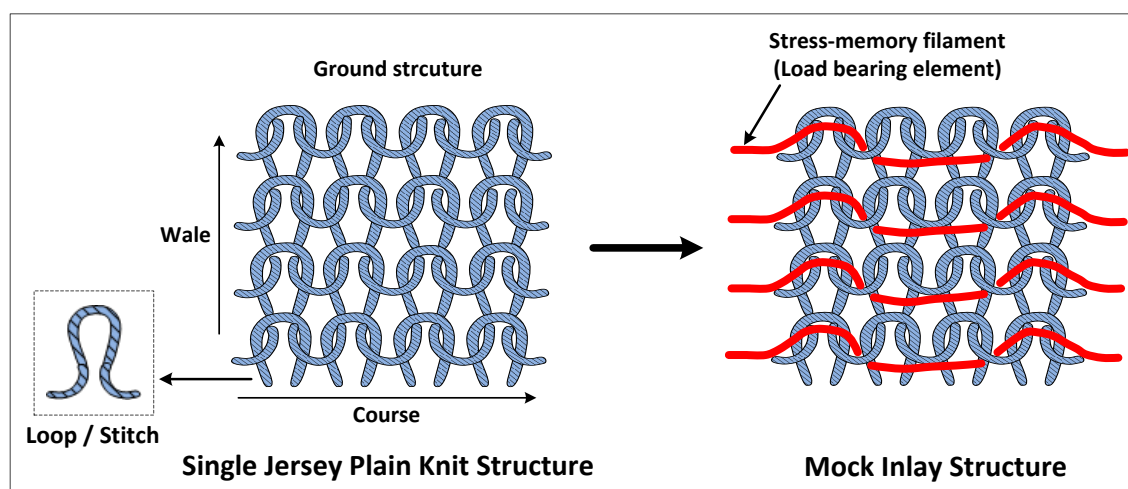


Figure 3.2: Scheme of stress memory filaments integration and structural details of the memory stocking.

The tension of 1 cN was maintained during the MP filament insertion. Single jersey simple plain knit structure was selected as a ground structure and Nylon of 70 denier (weight of 70 gms in 9000 meters of length) was used. The combination of knit, float, and tuck stitches were used to produce different patterns as shown in Figure 3.2 (Terminologies, Section: 3.2.4.1). Two different stitch lengths were chosen for knitting; 3.8 mm and 2.5 mm. The minimum float length is 2 and maximum is 5. Also, two series of fabric structures were made; A and B series. A series represents the structure with different float length in only MP filaments, whereas B series represents floats in both MP filaments and Nylon filaments in the ground structure. A schematic and notation diagram of designed knit structures are depicted in Figure 3.3. The as produced fabric samples were in the tubular form.

3.2.4.1. Terminologies

Knitted structure: Knitted structures are progressively made from the yarns row after row of intermeshed loops. The feeding yarn (Nylon or SMPFs) is converted into loops by the action of hook in needles. A good example of plain knitted structure is ‘single jersey’ fabric, in which the simple loops are knitted row by row. This is used in our study as a ground structure to insert the SMPFs as floats. Horizontal series of loops are called as wales and vertical series of loops are called as course [170].

Stitch density: Stitch density refers to the presence of number of loops in a measured area of knitted fabric such as square inch or square centimeters.

Stitch/loop length: The total length of the yarn consumed to make one loop in the knit structure is known as stitch length.

Float: The float stitch shows the missed yarn floating freely on the backside of the fabric of the knitted loops. It basically has the U-shape appearance as it can be noticed from Figure 3.1 and 3.2, where the red colored memory filaments is freely floating on the ground structure.

Tuck: The tuck stitch is produced when a new loop is inserted on the same needle (or loop). Example as it can be seen from the Figure 3.1, the red colored memory filaments is inserted on the ground Nylon loop and then formed the float stitch and then again formed the tuck stitch. This usually represents the inverted U-shape appearance on the fabric.

3.2.4.2. Thermal recovery of memory fabric tubes

As the memory filament tends to fix upon deformation, it was stretched while going through the passage of knitting process. The as produced all six type of fabric structures were treated at 60 °C in an oven to recover their original shape from the temporary deformation. The circumference of all the memory fabric tubes was reduced after the recovery under temperature.

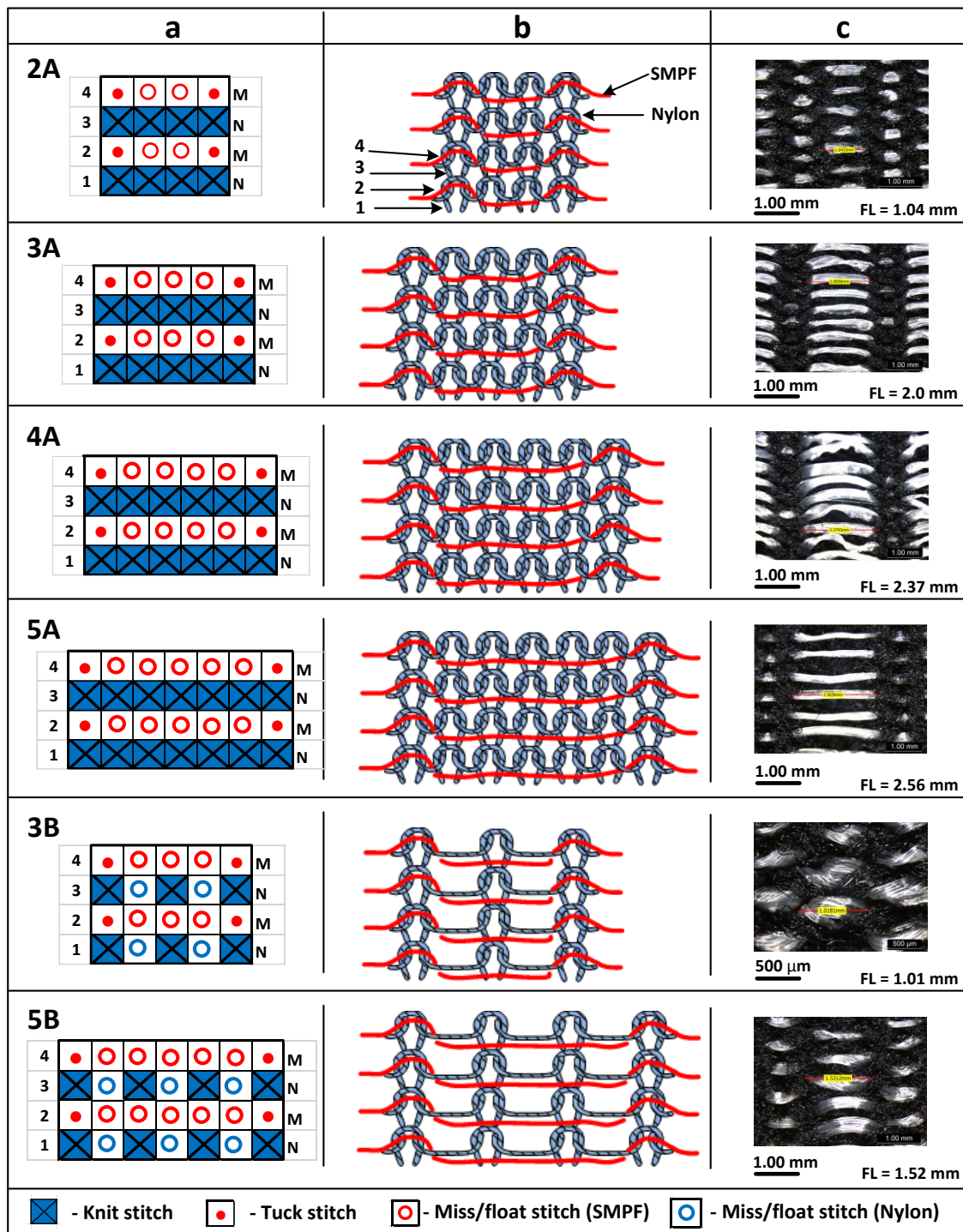


Figure 3.3: Scheme of memory fabric knit structures. a) Notation diagram, b) Schematic illustration of knit structures, c) Microscopic image of memory fabrics on technical back. M=Memory filament, N=Nylon filament, SMPF = Stress memory polymeric filament.

3.3. Characterization Techniques

3.3.1. Preconditioning for stress-memory polymeric material

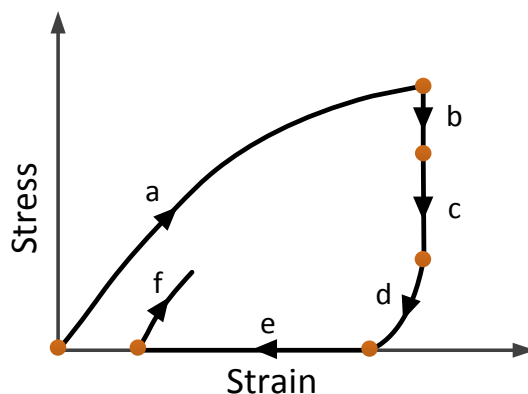


Figure 3.4: Stress-strain profile during a thermo-mechanical programming cycle. (a-f: different steps of the cycle)

Prior to the programming of the specimen, one of the measures to purify the memory stress in is to have preconditioning. The prepared MP film was taken as the specimen for beginning the preconditioning and then stress memory programming. Preconditioning is achieved by carrying out several thermo-mechanical conditioning cycles at a relatively higher strain level (100 %; more than initial strain (I.S)), used for stress-memory programming process). A thermo-mechanical preconditioning cycle (Figure 3.4) include the following steps:

Step a: Extending the specimen to 100% strain at a speed of $10 \text{ mm}\cdot\text{min}^{-1}$ at higher temperature ($T_{pc} = 60 \text{ }^\circ\text{C}; > T_{trans}$, T_{pc} : preconditioning temperature);

Step b: Holding the specimen under constraint for 30 min (Eliminating the viscous stress);

Step c: Cooling the specimen under constraint to lower temperature ($20 \text{ }^\circ\text{C}$), and holding it for next 30 min;

Step d: Relaxing of the internal stress to zero level by unloading the clamps;

Step e: Heating the specimen to $60 \text{ }^\circ\text{C}$ for strain recovery;

Step f: Begin of second cycle;

The specimen showed significant amount of plastic or irrecoverable strain (10-20%) at the end of first cycle. No plastic strain was observed after completion of 5 cycles, and the material is ready to emply for the next stage, i.e., programming. Pre-conditioning was carried out to avoid plasticity from the stress-memory polymeric network configuration so as to ensure its structural integrity over prolonged and repetitive use. Furthermore, preconditioning has to be performed at a relatively higher strain level, i.e., 100% (higher than I.S) so as to observe no elastic part remaining in subsequent programming and assured complete stress freezing in S_4 .

3.3.2. Stress-memory tensile programming test

Before conducting the stress memory test, specimens were programmed to freeze the memory stress in the polymeric network. Furthermore, this was also done to eliminate viscoelasticity from the polymer network. The testing machine was composed of a tensile tester (Instron 5566), for loading and unloading, anchored with temperature chamber for heating and cooling. The tensile load was measured using a load cell and the displacement of the gauge length was measured from the displacement of a cross-head. The specimen size was 80 mm in length and 10 mm in width. The specimen gauge length was 50 mm. The steps for a programming cycle (Figure 3.5a) are mentioned as:

Step 0: Heating the original relaxed specimen to higher temperature ($T_{Ph}=50\text{ }^{\circ}\text{C}$; $> T_{trans}$);

Step 1: Stretching the specimen to a particular strain level (hereafter called initial strain, I.S);

Step 2: Holding the specimen under constraint to relax the stress to a saturation level. This eliminates the viscous stress, i.e., step 2;

Step 4: Cooling the specimen under constraint to lower temperature ($T_{PI}=20\text{ }^{\circ}\text{C}; < T_{trans}$) for the charging/storing of the stress;

The I.S was chosen in the range of 10 to 80 %. The specimen was now ready to perform stress memory test without showing any plasticity, viscoelasticity and elasticity.

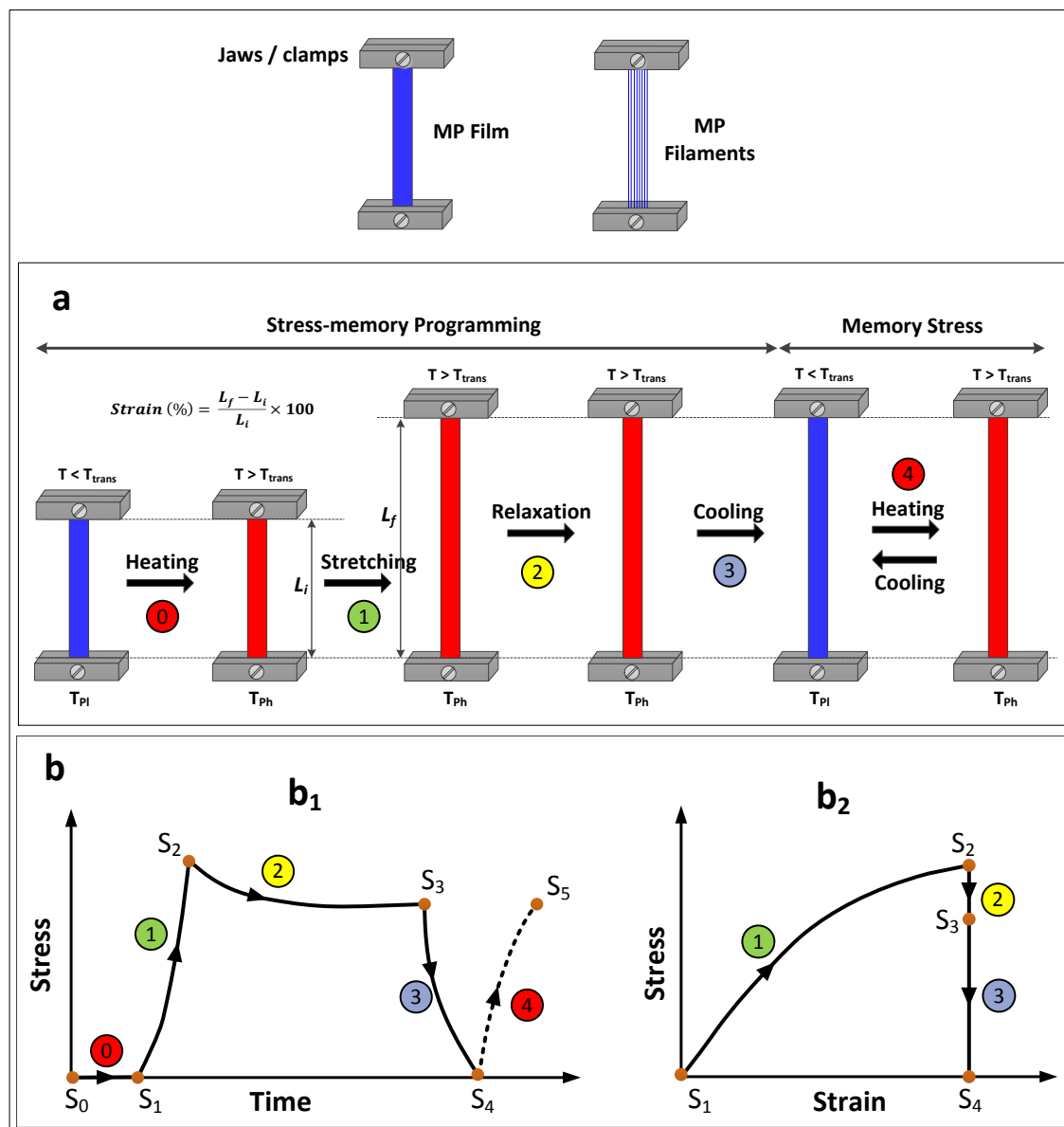


Figure 3.5: Scheme of stress memory programming. a) Representation of tensile programming. b) Profile of stress-time (b₁) and stress-strain (b₂) during programming. L_i :

Initial length; L_f : Final length; T: Temperature; T_{trans} : Transition temperature; T_{PI} :

Programming-low temperature; T_{Ph} : Programming-high temperature. ①: Total stress;

②: Viscous stress; ③: Memory stress. S_0 to S_5 : step zero to step 5.

3.3.3. Differential scanning calorimetry (DSC) analysis

In this project, the thermal property of memory polymeric film and filament test specimens was examined by Perkin-Elmer diamond differential scanning calorimeter (DSC) in a controlled nitrogen environment with an intracooler. The specimens were scanned from -50 °C to 150 °C at a scanning rate of 10 °C/min and kept in hold condition for 1 minute at -50 °C. This scanning process was repeated up to 3 cycles and the result of 2nd scan was considered to get the transition endothermic peak. In addition, stress-memory programmed film and filament specimens at different strain levels were also subjected for thermal scanning to determine the relative degree of crystallinity. The relative degree of crystallinity was calculated using the below formula.

$$\text{Crystallinity (\%)} = \frac{\Delta H_m - \Delta H_c}{\Delta H_m^\circ} \times 100 \quad (3.1)$$

Where, ΔH_m and ΔH_c refers to enthalpy of melting and cooling curves, and ΔH_m° is melting enthalpy of PHA soft segment.

3.3.4. Thermomechanical (TMA) analysis

The TMA analysis of the memory polymeric film specimen was carried out using Dynamic mechanical analyzer (DMA) in static mode to analyze the strain response of a stretched polymeric film under a constant load and it is known as creep behavior. Before testing, initially the polymeric film specimen was deformed and fixed under the room temperature. The deformed specimen was fixed between the jaws with a gauge length of 10 mm. A constant load of 1 mN was maintained to observe the response of strain as a function of temperature and time. The triggering of the specimen found in the range of melting transition of the specimen with a temperature ramp: 3 °C/min. The contraction strain of -5 mm was observed after the testing.

3.3.5. Characterization of memory polymeric film for constituent analysis

3.3.5.1. Stress and strain recovery test

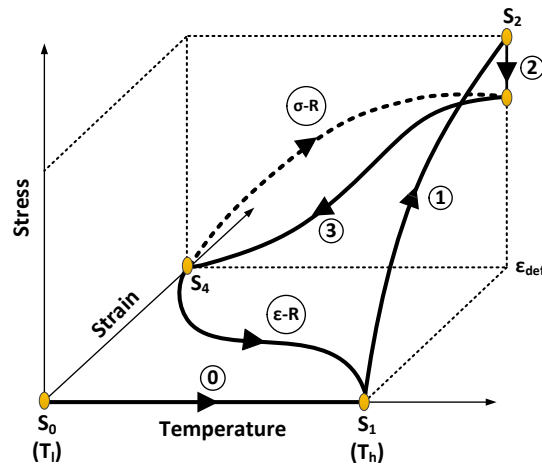


Figure 3.6: Schematic showing stress-strain-temperature profile during programming. T_l : low temperature; T_h : high temperature; σ - R : stress recovery; ε - R : strain recovery; ε_{def} : total deformation or initial strain.

The stress memory programming process was carried out using memory polymeric (MP) film specimen to store the programmed memory stress. Once the programmed stress is stored, the MP was discharged (heated) at high temperature under constraint (constant strain) to obtain the recovery stress (Figure 3.6; step σ - R). The temperature for discharging the stress was ranging from 20 to 60 °C. The specimen was held constant for 30 min to get the stabilized result at each temperature level. The programmed specimen was also subjected to strain recovery under no constraint (Figure 3.5; step ε - R). After the fixation of the employed strain (ε_{def}), the specimen was kept for free strain recovery in a heating chamber. The recovered strain (ε_r) was obtained at different temperature level ranging from 20 to 60 °C with an interval of 5 °C.

3.3.5.2. Measurement of initial and relaxed/memory modulus

During the stress memory programming process, the memory polymer undergoes stress relaxation if the applied deformation is held constant (Figure 3.4; step 2). This results in dissipation of viscous energy and finally a stabilized stress level is achieved. Figure 3.4b₁ shows the stress-time profile of stress relaxation during step 2. The initial modulus (IM) is the peak stress divided by the employed strain [44, 171], and the relaxed or memory modulus (RM) is obtained by dividing the saturated or relaxed stress with the strain. Both the initial and relaxed moduli were recorded at different strain levels. Also, the moduli were obtained at different temperature levels from 20 to 60 °C.

3.3.5.3. Measurement of thermal strain/stress of an unstretched MP film specimen

The length of the MP film specimen was measured at different temperatures from 20 to 60 °C under stress free condition. The measurement was done using Vernier caliper which has the least count of 0.001 cm. For the thermal stress, the MP film specimen was heated to higher temperature and then clamped to jaws of the Instron tensile tester. Thereafter, the temperature of the chamber was cooled down. Cooling results in the development of the retraction force due to inherent nature of thermal contraction of the clamped MP film. The thermal stress was collected at different temperature levels while cooling from 60 °C.

3.3.6. Fourier Transform Infrared (FTIR) spectroscopy analysis

In current project, IR characterization was carried out using Perkin Elmer model Spectrum 100, Fourier Transform Infrared (FTIR) spectrometer. Spectra for both MP film and MPFs were recorded in the range of 4000 to 500 cm^{-1} with a resolution of 4 cm^{-1} and a scan number of 4. In addition, Stress-memory programmed specimens at different strains were also subjected for scanning to record the spectra.

3.3.7. Wide angle X-ray diffraction (WAXD) analysis

Wide angle X-ray diffraction (WAXD) is basically used to get the diffraction patterns of crystalline or semi-crystalline polymeric materials when a beam of X-ray strikes the specimen. The scattering intensity is plotted as a function of the 2θ angle. The WAXD profiles of stress-memory programmed memory polymeric filament and film specimens were collected using Rigaku SmartLab X-ray diffractometer which was operated at 60 kV and 60 mA. The diffraction measurement was carried out in the 2θ angle range 10° to 40° at a rate of 0.02° /step. Stress-memory programmed and fixed specimens at different strain levels were used to get the diffraction peaks. The compactness of the internal structure of material was determined by calculating the d-spacings using Bragg's law:

$$2d \sin \theta = n\lambda \quad (3.2)$$

Where, d = spacing between diffraction planes, θ = incident angle, n = positive integer, λ = wavelength of the incident beam.

3.3.8. Evaluation of shape memory properties

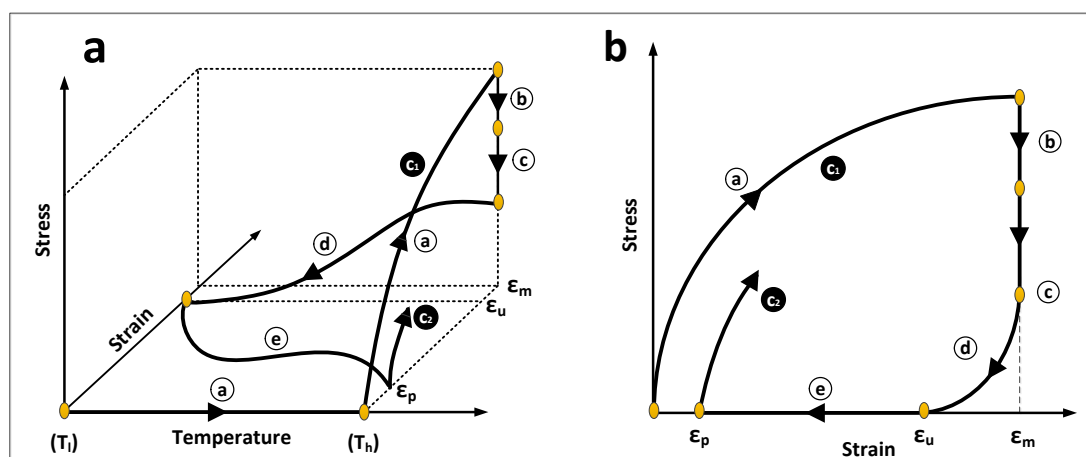


Figure 3.7: Scheme of thermo-mechanical cyclic test. a) Plot of stress with strain and temperature. b) Typical curve of stress vs strain. (T_1): Low temperature ($T < T_{trans}$); (T_h): High temperature; (ϵ_p): Plastic strain; (ϵ_u): Fixed strain; (ϵ_m): Programming strain; ($\epsilon_m - \epsilon_u$): Elastic strain; $\epsilon_r = (\epsilon_m - \epsilon_p)$.

Thermo-mechanical cyclic testing was carried out using INSTRON-5566 tensile tester equipped with controlled heating chamber. The tensile load and displacement of gauge length was measured from load cell (500N) and moving cross-head respectively. The specimen dimensions of film were 80 mm x 10 mm x 0.4 mm and 100 filaments/bundle for stress-memory filaments. Gauge length of 80 mm was maintained during testing. The total strain was 100% with an extension ramp of 10 mm.min⁻¹. The cooling at ambient temperature and heating at 60°C was done at a thermal ramp of 5°C/min.

The thermo-mechanical cycle includes:

- (a) Stretching of the specimen above T_{trans} to a desired strain level (100%)
- (b) Holding the specimen under constraint strain at elevated temperature for 10 mins to remove the viscous stress or visco-elasticity
- (c) Cooling the specimen under constraint strain for 10 mins
- (d) Releasing the employed constraint strain by unloading process

(e) Reheating the specimen above transition temperature for shape recovery.

Normally this procedure is repeated for five cycles and the last one is considered with the similar trend. The shape fixity ratio ($R_f(N)$) and shape recovery ratio ($R_r(N)$) can be expressed in %age as shown in Eq. (3.3) and Eq. (3.4) respectively. The shape fixity and recovery ratios, and total recovery ratio ($R_{r,total}$) Eq. (3.5) were obtained from the N^{th} cycle [85].

$$R_f(N) = \frac{\varepsilon_u}{\varepsilon_m} \times 100\% \quad (3.3)$$

$$R_r(N) = \frac{(\varepsilon_m - \varepsilon_p(N))}{(\varepsilon_m - \varepsilon_p(N-1))} \times 100\% \quad (3.4)$$

$$R_{r,total} = \frac{(\varepsilon_m - \varepsilon_p(N))}{\varepsilon_m} \times 100\% \quad (3.5)$$

3.3.9. Characterization of stress-memory filaments integrative stocking fabrics

3.3.9.1. Mechanical testing of memory fabrics

Extension of the stockings is very crucial factor to determine their performance and wear ability during application on the human leg. The extension occur only in the course (horizontal) direction and the fabric samples were cut into area of 150 mm x 50 mm. Instron-5566 tensile tester was used to determine the elongation behavior under different constant loads. The gauge length of 75 mm was maintained (distance between upper and lower jaws) and extension ramp was at 300 mm.min⁻¹. The extension percentage at different level of loads are taken and plotted for the discussion in the chapter 7.

3.3.9.2. Structural characterization of textile memory fabrics

All the memory fabric cylindrical tubes were relaxed under standard testing condition (Temperature: 20±2°C; relative humidity: 65±2%) according to AATCC 99 method.

Memory fabric tubes were split up, dimensions of the fabric tubes were measured and recorded before the relaxation (24 Hrs).

Fiber content

A length of 2 cm was marked on all the fabric samples and cut apart. The Nylon and memory polymeric filaments (MPF) were unraveled and measured the crimped length by straightening them. Based on the linear density of Nylon (70 denier) and MPF (150 denier), the corresponding weight, and the ratio of MPF was calculated. The percentage of MPF content was calculated from the Eq. (3.6). The MPF fiber content was then subtracted from 100 to get the percentage content of Nylon.

$$\text{Fiber content (\%)} = \frac{\text{Weight ratio}}{(\text{Weight ratio} + 1)} \times 100 \quad (3.6)$$

Structural properties

The float length of MP filament in each series of the fabric varies and which could be seen on the technical back side. This was observed using Leica (Model: M165C) classic stereomicroscopy and measured the length of floats in each type of memory fabric structures. The resolution of microscope is maximum 453 lp/mm with magnification in the range of 7.3x – 120x. The microscopic images of the technical backside showing float length is shown in the Figure 3.2c.

The loop length was measured by unravelling the Nylon filament from known number of loops (20 loops) and the same method continued for five readings to get the average values. The areal density (loops/square inch) was measured by the product of wales/inch and course/inch. The Loop shape factor was calculated from the ratio of course/inch to its wales/inch (Eq. (3.8)).

$$\text{Loop shape factor} = \frac{\text{Course/inch}}{\text{Wales/inch}} \quad (3.7)$$

The fabric weight (GSM - grams.meter⁻²) of each sample was measured by weighing the area of 5x5 cm. Fabric thickness was measured according to the ASTM-D1777 standard by taking the average of five readings with load of 20 cN.cm⁻².

3.3.10. Interfacial pressure measurement of the memory fabrics

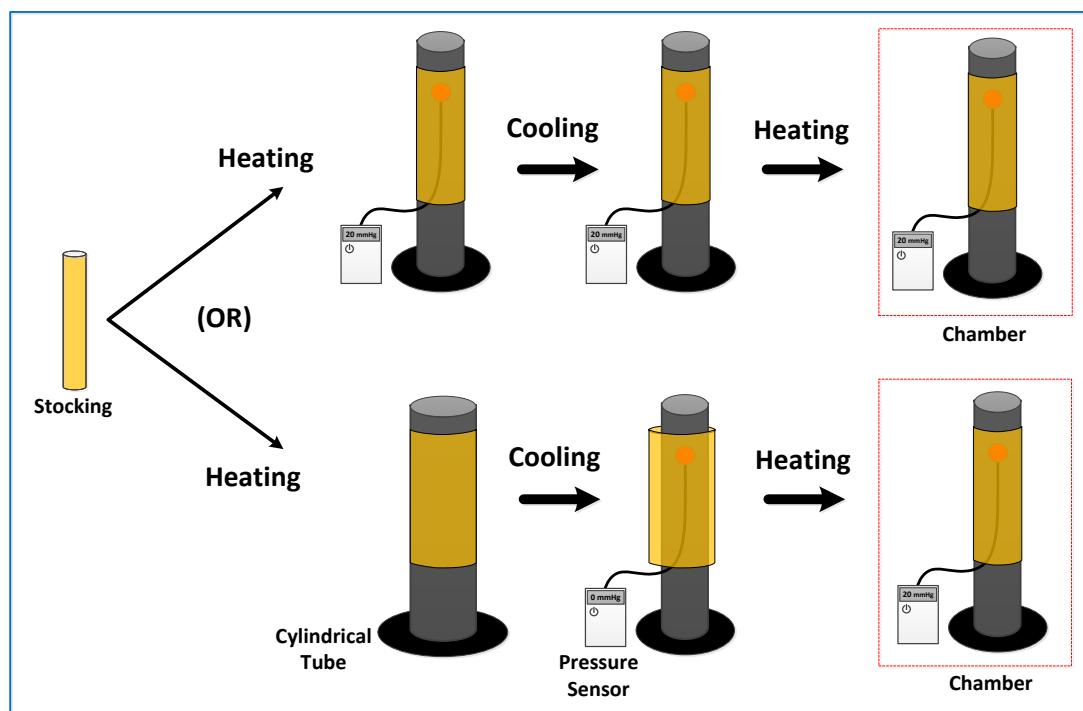


Figure 3.8: Scheme of interfacial pressure measurement in the stockings

In this project, interfacial pressure measurement of the memory fabrics was carried out using hollow cylindrical tubes having variable diameters. A general procedure for the pressure measurement is described here and the detailed section is included in the relevant chapters accordingly. For the all the pressure measurement, Kikuhime^{TR} pressure sensor was used to record the pressure in mmHg. The memory fabric tubes are integrated with the thermal responsive stress memory filaments. The memory stockings were having

circumference smaller than the cylindrical tubes and different sizes of the tubes were used to provide different level of strain, Eq. (3.9). The pressure knobs are attached on the cylindrical tubes and placed the stockings over on it as shown in the Figure 3.8. Initially stockings are heated above the transition temperature and then deformed to place on the cylinder for stress storage upon cooling. Further the stored stress is recovered upon heating above the transition temperature and this was performed in the heating oven. The oven with controlled temperature chamber was used to trigger the memory stress and measured the pressure accordingly. The two cases depicted in the Figure 3.8 is for reference and they are individually studied and reported in the respective chapters in further.

$$\text{Strain (\%)} = \frac{SC' - SC}{SC} \times 100 \quad (3.9)$$

Where, SC is cylinder circumference and SC' is stocking circumference.

The escalation of the interfacial pressure in the stockings on the cylinders due to stored memory stress is shown in the Figure 3.9. The mode of temperature can be controlled to get the static constant pressure in heating and dynamic massage pressure in heating and cooling steps successively (Figure 3.9).

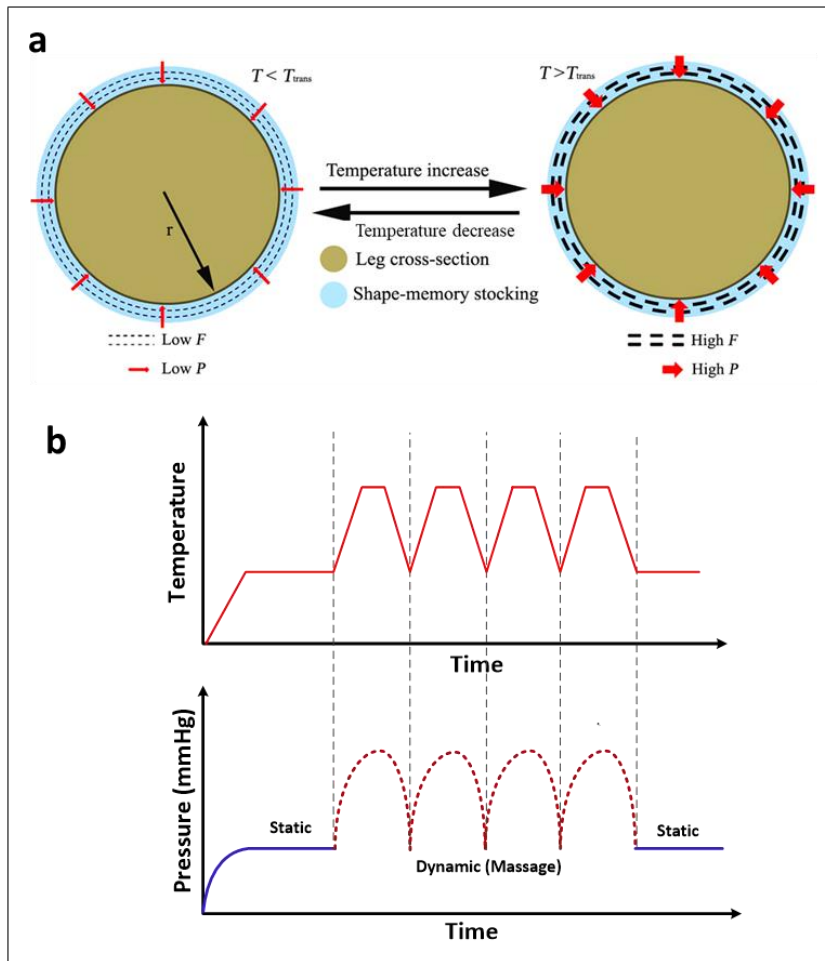


Figure 3.9: Schematic of pressure control. a) Cross-section of cylinder and the stocking,

b) Pressure-time and temperature-time profiles during pressure measurement

3.3.11. Doppler Ultrasound examination

The Ultrasound scanning was performed in a controlled room temperature (22 °C) using the Esaote MyLab™Six ultrasound unit in conjunction with a 3–13 MHz linear transducer (Esaote, Genoa, Italy). The memory stocking was first heated using dryer gun and then deformed to fix the temporary shape before application on the lower limb of the human subject. The stocking was then heated more than 50 °C using dryer gun, so that it can start compressing the lower limb. Using spectral Doppler ultrasound, the popliteal vein above the calf muscle was scanned longitudinally to measure the blood flow. Standardized Doppler settings were used for all ultrasound measurements: pulse repetition frequency (PRF) was 2.5kHz, wall filter was 100 Hz and sample volume was 2mm. The ultrasound scanning was done in four stages to find out the changes in the venous blood flow; 1) bare limb without stocking, 2) After stocking application, 3) After heating and cooling, 4) During heating to trigger the massage effect.

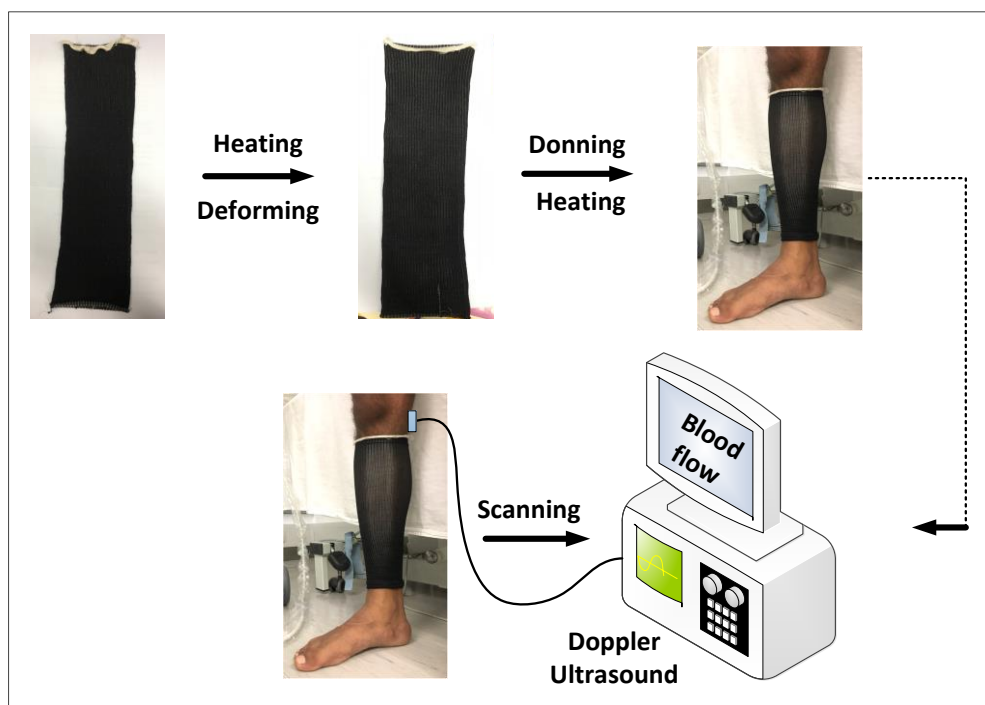
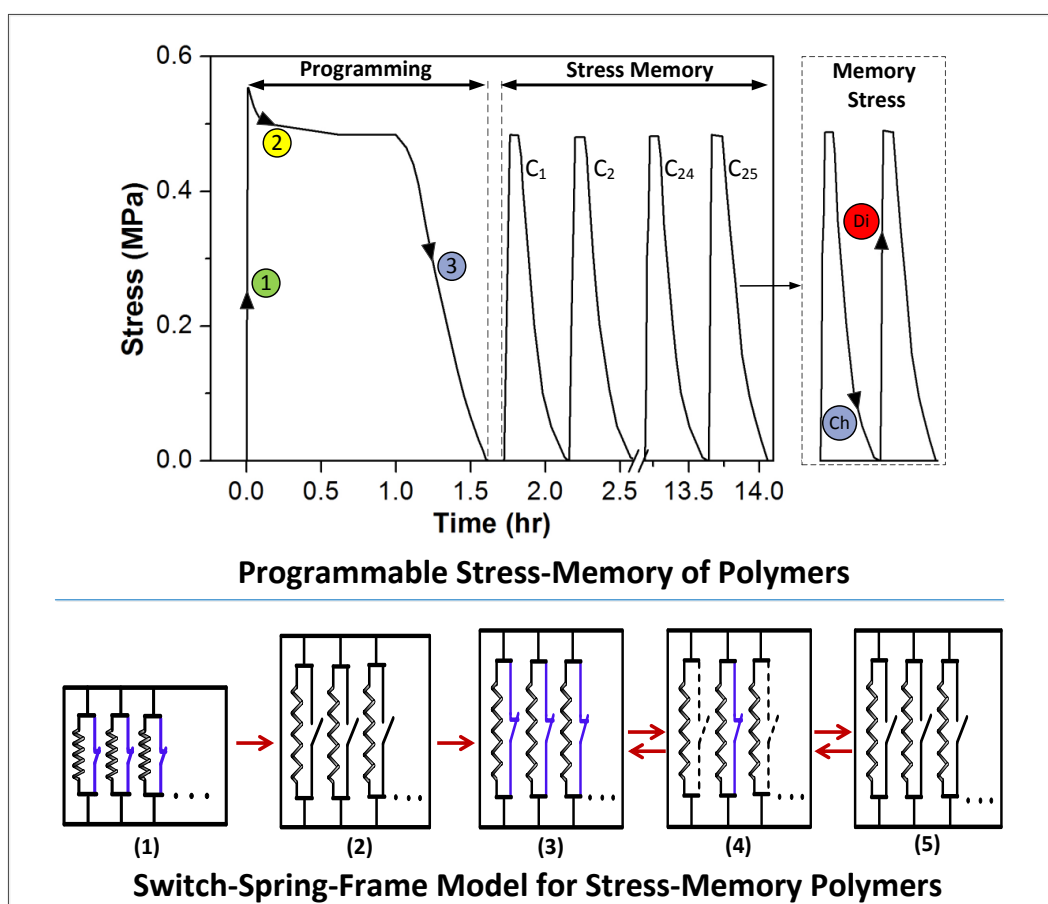


Figure 3.10: Set up for venous blood flow measurement using Doppler Ultrasound

CHAPTER 4: STRESS-MEMORY POLYMERS

Highlights of the Chapter

Even though smart polymeric materials have been researched in many areas in the past few decades, there are still opportunities to address their interesting behaviors. A novel stress-memory phenomenon of stimuli responsive polymers is discovered and reported in this chapter and a switch-spring-frame model is proposed to narrate such behavior. The concept and model represent a landmark in polymer physics. The discovery reveals promising potentials of such materials in many areas such as medical devices.¹



¹Relevant Publication

Hu, J. L., B. Kumar and H. Narayana (2015). "Stress memory polymers." *Journal of Polymer Science Part B-Polymer Physics* **53**(13): 893-898.

4.1. Introduction

Polymers responsive to an external stimulus are smart materials adaptive to our human demands [172-175]. Shape memory polymers are at the forefront of research in the broad range of explorations leading to both high impact academic publications [5, 14, 42, 176] and wide applications [11, 104, 177, 178]. Shape memory polymers (SMPs) are so named because of their ability to memorize shapes through programming processes using external stimuli. Thus, previously, we normally considered SMPs as programmable *shape* controlling materials [39] and considerable progress has been achieved in their shape capability development [1, 179, 180]. Similarly, the study of stress of SMPs in literature only serves the objective to evaluate their ability to recover the shape, namely, shape recovery force [47, 49]. Additionally, existing models explaining shape memory effect use dashpots in viscoelasticity [46, 109, 115], which overlooks the stimulus-responsive nature of SMPs and hinders the insights in analyses of polymers [14, 180]. Furthermore, recent advances demand more understanding of their stress behavior which hampers realistic and valuable applications [14, 181]. The discovery being reported in here is stemmed from a real case study into shape memory polymeric fibers in compression stocking for the management of phlebological and lymphatic deceases such as varicose veins and venous ulcers [92, 95, 155]. Here we show a novel phenomenon namely, *stress-memory* in which the stress of a material can respond to an external stimulus due to programming. This concept is further enlightened by a switch-spring-frame model. The discovery of stress memory can extend the concept of SMPs to memory polymers which can remember not only shapes, but also stress and temperature [6] and may forecast more fascinating properties of SMPs for future revealing. The model for understanding the stress memory effect is a landmark in polymer physics, particularly in smart polymers where the responsiveness to a stimulus can be vividly defined. Stress memory enables us to develop

applications needing stimuli-responsive forces, which broadens the horizon in emerging smart products of many fields.

4.2. Results and Discussion

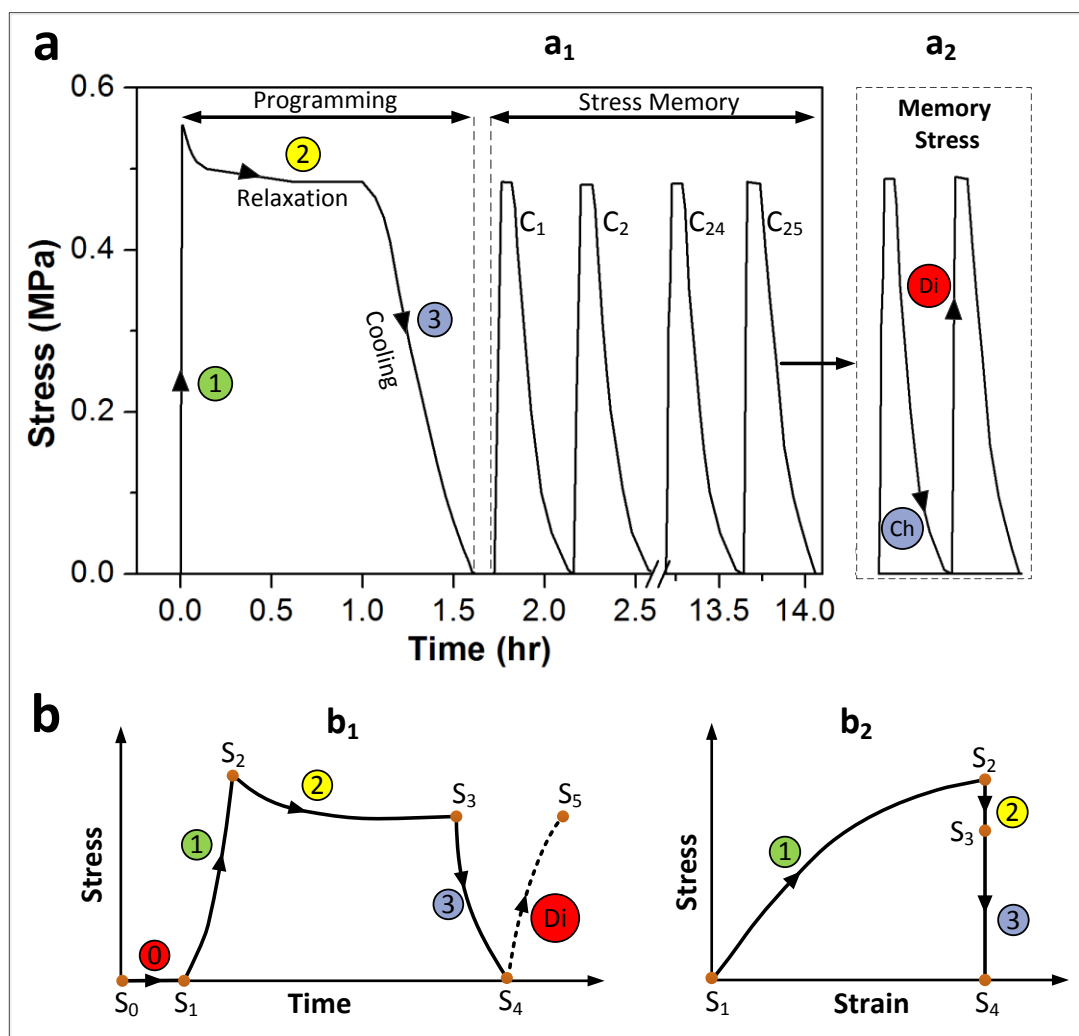


Figure 4.1: Thermal induced stress-memory of polymers. (a) Programming, stress memory and memory stress. (a₁): Experimental results showing stress-time profiles in programming and memory processes; (a₂): A stress memory cycle with stress charging (Ch) and discharging (Di) stages. (b) Stress-strain and stress-time profiles during programming. ①: Total stress; ②: Viscoelastic stress; ③: Memory stress. S₀→S₁: heating the original relaxed specimen; S₁→S₂: stretching the specimen; S₂→S₃: relaxing

the specimen; $S_3 \rightarrow S_4$: cooling/charging the specimen; $S_4 \leftrightarrow S_5$: Stress memory process, charging-discharging.

Stress-memory refers to a phenomenon where the stress in a material can be programmed, stored and retrieved reversibly with an external stimulus which can be temperature, electricity, magnetic fields etc. A thermal sensitive polyurethane with a melting transition is used, $T_{\text{trans}} = 42.6 \text{ }^\circ\text{C}$ as an example of discussion here (Figure 4.2). The stress memory programming (Figure 3.4; Chapter 3) was performed and the result is depicted here in Figure 4.1. The reversible stress can vary as heating and cooling cycles around T_{trans} as shown in Figure 1(a₁). The stress memory in one repeating cycle includes charging and discharging stages as in Figure 1(a₂). Charging is the process where a stress is being stored under cooling in the material just like storing electricity into a battery while discharging releases the stored stress at heating. Charging and discharging were continued for 25 cycles and the cyclic stress variation showed excellent repeatability and consistency.

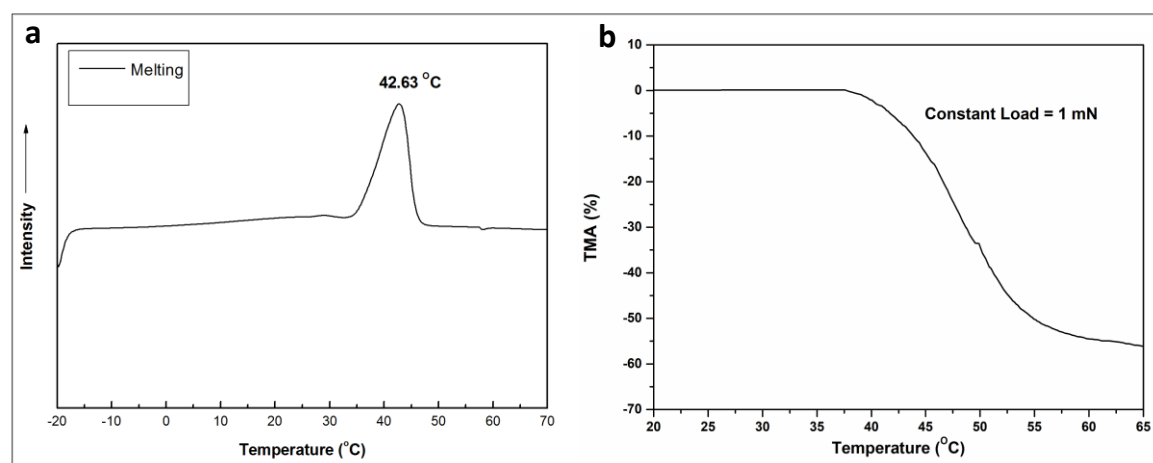


Figure 4.2: Thermal properties of stress-memory polymer. a) DSC thermogram, b) TMA curve at the temperature ramp: 3 °C/min

Memory stress is obtained through a programming process (Figure 4.1a & b), which includes steps of heating-stretching, heating-relaxing and cooling-fixing from S_0 to S_4 . This charge the memory stress in the material. The programming can be controlled with respect

to time, temperature, heating rate and constraint conditions. Herein, the programming strain was set in range of 10 to 80% ($< 100\%$), also denoted as initial strain (I.S). The stress memory process in the programmed specimen was started by heating at $T_{Di} = 50\text{ }^{\circ}\text{C}$ ($S_4 \rightarrow S_5$) under a constraint strain. Stress increases with time gradually, and then reaches a plateau; maximum memory stress (MS_{max}) is observed (Figure 4.1a₁). This MS_{max} obtained upon reheating is due to the previous programming which charged stress in the film as seen in Figure 4.1b and Figure 4.1(a₁). After a specific time of heating, the specimen was cooled down at T_{Ch} and the decrease of the stress from the plateau was traced and eventually reached zero ($S_5 \rightarrow S_4$). In fact, a stress memory should have viscoelasticity, elasticity, memory and plasticity (Figure 4.3).

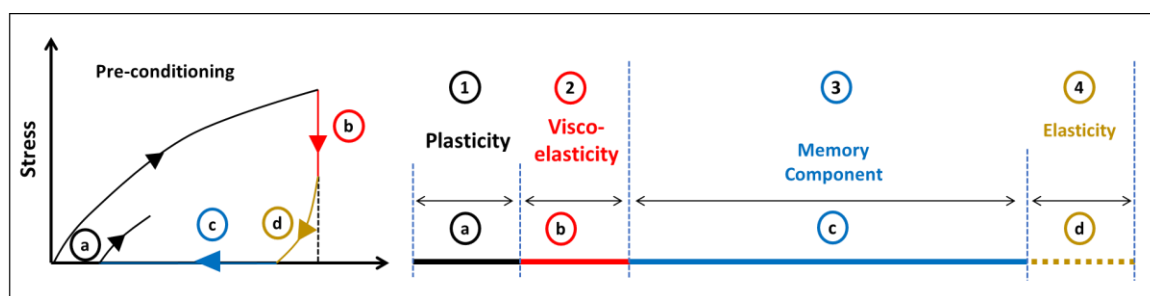


Figure 4.3: Components of stress-memory polymer revealed in this work

The memory stress should be pure so that the thermal-induced cyclic stress variation can be repeated, analysed and meaningful as signals for different applications. In order to obtain pure memory stress, all non-memory components must be eliminated. In programming, the viscoelasticity can be removed at step ② (Figure 4.1). Apart from viscoelasticity, plasticity of a polymer also needs to be removed, which was achieved by preconditioning using thermo-mechanical cycles (Section 3.4.1). Preconditioning eliminates the weak-link spots causing permanent slippages of polymer chains in the network, and ensures the structural integrity of the stress memory polymeric network configuration for its prolonged and repetitive usage. Furthermore, preconditioning needed to be performed at a relatively

higher strain level, i.e., 100% (higher than I.S) so as to observe no elastic part remaining in subsequent programming and assured complete stress freezing in S_4 (Figure 4.1).

4.2.1. Mechanism models of stress-memory process

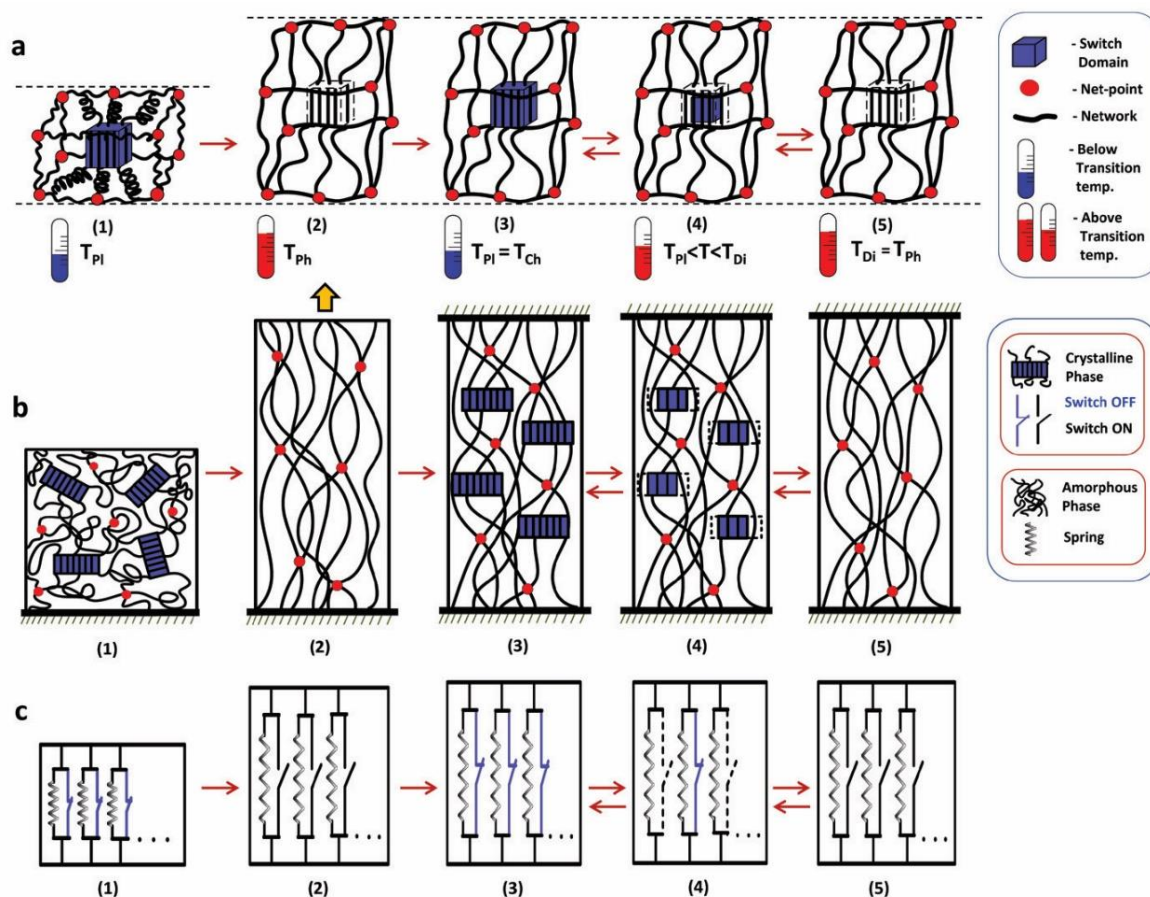


Figure 4.4: Mechanism models of a thermal-responsive MP in programming and stress-memory process. (a) Switch–matrix-netpoint unit cell model. (b) Crystal-coil-crosslink model. (c) Switch-spring-frame model. Single arrows from (1) to (3) represent programming process while double arrows from (3) to (5) for cyclic stress memory process. (1) Original length at relaxed state; (2) Stretched length at heating; (3) Charged state at cooling; (4) During transition around T_{trans} ; (5) Discharged state at heating.

The stress-memory phenomenon can be explained by Figure 4.4, where the mechanism is described in three related models from different view points: a unit cell model with switch-matrix-net-points (Figure 4.4a), a general morphological configuration (Figure 4.4b) using

crystal-coil-crosslink, and a mechanical system in switch-spring-frame (Figure 4.4c). The polymer has a physically cross-linkable hard segment and a crystallizable soft segment (Figure 4.4b). It is observable that switch is the soft segment crystal which can be 'OFF', that is, close-up, representing the well-aligned dense crystalline structure while it is 'ON', means opening, when the crystals are molten into free molecular chains. The matrix consists of molecular chains in amorphous regions at original state which is stretchable like a spring. It is coiled in its original state while highly stretched when the sample is tensioned and frozen. The netpoints are the hard segments formed by physical cross-links which keep the polymer frame and provide the integrity and basic mechanical properties of the polymer bulk. Framework is formed by the cross-linking points and their connected chains. A switch-matrix-netpoint unit cell is comprehensible for memory and the switch-spring frame is logical for mechanical process, which can explain how the pattern of a cyclic stress is formed.

All three models corresponding to the same series of states: the original, state (1), the specimen is totally relaxed at room temperature when crystals are randomly distributed, the polymer chains in the amorphous region are coiled and physical cross linkers form the network and support the whole structure. In state (2), the polymer is stretched under higher temperature than its transition when the crystals are molten and the coils in the amorphous region are straightened or highly oriented, then state (3), cooled down to lower temperature than its transition and the stretched specimen is constrained accordingly when the crystals are reformed. Between steps 3 and 5, the memory stress process starts, are in transition and completes as heating or cooling alternates, thus a state (4) is inserted to illustrate the partial melting of the crystals and the other part remains dense crystals. This means, as memory stress progresses, crystals melt step by step from edges to the core or smaller crystals melt first and the switches open one by one as time goes on to trigger the memory process

(Figure 4.4b). From states (3) to (5), it is the memory process in the range of transition temperature while from step (1) to (3) is the programming process where stress is stored in the polymer film. Internal molecular configuration in unit cell and the bulk polymer and the corresponding states of the switch-spring devices evolve from from step (1) to (5).

One-unit cell in Figure 4.4a forms one switch-spring paired device and Figure 4.4c is a collection of parallel devices. The stress profiles during programming and stress-memory process (Figure 4.1(a₁)) of a polymer can be interpreted by the switch-spring-frame model (Figure 4.4c). In the polymer mechanical system, there are a collection of switch-spring pair devices. When a strained spring is totally locked by a switch, the device is inactive, and then the stress is zero in this device. When a spring is released by opening the paired switch, the corresponding device is active and the stress is equal to the originally charged level. During the transition, a part of the switches is opened and the corresponding springs can release their stored entropy energy. The rest of switches are still closed up, which freezes the paired springs. Springs are coiled and switches are closed up when the specimen is at its original state (1). In the programming stage, entropy of the polymer chains is stored into the springs by heating-stretching and cooling-fixing the specimen. In a repeating unit of memory stress pattern, during the charging process (5)→(3), switches close up one by one to freeze the stretched springs from being active and store the energy in the polymer through the gradual formation of crystals by cooling, which leads to the slow decrease of the memory stress in manners demonstrated in Figure 4.1(a₂). During discharging (3)→(5), switches open up step by step through melting the crystals from edges to the cores at high temperature (Figure 4.4(c₄)), then the springs become activated where the stored entropy energy is released sequentially in the stress memory polymer. Correspondingly there is a gradual increase of memory stress due to the tendency of returning back to its original relaxed state of the strained springs. As the number of switches are finite, the memory

stress can reach MS_{\max} and MS_{\min} , then the cyclic variation of charging and discharging can be repeated with alternative temperature stimulation.

4.2.2. Stress-memory response with different constraint methods

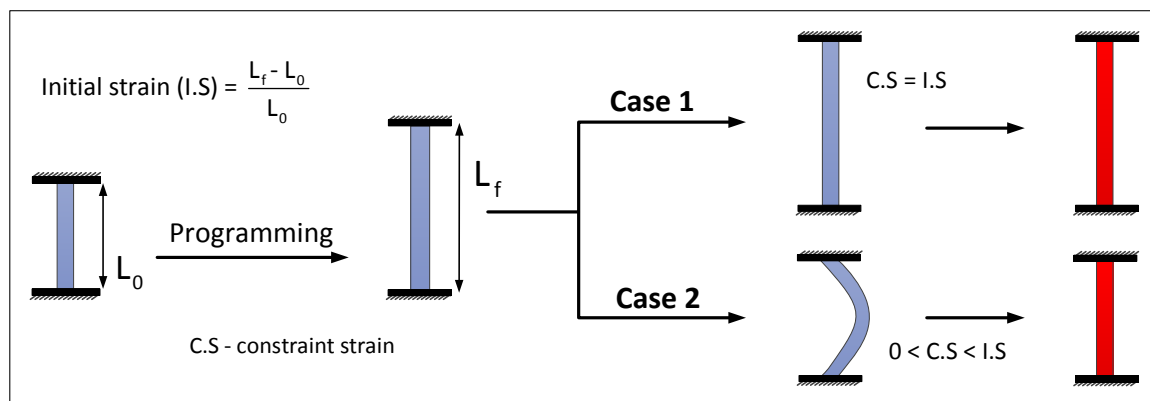


Figure 4.5: Scheme of stress-memory programming tests

The memory stress was dependent on the constraint level (level of constraint used for stress-memory cycle, hereafter termed as C.S), the I.S, discharging temperature and rate of heating or cooling. Different testing conditions are described as:

Case 1: The C.S is fixed same as I.S (Figure 4.5). Five specimens were programmed to different I.S levels (10 to 50%).

Case 2: The discharging is executed at a C.S smaller than the I.S, namely, partial constraint (Figure 4.5). Specimens were deformed to an I.S of 20% to 80% with 10% interval, but the C.S was fixed to 20% for all 7 specimens, which is equal to or lower than their I.S, namely, total or partial constraints respectively.

Case 3: Different temperature levels, i.e., 30, 40, 50, 60 and 70 °C, were set to obtain MS_{\max} at same C.S. It was detected that an increase in discharging temperature (T_{Di}) leads to the increase in memory stress (Figure 4.6). Again, according to Figure 4.4, assuming the same number of switches closed during the programming, at a higher temperature, more switches are opening up in the polymer system due to the melting of more crystalline soft segments, which makes more springs at work and leads to the higher MS_{\max} during discharging. It

was also observed that above 70 °C there was no further increase in memory stress as all the switches have been opened, thus the finite number of springs are all active and participating in the system in contributing to the MS_{max} . The reported behaviour is well corresponding with the DSC result where, the crystals melting broadness is in the range of 34 °C to 48 °C and around the same range of temperature MS_{max} is achieved by discharging at 50 °C (Figure 4.6).

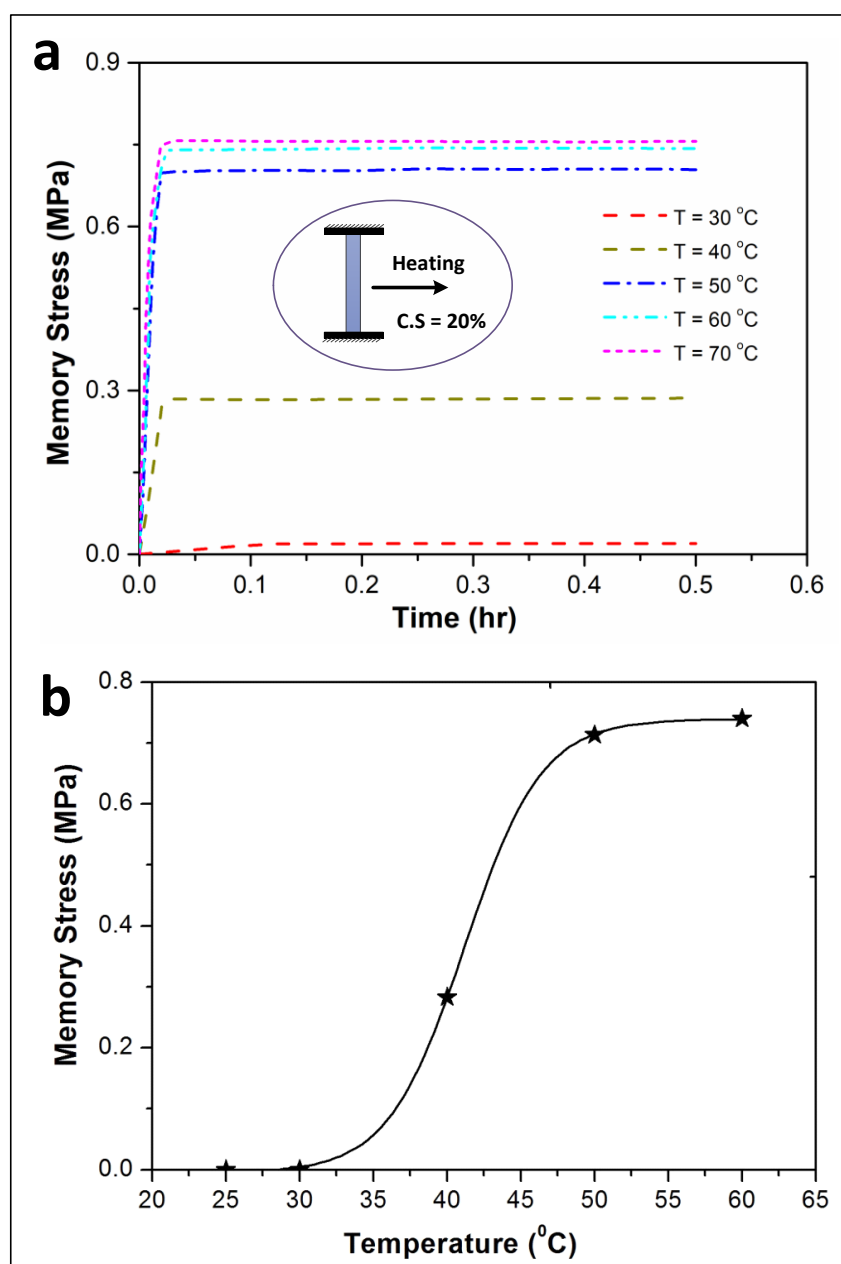


Figure 4.6: Evolution of memory stress at different discharging temperatures. a) Memory stress-time profile. b) Memory stress-temperature profile

Case 4: Figure 4.7 shows that different profile of stress memory can be modulated by controlling the amount of charging and discharging in a continuous usage. Level of charging and discharging are indicated as T_1 , T_2 and T_3 in the figure denotes different temperature levels. This profile was achieved by controlling the combined effect of different temperature levels, different time intervals and rate of charging/discharging. The different time intervals are denoted as “ t ”; $t_1=6$ min, $t_2=12$ min, $t_3=5$ min, $t_4=6$ min, $t_5=50$ sec, and $t_6=2.5$ min.

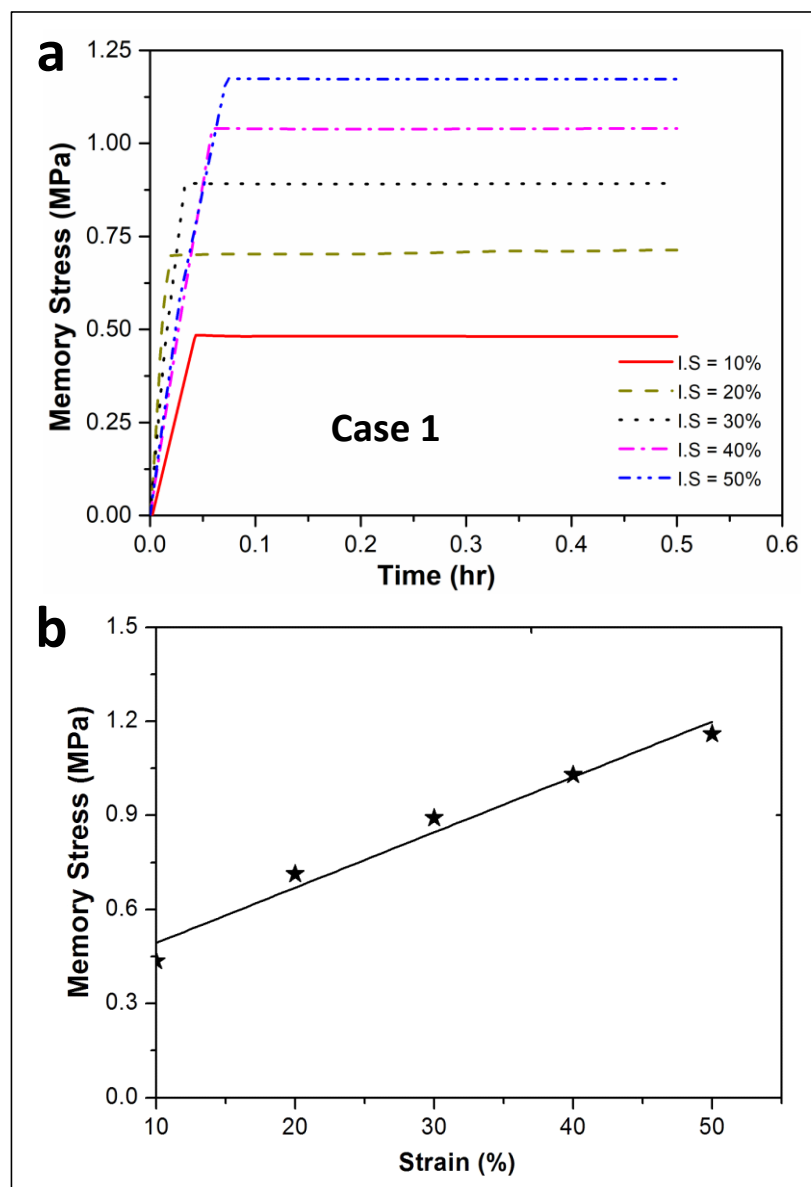


Figure 4.7: Maximum memory stress discharged at constraint strain (C.S) equal to the initial strain (I.S), total constraint. a) Stress-time profile. b) Stress-strain profile.

To consolidate the concept of stress memory as well as prepare for specific applications, it was investigated the effects of I.S and constraint strain (C.S) on memory stresses. For Case 1 where the C.S is equal to its respective I.S, namely total constraint, the memory stress, MS_{\max} , is found to increase with the I.S level (Figure 4.7). Here the switch-spring-frame model still applies. The higher the I.S, the more stretched the springs originally are, the more entropy energy stored in the devices and contributed to the increase in MS_{\max} during discharging.

On the contrary, it was encountered that memory stress was inversely proportional to the I.S (Figure 4.8) where the discharging was executed at a C.S smaller than the I.S, namely, partial constraint in Case 2. From this result, it is clear that, the partial recovery of the strain from the programmed I.S in a partial constraint, can lead to the loss of memory stress. We assume that all specimens have the same number of switch-spring devices. According to the mechanism described in Figure 4.4, due to the heterogeneous nature of a polymer in gradual melting (Figure 4.4(b₄)), it is possible that some stretched springs had returned to their coiled state (related to Figure 4.4(c₄)) completely during the constraining process. This is corresponding to the recovery from the I.S to the C.S, which leads to fewer active springs during the later stress discharging in a larger I.S specimen, thus releasing less entropy energy and leading to the decrease in MS_{\max} .

4.2.3. Stress-memory response with different initial strains at single constraint

On the other hand, if an I.S is totally constrained where no springs is allowed to recover, but fully stretched during discharging, the highest memory stress can be obtained due to the fact that all springs are at work. Just like many signals, a memory stress profile can be characterized by magnitude and frequency, which can be modulated in many ways by factors such as I.S, C.S, temperature, time and rate of stimulus change, etc. Figure 4.9

further demonstrates the combined effect of time and temperature in memory stress in charging and discharging under a continuous usage of the material.

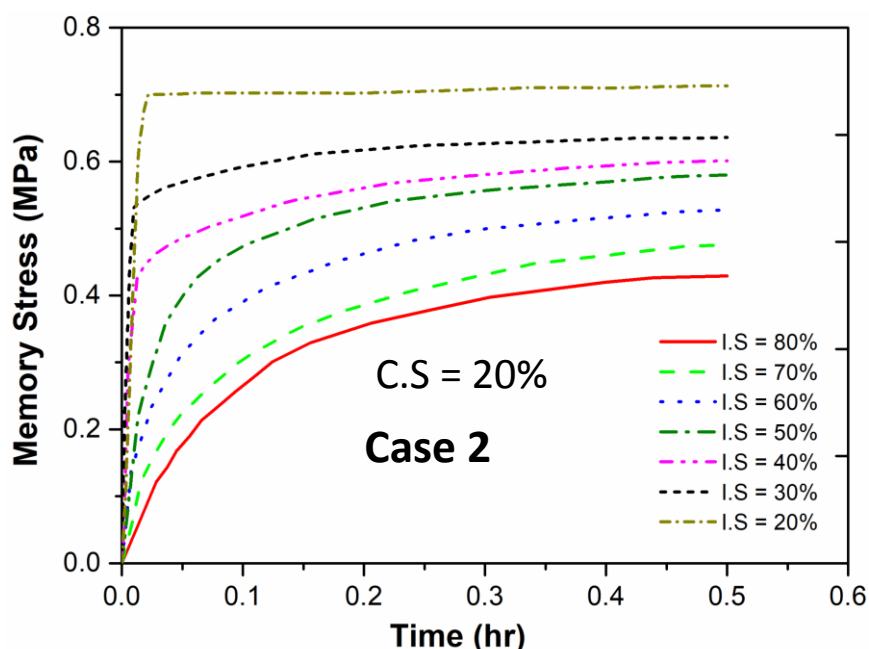


Figure 4.8: MS_{max} programmed at different I.S but discharged at the same C.S.

In the above, although a thermal responsive stress memory phenomenon is reported and modeled of a polymer, such concept may be universally applicable to polymers responsive to other stimuli such as solvent responsive polymers [182]. Unfortunately, like another report [183] by the same authors, the stress memory phenomenon was not identified in the literature, thus memorized stress was not separated in these cases. Instead the stress answer in their terms is a mixture of all components, namely, elastic, plastic, viscoelastic and memory parts. Thus, the report of this research represents a significant progress in terms of conceptualization and systematic understanding of stress memory of smart polymers.

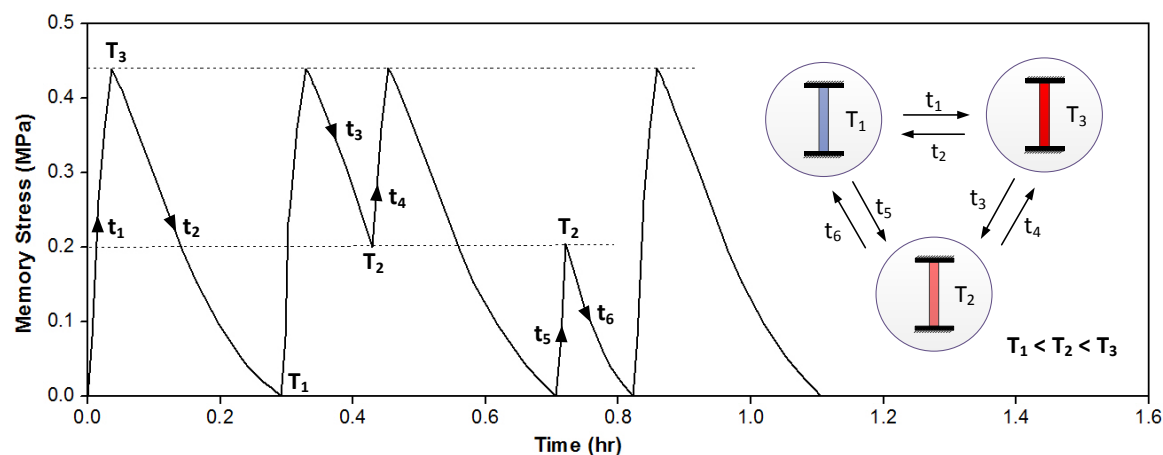


Figure 4.9: Controllability of memory stress, a combined memory stress profile under different conditions, partial constraint. $t_1 \rightarrow t_6$: different time intervals; $T_1 \rightarrow T_3$: different temperature levels.

4.3. Application of Stress-Memory Concept

The application of stress memory of polymers was first attempted in the development of smart compression stocking to control the interface pressure critical for the management of chronic venous diseases [120, 184]. Maintaining the gradient pressure from ankle to knee in the stocking is one of the key factor to achieve the efficient compression therapy but none of the current commercial stockings provide this benefit effectively. In this application, we utilized the principle learned from Case 2 in Figure 4.8, where different MS_{max} can be obtained from programming with the same C.S but different I.S levels.

The experimental procedure of preparing the stress memory polymeric filament integrative stocking is discussed in Chapter 3. Figure 4.10 shows the scheme of stress memory programming and pressure testing methodology to achieve the different pressure levels in the same size of the stocking.

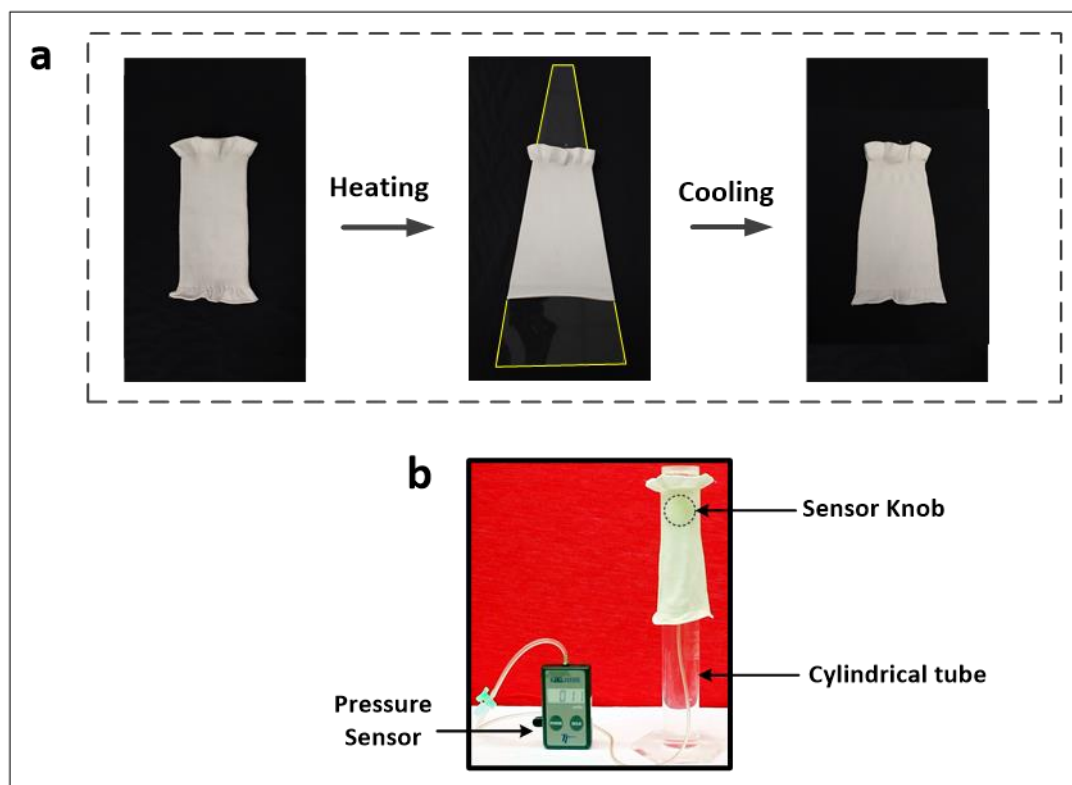


Figure 4.10: Application of stress memory. a) stress memory programming of stocking for gradient pressure. b) Pressure measurement set up.

The pressure measurement was done using a KikuhimeTM pressure sensor (Figure 4.10). For the demonstration, the stocking was initially programmed that included different processing steps, i.e., heating, deformation, relaxation and cooling. The stocking was initially heated using a heating element (air blower), and applied to a trapezoidal template (Figure 4.10a). The template was made of acrylic sheet. The whole system was allowed to cool at the ambient temperature for 30 minutes to fix the deformed shape of the stocking on the template. Finally, a trapezoid shape of stocking was obtained with lower and higher circumference of 14 and 17 cm respectively. The pressure measurement was obtained on a glass tube that provide the similar constraint level (circumference: 14.5 cm) for the entire length of the stocking. Extreme tight and loose states were obtained along the length of the stocking respectively at the top and bottom points (Figure 4.10b). For the activation, the hot water (70 °C) was poured in the tube, and the pressure increase over time was noted

using stop watch. As a demonstration, the pressure profiles at two different locations are shown in Figure 4.11, where the highest and lowest pressure readings are observed at upper and lower region respectively.

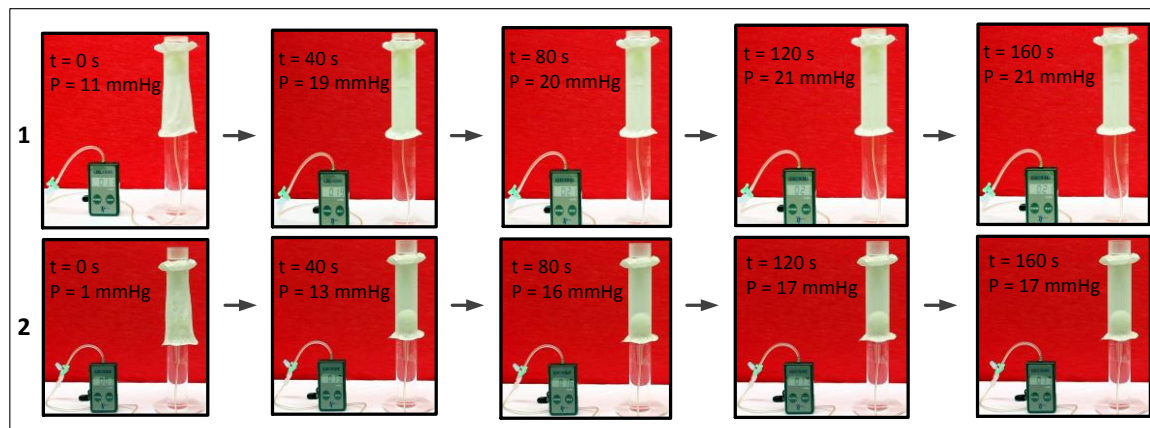


Figure 4.11: Results showing the pressure gradient (difference in two cases with pressure knob placement)

The stocking shows different pressure levels at different positions (Figure 4.11) from an originally cylindrical tube programmed using a trapezoid template in Figure 4.10a. This enables us to develop one-size stocking suitable for multiple leg sizes with the same level of pressure or attaining multiple compression levels on the same leg for different stages of chronic venous disorders [146]. Furthermore, we actuated the stocking by heating and cooling alternatively, a cyclic pressure variation was also monitored (Figure 4.12a). This is consistent with the stress-memory behavior of the polymer film as shown in Figure 4.1(a), where only the Laplace's law is needed to convert the internal stress developed in the textiles into the interface pressure related to the limb circumference [61, 185]. This can provide an exciting new function, namely the massage effect to the sick limbs (Figure 4.12b) to replace the existing cumbersome compression devices such as Intermittent Pneumatic Compression (IPC) [58].

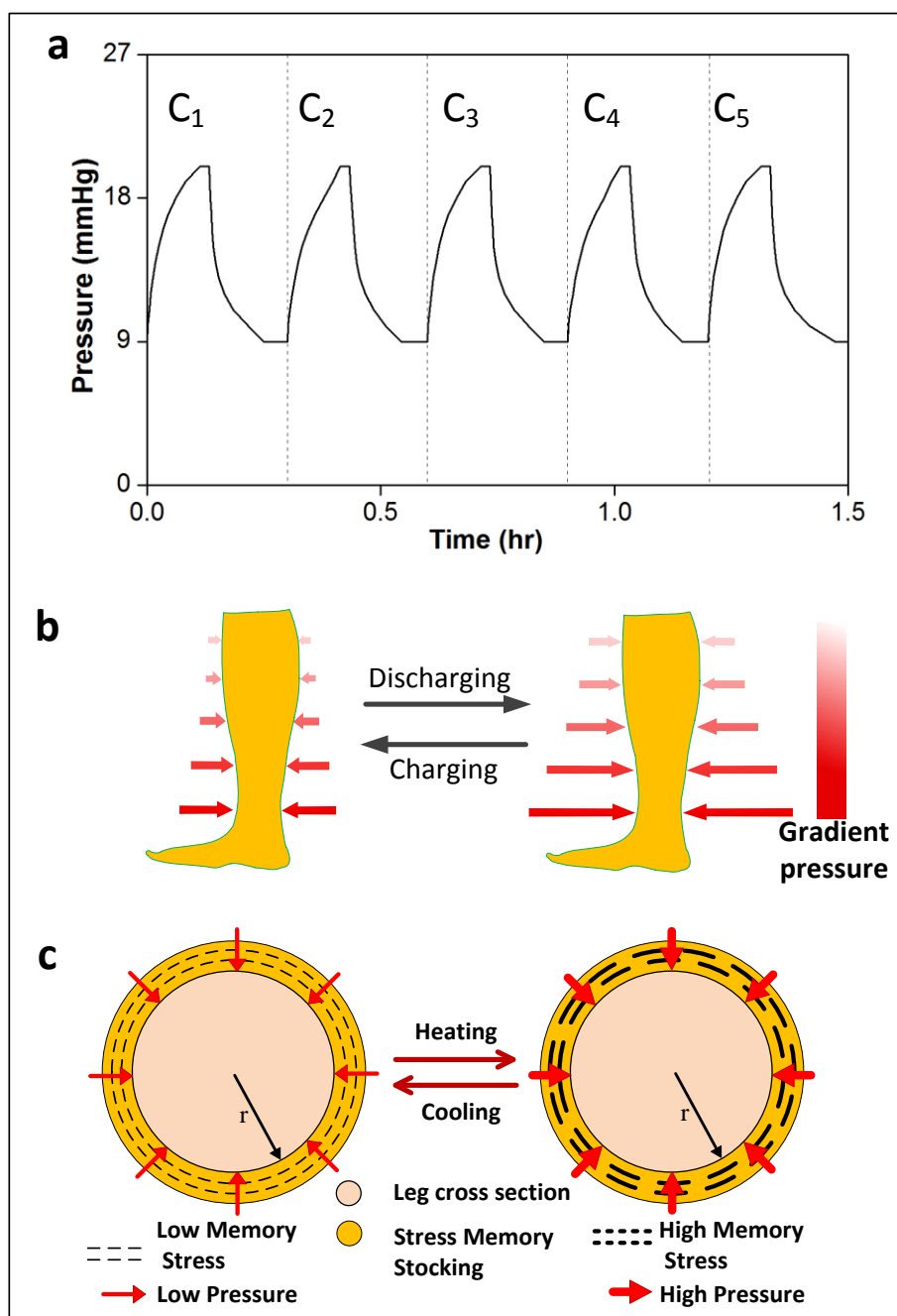


Figure 4.12: Dynamic compression pressure. a) Pressure profile of the stocking for massage effect. b) Compression stocking with massage effect. C_1 to C_5 : Cycles. c) Cross section of stocking and the leg showing pressure change with memory stress.

Memory polymers could be processed into different other forms such as filament, foam, and film to implicate them scientifically and practically into diversified applications. A generalized form in Figure 4.13 represents the modes of memory stress applications. The

discovery and understanding of stress memory in polymers enable us to develop applications where stimuli-responsive forces are required in emerging smart products including massage devices [58], sensors [186], stress garments [187], artificial muscles [4, 188] and electronic skins [189]. Stress memory polymers and their mechanism models are milestones in smart polymer physics which may forecast more fascinating properties for future revealing and their applications.

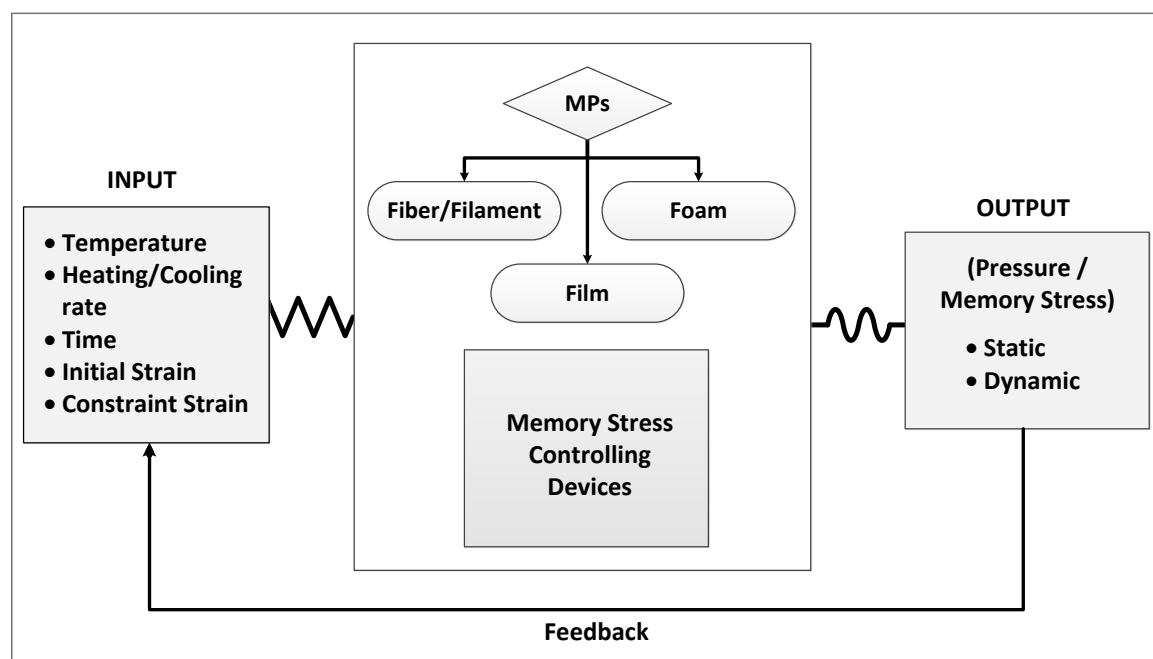


Figure 4.13: A generalized model of stress memory potential for applications

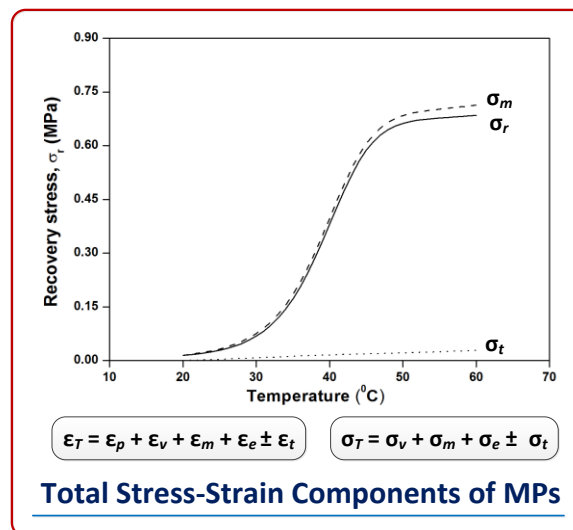
4.4. Summary

1. A novel phenomenon of stress memory in stimulus-responsive-polymer, namely stress memory polymer has been discovered. To narrate this unique behavior, it is further enlightened with the switch-spring-frame model. The model for the memory effect in polymers is a landmark in polymer physics and could be useful for other type of smart materials too.
2. This is the first study to apply stress memory programming technique into smart compression stockings for the management of chronic venous disorders. The level of interfacial pressure in the stockings can be maintained/controlled externally by means of temperature change. Also, the pressure level can be modulated by the initial and constraint strain.
3. Multi-functional compression benefits can be achieved in the stocking including gradient pressure, dynamic pressure (massage effect), static pressure, selective pressure control, and single size for all.

CHAPTER 5: CONSTITUENT ANALYSIS OF STRESS-MEMORY IN SEMI-CRYSTALLINE POLYURETHANE

Highlights of the Chapter

A new approach is made in this study to unveil the total stress-strain components in the memory polymer. Stress memory behavior of semi-crystalline polyurethane is analytically studied by quantifying the stress components in tensile mode of programming using constituent equations based on phase transition approach and a novel memory modulus (MM). The predicted results are having significant agreement with the experimental data. The model is used to design and predict the pressure in a memory bandage based memory film actuator. This approach can help researchers to engineer the products needing memory stress more precisely in multidisciplinary areas by predicting their behavior accurately.²



²Relevant Publications

Narayana, H., J. L. Hu, B. Kumar and S. M. Shang (2016). "Constituent Analysis of Stress Memory in Semicrystalline Polyurethane." Journal of Polymer Science Part B-Polymer Physics **54**(10): 941-947.

Kumar, B., J. L. Hu, N. Pan and H. Narayana (2016). "A smart orthopedic compression device based on a polymeric stress memory actuator." Materials & Design **97**: 222-229.

5.1. Introduction

Memory polymers (MPs) are smart polymeric materials and have the ability to recover the original shape (undeformed) from a temporarily shape (deformed) upon exposure to various external stimuli [11, 14, 87]. This *shape memory* phenomenon allows deriving several useful functions from SMPs including deployment, fixation, actuation, self-healing, and fitting [14]. Many of these functions are found to be useful for numerous applications including textiles, biomedical, aerospace, electronics, transport, construction, etc. [11, 12, 14, 178, 190]. In the earlier work (Chapter 4), discovered the stress memory phenomena and linked to an authentic application in compression stocking for varicose veins [110]. However, there is a further need of the quantitative analysis of the stress components during freezing (crystallization) or recovery (melting) of the memory polymer. A systematic and contemporary approach is shown in this work via experimental work to measure the “memory modulus” and to use it to quantify the pure memory stress of memory polymers under tensile stress memory programming condition. All the stress components generated in the thermo-mechanical process are identified and examined carefully. Furthermore, the stress evolution of the programmed memory polymer was modeled using the constitutive model, based on the phase transition approach [5]. This novel approach would further improve comprehending of the stress memory and help in designing or engineering of related application products with precision. The memory polymer used in the Chapter 4, was integrated into textile fabric base to prepare the smart bandage system with a flexible heating embodiment. The same model approach has been applied to predict the interfacial pressure in the memory polymeric actuator integrative smart bandage system to prove the practical feasibility of the concept.

In this work, the *stress-memory* behavior of the memory polymer (MP) has been taken into more consideration to explore further. Herein, the stress is stored (termed as charging or

cooling of the MP) upon inducing certain strain level beyond the T_{trans} (transition temperature) and cooling below this point. The stress is further released (discharging or heating of the MP) upon triggering by an external stimulus such as heat. Although the stress freezing can be obtained via a normal shape fixing process of the MP where the internal stress is also frozen or stored at lower temperature ($< T_{\text{trans}}$) in a deformed MP, but upon triggering the MP under constraint, the recovered stress do not remain stable but decreases over time [191, 192]. This is primarily because of the viscous stress that causes stress relaxation phenomenon. This adds limitation to use MP for some applications where the stress level should maintain or a stable cyclic stress variation is required such as pressure bandage and other massage devices. To obtain the *stress memory* phenomena, the recovery stress should be pure so that it can be repeated, analyzed, and meaningful as signals for diversified applications.

In the previous work (Chapter 4), the novel *stress-memory* in a semi-crystalline polyurethane was reported [110]. It has been found that the deformation in a thermally induced MP during a thermo-mechanical process has 4 major components; 1) plasticity ε_p , 2) viscoelasticity ε_v , 3) memory ε_m , 4) elasticity ε_e . Thermal strain ε_t causes the expansion or contraction upon heating or cooling, this is also one of the component, and hence the total deformation ε_T can be expressed as: [193]

$$\varepsilon_T = \varepsilon_p + \varepsilon_v + \varepsilon_m + \varepsilon_e \pm \varepsilon_t \quad (5.1)$$

In generic term, the total stress σ_T in a typical *thermo-mechanical cyclic* process can be divided into viscous σ_v , memory σ_m , residual σ_r , and thermal stress σ_t [193].

$$\sigma_T = \sigma_v + \sigma_m + \sigma_r \pm \sigma_t \quad (5.2)$$

Viscous stress is an impeditive or negative part which results in the relaxation of the total stress produced in the MP after initial deformation at high temperature under constraint strain condition. After cooling the deformed MP, some part of the stress will be frozen in

the polymeric matrix. This stored stress can have viscous, memory and thermal parts. The remaining residual stress (elastic) is released quickly if the external constraint is removed in the cooled MP. Heating or cooling also causes expansion or contraction of the material resulting in thermal stress and this could be either contributive or impeditive in the compression and tensile stretch programming process [44]. To obtain the pure *stress memory* effect with no energy dissipation, it is imperative that the stored stress should have primarily pure memory component.

The pure stress recovery or freezing can be obtained from a MP if it has been employed to certain thermo-mechanical processes, i.e. preconditioning and programming (Chapter 3; Figure 3.4). The pre-conditioning process was done to eliminate the plasticity and elasticity in the polymeric network (Figure 3.3). Plastic deformation is usually found in the first few cycles [82, 85, 88] and thereafter the MP is mechanically trained to show similar stress-strain response for more number of cycles. Programming is a process of storing stress, also termed as charging the memory polymer. The critical part is to eliminate another impeditive component that is viscous stress, and prepare the material to retrieve or freeze the stress at different magnitudes and levels upon controlled triggering.

The steps for a programming cycle (Figure 5.1) are as follows: **(0: $S_0 \rightarrow S_1$)** Heating the original relaxed specimen ($T_h = 60\text{ }^\circ\text{C}; > T_{trans}$); **(1: $S_1 \rightarrow S_2$)** Stretching the specimen to a particular strain level (10 to 50%); **(2: $S_2 \rightarrow S_3$)** Holding the specimen under constraint to relax the stress to a saturation level. This step eliminates the viscous stress; **(3: $S_3 \rightarrow S_4$)** Cooling the specimen under constraint to lower temperature ($T_l = 20\text{ }^\circ\text{C}; < T_{trans}$) for the charging/storing of the stress in the polymer network. No residual stress was observed up to 50 % strain after cooling for the present MP. After programming the MP, now it is ready to perform *stress memory* test.

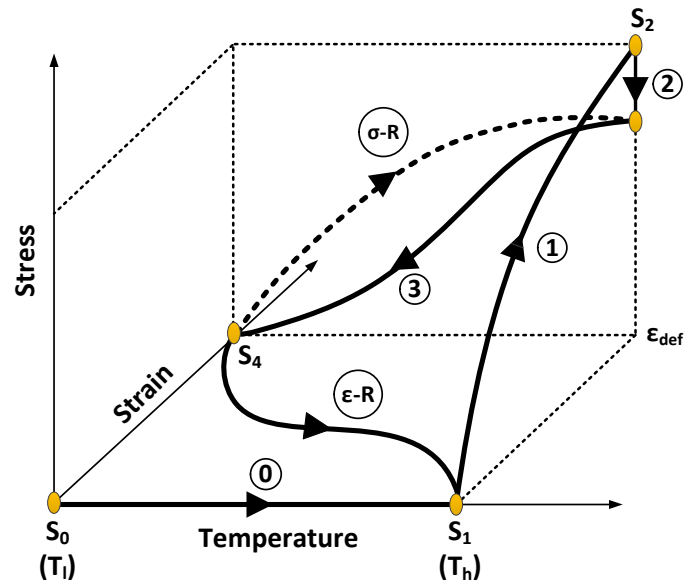


Figure 5.1: Stress-strain-temperature profile during programming. T_h : high temperature; T_l : low temperature; σ -R: stress recovery; ε -R: strain recovery; ε_{def} : total deformation or initial strain.

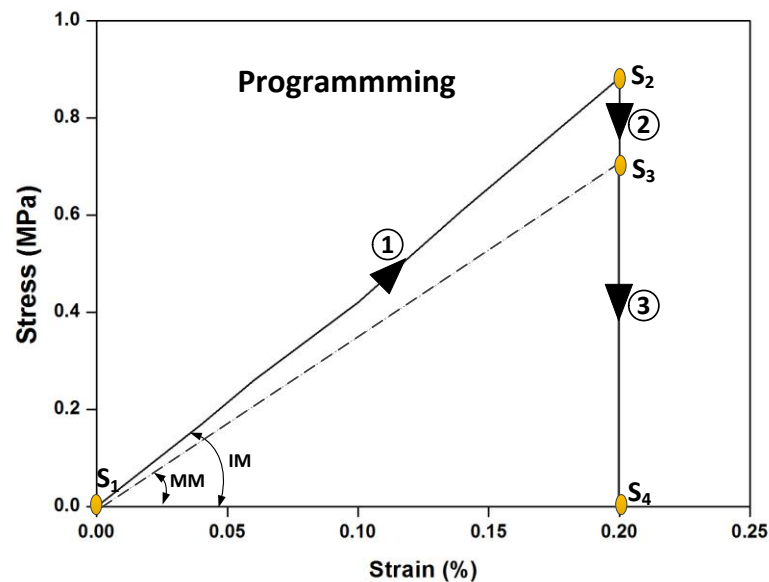


Figure 5.2: Experimental results of stress-strain profile (Initial modulus: IM; Memory modulus: MM) ($\varepsilon = 20\%$, $T_h = 60\text{ }^\circ\text{C}$)

After the stress memory programming process, stress (Fig.48a; step σ -R) and strain (Fig. 48a; step ε -R) recovery tests were performed in constraint strain and stress-free conditions

respectively. The total modulus (E_T) during the programming while stretching and memory modulus (E_M) (Figure 5.2) after the stress relaxation process were obtained at different temperature levels. The experimental results of stress recovery during stress memory test I shown in the Figure 5.3 with stress-time profile. This shows the relaxed stress obtained to calculate the memory modulus and well described in the Chapter 3; section 3.4.5.2.

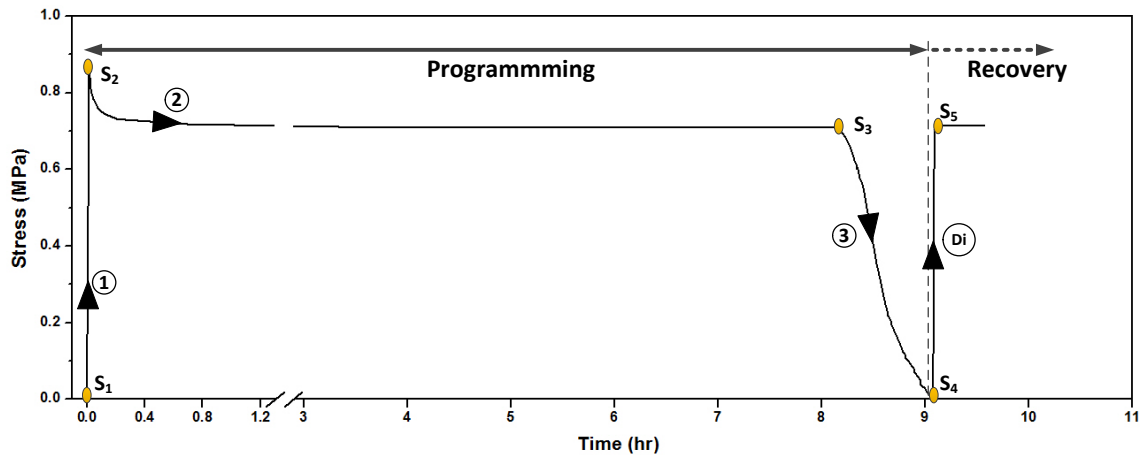


Figure 5.3: Experimental results showing the stress-time profile during programming and recovery process. Di: Discharging or heating above the transition.

5.2. Experimental Results

5.2.1. Evolution of the recovery stress

The results under the uniaxial tensile mode are discussed here. The results at 20 % strain level are shown and discussed here. Similar trends were observed at different strain levels (10 to 50%). Once heated the MP to a particular level of temperature, the recovery stress increased rapidly initially and reached to the plateau (Figure 5.4a) and remaining constant for several hours indicating no component of viscous stress. Once the activated MP was cooled again, all stress was freezing again to zero level. This indicated pure *stress memory*

phenomena which can be repeated for multiple cycles with no energy dissipation. Different stress peaks are observed at different temperatures (Figure 5.4b).

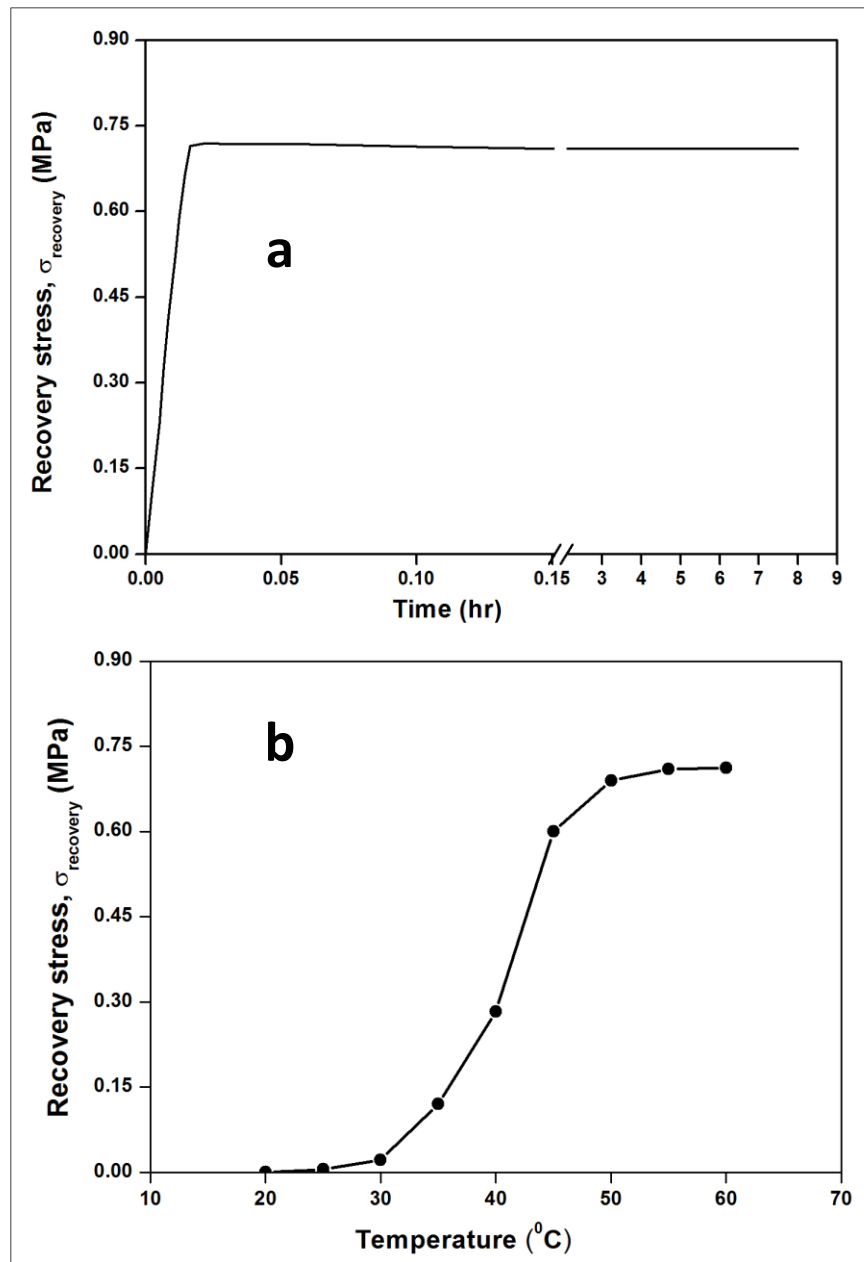


Figure 5.4: Evolution of stress with time and temperature. a) Variation of recovery stress over time ($T = 60\text{ }^{\circ}\text{C}$). b) Recovery stress at different temperature levels during discharging ($\varepsilon_{\text{def}} = 20\%$).

Here, we can use the switch-spring-frame model to explain these results (Chapter 4). The polymer has a physically cross-linkable hard segment and a crystallizable soft segment

(also termed as *switch*). At low temperature, the *switch* represents the well-aligned dense crystalline structure (*off* state), while at high temperature the crystals are molten into free molecular chains (*on* state). The detailed mechanism of the switch-spring-frame model is well explained in the Chapter 4; Figure 4.4.

5.2.2. Free strain recovery

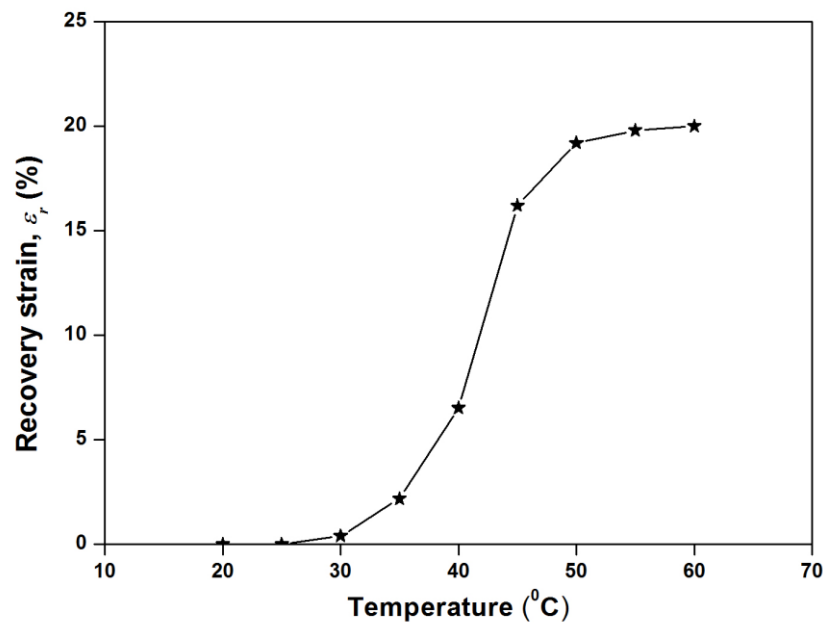


Figure 5.5: Experimental results of the recovered strain (ϵ_r) under no constraint condition

Figure 5.5 shows the free strain recovery (ϵ_r) results of a pre-deformed specimen ($\epsilon_{def} = 20\%$). It can be noticed that, a significant large recovery was observed between the temperature ranges of 35 to 50 °C near the vicinity of transition (T_{trans}) of the polymeric network (~ 42.63 °C). As the temperature increases, the *switches* in the polymeric network gradually release the stored entropic strain [110]. At around 55 °C, all the crystal *switches* (Figure 4.4) are activated which releases all the stored strain.

5.2.3. Moduli at different temperature levels

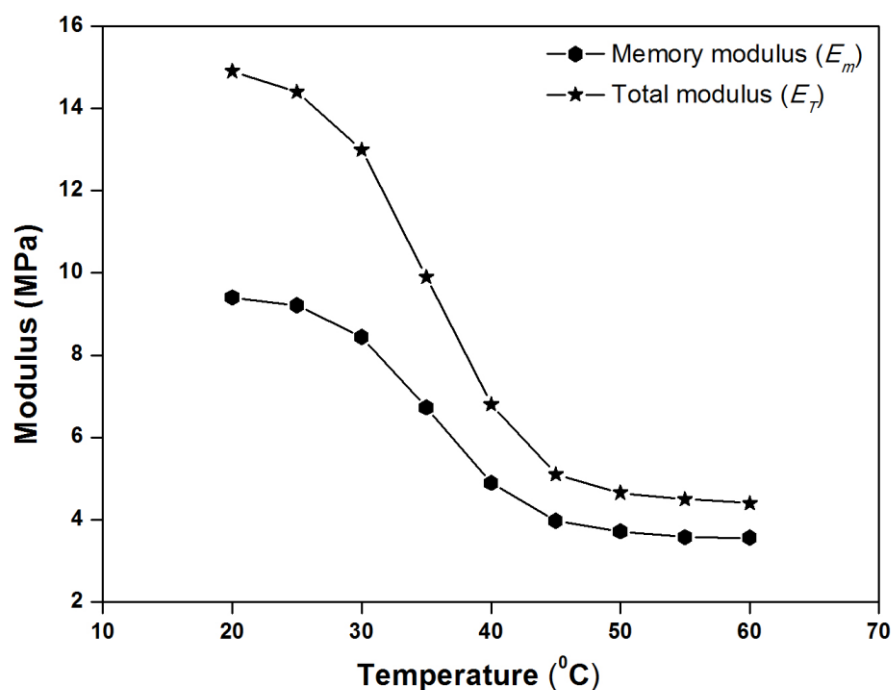


Figure 5.6: Results of initial (IM) and memory modulus (MM) at different temperature levels ($\epsilon_{def} = 20\%$).

Figure 5.6 shows the results of initial or total modulus (IM) and memory modulus (MM) as a function of temperature. The results show higher modulus at lower temperature ($< T_{trans}$). The modulus dropped significantly near the vicinity of temperature range from 30 to 50 °C which is consistent with the microscopic mechanism underlying the transition temperature of the memory polymer. The vitrified chains of soft segments are predominant below T_{trans} which restricts the conformational motion of the MP, inducing high modulus. Above T_{trans} , the melting of crystals allows significant entropic motions within polymer chains resulting in low modulus.

5.2.4. Evolution of thermal stress and strain

The measurement of the thermal stress and strain is well explained in the Chapter 3; section 3.4.5.3. Figure 5.7a and 5.7b shows the results of thermal strain and stress of an unstretched

MP. As shown in Figure 5.7a, the glassy and rubbery linear coefficient of thermal expansions is around $6.5\text{E-}5/^{\circ}\text{C}$ and $1.4\text{E-}4/^{\circ}\text{C}$ respectively.

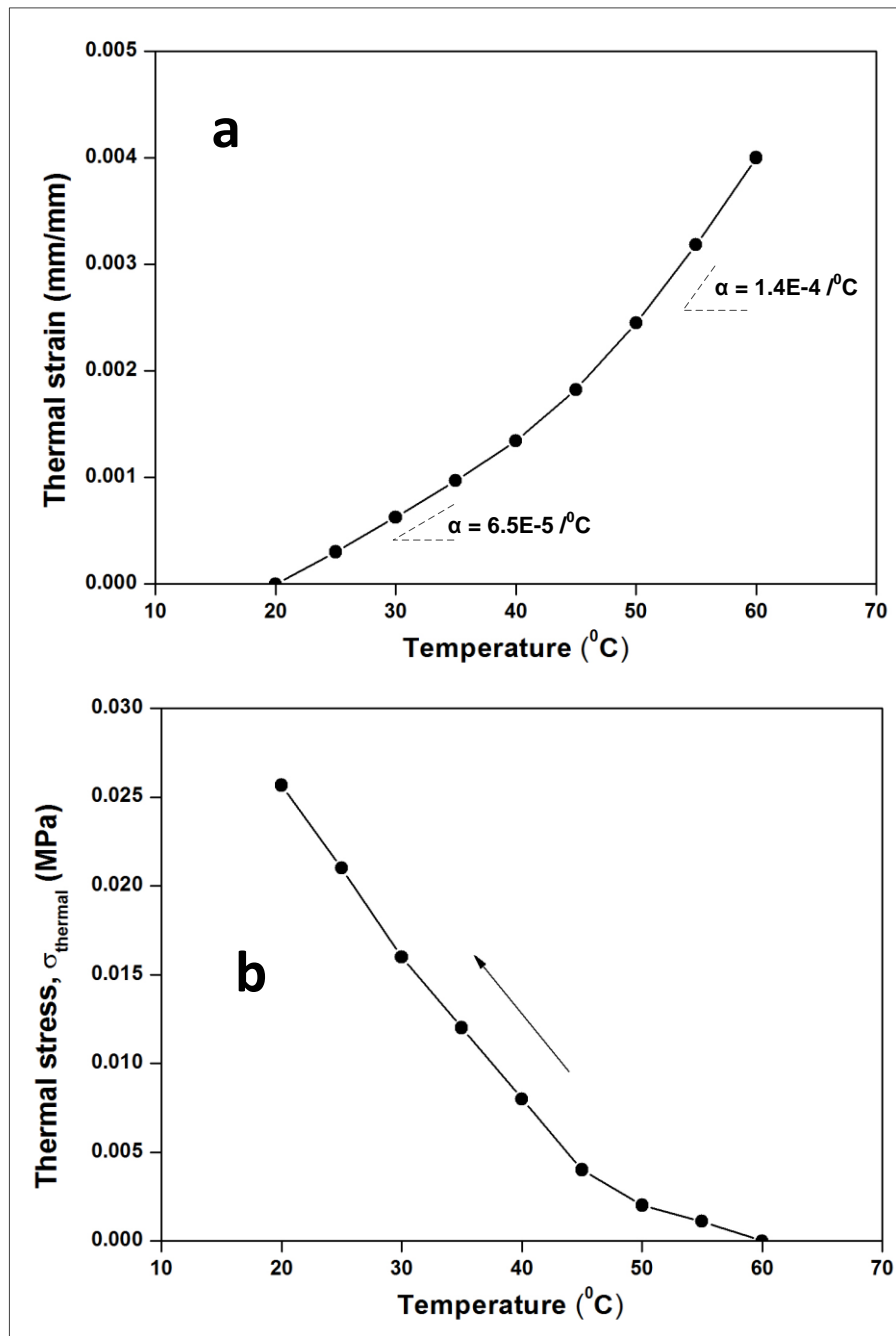


Figure 5.7: Evolution of the thermal strain and stress. a) Thermal strain in an unstretched MP upon heating under no constraint. b) Evolution of thermal stress in an unstretched MP upon cooling under constraint.

Cooling results in thermal contraction, and therefore the thermal stress is generated in an unstretched memory polymeric film specimen, if it is under constraint (Figure 5.7b). However, the amount of thermal stress in the temperature range (20 to 60 °C) is found to be low compared to maximum recovery stress; only 3.6 % of the maximum recovery stress (0.712 MPa; (Figure 5.3/5.4b) at 60 °C temperature. It can be therefore inferred that the maximum contribution of the recovery stress in a programmed memory polymer is due to presence of the memory component.

5.2.5. Stress components during recovery

Based on the above observation of *programmed MP*, the recovery stress σ_r (Figure 5.4a) can be expressed as:

$$\sigma_r = \sigma_m - \sigma_t \quad (5.3)$$

(1) The memory stress σ_m is the contributive part to the total stress as the triggering of the MP increase entropic elasticity inducing contractive nature results in tensile stress under strain constraint. The magnitude of the memory stress depends on the value of the final relaxed stress obtained after stress relaxation (step 2; Figure 5.3). (2) The other part is the thermal stress σ_t whose contribution is impeditive or negative, i.e. decreases the recovery stress. Heating tends to increase the length of the memory polymer, and thereby causes thermal expansion.

Several constitutive models have been discovered to do the stress or strain analysis in the MPs. These models can be classified into two main categories. The first approach is based on phase transition where the polymeric network is considered as active and frozen phases (Chapter 2; section 2.6.1). Based on the ratio of active and frozen parts, the shape memory response can be predicted. The second approach is the thermo-viscoelastic approach, which attributes to the rate-dependent behavior of a polymer and uses spring or dashpot elements

to describe recovery behavior [14, 49, 191, 194]. Herein, we followed the earlier approach based on the phase transition model [5].

Cooling below the transition level (T_{trans}) results in crystals development in soft segment, that transfers external stress from deformation strain (work done externally) into internal forces (energy). Crystal formation depends on temperature as well as the state or level of strain. In fact, the stress memory of the polymer does not only depend on crystallinity, but also the interplay of crystallinity with temperature and deformation strain. The crystal structure for stress memory is not only related to super-cooling, but also heating conditions. In this current work, we employed the heating and cooling conditions which are around transition (T_{trans}) temperature of the memory polymer. Under these common/standard conditions, we can assume that morphological transition of the polymer is uniform throughout the polymer network and path independent, which, to some extent, means that the crystal formation fits to the stress memory requirements where proper /ideal temperature and strains are involved. Otherwise, the results would be quite different.

The phase transition approach is based on the thermodynamics where the change in the internal energy, entropy and dissipation occurs during a thermo-mechanical cycle. The deformation internal energy is converted into a free conformational entropy change during the transition. In the absence of dissipation, it is possible to switch to different states by changing temperature. The internal energy change is related to non-conformational motion captured by frozen phase while entropic conformational motion is the characteristics of the active phase. This transition can be captured by the frozen fraction φ_f which represents the volume fraction of the frozen phase at a given temperature. There exist two limits for φ_f , i.e., $\varphi_f = 0$ and $\varphi_f = 1$, related to extreme temperatures. The zero value refers to the complete melting of the crystals in the soft segment above T_{trans} where, the value at one refers to crystallization of the molten crystals in the amorphous region ($< T_{trans}$). For any other

temperature between the extreme boundaries, both active and frozen phase coexists and the φ_f is temperature dependent which is expressed as:

$$\varphi_f(T) = 1 - \frac{1}{1 + C_f(T_h - T)^n} = \frac{\varepsilon_s}{\varepsilon_{\text{def}}} \quad (5.4)$$

Where, ε_s is the stored strain (i.e, $\varepsilon_{\text{def}} - \varepsilon_r$) at a given temperature. Using the experimental results of the $\varepsilon_s/\varepsilon_{\text{def}}$ (Figure 5.5), the temperature relation of φ_f can be determined. The experimental data $\frac{\varepsilon_s}{\varepsilon_{\text{def}}}$ gives the path of frozen fraction $\varphi_f(T)$ which is sigmoidal in nature (Figure 5.8). And the parameters, C_f and n , are the empirical constants of the phenomenological function chosen to best fit this experimental curve. C_f and n are related to the stress recovery rate separately and collectively, that is, the higher the two values, the quicker the stress recovery when temperature changes. The $\varphi_f(T)$ assists to capture the temperature and strain dependent stress memory behavior in a simplified approach because it is easy to quantify experimentally by strain recovery test (Figure 5.5) to measure the values of stored strain (ε_s) and deformed strain (ε_{def}). Using $\varphi_f(T)$ instead of crystallinity is beneficial in the model to explain stress recovery or storage. The frozen fraction is applied in the model partly because it can integrate all key elements, responsible for stress memory, namely, temperature (programming and recovery), development of strain (initial and stored strain), and crystals (heating and cooling). Furthermore, $\varphi_f(T)$ can model the stress response of MPs with glass (T_g) transition type polymer too, since originally derived by Liu et al. [171] where there is no crystallinity at all.

This φ_f is a good indicator of changing modulus of the polymer network with temperature; at $\varphi_f = 0$ and $\varphi_f = 1$, the modulus is lowest and highest respectively. The modulus can be expressed as:

$$E(T) = \frac{1}{\frac{\varphi_f}{E_i} + \frac{1 - \varphi_f}{E_e}} \quad (5.5)$$

Where, E_i and $E_e (= 3NkT)$ are corresponding to the modulus of an internal energetic deformation ($\varphi_f = 1$) and entropic deformation ($\varphi_f = 0$) respectively. From the experimental results, two different values each for E_i and E_e are available, i.e., during initial stretching and after relaxation. However, the relaxed memory modulus is more reasonable in the present case to predict the stresses of a programmed sample as there is no energy dissipation. The memory and thermal stress components can be determined by using the following relations [191]:

$$\sigma_m = E(T) \cdot \varepsilon_r \cdot (1 - \varphi_f) \quad (5.6)$$

$$\sigma_t = \int_{T_1}^{T_h} E(T) \alpha(T) dT \quad (5.7)$$

Where, $\alpha(T)$ represents the thermal expansion coefficient of the stress memory specimen and T_1 is the ambient temperature used for cooling during tensile experiments (~ 20 °C).

5.2.6. Modelling results

The experimental and modelled results are discussed here in this section. The model coefficients are tabulated in the Table 5.1. Experimental results of free strain recovery are used for the theoretical prediction of φ_f (Figure 5.8 & Eq. 5.4). Figure 5.9 shows the plot of experimental and simulated results of the memory modulus (MM) and initial modulus (IM) modulus as a function of temperature. The maximum change in φ_f and moduli is near the vicinity of T_{trans} . The σ_m and σ_t were calculated using Eq. 5.6 and 5.7 (Figure 5.10 & 5.11). The experimental data are fitting well with the theoretical curve. The memory and thermal

stress is contributive and impeditive parts respectively as described above, and the total recovery stress is calculated using Eq. 5.3.

Table 5.1: Values of model parameters

Coefficients	Unit	Values
n		6
C_f	(1/K ⁴)	3.02E-08
E_i	(MPa)	9.40 (RM), 14.9 (IM)
N ($E_c=3NkT$)	(mol/cm ³)	2.59E+20 (MM), 3.19E+20 (IM)
k (Boltzmann constant)	m ² .kg.s ⁻² .K ⁻¹	1.38E-23

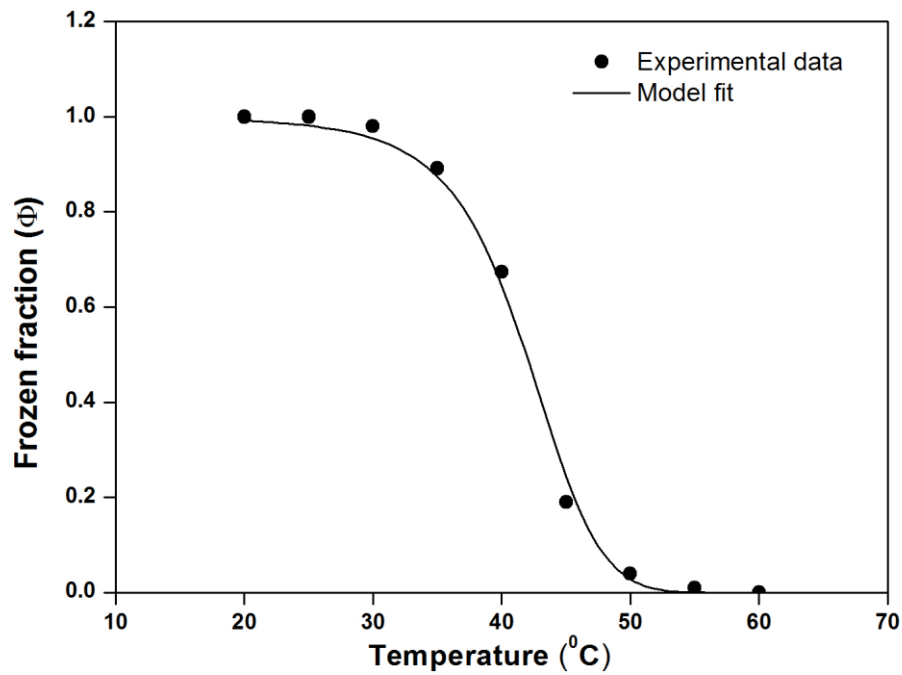


Figure 5.8: Theoretical prediction of the frozen fraction. Model fitting of experimental frozen fraction data to get C_f value for the modulus prediction.

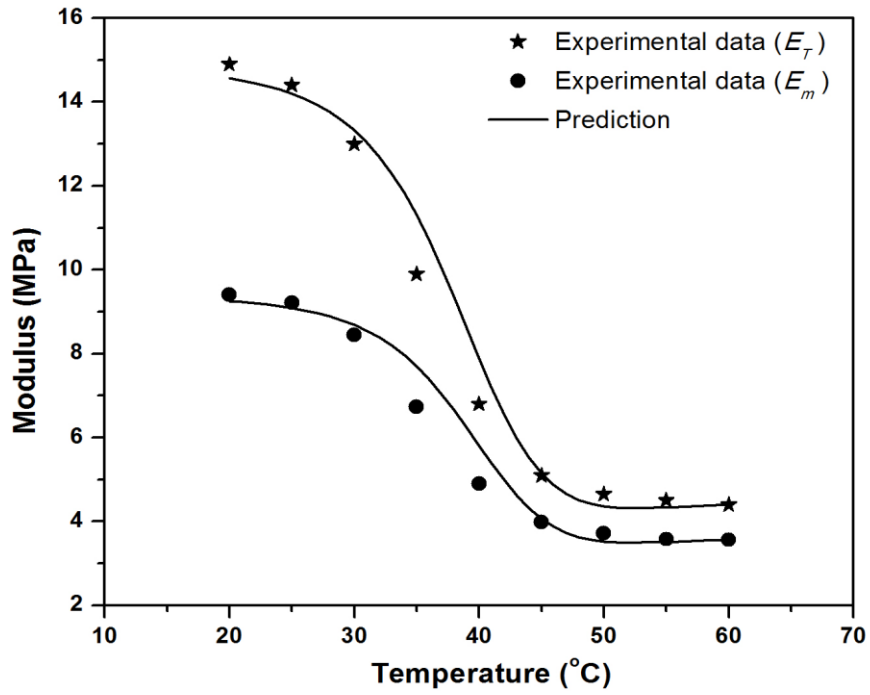


Figure 5.9: Prediction of MM and IM evolution at different temperature levels

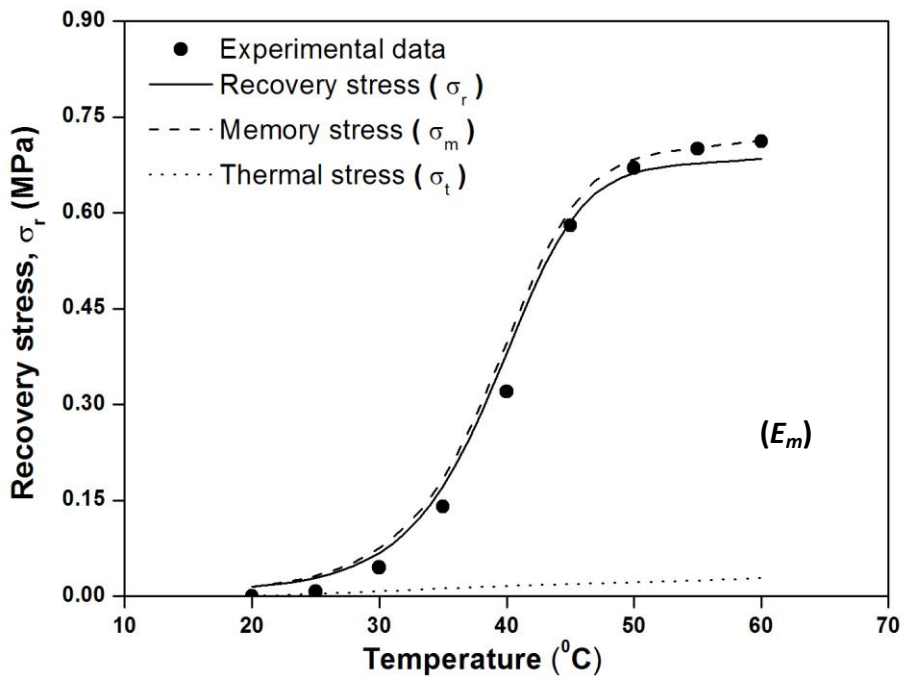


Figure 5.10: Prediction of recovered stress using memory modulus (E_m)

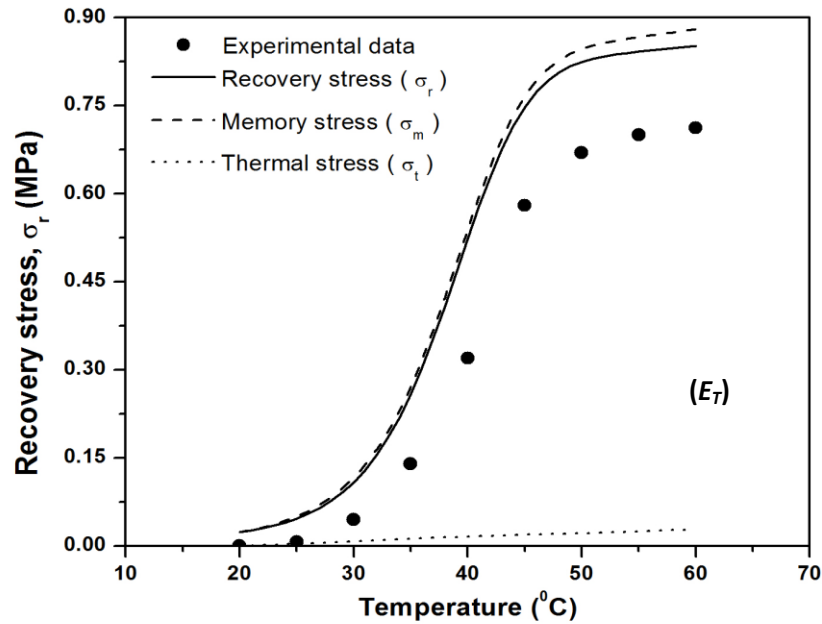


Figure 5.11: Prediction of recovered stress using initial or total modulus (E_T)

In case of tensile programming, thermal expansion of the specimen will affect the recovery stress. The σ_r prediction using MM (Figure 5.10) is in well agreement with the experimental data with maximum difference of 3.87%, rather than using IM (Figure 5.11) with a big deviation of 19.61%. A novel method of finding memory modulus (MM) being presented here is meaningful to use for the prediction of the actual memory/recovery stress. However, the contribution of thermal stress (0.0256 MPa) to the memory stress (0.712 MPa) is comparatively less (3.6%) compared to recovery stress (0.684 MPa). Henceforth, the recovery stress can be regarded as memory stress.

The parameters (Table 5.1) can only describe the stress response for a single strain level, i.e. 20%. The present constitutive model for stress recovery depends on the applied strain. Using the same parameters (Table 5.1), we have attempted to predict the stress behavior for other strain levels, i.e. 10% (Figure 5.12a) and 50% (Figure 5.12b). It can be observed that the prediction is underestimating the stress recovery at lower strain (10%) and

overestimating the stress at higher strain (50%). This inferred that the model does not capture the strain-independent phenomena. It is therefore recommended to calculate the model parameters at individual strain for accurate description of the stress recovery.

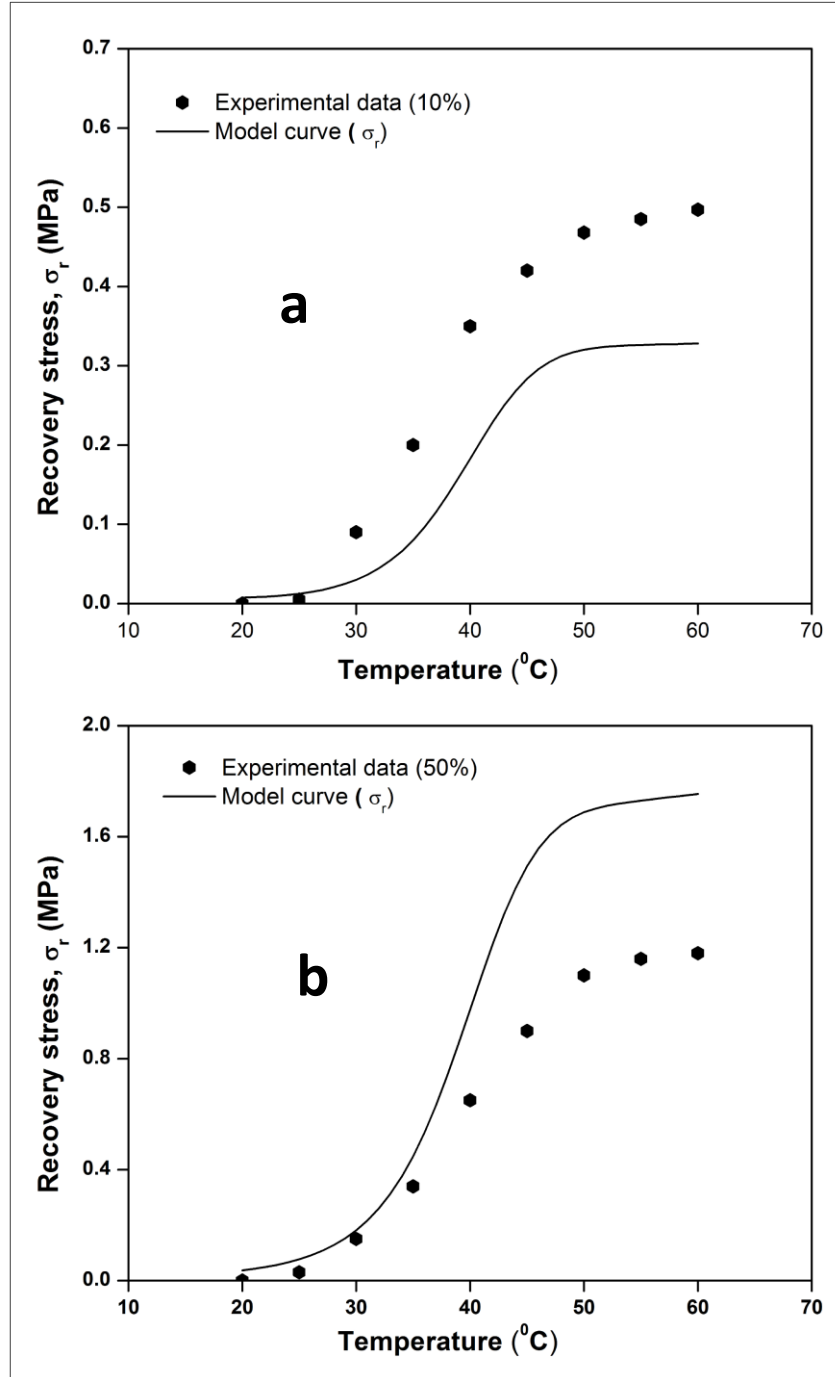


Figure 5.12: Model prediction at different strain levels (10% and 50% strain). Same model parameters (obtained at 20% strain; Table 5.1) are used to plot the model curves for different strains.

Most of the polymers shows non-linear viscoelasticity, and hence different amount of stress relaxation are expected at different applied strains. More relaxation is expected at higher strains as compared to lower strain. These differences are not captured by the model, and therefore the parameters, shown in Table 5.1, are restricted to one strain level, i.e. 20%.

This constitutive analysis on the *stress memory* could have direct impact on the designing and engineering of the MP actuators for some real applications such as in pressure bandage or massage devices. One can modulate the stress magnitude and also maintained it for long time to deliver a sustained compression required for venous ulcers [195, 196]. A stable and dynamic stress cycles can be obtained for the massaging related to orthopedic problems such as muscle spasms, cramps, and aches. Furthermore, the compression level exerted by the memory product on the affected body portion can be predicted using the above constitutive model. The interface pressure exerted by a compression product is primarily dependent on the stress in the material [61, 197, 198]; therefore, the variation of pressure at different triggering temperatures can be obtained.

5.3. Application of Stress-Memory Analysis

To practically apply the constituent analysis of stress memory, a bandage prototype was designed and using the same memory polymeric film which was used for the theoretical analysis. Figure 5.13 shows the detailed embodiment of the bandage and it has basically 3 parts; 1) base fabric, 2) MP film actuator, 3) heating unit. The layers of base fabric are a normal woven fabric made from polyester yarns. The MPU film is used as the actuator for compression. For the heating element, a normal electrical heating wire made of copper (diameter = 1.8 mm; resistivity = $1.68 \times 10^{-8} \Omega \cdot \text{cm}$) was used. The wire is first twisted and secured using plastic tape fasteners, and then embedded between the fabric layers. The path

of the embedded wire was shaped as square wave to obtain uniform temperature distribution (Figure 5.13b). This design does not significantly affect the mechanical property of the device and allows sufficient flexibility for easy wrapping of the prototype over a curved surface. Carbon nanotubes or other fillers can also be used to generate heat, but these particles can compromise the mechanical properties of the MPU. The fabric layers were then stitched together along the seams to secure the location of the heating layer for safety and tactile comfort.

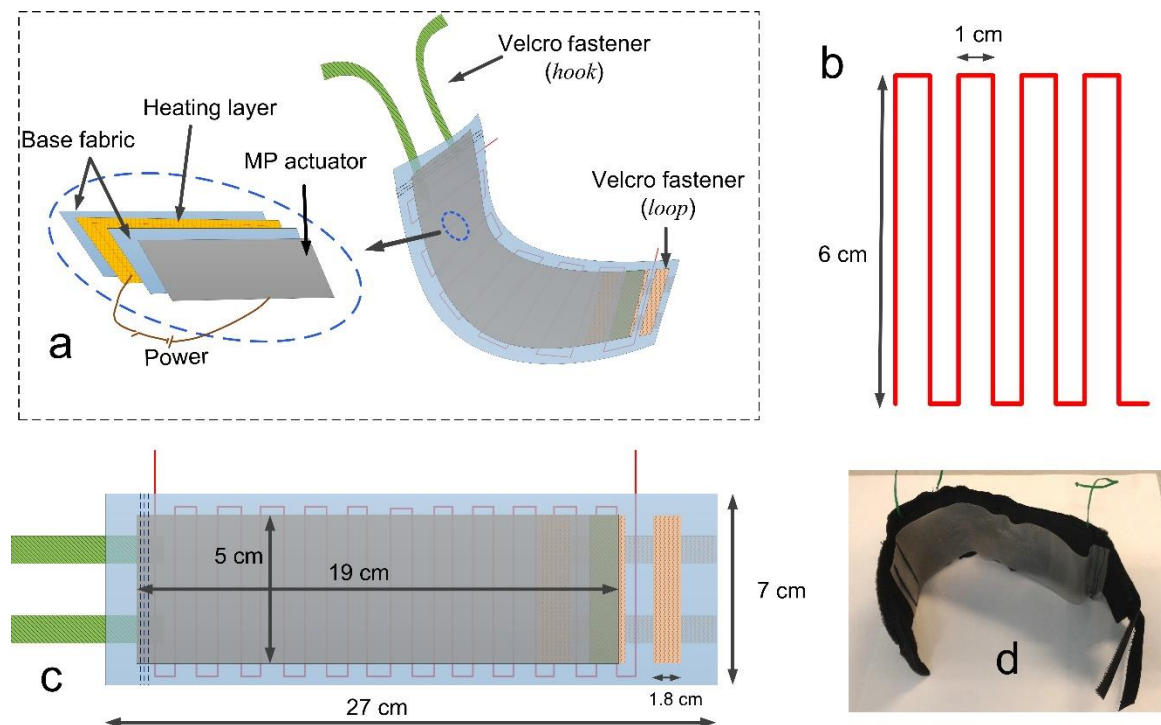


Figure 5.13: Embodiment of the memory bandage. a) Schematic of the proto type, b) Arrangement of embedded electric heating wire, c) Top view, d) Photograph of the prototype

The MPU film actuator was then integrated with the base fabric using a Velcro *hook* and *loop* system attached to the film and fabric respectively. The Velcro strip (*hook*) is stitched to the end of the film along its width, and several Velcro strips (*loop*) to the fabric at different locations as shown in the Figure 5.13c, thus allowing different sizes or different

magnitudes of pressure. If just the thermal therapy is needed, one can detach the MPU actuator. In its fully developed form, the prototype can be easily wrapped onto the body part and held in position by the Velcro fasteners.

For the power supply to the heating wire, a single output DC power source (MCH model K3050) was used with variable voltage levels up to 30 V. To test the performance, the assembled prototype was wrapped on a solid tube (circumference: 23.5 cm) mimicking the body part that also provides an external constraint (strain) to the MPU actuator. The temperature change on the surface of the device at different voltage levels is measured using a digital infrared thermometer (Fluke 62 MAX; Model no: 130474), and the pressure measurement was done using a KikuhimeTM pressure sensor. The experimental set-up is shown in Figure 5.14.

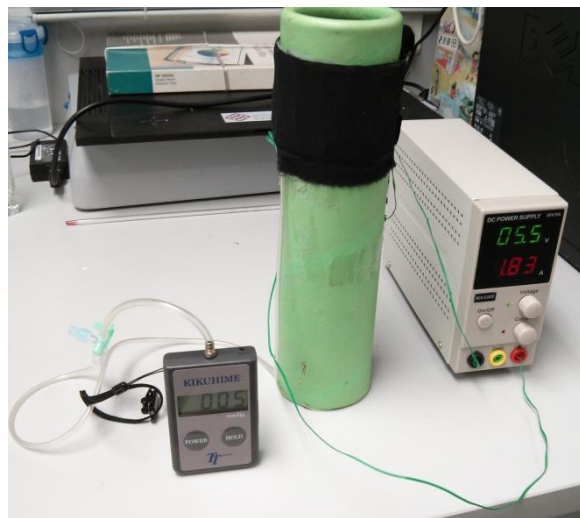


Figure 5.14: Experimental set-up for pressure measurement

5.3.1. Theoretical and design considerations for the MP actuator

If a compression bandage is mounted over a curved body section (limb or neck), the applied interface pressure is related to the properties of bandage and body part known as the Laplace Law: [61, 198, 199]

$$P = \frac{\sigma \times h}{r} \quad (5.8)$$

Where, P is the interfacial pressure (N/m^2), σ is the internal stress (N/m^2) in the bandage and h is its thickness, and r the radius of the limb. Once the bandage is stretched to fit to a limb, a constraint (strain) and hence a stress σ is established in the bandage. It is therefore possible to predict the amount of pressure P the bandage exerted on the limb, once the amount of the stress σ is known. However due to the plastic and viscoelastic nature of the material, both strain and stress developed in the bandage are fading away with time - the stress reduction in a MPU actuator as high as more than 50% at temperature $> T_{trans}$ has been reported in [50]. So even a desired pressure level P is selected initially, it will inevitably decline, unless of course a stress memory polymer is used which can “remember” and hence compensate the initial internal stress σ , controlled by an actuating heat trigger so as to maintain externally the applied pressure P .

5.3.2. Experimental and modeled results of memory actuator/bandage

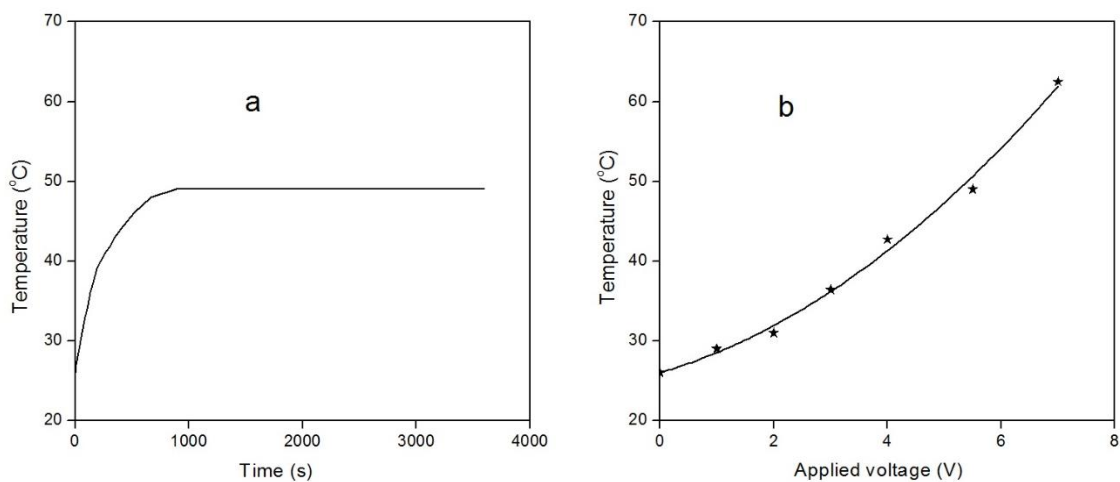


Figure 5.15: a) Variation of surface temperature with time (5.5 V). b) Results of maximum surface temperature with applied voltage.

For the heating therapy, the surface temperature of the prototype bandage is recorded in Figure 5.15a, where for a given applied voltage level, the temperature starts increasing and then levels off in a relatively short interval of time (< 10 min). Thereafter, the temperature is stabilized, and the prototype can hold the temperature level for desired period. The applied electric voltage can be altered to achieve different temperatures (Figure 5.15b). The configuration of the embedded wire (square wave; Figure 5.13b) helps to maintain a uniform temperature distribution over the area as required when using MPU [200]; this was also confirmed after examining the temperature at multiple locations on the prototype using a digital infrared thermometer.

Table 5.2: Values of model parameters used for pressure prediction

Parameters	Unit	Values
r (radius of cylinder)	m	3.74E-2
h (film thickness)	m	4E-4

Once the prototype is wrapped across a curved surface as in Figure 5.14 and the power source for the heating wire is switched on, the programmed MPU actuator starts to activate to generate compression. The pressure prediction was done using the equations obtained (Eq. 5.3 to 5.8) and Table 1 & 2 lists the values of the parameters used. Corresponding to the temperature profile in Figure 5.15a, Figure 5.16 shows the interfacial pressure developed by the prototype due to the recovered stress in the MPU. This adds to the inward pressure to the cylinder as described by Laplace's law (Eq. 5.8). Different pressure levels were achieved by adjusting the surface temperature as indicated in Figure 5.17, where a

consistent agreement is also shown in comparison between the predicted and actual results of the pressure against the temperature.

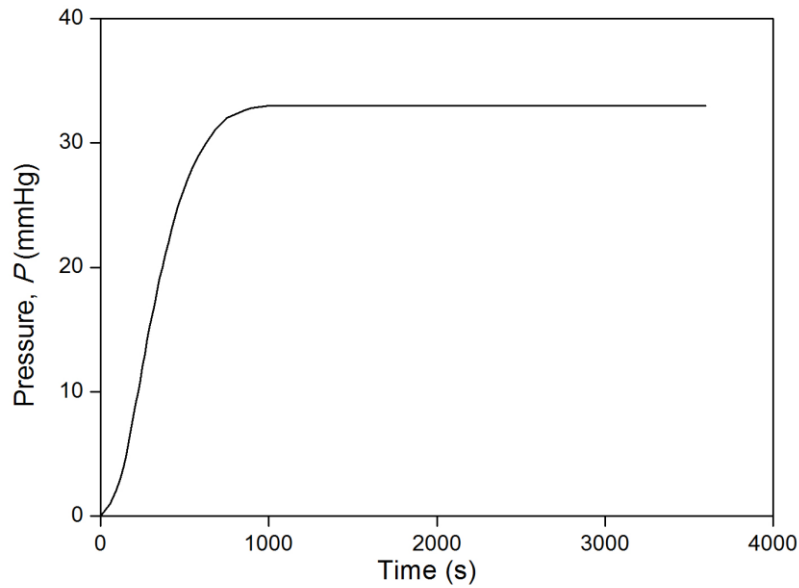


Figure 5.16: Experimental result of pressure variation over time.

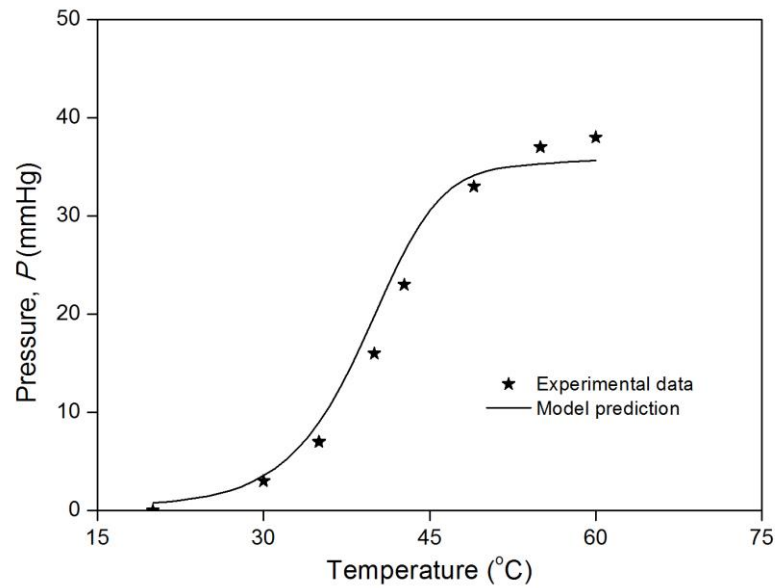


Figure 5.17: Experimental and theoretical predicted results of pressure at different levels of temperature.

The pressure response to temperature change in Figure 5.17, around 35-45 °C is the most significant to show the consistence with the microscopic mechanism underlying the glass

transition (~ 42.63 °C) of the MPU. For actual compression therapy, the pressure range from 20 to 60 mmHg is needed depending on the severity of the venous disease at the affected limb (36). According to Eq. 5.8, this pressure range can be achieved by changing the thickness of the bandage, or controlling the recovery stress via either the strain (5-20%) or the temperature (30- 60 °C) levels; both are in the desirable limits of the model validity and overheating of the body surface. Apart from static compression benefits, the prototype can also deliver dynamic cyclic compression if an alternating temperature variation is provided. Figure 5.18 shows the dynamic results of compression obtained from this prototype after power supply is sequentially ON and OFF for 900 seconds each, highly repeatable and steady.

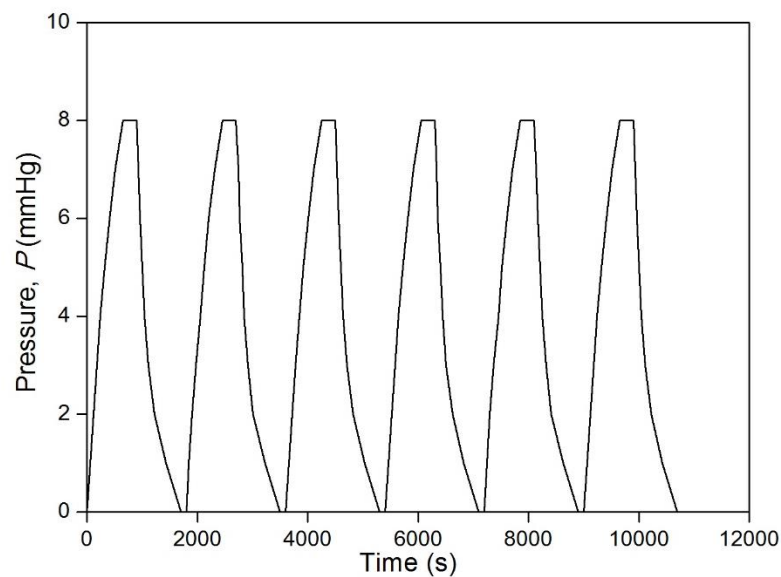


Figure 5.18: Dynamic compression using prototype (2.5 V; $\epsilon_{pre}=10\%$; Heating/cooling time = 900 s)

5.3.3. Limitations of the memory actuator/bandage

Several limitations must be born in mind before advocating the above prototype as a potential commercial product. The breathability of the prototype can be a potential issue as the MPU film actuator has very limited permeability if the covered area is too large; in the

case of static pressure, the compression is recommended for an extended time (> 10 hour), and the tolerance of the patient must be considered. Converting the MPU into filaments to develop fabric structure with good porosity could potentially eliminate the above problem. The second limitation is the validity of the uniaxial tensile model in dealing with the tensioned contact problem used in this study. Also, a solid tube is used here for pressure measurement; however, if the MPU is used onto a body part, the condition of fixed constraint may not be true as the underlying soft tissues can easily deform. The third limitation is due to the relatively slow activation of the MPU, thus restricting the duration of the massage cycle. Currently, dynamic compression is provided by pneumatic or mechanical system where a very fast response can be obtained. As an example, the massage cycle for the intermittent pneumatic compression (IPC) device ranges from 30 to 180 seconds. However, the above prototype takes a much longer time (> 10 min) to complete a massage cycle. So, development of MP with quick response is highly desirable.

5.4. Summary

The *stress-memory* behavior of semi-crystalline polyurethane is systematically investigated both experimentally and analytically using thermo-mechanics based constitutive model. The simulated results are significant and in well coherence with the experimental data. Following points can be highlighted based on the above study:

- 1) Elimination of plasticity, viscoelasticity, and elasticity are important to obtain a pure stress memory results from a MP actuator. In the programmed MP, the stress evolution during heating is exactly the reverse process of the stress freezing during cooling with no energy dissipation.
- 2) Stress components including memory and thermal stress, are aroused upon recovery in a tensile programming. The memory and thermal stress are contributive and impeditive to the total recovery stress respectively.

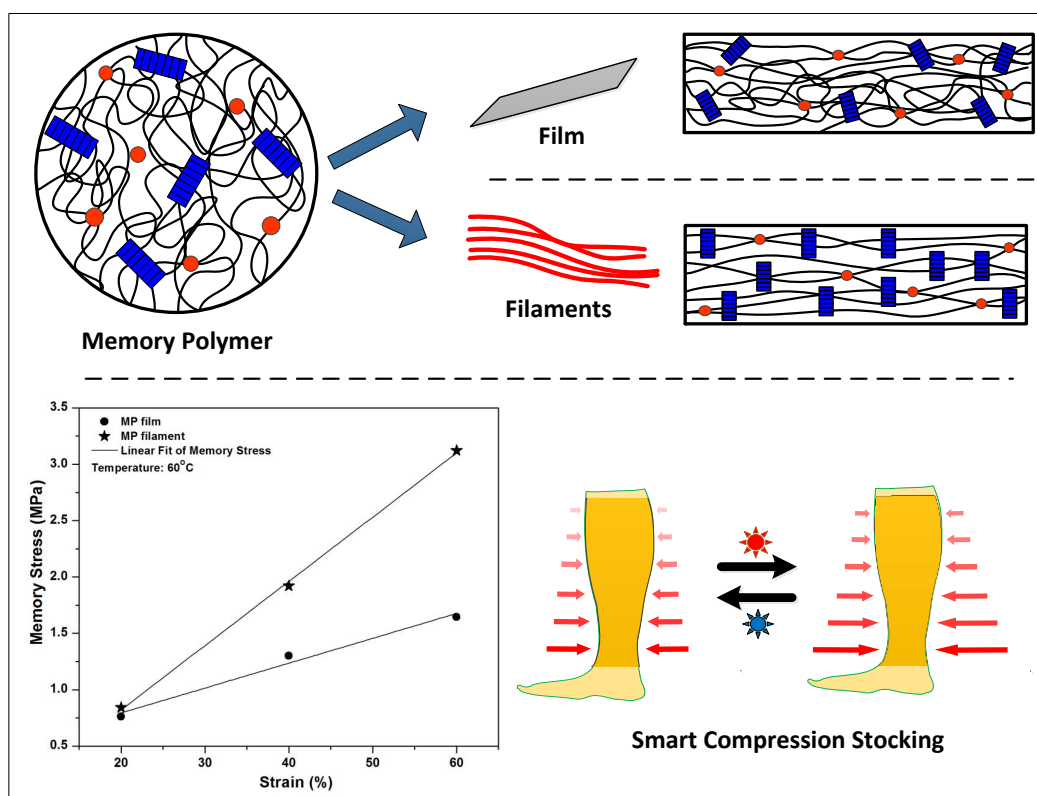
- 3) The maximum transition of the ϕ_f , moduli, recovered strain and recovered stress occur in the vicinity of the T_{trans} of the MP.
- 4) The proposed scheme to find the Memory modulus (MM) should be preferred for the prediction of the actual recovery/memory stress.
- 5) The smart bandage provides multi-functional benefits such as heating therapy, static and massage pressure, and selective pressure control.

There are a few limitations in using this MPU-based smart compression bandage. First, like any thermal technique, the system response is relatively slow. In addition, lack of air permeability of the membrane presents a comfort concern when employed on larger area and over long period of time. These may limit the application of this product in certain cases. Finally, the original theoretical model assumed a uniaxial tension, and the pressure measurements in this work used a solid substrate in contact with the MPU, future modifications are expected when dealing with soft human body parts.

CHAPTER 6: STRESS-MEMORY FILAMENTS FOR ADVANCED COMPRESSION THERAPY

Highlights of the Chapter

For the first time, the novel stress memory behavior is revealed at filament/fiber level based on semi-crystalline memory polymer in this chapter. PHA-3000 based memory polymer was synthesized and prepared film and melt spun filaments for the comparison. The evolution of memory stress is studied with comprehensive thermal, mechanical, and structural characterizations. The stress memory behavior is also realized in the filaments integrative smart compression stockings with pressure related studies.³



³Relevant Publication

Narayana, H., J.L. Hu, B. Kumar, S. Shang, J. Han, P. Liu, T. Lin, F. Ji and Y. Zhu (2017). "Stress-memory polymeric filaments for advanced compression therapy." *Journal of Materials Chemistry B* 5(10): 1905-1916.

6.1. Introduction

Smart fibers can sense, react, and adapt in response to an external stimulus such as thermal, electrical, and magnetic field. Fibers are basically a fine substance having high ratio of length to its thickness. Shape memory polymers (SMPs) are one of the major category in smart materials which have been attracting the researchers from both academia and industry due to their fascinating behavior [1, 5, 201, 202]. SMPs can be deformed, fixed, and recovered spontaneously from a temporary shape upon an external stimulus such as heat, light, and solvent [11, 14]. Other than shape, SMPs also provide the platform to program, store, and retrieve other physical parameters such as stress (stress-memory) [40], temperature (temperature-memory) [90], chrome (chrome-memory) [41], and electricity (electric-memory) [91]. Hence, these smart polymeric systems could also be termed as memory polymers (MPs). MPs can also be spun into filaments via melt, dry, wet, electro, and reaction spinning methods [78, 95]. Recent research works in MP fibers have been focused into vivid applications such as fiber supercapacitors [99], bone tissue engineering [203], vibration damping structures [101], self-healing fibers [204], composites [205], and other functional yarns [110].

Considerable research work has been done on synthesis, processing, and characterizing shape memory and physical properties of MP filaments (MPFs) over a decade. Hu et al. have versatile experience in synthesizing MPs and developed fibers with applied science and technology to implement into various textile applications [14, 27, 28, 92]. Agrawal et al. studied the effect of post spinning operations on fiber morphology of polyol based MPFs [206]. Zhu et al. have compared MPFs with other manmade fibers and engineered melt spun MPFs to enhance the complete shape recoverability [207]. Whereas, Meng et al. investigated the influence of spinning method/post treatments on fiber morphology, phase separation, thermal, and mechanical properties of melt and wet spun MPFs [93, 95-97]. In

addition, their further study was directed to produce filament with thermally sensitive internal diameter suitable for smart functions such as smart filtration and controlled drug release [208]. In the later stage, Nano MPFs were also electro-spun towards application into antibacterial nanomaterials and nonwovens [209-211]. (Well discussed in chapter 2)

To date, all the current available research works in MP fibers are completely focused and limited to only development via different polymerization and spinning methods to investigate their shape-memory, thermal and mechanical properties. Nobody has attempted to unveil their unique stress-memory behavior other than shape-memory properties specifically at filament level.

As discussed in the Chapter 4 and 5, pure memory stress can be derived from memory polymers to utilize as meaningful signals in the applications such as compression devices [56, 212]. Ahmad et al. have developed a compression bandage using thermal sensitive shape memory polymeric film as an actuator and studied the feasibility. They encountered a huge and significant pressure loss (up to 80%) over time and the reason could be ascribed to presence of impeditive component called viscous stress. This kind of devices have considerable limitations such as not breathable, unavoidable stress relaxation, and instability of pressure with no external readjustment. This implies that there is a need of more scientific way to address the problem. Smart stress-memory programming technique can eliminate all impeditive components and to have pure memory stress. Comprehensive understanding of fundamental stress-memory behavior in MP filaments and integrating them into suitable structure could undoubtedly overcome several limitations.

In this current study, the more importance has been given to study the response of memory stress (M.S) in thermal sensitive semi-crystalline segmented polyurethane filaments and film with melting type transition (T_m). The MPs were bulk polymerized and spun into filaments via melt spinning method. The response of M.S at different strain level (20, 40,

and 60%) was experimentally studied as a function of temperature with time. The thermal, mechanical, and structural properties were also comprehensively characterized by FTIR, DSC, and XRD for comparison and to comprehend the underlying relationships with evolution of memory stress. Pressure related studies were carried out in MPFs integrative stockings to confirm this unique behavior. Based on the memory behavior of MPFs as a function of temperature and strain, compression stockings can be precisely tailored for smart compression management. Systematic characterization and comprehending the underlying physics of filaments is very much crucial and prerequisite step towards optimization of M.S required for smart compression benefits.

6.2. Experimental Results and Discussion of MP Film and Filaments

6.2.1. Mechanical properties of MP filaments

The mechanical tensile testing of MPFs were carried out in the standard testing condition and the results are tabulated in the Table 6.1 below. The melt spun filaments are having the average tenacity of 0.567 cN/dtex with 142% of breaking elongation. In general, melt spun MPFs have a good phase separation with hard segment stability compared to wet or dry spun MPFs and high molecular weight soft segment content allows to have good stretchability [95]. The study is still underway towards optimizing the mechanical properties of MPFs and it can be achieved with optimum spinning conditions and further post treatment process such as heat setting.

Table 6.1: Mechanical properties of MP filament

Sample	Linear density (Denier)	Tenacity at break (cN/dtex)	Elongation at break (%)	Initial modulus (cN/dtex)
Melt spun MPF	150	0.567	142	0.918

dtex: weight in grams of 10 kilometers of length.

6.2.2. FTIR Analysis of Memory Polymeric Film and MPFs

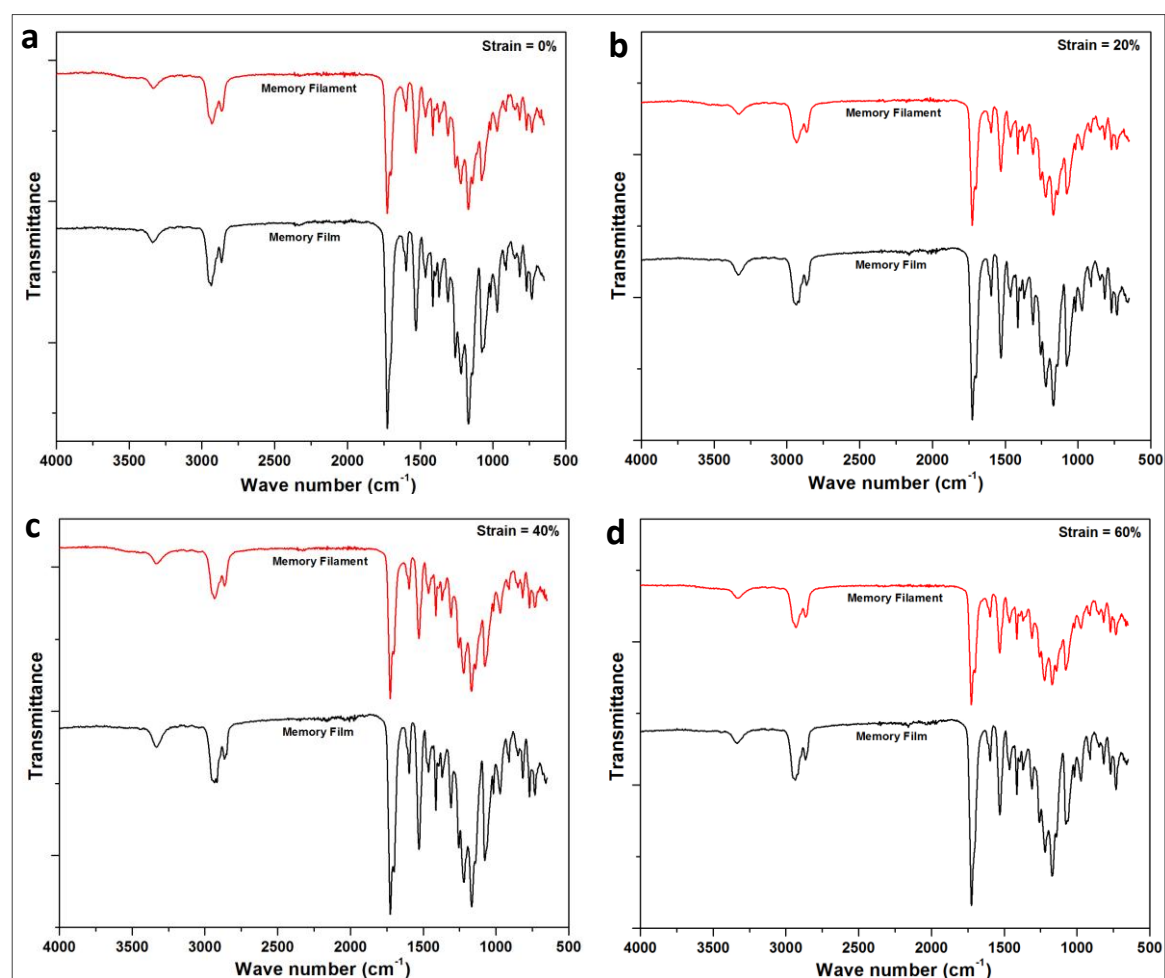


Figure 6.1: FTIR spectra of memory polymeric film and filaments at different programmed strain levels.

The Fourier transform infrared (FTIR) spectra of MP film and filament are shown in Figure 6.1. The absence of band at 2250–2270 cm^{-1} is indicated that there is no free -NCO group present in the polymer structure, which suggests completion of the reaction. The most important characteristic features of MP are the band at 1075-1079 cm^{-1} (C–N stretching vibrations), 1166-1171 cm^{-1} (C–O stretching vibrations), 1527-1531 cm^{-1} (C–N stretching and N–H bending character), 1724-1729 cm^{-1} (C=O stretching vibrations from urethane groups), 2861-2866 cm^{-1} (CH_2 symmetric stretching vibrations), 2929-2935 cm^{-1} (anti-symmetric stretching and 3430 cm^{-1} (O–H free and N–H stretching from urethane group stretching vibrations). Presence of those bands in MP reflects the formation of urethane linkage, (-NH-C(=O)-O-). There was no significant change found in the IR spectra for programmed specimens at different strains [213, 214].

6.2.3. Thermal Properties of MP Film and MPFs

Reversible soft segment phase could be theoretically either amorphous or crystalline and which decide the transition type [14]. Here in this study, crystalline 1,6-poly (hexamethylene adipate) diol as a soft segment with melting (T_m) transition type and MDI/BDO was used as hard segment content. The thermal properties of both MP film and filaments were investigated by DSC and tabulated in Table 6.2. Where, ΔH_m and ΔH_c refers to enthalpy of melting and cooling curves.

Table 6.2: Thermal properties of MP film and filament.

Sample	T_m	ΔH_m	ΔH_c
	(°C)	(J.g ⁻¹)	
MP Film	41.77	15.9	-19.91
MP Filament	42.05	17.71	-29.42

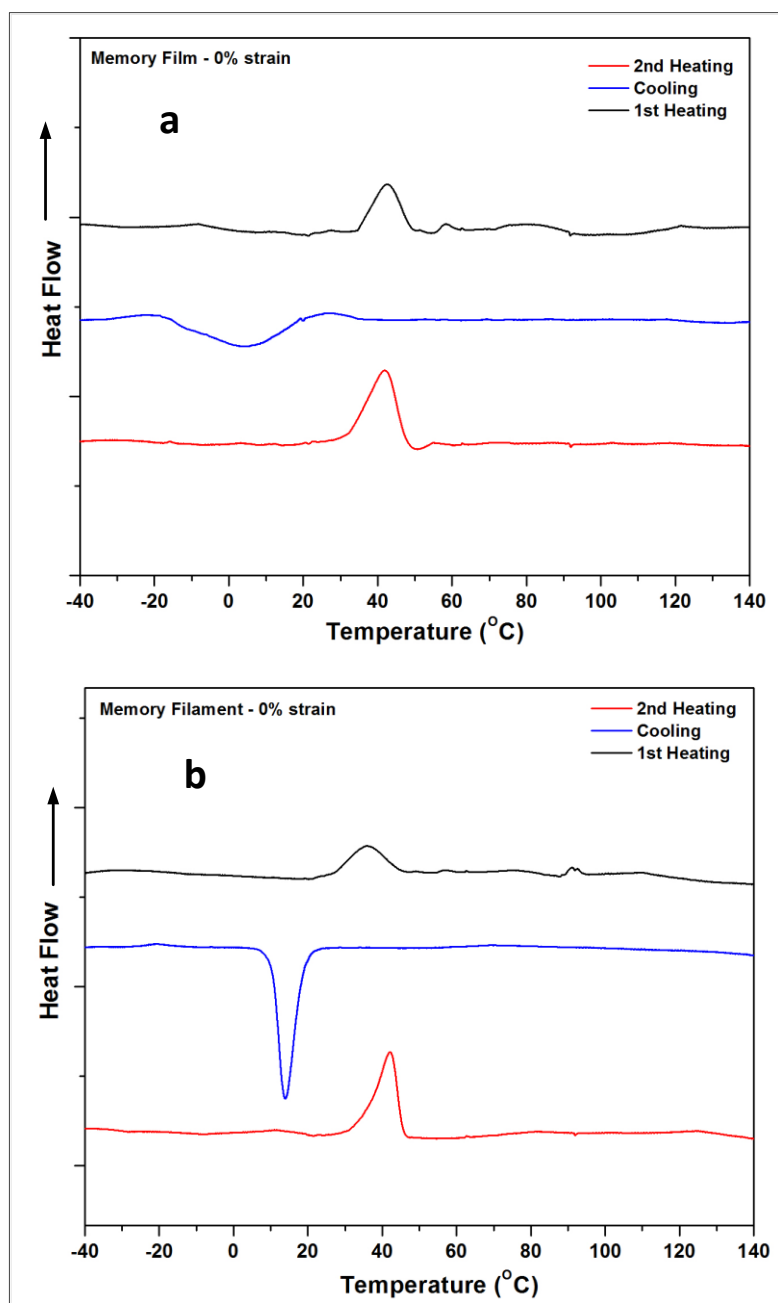


Figure 6.2: DSC thermograms of film (a) and filament (b).

Figure 6.2 shows the DSC thermograms of both MP film and filaments and each graph is showing three curves; 1st heating, cooling, and 2nd heating. Second heating is considered to determine the peak value transition to avoid the previous thermal history. At higher temperature both specimens showed apparent melting transitions, and which were attributed to melting of soft segment phase. The detailed thermal properties of the specimens are tabulated in Table 6.2. It is visible that the peaks of heating and cooling

curves are more prominent in the filaments compared to film. The higher melting transition temperature of soft segment and more prominent peak during cooling indicates that melt spinning has induced perfect crystallinity to the filaments. Simultaneously, MPFs shown higher melting enthalpy (heat of fusion) compared to film and it suggests that melt spinning has induced more ordered and packaged region in the material.

6.2.4. Thermo-mechanical properties

The experimental results of thermo-mechanical cyclic tests are summarized and depicted in Table 6.3 and Figure 6.3 respectively.

Table 6.3: Thermo-mechanical cyclic properties of film and filament

Sample	Fixed strain, ϵ_u (%)	Plasticity, ϵ_p (%)	Shape fixity, R_f (%)	Shape recovery, R_r (%)
MP film	88	17.5	88	82.5
MP filament	82	24	82	76

Shape memory properties of MP film and filaments were examined with series of thermo-mechanical cyclic tests and it is evident that both are having similar behavior. It can be seen from Table 6.3 and Figure 6.3 that film is having higher shape fixity and recovery ratios in comparison with filaments. Figure 6.3 represents five cycles of thermos-mechanical test results and the readings are obtained from the fifth or last cycle. It should be noted that the level of stress is higher in filaments and it would enhance the recovery stress in further stress memory programming and the reason could be ascribed to improved molecular orientation, crystallization, and stability of physically cross-linked networks. Increased level of stress and incapability to freeze the total stress at room temperature might have

caused to get the reduced shape fixity in MPFs [215]. Further optimization in synthesis and spinning conditions would help to improve the shape memory properties.

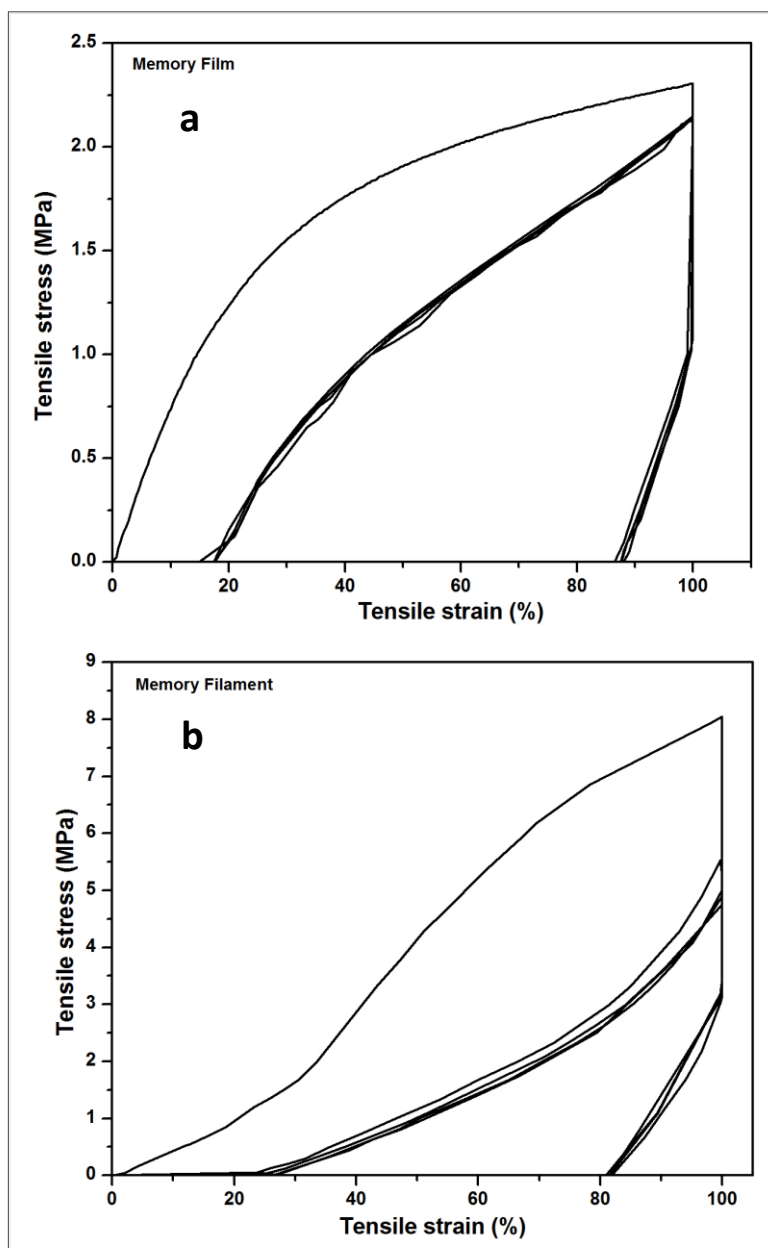


Figure 6.3: Thermo-mechanical cyclic test curves of MP film (a) and filaments (b). Note: Curves plotted for single filament in (b).

6.2.5. Stress-memory response in MP Film and Filament

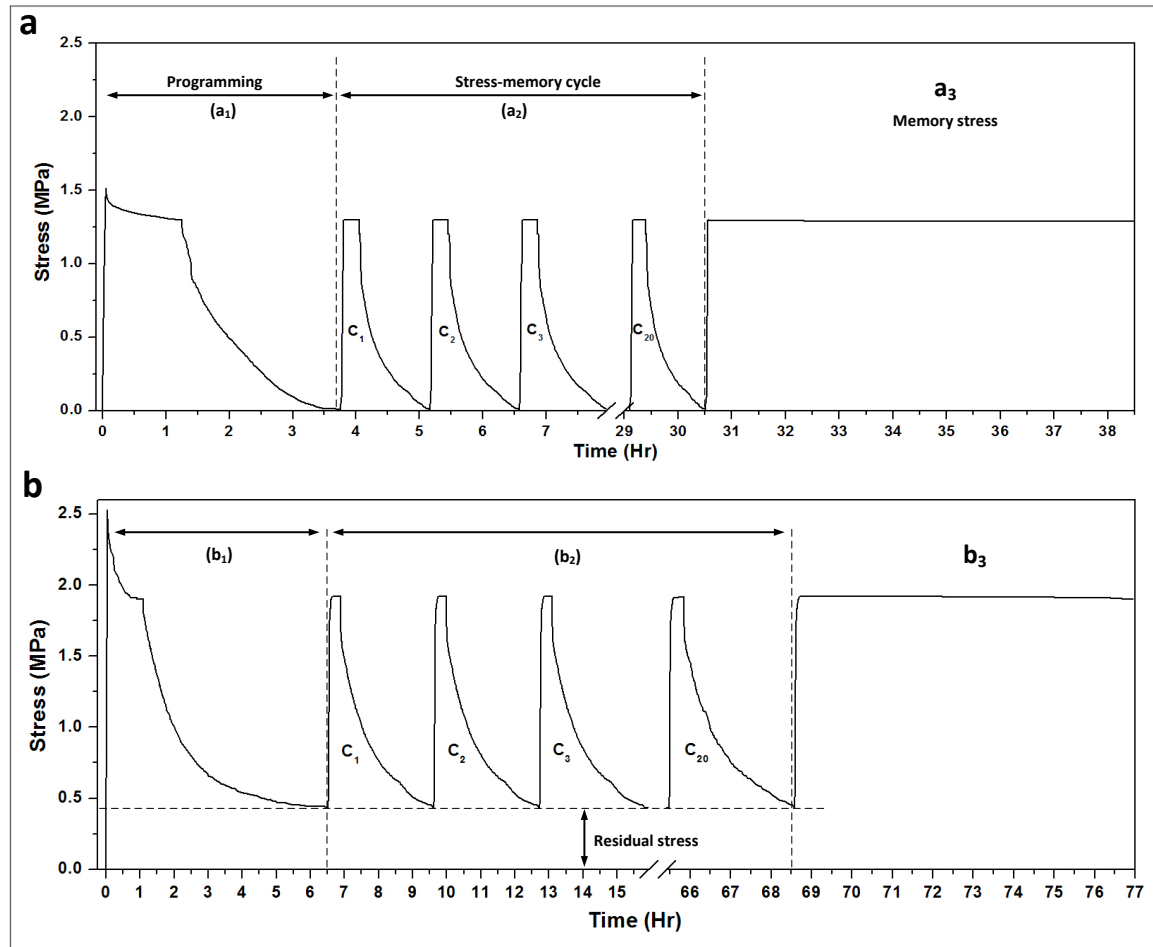


Figure 6.4: Experimental results of stress-memory response in MPs. Stress-time profile of MP film (a), and filament (b). (a₁, b₁) Programming process; (a₂, b₂) Cyclic response of M.S; (a₃, b₃) Time dependent behavior of M.S with heat stimulus.

Stress-memory is a novel phenomenon, which can be achieved by smart programming process and comprehensive steps are discussed in the Chapter 3 (Section 3.4.2). Figure 6.4 illustrates the experimental results of programming (a₁,b₁), cyclic (a₂,b₂), and time dependent (a₃, b₃) nature of M.S in film and MPFs with response to an external heat stimulus. Deformation during the thermo-mechanical process induces 5 major components in MPs and they are plasticity (ϵ_p), visco-elasticity (ϵ_v), memory (ϵ_m), elasticity (ϵ_e), and

thermal strain (ε_t) (Eq. 6.1). Whereas stress components (Eq. 6.2) are viscous (σ_v), memory (σ_m), elastic or residual (σ_e), and thermal stress (σ_t) [168]. (Well discussed in Chapter 5)

$$\varepsilon_{Total} = \varepsilon_p + \varepsilon_v + \varepsilon_m + \varepsilon_e \pm \varepsilon_t \quad (6.1)$$

$$\sigma_{Total} = \sigma_v + \sigma_m + \sigma_e \pm \sigma_t \quad (6.2)$$

The programmed stress will be stored in the polymer matrix during cooling the deformed specimen and it is imperative to nullify impeditive or negative components other than memory component to obtain pure M.S. Thermo-mechanical cyclic testing was done at higher strain than the programming strain level (Figure 6.3) to remove the plasticity and elasticity. Figure 6.4(a₁), (b₁) shows the stress relaxation process at higher temperature and constraint strain, where viscous stress was eliminated and followed the stabilized line in the graph. However, thermal stress is an impeditive component in the tensile programming, results from the thermal expansion of the material and it is negligible also unavoidable [168]. Further M.S was reached to zero in MP film (Figure 6.4a) and it indicates storage of pure M.S in the polymeric network assisted by vitrification (crystallization) process. Whereas stress level was reached plateau during cooling with some residual stress in MPFs (Figure 6.4b) and this will be discussed in detail in the next section. The stored M.S was further recovered to maximum peak level triggered by heat stimulus and it can be noticed that the level of stress is equal to relaxed stress ((Figure 6.4(a₁), (b₁)) obtained before cooling. Interestingly, the actuation time was less than 2 minutes to reach the peak stress level. The recovered stress can be stored and retrieved for several cycles to exhibit stress-memory nature ((Figure 6.4 (a₂), (b₂)) and the repeatability was investigated up to 20 cycles ((Figure 6.4 (a₃), (b₃)). This behavior is a prime important factor and would enable MPFs for constituting the massage effect in the smart compression stockings at a fixed deformation level. In addition, time-dependent behavior of triggered M.S was also

examined for 8 hours and the stability was very good with less than 2% stress decay over time. Apart from massage effect, maintaining the pressure gradient in the stockings for long-time is also a serious issue [75, 147, 196] and this could be solved with scientific approach based on this stabilized M.S in the MPFs. Series of experiments was conducted in MP film and filaments followed by smart programming procedure and the peak stress values were recorded as a function of temperature and presented in the next section for discussion.

6.2.6. Evolution of memory stress (M.S) in Film and MPFs

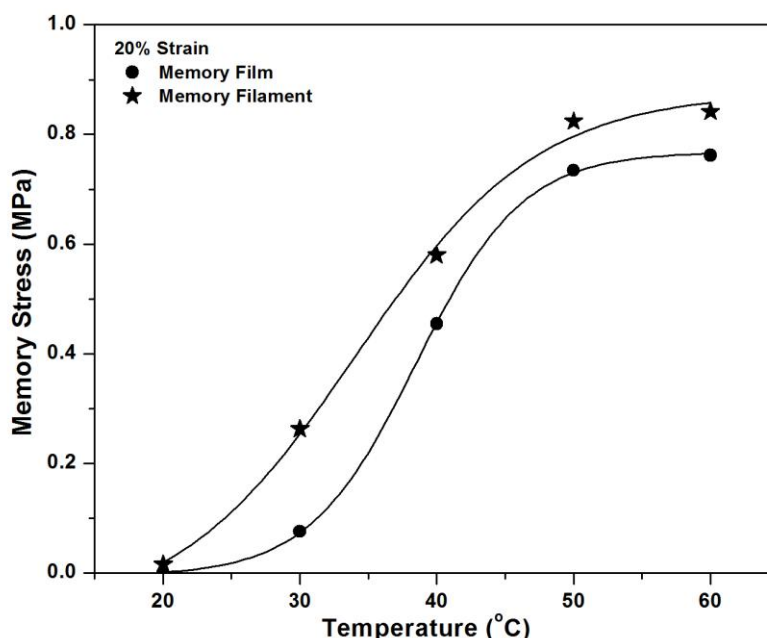


Figure 6.5: Memory stress-temperature profile at 20% strain.

Figure 6.5, 6.6, and 6.7 show the M.S and temperature profile of film and filaments at 20%, 40%, and 60% strain levels. The points in the graph shows the experimental results and they are fitted with sigmoidal function. The curves are well fitted with all the experimental data at every strain and temperature levels. Interestingly, the level of M.S response in MPFs is higher than the film specimen at all the strain levels.

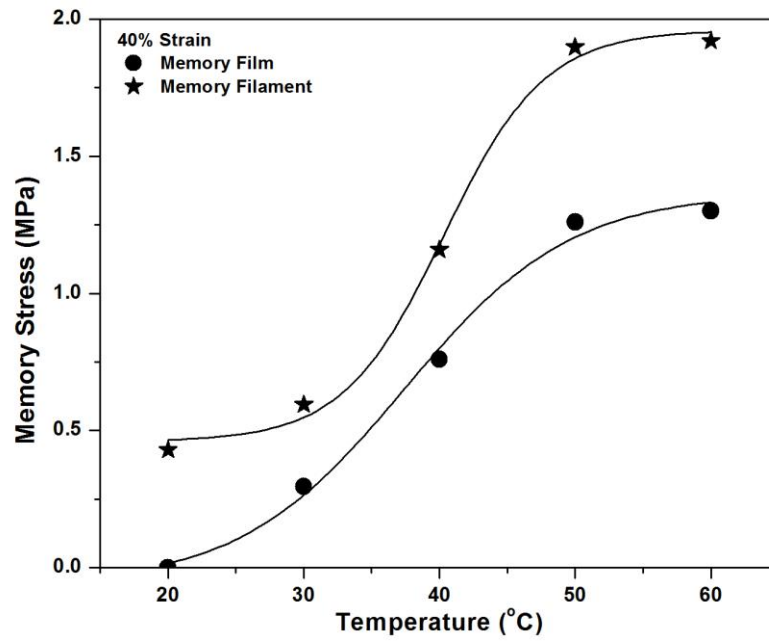


Figure 6.6: Memory stress-temperature profile at 40% strain.

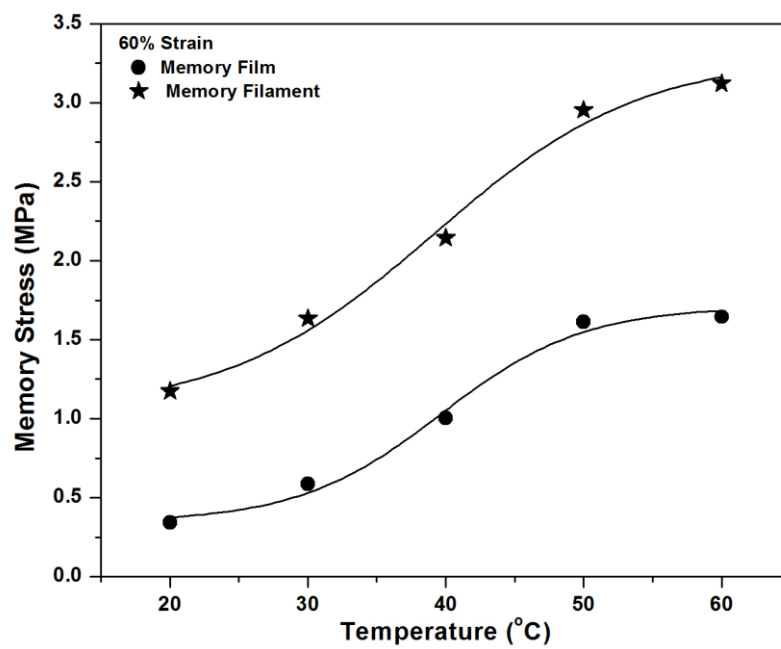


Figure 6.7: Memory stress-temperature profile at 60% strain.

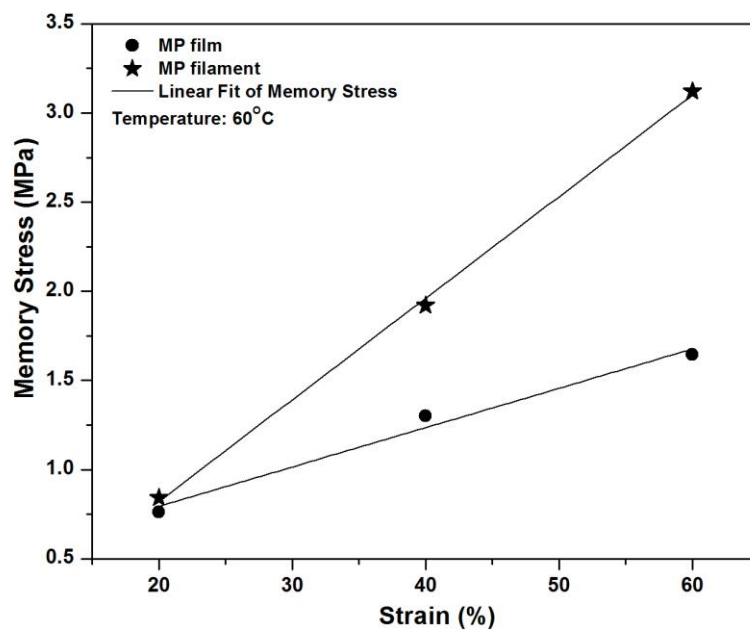


Figure 6.8: Memory stress-strain profile at constant temperature (60 °C)

Table 6.4: Peak memory stress values of film and filament as a function of temperature

Temperature (°C)	Film				Filament			
	Memory Stress (MPa)			R ²	Memory Stress (MPa)			R ²
	20% ϵ	40% ϵ	60% ϵ		20% ϵ	40% ϵ	60% ϵ	
20	0	0	0.341	-	0.016	0.429	1.174	-
30	0.076	0.296	0.588	0.99	0.263	0.594	1.635	0.91
40	0.455	0.759	1.004	0.99	0.580	1.159	2.144	0.97
50	0.734	1.260	1.613	0.98	0.824	1.897	2.953	1.00
60	0.762	1.300	1.644	0.98	0.842	1.920	3.121	0.99

The maximum difference in M.S was observed between 30 to 40 °C as it is close to the transition temperature range and activating the polymeric network to release the stored stress. The drastic change in the M.S was encountered with 498% in film and 120% in the filament at 20% strain from 30 to 40 °C (Table 6.4). Increase in the strain level (60%) has reduced the difference and it is around 71% and 31% for film and filament respectively. However, if we compare the M.S of film and filament as a function of temperature, the maximum difference was found to be 246% at 30°C with 20% strain. MPFs have perfect crystallization with an exothermic peak (Figure 6.2b) below room temperature and this might have caused to release maximum stored stress quickly as compared to film. In contrast, above the transition temperature, the difference in MS was significantly reduced (max. 90%) between film and filament as expected. The increase in strain and temperature gave rise to increase in M.S as well. This could be well explained by the “switch-spring-frame” model which has been reported in Chapter 4.

Based on this model, polymeric soft segment consists of amorphous and crystalline region. Here the crystalline region refers to switch and amorphous molecular chains as springs. Deformation at high temperature opens the switch and causes spring to be strained, subsequently switches gets closed at lower temperature and constraint strain with crystallization process to freeze the internal stress (Figure 6.9). As the strain level increases, number of paired spring and switches in the soft segment also increases thus helps to store the maximum level of M.S as shown with schematic in Figure 6.9. This can also be explained by strain induced crystallization,[216] where new network structure forms to reinforce the net-points and thus leads to higher crystallinity in the strained specimens. Similarly, increase in the temperature triggers the strained spring (amorphous molecular chains) to release the stored M.S by opening the switches (i.e gradual melting of crystals in the soft segment). Higher the number of opening switches more will be the released M.S

under the constraint condition as a function of temperature. The experimental data plotted for film and filament in Figure 6.5, 6.6, and 6.7 are summarized and tabulated in Table 6.4.

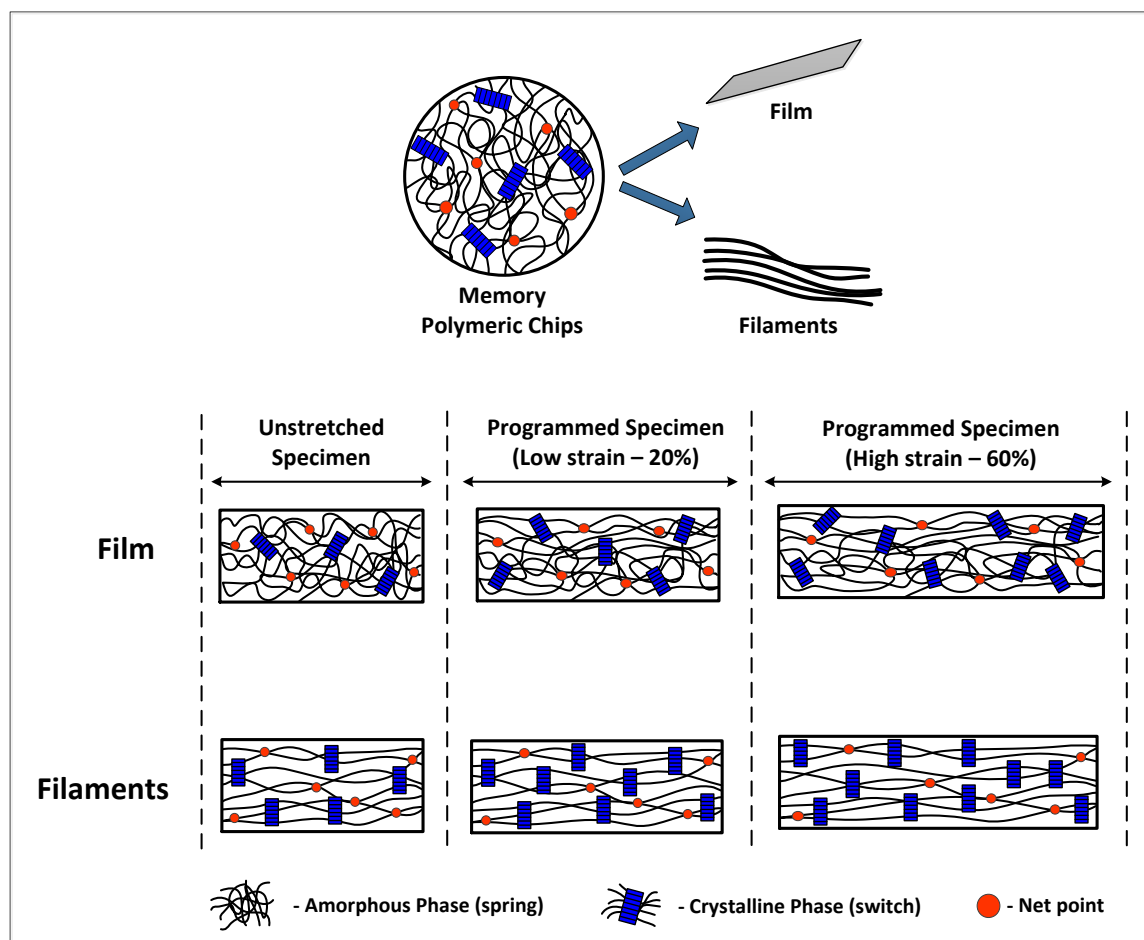


Figure 6.9: Schematic representing the structural changes in film and melt spun filaments on strain.

Both film and filament specimens allowed to cool down to room temperature (20-21 °C) after stress-memory programming process. It can be seen from Figure 6.2 that the melt spun filament has shown higher melting enthalpy compared to film (Table 6.2). As stated previously, crystallization during cooling process allows material to store the M.S. In this case, it is more prominent in the filaments leading to maximum amount of M.S storage and releasing upon cooling and thermal actuation respectively. The elevation of M.S response in both film and filaments at all the strain and temperature levels showing linear trend

(Figure 6.8) and it is statistically significant with correlation coefficient value nearly 1 (Table 6.4).

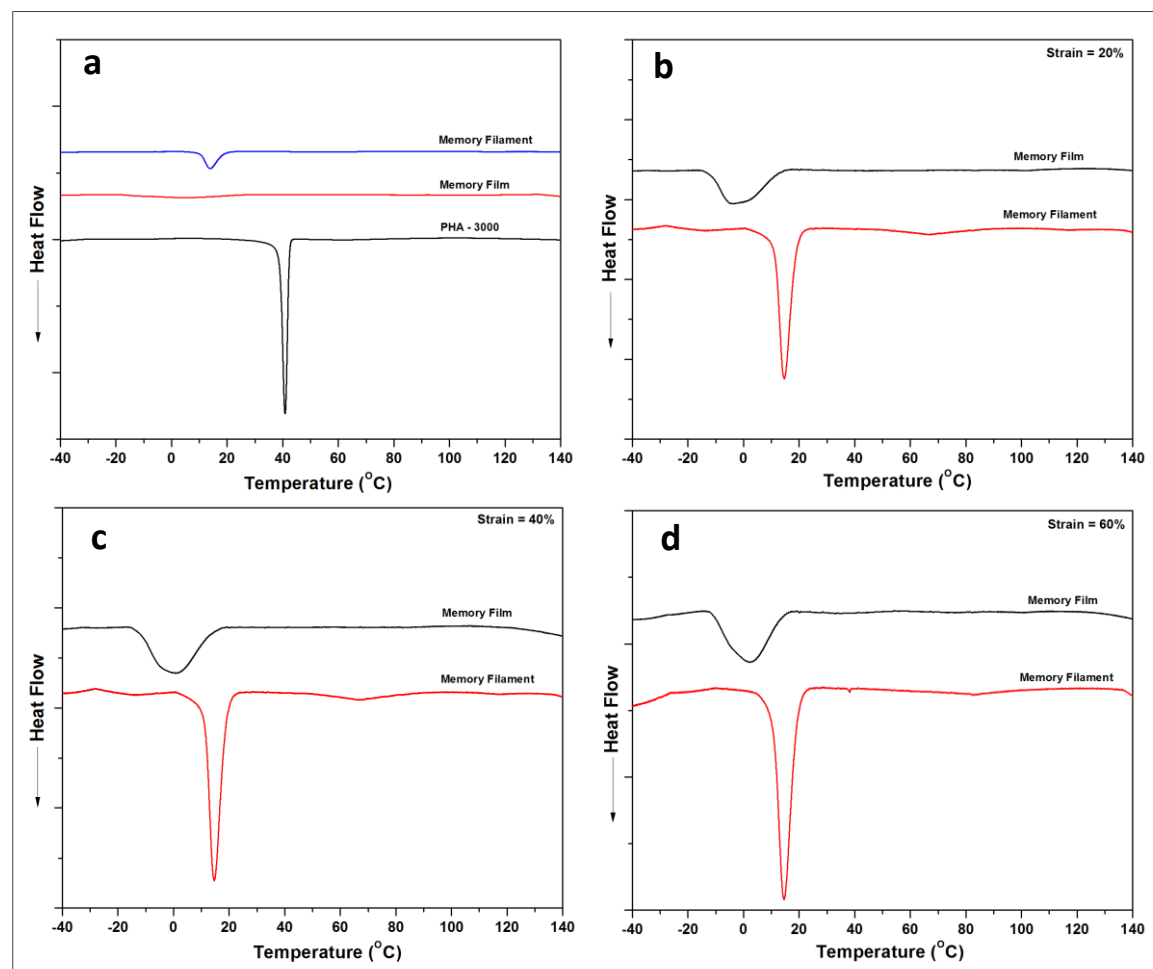


Figure 6.10: DSC thermograms (cooling curves) of film and filaments at 0% (a), 20% (b), 40% (c), and 60% strain (d).

If carefully observe the graphs in Figure 6.5, 6.6, and 6.7, the stress in the film specimen was reached to zero at lower strain (20% and 40%) except 60% strain compared to filament. The reason could be ascribed to well aligned molecular chains in the filaments in its axial direction with perfect and increased crystallinity (Figure 6.10) caused by orientation in melt spinning process (Figure 6.9). This is evident and can be clearly seen from the DSC traces of filaments (Figure 6.10) showing sharp peak during the

crystallization/cooling process and from XRD diffraction peaks (Figure 6.11). The relative degree of crystallinity of filaments is higher than the film and the crystallization peak is not very prominent in the film and this might have caused film specimens to reach the zero stress upon cooling compared to filaments. Increase in the strain level gave rise to increase in the M.S and this was higher in the filaments due to high relative degree of crystallinity and it was confirmed from the DSC cooling curves of programmed specimens ranging from 20 to 60% strain (Figure 6.10) and tabulated in Table 6.5.

Table 6.5: Thermal properties of film and filaments at different programmed strain levels

Programmed Strain (%)	Specimen	ΔH_m (J.g ⁻¹)	ΔH_c (J.g ⁻¹)	Crystallinity (%)
20%	Film	17.249	-22.993	48.92
	Filament	17.998	-26.959	54.65
40%	Film	18.373	-22.5626	49.76
	Filament	20.05	-25.468	55.33
60%	Film	17.044	-24.576	50.60
	Filament	20.32	-25.867	56.15

(Note: The relative degree of crystallinity for soft segment was calculated from the enthalpy data, ΔH of crystallization by using 82.61 J.g⁻¹ enthalpy value for PHA-3000.)

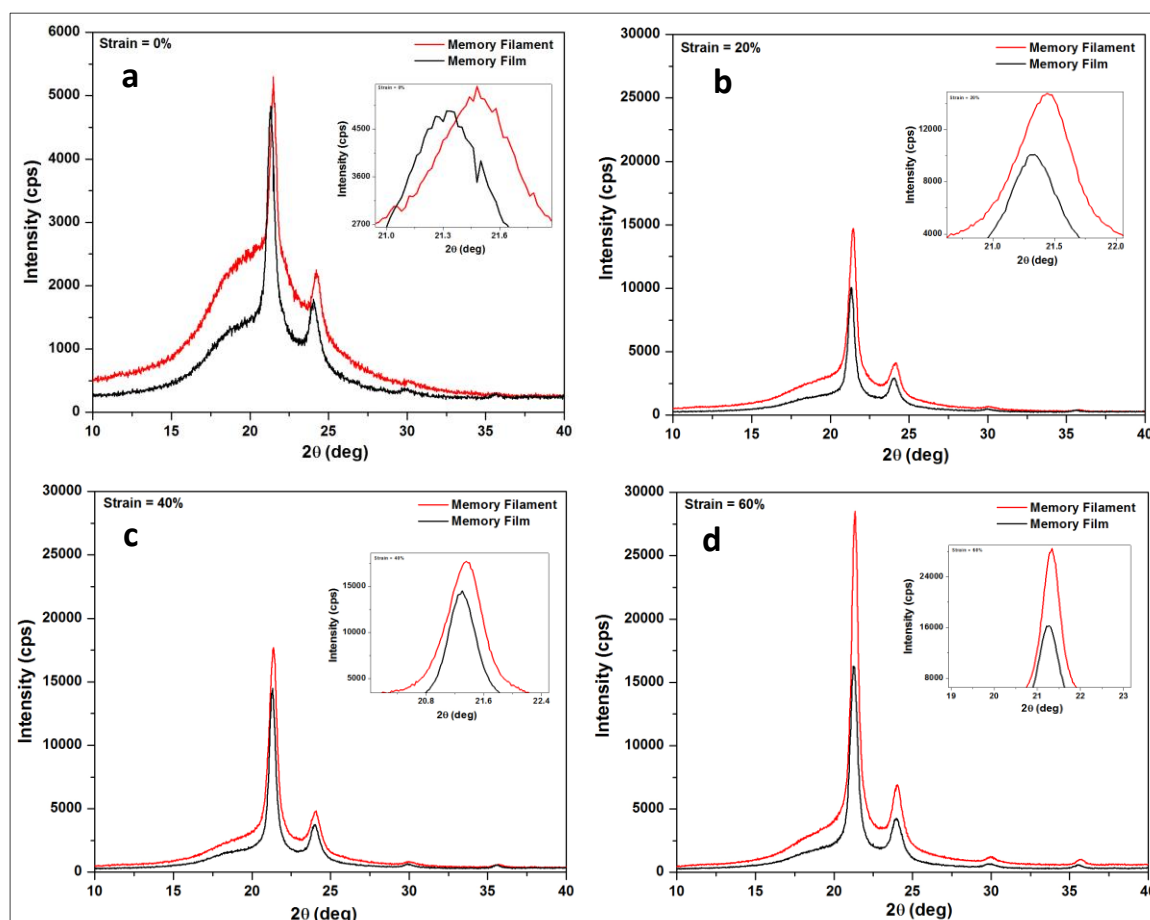


Figure 6.11: WAXD profiles of MP film and filaments at different stress-memory programmed strains. (a) Diffraction profiles of un-stretched specimens. (b) Diffraction profiles at 20% strain. (c) Diffraction profiles at 40% strain. (d) Diffraction profiles at 60% strain.

To further confirm the presence of crystallinity, we performed WAXD analysis. Figure 6.11 shows the WAXD profiles of un-stretched and stress-memory programmed MP specimens at different strain levels. The crystalline diffraction peaks of MP film and filament were found at $2\theta = 21.31^\circ$ (d-spacing=4.16 Å) and $2\theta = 21.48^\circ$ (d-spacing=4.13 Å) respectively. This slight decrease in d-spacing in the filament was observed due to compact polymer packaging. WAXD profiles also demonstrated that the intensity of

crystalline diffraction peaks was increased with strain (20% to 60%) in both film and filaments as well as the filaments showed highest intensity compared to film at same strain level. It suggests that the presence of crystalline domain increased with programming strain level (Figure 6.9). It infers that melt spinning has caused the ordered conformation of molecular chains in the soft segment and resulting in more crystallinity in filament. These results are well correlated with the DSC exothermic results as shown in Figure 6.10. This could be the reason for getting high memory-stress response with increase in strain and temperature level in comparison to film.

6.3. Potential application of stress-memory filaments

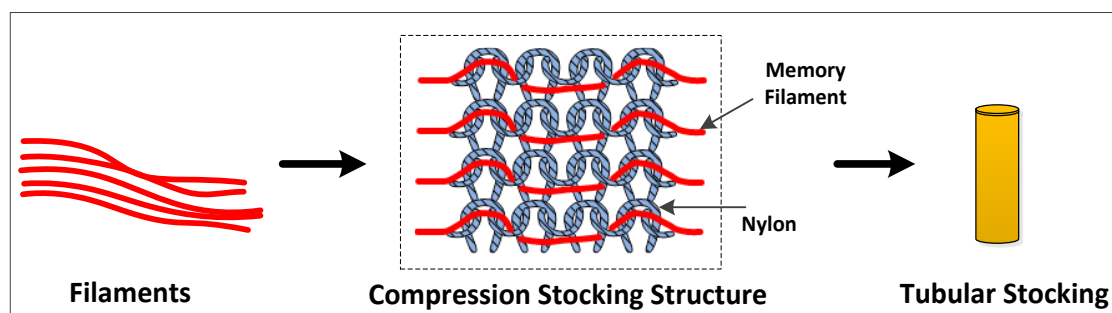


Figure 6.12: Integration of stress-memory filaments into textile knit structure

The detailed methodology related to the integration of stress-memory filaments into textile knit structure is well explained in the Chapter 3. Based on the DSC exothermic results (Figure 6.10), it can also be noticed that higher crystallinity with sharp crystallization peak of filament is around 15 °C and whereas the cooling temperature is 21 °C during the stress-memory programming. This also could be the main reason filaments are incapable to freeze the higher stress to reach zero level at room temperature and left out with some residual stress. At this condition, it still behaves like elastic and exhibits as the elastic stress.

However, it is known that melt spinning has induced more crystalline domain and change in exothermic peak leading to some amount of residual stress in the filaments and this is

also very much useful and advantageous in certain applications such as smart compression stockings.

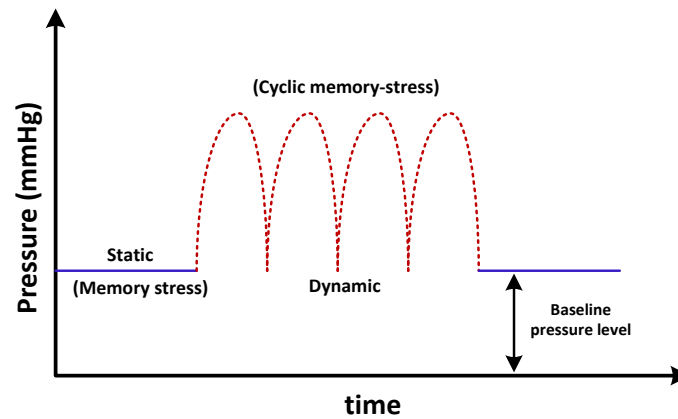


Figure 6.13: Schematic showing the baseline pressure during rest condition

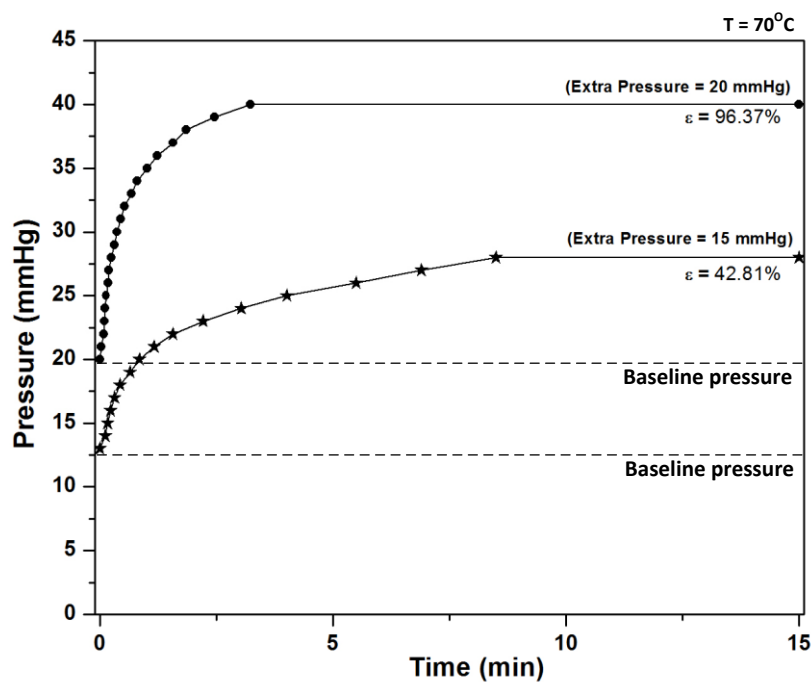


Figure 6.14: Experimental results of MPFs integrative stocking. Pressure-time profile at different strain level

For an efficient compression therapy, the pressure level should not completely reach the zero and stockings should maintain a minimum of 20 mmHg of baseline pressure to assist

venous return during resting condition (Figure 6.13)[58]. The pressure testing results of MPFs integrative compression stocking structure also confirmed the similar behavior. In addition, these smart fabrics also provides extra pressure (Figure 6.14) and massage effect (Figure 6.15) in the same deformation constraint just by change in an external heat stimulus to trigger the M.S. In both static and dynamic pressure profile cases, the baseline can be seen and this is due to result discussed before according to Figure 6.4b.

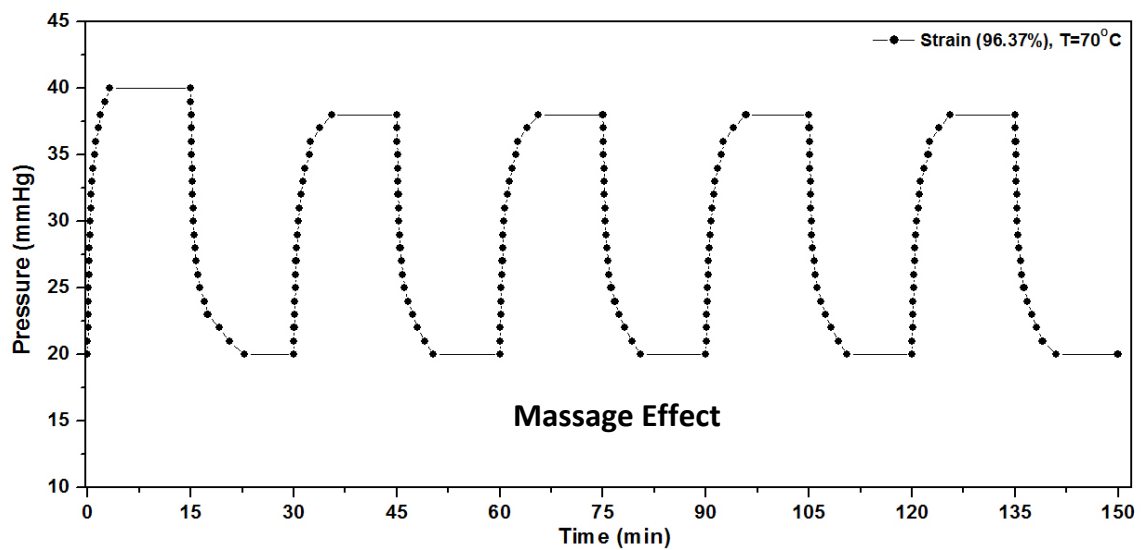


Figure 6.15: Experimental results of MPFs integrative stocking. Pressure-time profile showing massage effect

The internal pressure profile in the stockings can be controlled with memory stress via either deformation or temperature level as shown in the Figure 6.14. It is also depicted in the Figure 6.16b as a schematic curve. The novel stress-memory phenomenon can be implemented scientifically with applied technology in multi-disciplinary arenas such as massage devices, artificial muscles, and smart fabrics, where the stimuli responsive stress is needed.

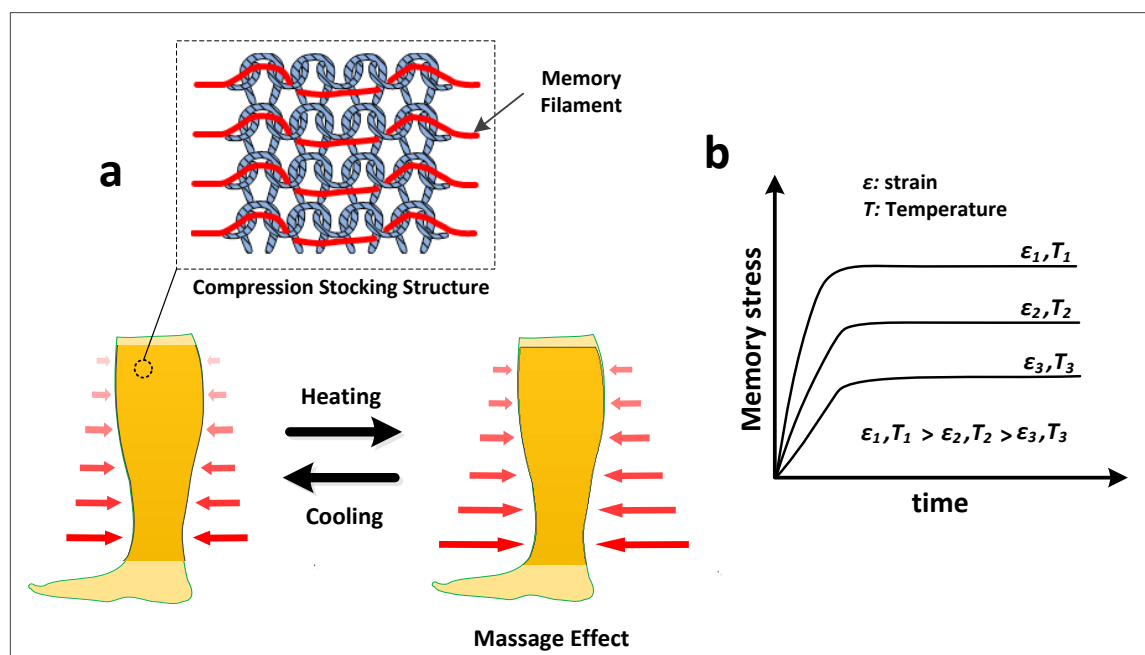


Figure 6.16: a) Schematic of MPFs integrative stocking structure and the effect of massage on human limb upon thermal stimulus. b) Plot showing the relationship between memory stress and the strain as a function of temperature.

6.4. Summary

In this work, a semi-crystalline segmented polyurethane was synthesized using 1,6-poly (hexamethylene adipate) diol as a soft segment and the synthesized polyurethane was used to prepared MPFs and film. A systematic investigation was carried out in MP film and filaments to compare and understand the stress-memory behavior towards optimization of memory stress. This study would assist a material scientist to perceive the unique stress-memory behavior of filaments and to precisely engineer the stockings with smart functions. Based on the experimental results and stress memory properties, the following points can be highlighted.

1. The thermal properties; melting transition and enthalpy of MPFs is higher than the film. Melt spinning has improved the thermal properties. Shape fixity and recovery

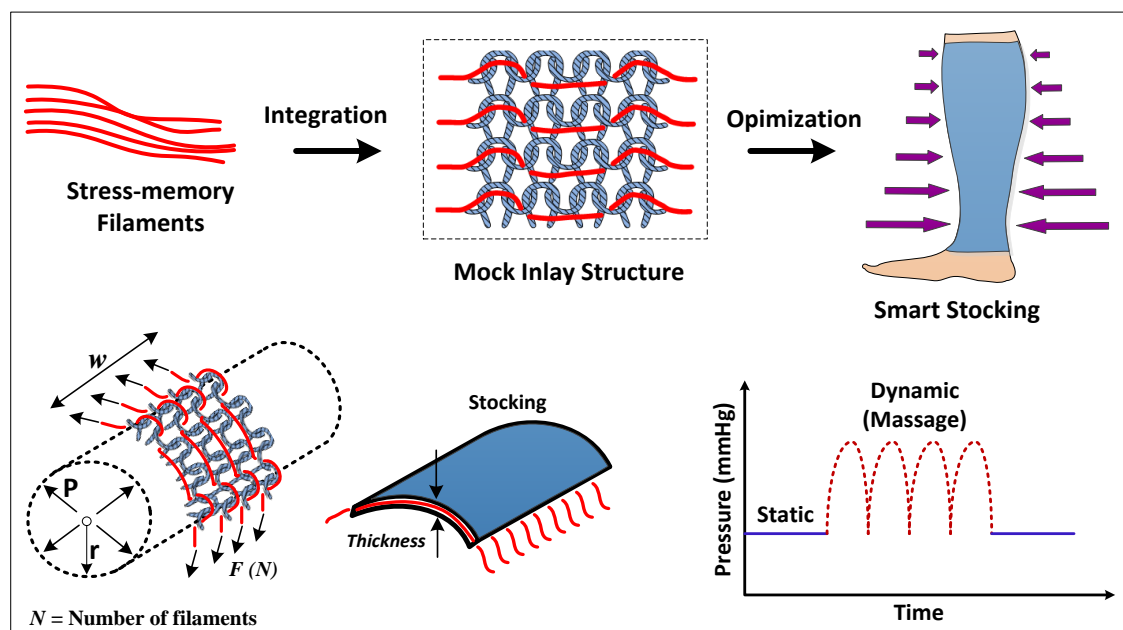
ratios of film is higher than MPFs. The incapability of freezing higher stress at room temperature might have caused to have reduced shape fixity with some residual stress.

2. The elevation of M.S with strain and temperature following a linear trend with maximum value in MPFs due to perfect crystallization, ordered polymer package which is evident from DSC traces and WAXD diffraction peaks. The maximum change in the M.S was observed between 30 to 40 °C. Melt spinning has induced oriented conformation of molecular chains in the filament axis.
3. Increase in the stain level has caused higher M.S due to strain induced crystallization with some residual stress upon cooling and this is significant in the MPFs, which is advantageous to utilize in the smart compression stockings to maintain the minimum baseline pressure and confirmed by pressure testing results.
4. Thermal sensitive MPFs integrative smart fabric structure and provides extra pressure and massage effect in the constraint strain by triggering the stored M.S just by change in temperature.

CHAPTER 7: DESIGNING OF ADVANCED SMART MEDICAL STOCKING USING STRESS-MEMORY FILAMENTS FOR PRESSURE CONTROL AND MASSAGING

Highlights of the Chapter

In this work, a pioneer approach is made to design and optimize the smart stocking structure by integrating the stress-memory filaments as a main load bearing element to control the internal stress. Six different textile knit structures were employed and investigated for pressure analysis and studied their effect together with physical parameters and leg radius. An empirical relationship is derived, which provides the knowledge for how to control the stocking pressure with structural modifications like never done before. In addition, the effect of massage function on venous blood flow is measured by Doppler Ultrasound.⁴



⁴Relevant Publication

Narayana, H., J.L. Hu, B. Kumar, S. Shang, M. Ying, R.J. Young (2017). "Designing of Advanced Smart Medical Stocking using Stress-memory Polymeric Filaments for Pressure control and Massaging." *Materials Science and Engineering-C*, (Manuscript Submitted).

7.1. Introduction

The human beings on this planet are more concerned about their health-related issues and outstanding related research are being carried out at various levels [217-220]. Even though, many problems are yet to be resolved with proper medical treatment and modalities such as lymphatic and phlebological disorders including varicose veins, venous ulcers, edema, lymphedema, deep vein thrombosis (DVT), and venous stasis [221-223]. Gravity is the main reason, why these disorders do occur in the lower extremities of human limb. Compression therapy is considered as a cornerstone in the conservative treatment of phlebological and lymphatic diseases, which provides a proper level of pressure around the affected tissues to push the blood returning heart through veins by reducing the venous hypertension [120, 224].

In the current practice, compression therapy has notable shortcomings which may lead to an inefficient treatment. It has been a great challenge in the selection of proper size stockings for both health practitioners and manufacturers for effective patients' compliance [76]. There are different class of stockings based on compression level [146]. Achieving the targeted level of pressure and maintaining for prolonged period of time are difficult tasks due to several reasons including different leg attributes such as shape and size, difference in inherent materials (both stockings and legs), and time and temperature dependence. Another major complication is the pressure drop over time in the wrapped position of the bandage or stocking on the limb. They are made of textile fibers including PET, Nylon, Cotton, Viscose, elastane which have a common phenomenon of stress relaxation over time in the stretched state and thus pressure drop occur [196, 225, 226]. Once the pressure drops below a stipulated level, the stocking must be replaced, and unfortunately this is tedious and not affordable by all. For dynamic treatment, the equipment like IPC is too expensive, noisy, bulky, and once attached requires immobility

from the patients [58]. It is also not breathable, uncomfortable and may not be efficient as it may not contact the skin surface evenly. Except for IPC, other means are passive, meaning that they only provide a fixed level of initial pressure, which has no pressure control and are incapable of having massage effect required for senior and non-active patients to improve blood flow. In present scenario, stockings can only give static mode of pressure, and not provide dynamic compression as obtained from IPC device. *These challenges, particularly stocking could be resolved if there is a possibility of stress control in the flexible textile fabric materials, which would be a great invention to the chronic patient community.*

However, there are other few works which have focused in the stocking structure development using elastomeric textile yarns [227-230]. Incorporating more elastomeric content and creating tighter construction helps to provide a more homogeneous pressure distribution and sustenance during the course of treatment [162]. One can control the linear density of mock inlay or inlay yarns and input yarn tension to optimize stocking structure for the pressure generation [164, 165]. Dias et al.,[166] have invented customized production of pressure garments quickly and accurately by defining the shape characteristics of the body extremity and specifying knitting pattern. Such garments have the problem of loosening their elasticity due to continuous wear with no extra benefits of massaging for elderly or inactive patients. Kumar et al. have incorporated shape memory filaments in the stocking structure to control the pressure externally with temperature but they faced a relaxation in the structure leading to pressure loss over time and which needs further optimization [231].

The optimization of smart stockings is still unexplored till now to provide both static and dynamic compression (massage effect) benefits. Hence, there is an imperious need of

developing a smart structure which can sustain the pressure, provide controllable static and dynamic compression by utilizing smart fibers.

In this work, an attempt has been made to integrate the memory polymeric filament (MPF) into stocking in conjunction with Nylon filaments via structural optimization to obtain the optimum pressure results. The stocking structure was knitted using variable parameters, including stitch/loop length, combination of floats or miss stitch in SMPFs and Nylon filaments. The effect of fabric structures on the interfacial pressure development was experimentally studied and compared to obtain the optimum stocking structure which could generate optimal compression. The influence of physical parameters on interfacial pressure such as leg radius, temperature, and strain was also investigated using the optimized stocking structure. Importantly, the ability of smart stocking for dynamic compression (massage effect) was also studied with change in heat stimulus. The as developed smart compression stocking can provide both static and dynamic pressure profile with change in the temperature. An empirical relationship is also derived to elucidate the effect of stocking structural parameters on the generation of interfacial pressure on the cylinder. This relationship explains how to control the compression pressure by varying the stocking structural and physical parameters. In addition, the effect of massage function on lower limb blood flow velocity was objectively measured using Doppler ultrasound equipment. This novel approach of controlling the stress or pressure in the stockings via changes in the smart structure would enable a material scientist to optimize the desired level of compression required for efficient treatment to manage chronic disorders. The stress control via fabric structure using smart stimulus responsive filaments would broaden the horizon of applications into multidisciplinary areas.

7.2. Major Key Issues and Approach to Solve

Prior to the designing of smart stocking there are some important key issues to be addressed scientifically to choose the right material and method for advanced compression therapy.

7.2.1. Polymer optimization and its transition temperature

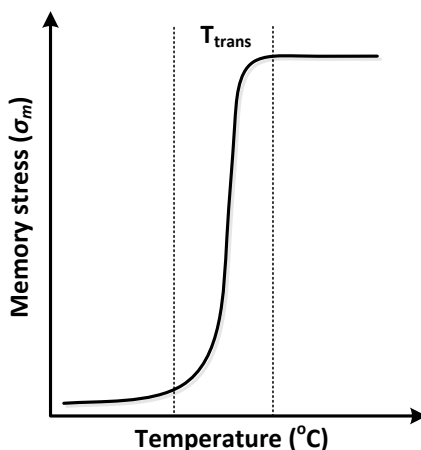


Figure 7.1: The thermal transition in Memory Polymers (MPs).

A stimulus responsive smart memory polymer is needed to achieve the shape fixation. Its transition temperature (Figure 7.1) should be in the normal usage temperature, so that reversible shape or stress can be retrieved upon external heat stimulus. To achieve this objective, a semi-crystalline memory polyurethane was synthesized and obtained transition around 42.13°C . The results are discussed in the previous Chapter 6 (Figure 6.2b).

7.2.2. Stress-memory and its relaxation optimization

In general, the as generated stress vanishes or decrease over time in a constant strain and this affects the performance of memory polymer for pressure application [50, 231]. The main reason for this problem, is presence of ‘viscous stress’ in the material and it needs a proper training before application. As discussed in the Chapters 4,5, and 6, novel stress-memory programming was carried out to remove the viscous stress by adopting a stress-

relaxation process and to get pure memory stress, which can be used for several cycles without any loss (Figure 6.4). This is the most required factor for solving the pressure loss in the stockings.

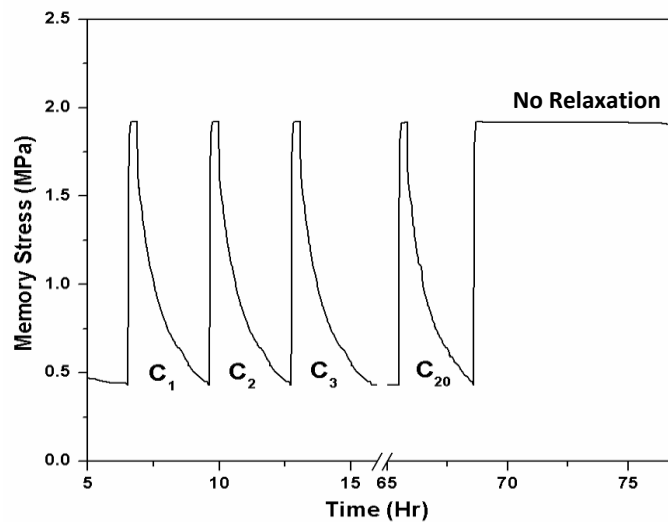


Figure 7.2: Experimental results stress-memory cycles in filaments (Chapter 6)

7.2.3. Memory filament preparation and stocking structure optimization

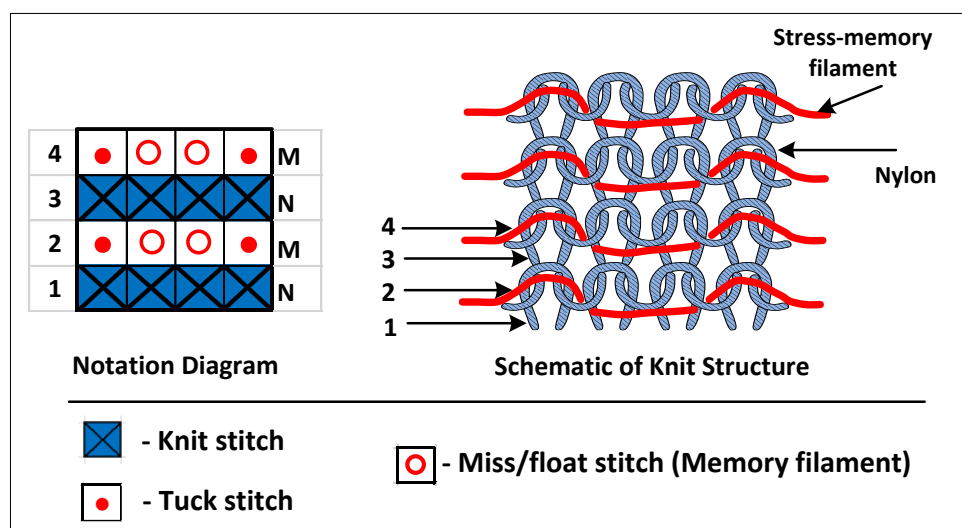


Figure 7.3: Schematic showing the integration of stress-memory filaments to fabric structure. M: Memory filament, N: Nylon filament.

The first question arises for developing smart stocking is, how to incorporate a smart memory polymer and structure optimization for getting optimum pressure results upon

application. The stress-memory polymer was spun via melt spinning (Chapter 6) and prepared continuous strand of filaments (MPFs) which can be easily integrated into stocking structure via knitting technology (Figure 3.1 & 7.3) to make the textile fabric. MPFs alone cannot be made into structure and thus Nylon filaments added as a ground structure in the point of comfort issues (Figure 3.1). The main objective is to keep the MPFs in such way that, which can act as a load bearing element because it is responsible to store, retrieve the stress and thus pressure. The length of MPFs in structure were varied by providing some intersection points (tucks) as it maintains the integrity and provides dimensional stability to the structure for even pressure distribution. Six different structures were prepared to do the pressure investigation structure optimization (Figure 3.2).

7.2.4. Achieving the target level of static and dynamic pressure

Maintaining the proper level of pressure in the stocking has always been a great challenge. None of the stockings provides dynamic pressure profile. A pressure dose of 40-50 mmHg has been found efficient in limb volumetric reduction (69 ml) and also comfortable to patients [58]. Activating the stored pure memory stress in the filaments can maintain constant pressure in the stockings for long time without any significant loss. The change in pressure is directly related to change in the temperature as the polymeric filament is a stimulus responsive smart material. Subsequent change in the heat stimulus (heating and cooling) results in triggering and storing the internal stress and thus dynamic pressure profile can be achieved similar to stress-memory cycles (Figure 7.2 & 6.13). The level of stress can be controlled easily in the filament integrative stockings to achieve the target pressure by optimization of structural parameters such as loop length, number of filaments/unit area, float length of MPFs.

7.2.5. Relationship between pressure and stocking structural parameters

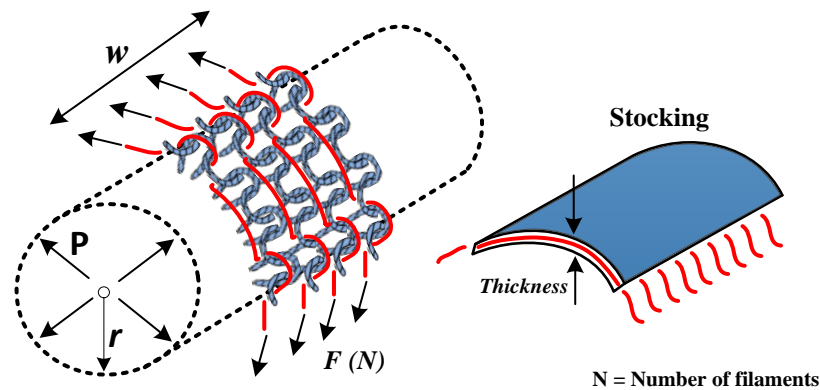


Figure 7.4: Scheme of relationship between pressure and stocking particulars

It is still unknown how to control the interfacial pressure in the stockings externally once it is applied on to a limb except temperature. There are several factors to be considered in the stocking fabric structure to unveil their relationship with the pressure escalation, which helps to design the stocking efficiently. The one aim of this current work is to justify this relationship with concrete experimental pressure test results. The following equations elucidate the underpinning relationship between smart stocking fabric structure and pressure.

Assuming the stoking-limb interaction as a cylindrical model, the pressure of a stocking can be derived from the Laplace's law (Figure 7.4).

$$P = \frac{\sigma \times thickness}{r} \quad (7.1)$$

Where, P is the interfacial pressure (N/m^2), σ is the internal stress in the stockings (N/m^2), and r is the leg or cylinder radius (Figure 7.4). The internal stress in the stocking fabric is contributed by the memory filament and the stored memory stress. Thus, Eq. (7.1) can be rearranged as:

$$P = \frac{\sigma_f \times D_f}{r} \quad (7.2)$$

Where, σ_f is the stored memory stress in the filament and D_f is the filament thickness or diameter, this varies with the linear density of the filament being used. As the stocking consists of memory filaments that allows to change the σ_f by external temperature T due to rubber elasticity:[231]

$$\Delta\sigma_f \propto \Delta T \quad (7.3)$$

The change in stress in the memory filament on the limb by temperature variation will guide the pressure change ΔP by the stocking whose magnitude can be expressed in major parameters - memory stress and filament diameter. Laplace's law is followed here for pressure determination, but it is assumed the stocking as a rigid cylindrical surface. Whereas, stocking fabric is a porous textile structure and integrated with the Nylon and Memory filaments. The generated pressure depends on several factors such as Nylon filaments between the memory filaments, free space, and interaction of Nylon filaments during actuation of the stocking. Hence, there should be a correction factor (K) to consider to know the contribution of other factors, and the Eq. (7.2) can be rearranged as:

$$\Delta P = \frac{\Delta\sigma_f \times D_f}{r} \times K \quad (7.4)$$

This equation ((Eq. (7.4)) could be used for design optimization of the stocking and selecting desired temperature range to get the different level of targeted pressure on the limb. The following are the highlights in this current work towards optimization of smart memory stocking structure:

- Thermal stimulus responsive memory polyurethane is synthesized, optimized, and processed into continuous filaments. Stress-memory programming is carried out to obtain the cyclic and stable pure memory stress to avoid the relaxation and pressure loss.
- Integrated the memory filaments as a load bearing element in conjunction with Nylon filaments and prepared the stocking structure. Comprehensively investigated the effect

of loop length and float lengths on compression pressure distribution in the stockings experimentally.

- In addition, influence of physical parameters such as temperature, leg radius, and strain level on the static and dynamic compression pressure performance and sustenance also studied with optimized structure.
- Established a relationship between the interfacial pressure and stocking structure parameters to control the static and dynamic compression (massage effect) externally. The relationship is validated and also justified with the experimental results.

7.3. Experimental Results and Discussion

The memory stocking fabric structures are shown in the Experimental section (chapter 3), Figure 3.2.

The interfacial pressure of stocking wearing on a particular limb size depends on several attributes and which can be adjusted externally in a MPF integrative one by just change in heat stimulus. The influence of fabric structure and physical parameters on static and dynamic interfacial pressure profiles are experimentally evaluated and thoroughly discussed in this chapter for better understanding of memory behavior.

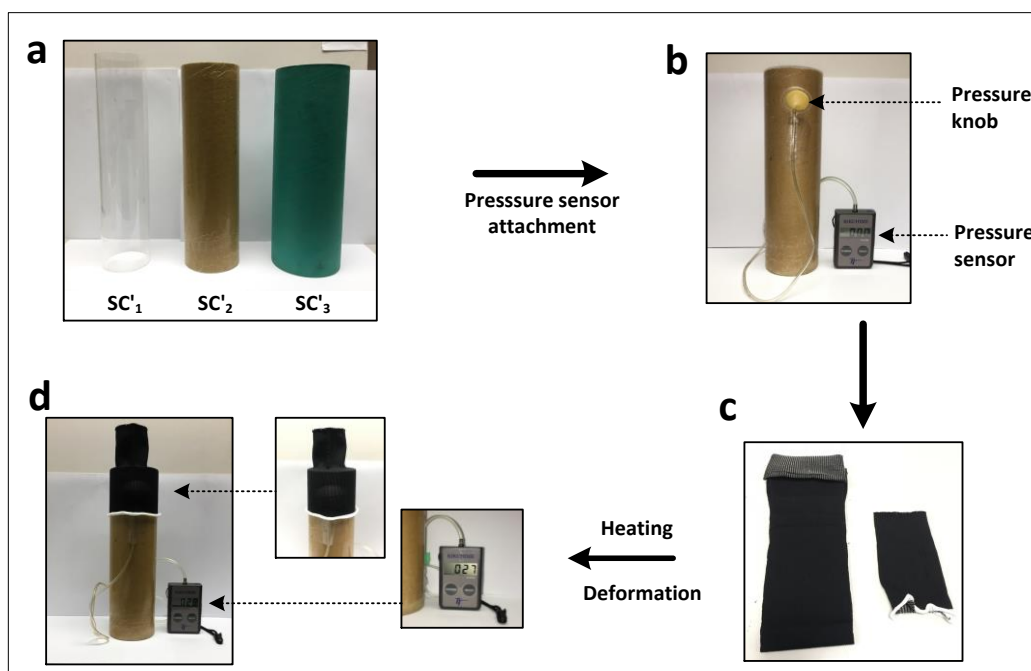


Figure 7.5: Set up for interfacial pressure measurement. a) Cylinders with different circumferences. b) Cylinder with pressure sensor. c) Memory stocking. d) Pressure measurement.

Memory stockings were having variable circumferences due to presence of different structures. All the stocking tubes were stitched into one circumference of 17 cm (SC) using single needle lock stitch machine and then made the cover stitch to avoid the fraying out of yarns. Here the circumference of the stocking is denoted as SC. All the pressure measurement was performed on the rigid cylinders to mimic the human limb. Three different cylinders (Figure 7.5a) were chosen with circumferences of 23.55 cm (SC'_1), 26 cm (SC'_2), and 31.42 (SC'_3). The circumference of the cylinders is denoted as SC' .

The MPF integrative stocking was heated at 70°C inside an oven for 5 minutes. Then the stocking was taken out, stretched, and placed on the cylinder having pressure sensor knob. The corresponding pressure was recorded and the cylinder with stocking was kept inside the oven (70 °C) for 30 minutes to record the elevation of pressure with time.

7.3.1. Structural properties of memory stocking fabrics

Table 7.1: Structural properties of memory stocking fabrics

Sample Code	Loop length (mm)	Wales/inch	Course/inch			Areal Density (Loops/Sq. inch)	Loop shape factor	Fabric thickness (mm)	Fiber content (%)	
			MPF	Nylon	Total				MPF	Nylon
2A	3.9	74	43	42	85	6290	0.87	0.8	34.39	65.61
	2.5	80	57	56	113	9040	0.71	0.70	39.4	60.6
3A	3.9	35	46	45	91	3185	0.38	0.82	38.12	61.88
	2.5	39	60	59	119	4641	0.33	0.81	39.61	60.39
4A	3.9	38	44	44	88	3344	0.43	0.90	35.71	64.29
	2.5	41	59	57	116	4756	0.35	1.07	39.13	60.87
5A	3.9	42	43	43	86	3612	0.49	0.92	30.42	69.58
	2.5	47	57	56	113	5311	0.42	1.13	34.32	65.68
3B	3.9	26	37	37	74	1924	0.35	0.83	40.54	59.46
	2.5	54	47	46	93	5022	0.58	0.89	43.24	56.76
5B	3.9	27	37	37	74	1998	0.36	0.95	40.5	59.5
	2.5	30	45	45	90	2700	0.33	0.80	45.91	54.09

The memory stockings were fabricated into two series (A and B) of structures with two stitch lengths on circular weft knitting machine. The detailed structural properties are tabulated in the Table 7.1 for the discussion. It can be seen from the table that, longer the stitch length (3.8 mm), lesser the wales and course/inch and thus reducing the total number of loops per unit area (Wale: vertical series of loops; course: horizontal series of loops). Whereas, shorter loop length is influencing to have more stitches/loops per unit area. In addition, the memory fiber content (%) is also more with fabric structures those having shorter loop length (2.5 mm). The number of loops/unit area is more in the fabric structures of series-A rather than series-B due to presence of more number of floats or miss stitches.

7.3.2. Effect of fabric structure on stocking pressure

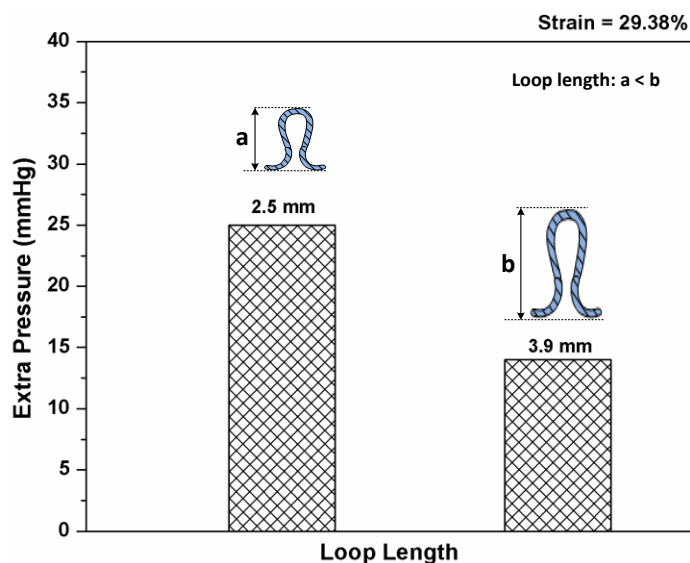


Figure 7.6: Effect of loop length on pressure profile (Series 3A)

Controlling the applied pressure of any stocking by the internal structural modification is a new approach using the smart memory filaments as an integral part. Figure 7.6, 7.7, and 7.8 shows the structural parameters those can be changed for the pressure control for a given temperature range and strain level. The loop or stitch length plays a major role in deciding the stocking structural stability and interfacial pressure evolution. The results of optimum stocking structure series-3A is plotted in Figure 7.6 for comparison with two different stitch lengths. The shorter stitch length (2.5 mm) produced highest extra pressure (25 mmHg) compared to longer stitch length (3.9 mm) and the reason ascribed is the presence of high thread density as shown in Table 7.1, and deduced in Eq. (7.5). More thread density leads to maximum amount of stress to be stored in memory filaments and that could be retrieved upon an external heat stimulus. In addition to thread density, the smaller loop length also ascribed the maximum extension in the yarns during loading. While extension of a knitted fabric, the loops of the filaments gets open up and then actual extension in the filaments happens. So, under same fabric extension level, the memory

extension is more for a structure with low loop length (2.5mm) compared with high loop length (3.9mm). There is almost 12 mmHg of pressure difference is visible between two stitch lengths.

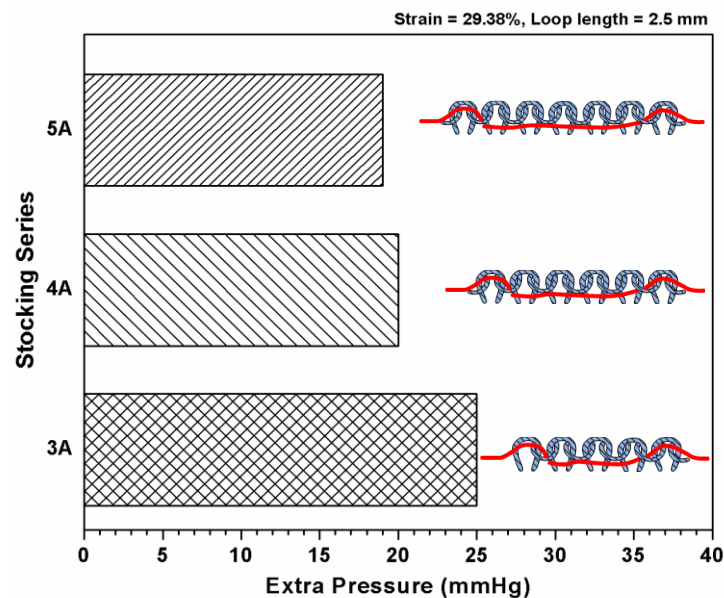


Figure 7.7: Effect of fabric structures on pressure profile (Series A – 2.5 mm loop length)

Another factor is the float length of MPFs to control the pressure magnitude. Due the floats the filaments remain in straight position and therefore more extension in the filaments is expected, but the overall structure become loose if there are too many floats due to lack of intermeshing of the loops. It can be seen from Figure 7.7, that the structure 3A is showing highest extra pressure (25 mmHg), followed by 4A, and 5A. It clearly suggests that number of intersection points of memory filament in one row is very much important and which decides the pressure controllability and sustainability. Lesser the intersection (more floats) provides poor dimensional stability and thus leads low pressure development. The structure 3A is an optimum series to be chosen for getting highest pressure profile. To achieve maximum interlacement, the floats can be completely eliminated but this would not be ideal for pressure change as the both memory and Nylon filaments will be extended to similar

level for a fabric extension. This will therefore restrict the extension of the memory filament up to the breaking extension of Nylon, up to 20%. Due to floats the memory filament remains straight and therefore extend more as compared to Nylon in the similar fabric extension. As Nylon has no contribution in pressure change, so the ideal structure for pressure variation will be when the maximum load (or extension) is achieved in the memory filaments during loading.

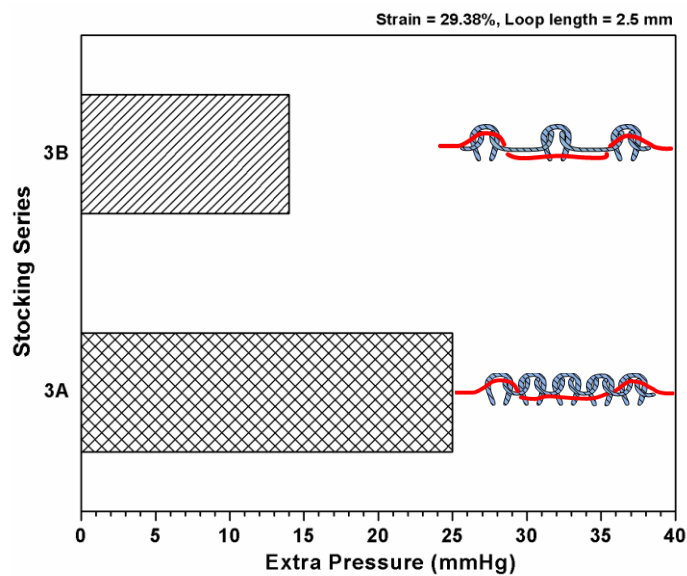


Figure 7.8: Pressure profile of series A vs series B (2.5 mm loop length)

Apart from the float length and stitch lengths, another parameter is to have floats for the ground filaments (Nylon; B series) for pressure control. Figure 7.8 shows the pressure profiles of structure 3A and 3B series. The results showed a difference of 11 mmHg in the pressure escalation upon thermal actuation with lowest peak in the structure B series. The stocking structure with more floats in both memory and Nylon filaments leads to unstable structure and thus leads to low pressure generation for 3B compared to 3A. Also, the floats in Nylon make it straight in the structure, and therefore restricts the memory filament extension.

7.3.3. Effect of physical parameters

The stocking series 3A (stitch length-3.8 mm) was stitched to three different circumferences (17cm, 20cm, 24.26cm) to have the same tension with strain of 29.38% (Eq. 3.9) on three different cylinders (SC'_1 , SC'_2 , SC'_3) respectively. Then the pressure test procedure was carried out to record the corresponding interfacial pressure. Whereas effect of temperature was studied for stocking-3A (stitch length-2.5 mm) with 53.40% strain (SC'_2) at different temperature level (30,40,50,60, and 70 °C) and effect of strain with all three different cylinders at a temperature of 70 °C for 30 minutes.

The generation of interfacial pressure on the human leg/limb is governed by several attributes such as different sizes of human leg, stockings, and fiber rheological characteristics or time dependant behaviours [63, 232]. Figure 7.9, 7.10, and 7.11 shows how to control the pressure in the stockings by changing different physical parameters. An attempt has been made in this work to study the significant influence of various physical parameters on the pressure development such as cylinder circumference, temperature range, and initial strain or deformation. According to Laplace's law for thin walled cylinder, the amount of pressure depends on the radius of the cylinder (Figure 7.4, Eq.7.1). Stocking series-3A was chosen and stitched them into different circumferences ($SC_1 < SC_2 < SC_3$) to apply on cylinders with those having three different circumferences ($SC'_1 < SC'_2 < SC'_3$) to maintain the same wall tension (Figure 7.9). The extra pressure profile of stocking with smaller circumference (less radius) showed highest range, followed by increasing trend of cylinder circumference. From Eq. 7.4, it can be deduced that the internal pressure decreases as the radius of the cylinder increases.

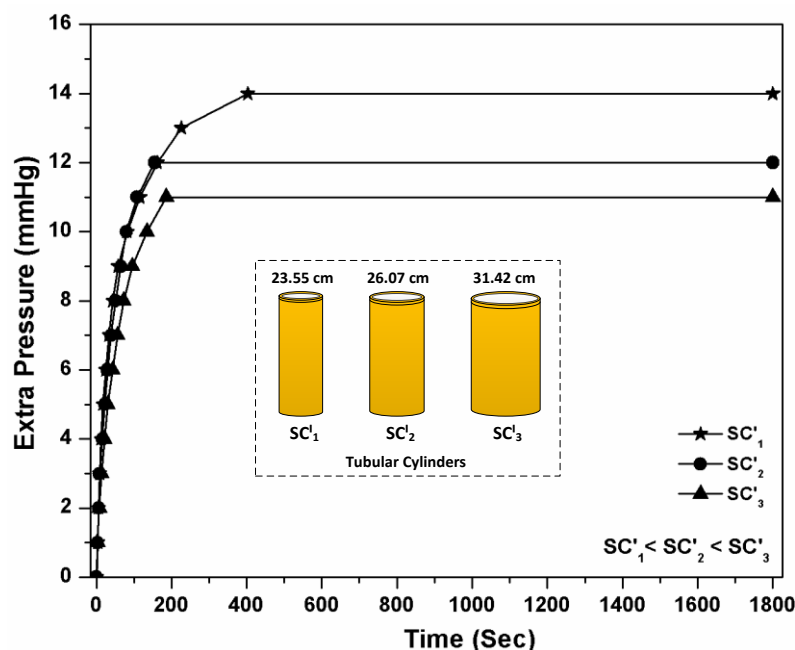


Figure 7.9: Effect of cylinder circumference on pressure under same tension

The smart memory filaments present in the stocking structure is responsible to store and the internal stress upon deformation and retrieve upon actuation above the transition temperature [169]. The pressure escalation is basically depending on the amount of stored internal stress in the memory filaments. Figure 7.10 shows the response of pressure in stocking (series-3A) on the cylinder with the strain of 53.40% at temperature ranging from 30 to 70 °C with an interval of 10 °C. The increase in the pressure level is proportional to increase in the temperature level. As the temperature increases, more number of crystals in the soft segment of memory filament melts and thus releases the stored internal stress from the strained amorphous molecular chains. The further increase in the pressure level is due to gradual melting of crystals in the semi-crystalline polymeric chains in the memory filament and this can be explained by switch-spring-frame model [40, 169]. It can be noticed that, there is a huge difference between the pressure level at 40°C and 50°C temperature. The melting transition temperature of the memory filament is around 42.05°C, where the maximum decrease in the modulus or melting of the crystals do occur.

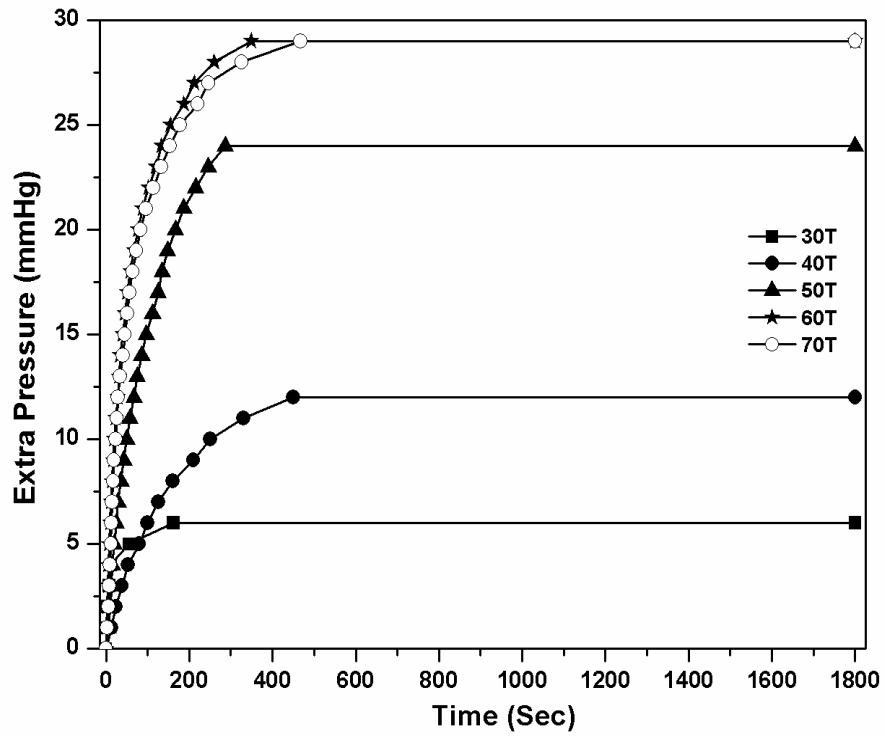


Figure 7.10: Pressure v/s time at different temperature levels

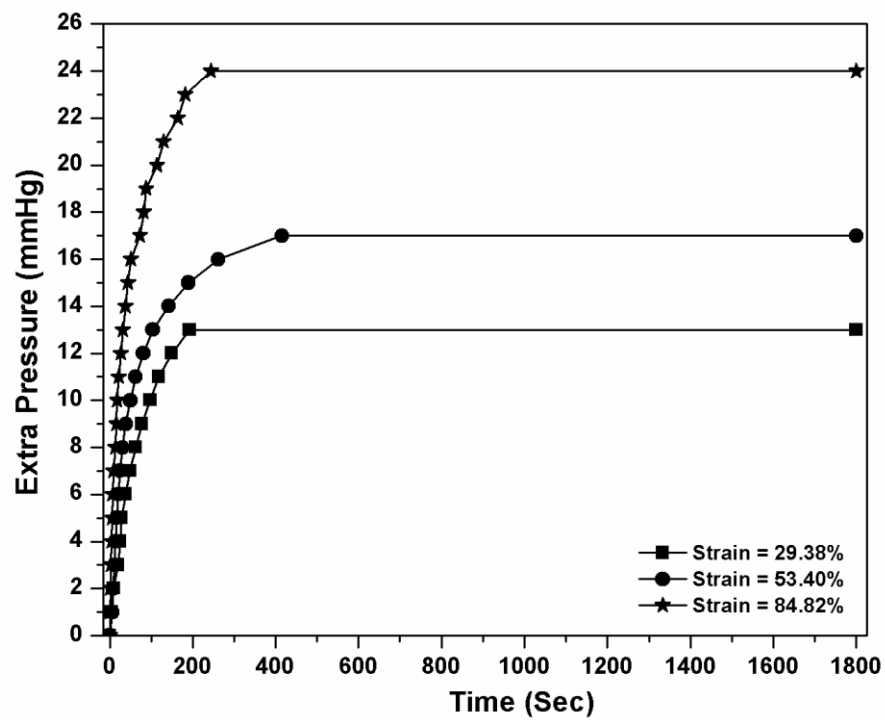


Figure 7.11: Pressure and time profile at different strain levels

Hence, particularly in this temperature range there is a sudden escalation of pressure is clearly visible. *It is imperative to note that the internal pressure in the memory stockings can be readjusted externally* by means of change in the temperature without changing the stockings unlike conventional ones.

In addition to the above parameters, effect of initial strain on the pressure performance of same stocking circumference (SC_1) was also studied and the results are presented in the Figure 7.11. The pressure escalation of the stocking was increased with increase in the circumference of the cylinders upon thermal actuation with time. From the Laplace's law it is known that the circumferential tension increases with increase in the radius of a cylinder and thus corresponding pressure also increases.

The level of the interfacial pressure in the memory stockings can be controlled in different ways using several combinations of physical parameters as discussed in this section. By knowing the effect of physical parameters on the interfacial pressure profile, it is possible to optimize in the process of designing the memory stockings for efficient and advanced compression therapy to manage chronic venous disorders [74, 120].

7.3.4. Controlling massage effect via stocking structure

It has been demonstrated that the memory filaments can store and retrieve the stress reversibly in presence of heat stimulus under constraint [40, 169]. Utilizing this property, the massage effect or dynamic compression can be obtained from the memory stocking using alternating temperature modulation (Figure 7.12).

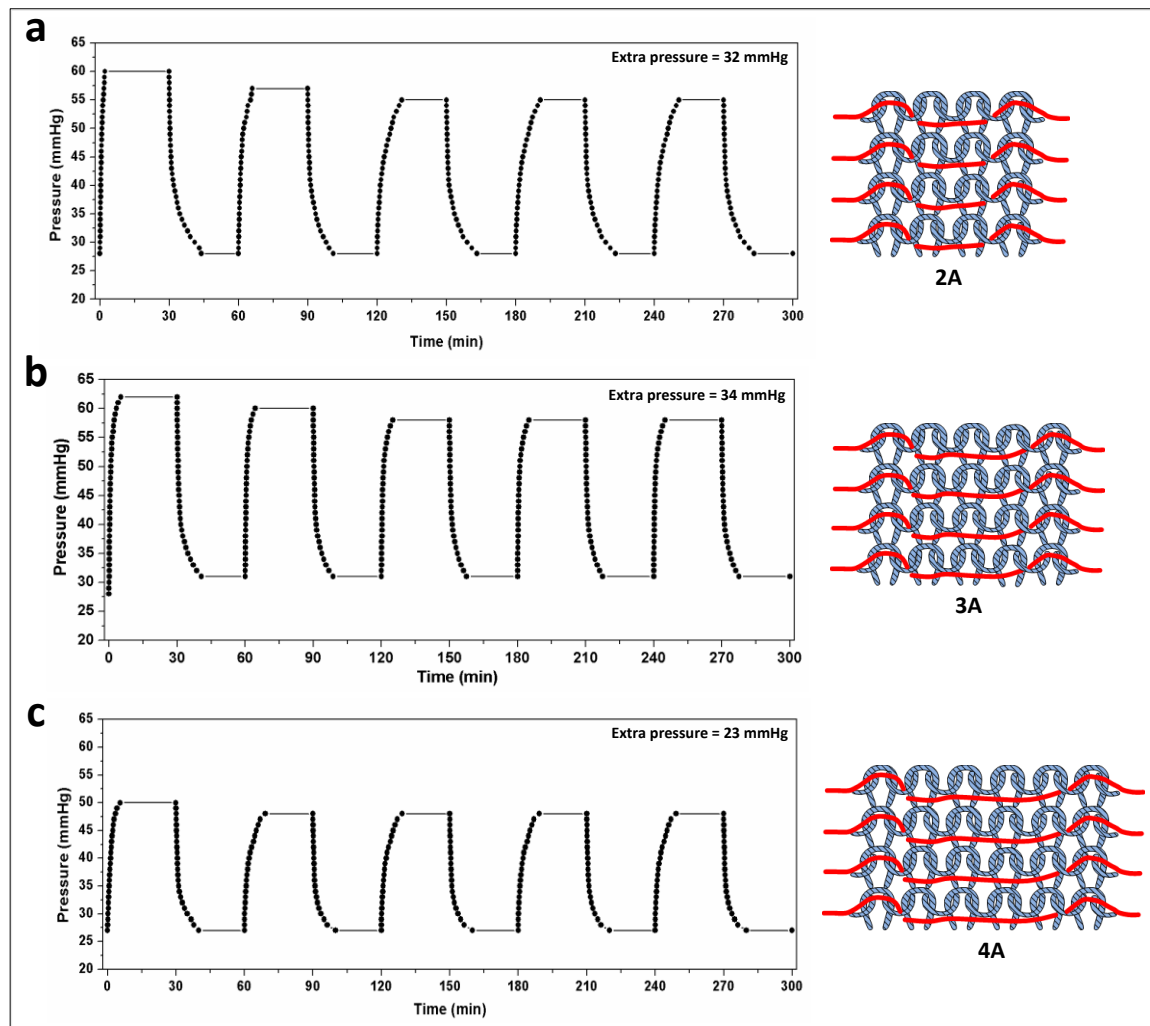


Figure 7.12: Controlling massage effect via stocking structures; (a) 2A, (b) 3A, (c) 4A.

(Loop length: 2.5 mm)

The magnitude of the pressure peaks can be controlled via structural modification (floats) of the stocking. The floats and the number of intersection points for the memory filaments in the structure are critical here, although more floats for memory filaments allows them to extend more and store/release more stress under same fabric extension level but it also makes the structure loose due to less intersection of memory filaments with the ground yarn (Nylon) and the effect of stress variation in memory filament would not be able to transfer to the entire fabric structure. In our case the series-3A produced maximum massage effect in the same temperature range compared with 2A or 4A series. So, the optimization of floats

and the number of intersection points should be achieved for the stability of the stocking and maximum pressure peaks. This structural input would undoubtedly enable a material scientist and clinical therapist to design the right structure for specific requirement.

7.3.5. Ultrasound examination of blood flow

The experimental set up for the Ultrasound investigation is shown in Figure 3.9 and explained in the Chapter 3. The internal compression pressure of the stockings can be readjusted or controlled externally by just change in the temperature. Experimental pressure investigations were performed on the hard surface of the hollow cylinders. To objectively confirm the effect of massage in the stockings, the Doppler ultrasound scanning was carried out on the human subject limb to measure the blood flow velocity of the popliteal vein which carries the impure blood back to the heart. The memory stocking was first heated, deformed and applied on the human limb then again heated to recover the shape and provide the compression (Figure 3.9). The transducer was placed longitudinally over the area where popliteal vein (Figure 7.13a) is located and measured its blood flow velocity four times: bare limb, after wearing stocking, after heating and cooling, during massage (Figure 7.13b). Figure 7.14 shows the blood flow velocity measured at four stages and there is a notable change in each of the stage. The highest peak velocity (5.3 cm/s) was observed during heating the stocking to trigger the stored memory stress in the filaments. It is confirmed that, memory stockings improve the blood flow by just change in temperature to provide controlled and selective static or dynamic massage benefits. This multifunctional stocking would revolutionize the treatment towards smart compression management.

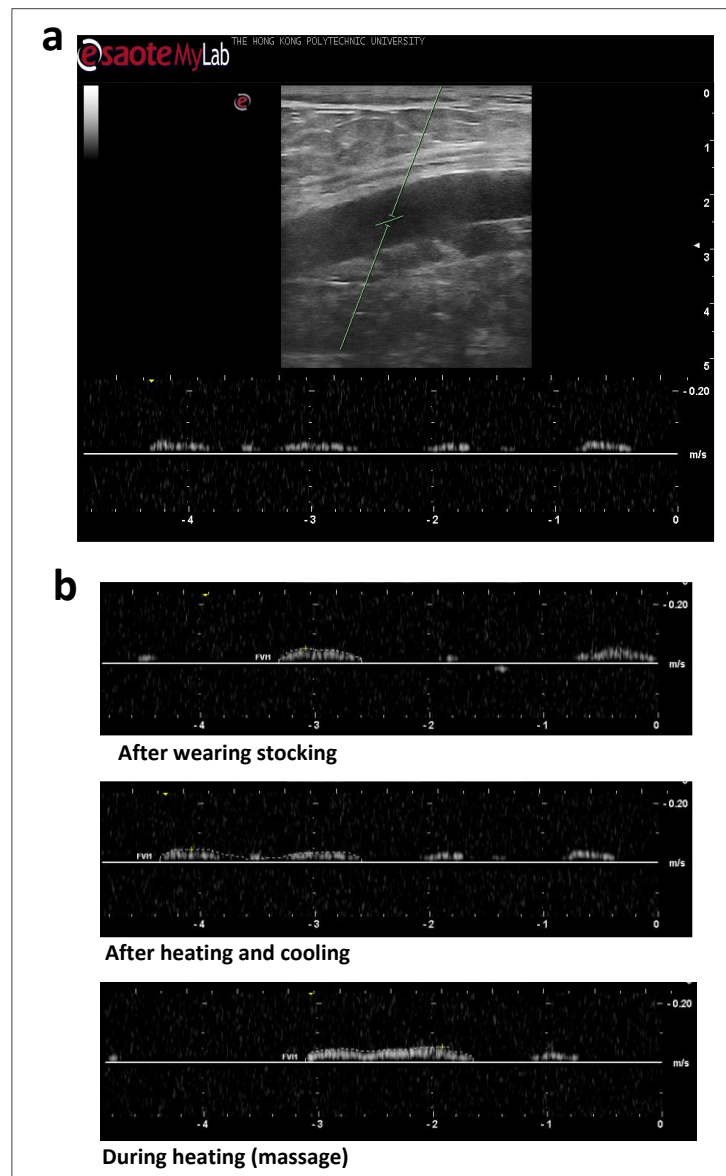


Figure 7.13: Measurement of blood flow via doppler ultrasound scanning. a) Scanned image of popliteal vein carrying impure blood. b) Graphs showing the change in blood flow velocity.

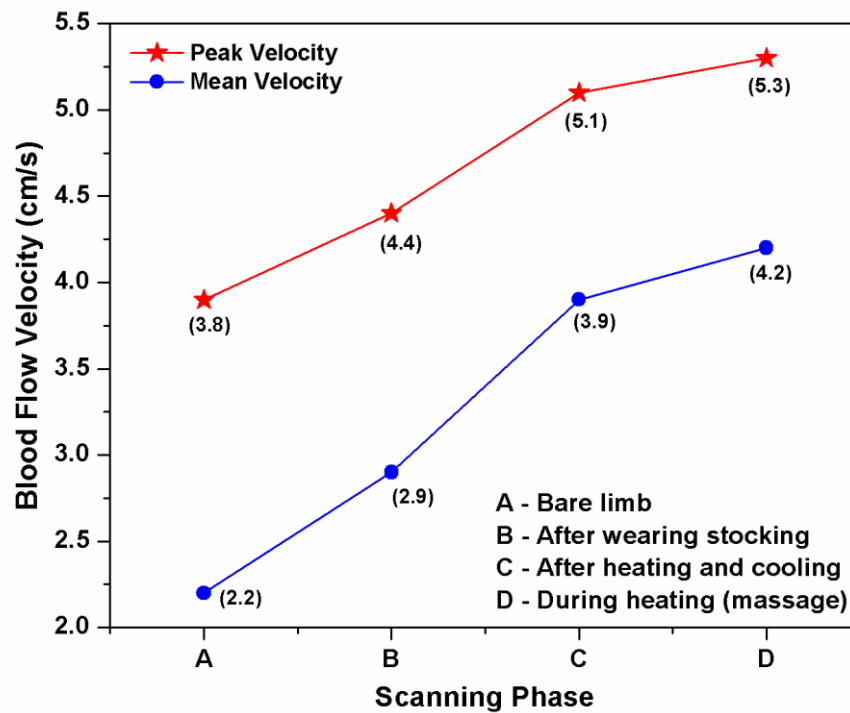


Figure 7.14: Blood flow velocity comparison at different testing phase

7.4. Pressure model validation

Once the stocking is applied on the leg and thermal stimulus provided, the stored memory stress in the filament actuates, and thus interfacial pressure generates. The pressure prediction has been done using the equations obtained and the model parameters are tabulated in the Table 7.3. The experimental pressure response (Figure 7.10) of optimized structure 3A (2.5 mm loop length) at different temperature levels has been taken into consideration (Figure 7.15b). Figure 7.15a shows the evolution of memory stress in the filament as a function of temperature at a strain level of 53.40%. Figure 7.15b shows the plot of experimental and theoretical pressure prediction results and they are in well agreement.

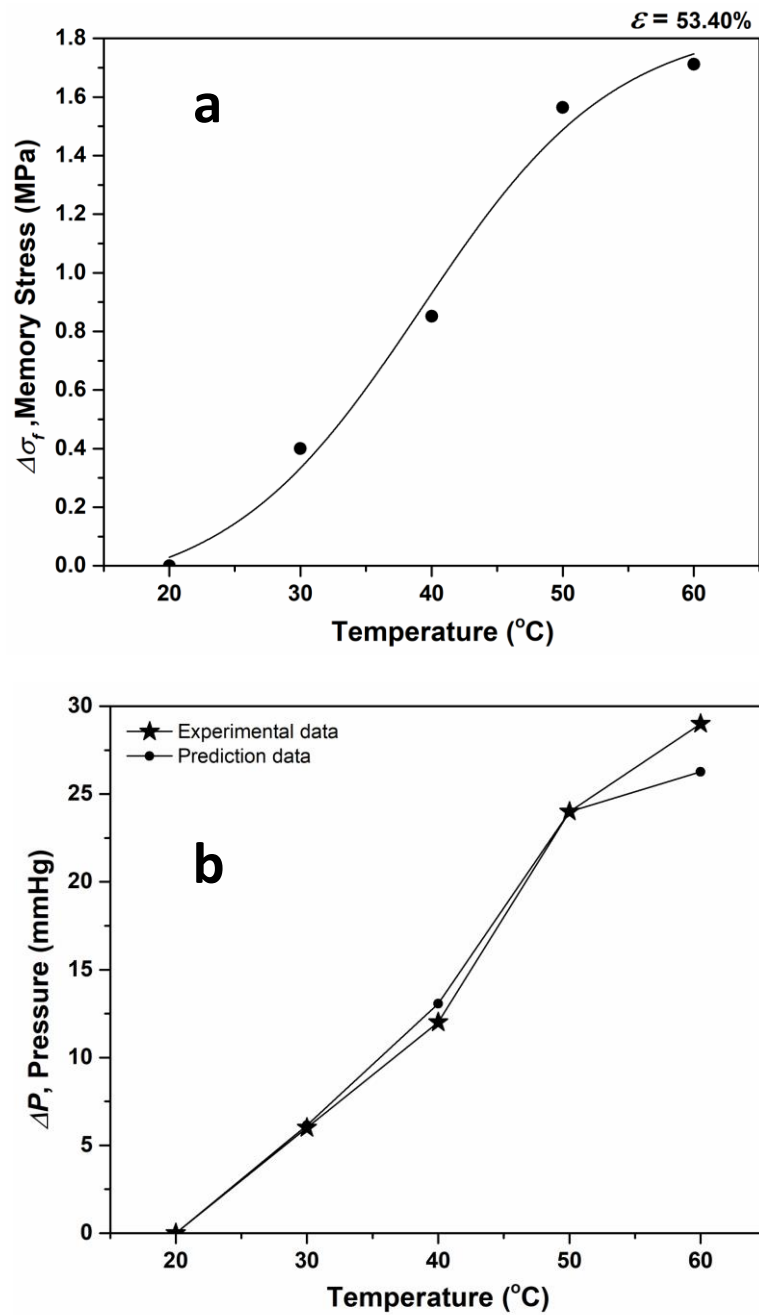


Figure 7.15: a) Memory stress in the filament at 53.40% strain with temperature level. b)

Experimental and theoretical pressure results at different levels of temperature.

Table 7.2: Pressure model parameters

Parameters	Unit	Value
Filament Diameter (D_f)	Meter	0.0001388
Cylinder radius (r)	Meter	0.0414
Average correction factor (K)		0.61

The average correction factor for the optimized structure 3A is 0.61 and this depends on the several factors. The pressure prediction using Laplace's law should be higher than the experimental results as the stocking is considered as a non-porous surface. It is imperative to include the average correction factor (K) for pressure prediction and it depends on factors as explained below.

- 1) According to the model, stocking is considered as a film without pores. But, the stocking is composed of fibers and there is a space between the memory filaments and they are not evenly distributed. Upon activation of memory stress and interfacial pressure, it is distributed among the neighboring filaments and the average pressure will be lesser due to loss. Thus, the average pressure should be less.
- 2) Another factor is, presence of Nylon filaments between the memory filaments. Upon actuation, Nylon filaments could join in together or shrink and act as a positive contribution to the resultant pressure.

7.5. Summary

In the current work, a semi-crystalline polyurethane based thermal responsive smart memory filaments were integrated into flexible textile knit structure in conjunction with

Nylon filaments for structure and compression pressure optimization. The smart structure was optimized via parameters such as loop length and floats in memory and Nylon filaments. The effect of fabric structure, physical parameters, and leg attributes on the interfacial pressure was studied experimentally and then developed an empirical relationship for pressure control. Based on the experimental investigations and understanding, following points can be highlighted:

1. First study to reveal that, interfacial pressure of stockings can be modulated and controlled via structure optimization such as float lengths, loop length, and loop/stitch density. It is possible to control the stress in the memory filaments integrative smart fabrics and thus compression pressure.
2. Maintaining the optimum float length of memory filaments is crucial factor to obtain the maximum pressure. The structure 3A with shorter loop length (2.5 mm) showed highest extra pressure (25 mmHg).
3. Apart from structural control, the internal pressure of the stockings can also be controlled via temperature and strain or deformation level.
4. Pioneer to unveil that massage effect (dynamic pressure) can be controlled as needed by fabric structural modification. The 3A structure showed maximum massage effect (up to 34 mmHg) and this is an optimal structure to be considered for efficient stocking.
5. Ultrasound scanning has revealed that there is a significant change of blood flow velocity in the vein to confirm the effect of massage effect controlled by stockings.

Hence, this would be a multifunctional stocking, where static, dynamic pressure (massage effect), one size for all, and easy donning can be achieved in a revolutionary way by overcoming the current problems towards smart and advanced compression therapy.

CHAPTER 8: CONCLUSIONS AND SUGGESTIONS FOR FUTURE WORK

Highlights

The conclusions for the entire research work and suggestions for the future work is summarized and discussed here in this chapter.

8.1. Conclusions

The proposed objectives in the chapter 1, are successively accomplished with an unprecedented approach of discovering the novel stress-memory phenomenon in the semi-crystalline memory polymeric (MP) film, filaments, and filament integrative textile knit structures towards designing the advanced smart medical compression stocking for the management of phlebological and lymphatic disorders. Based on the innovative and interesting results obtained through an intensive research work carried out in this project, the conclusions for each of the work discussed in chapter 4, 5, 6, and 7 are drawn and summarized in this current chapter.

8.1.1. Discovery of stress-memory in semi-crystalline MP

To fulfil the objective No. 1, a semi-crystalline memory polyurethane based on Poly(ϵ -caprolactone) diol was bulk synthesized and optimized via pre-polymerization method to prepare the polymeric film. Based on the literature gap and an unexpected tensile programming result led the way to discover the novel phenomenon of stress-memory in thermal stimulus responsive polymer, namely stress-memory polymer. Stress-memory programming and pre-conditioning technique, helped to nullify the unwanted components such as viscoelasticity and elasticity in MP to get the pure memory stress. In further, this helped to achieve the stress-memory behavior in continuous cyclic manner without efficiency loss and stable memory stress. To narrate this unique concept, it was further enlightened with the switch-spring-frame model, which represents the landmark in polymer physics. For the first time, stress-memory programming technique was successively applied to stockings for getting the pressure gradient and massage effect with external pressure control like never done before.

8.1.2. Quantitative stress-memory analysis & design of memory film actuator

Based on the stress-memory results, the next objective was to analyze the stress-memory components using thermo-mechanics based phase transition constitutive model. A new scheme was shown to find out the memory modulus for the prediction of pure memory stress. The experimental investigation was performed from 10 to 50% strain level and the result of single strain (20%) was used for model prediction. Both experimentally and analytically shown the effect of thermal stress or strain in memory polymer during tensile programming. It was confirmed that thermal component is an impeditive element and thermal stress has a negligible effect (3.6%) on memory stress. This model depends on the applied strain for stress prediction with given temperature and do not capture the strain-independent phenomena. It is therefore recommended to calculate the model parameters at individual strain for accurate description of the stress recovery.

This constitutive analysis of stress-memory has direct impact on designing and engineering the MP actuators for some real applications. The practical implementation of the modeling results was performed to design the smart pressure bandage using same stress-memory polymeric film. The interfacial pressure in the bandage is primarily depending on the internal stress in the memory film actuator. The model was further used to predict the interfacial pressure profile using Laplace's law and it is well in agreement with experimental results. A stable and dynamic stress cycles can be obtained in the multi-functional smart bandage for the massaging related to orthopedic problems such as muscle spasms, cramps, and aches.

There are a few limitations in using this MP-based smart compression bandage. First, like any thermal technique, the system response is relatively slow. In addition, lack of air permeability of the membrane presents a comfort concern when employed on larger area and over long period of time. These may limit the application of this product in certain

cases. Finally, the original theoretical model assumed a uniaxial tension, and the pressure measurements in this work used a solid substrate in contact with the MP, future modifications are expected when dealing with soft human body parts.

8.1.3. Engineering and optimization of stress-memory filaments

The accomplishment of objective No. 3 was aimed to reveal the stress-memory behavior especially at the filament level for the first time, which further helped to overcome the limitation of smart bandage such as problem of breathability/air permeability. A Semi-crystalline memory polymer based on Poly(1,6-hexamethylene adipate) diol was bulk synthesized, processed, and prepared film and multi-filaments via melt spinning method. A systematic investigation was carried out in MP film and filaments (MPFs) to compare and understand the stress-memory behavior towards optimization of memory stress (M.S). Thermal properties of the memory filaments were higher than the film. The elevation of M.S with strain and temperature following a linear trend with maximum value in MPFs due to perfect crystallization, ordered polymer package which is evident from DSC traces and WAXD diffraction peaks. Melt spinning has induced oriented conformation of molecular chains in the filament axis. Importantly, MPFs left out with some residual stress upon cooling caused by incapability of stress storage under room temperature and this is helpful to maintain the base level pressure in the stockings. Further massage effect can be obtained by triggering the stored memory stress for an efficient compression therapy to overcome the problems highlighted in the Chapter 1. Hence stress-memory filament is the right choice for designing the smart compression stockings. Thus, comprehending the stress-memory behavior at filament level is a must and pre-requisite method before designing the compression stockings with optimization of textile structures.

8.1.4. Designing of smart compression stockings for static and massage pressure

After the revelation of stress-memory potential in memory polymeric film and filament, the last objective was to design the smart compression stockings via textile engineering. MPFs were integrated into six different textile knit structures (fleecy or mock inlay structure) as a main load bearing element in conjunction with Nylon filaments as a ground structure. The smart structure was optimized with parameters such as loop length and floats in memory and Nylon filaments. First time, it was showed that the interfacial pressure can be modulated via structure optimization such as float lengths, loop length, and loop/stitch density. This has been shown with an empirical relationship in Chapter 7. Maintaining the optimum float length of MPFs is crucial factor to obtain the maximum pressure. Apart from structural control, the internal pressure of the stockings can also be controlled via temperature and strain or deformation level. Massage effect can also be controlled with fabric structural optimization. For the pressure prediction in the stockings, the correction factor K , should be used. The Ultrasound scanning has objectively proven the potential of massage effect upon venous blood flow in the popliteal vein.

To sum up,

- Optimization of memory polymeric composition, tuning the transition/activation temperature range, engineering MPFs and comprehending stress-memory behavior at filament level, textile knit structure optimization was the key instrumental to harness the potential of stress-memory polymer and implicate successively into smart compression stockings.
- The stocking structure series 3A (loop length: 2.5 mm) showed maximum extra pressure and massage effect. Hence, this structure can be considered for designing the optimum and efficient smart compression stockings.

- Multi-functional benefits can be achieved in the memory stockings such as pressure gradient, controlled static and dynamic pressure profile (massage effect), selective external pressure control, single size stocking for all, easy application, and size fitting.
- In addition to the multi-functionalities, there are several benefits such as low cost and simple knitting method, massage function for those who are having limited calf muscle function including people in long air travel, Intensive care unit (ICU) care unit, and elderly ones.
- An attempt has been done to scientifically solve the major shortcomings of current compression therapy highlighted in the Chapter 1 with an unprecedented research work reported in this PhD Thesis. The advent of smart medical compression stocking based on stress-memory polymeric materials would undoubtedly revolutionize the compression treatment and become a futuristic option as a medical solution for untapped applications.

8.2. Suggestions for future work

Although an intensive and thorough research work has been carried out to accomplish the proposed objectives, there are still some limitations or window for exploring the stress-memory potentials in designing and optimization of the smart compression stockings. Following are the future suggestions or recommendations could be followed for further research direction.

- 1) *Optimization of MP and its transition/actuation temperature*: The actuation temperature of the MP reported in this current work is around 42 °C and pressure related testing were performed around 60 °C to obtain the maximum memory stress. For the practical feasibility, “**body-temperature**” sensitive memory polymer can be

synthesized and tune the transition range (~ 32 to 34 °C) for achieving desirable memory stress response. Stress-memory behavior of body-temperature sensitive MP is still unexplored and it can be further extended. Study of crystallinity in semi-crystalline stress-memory polymer and changes in crystallinity with temperature by various analytical techniques such as XRD could be carried out for more interesting results and behaviors.

In addition, new methodologies shown in this current work to identify the pure memory stress could be followed to unveil untapped potentials of other soft polymeric materials for diversified applications.

- 2) *Optimization and engineering the stress-memory filaments:* Melt spinning operation is performed relatively at high temperatures around 190 to 220 °C, this could damage or modify the structural morphology of filaments. Hence, other alternative methods of memory polymer synthesis, processing, and filament spinning could be followed for the optimization. Preparation of mono-filament with desirable linear density might be helpful in further knitting process to avoid problems such as unwinding and fiber fraying out. Revelation of stress-memory behavior in the body-temperature sensitive memory filaments could be another distinct study to explore untapped applications as well.
- 3) *Soft surface pressure studies:* The current work limits to study of interfacial pressure on hard surface using cylindrical tubes. Further it can be extended to soft surface to mimic the human limb and study the pressure related parameters to deeply understand the influence of skin deformations on the applying pressure. Thus, based on scientific approach, the internal pressure can be adjusted to required level by optimizing the memory stress in the memory polymer, filament, and fabrics. To

measure the minute changes in the pressure level on soft surface, highly sensitive piezo-resistive based pressure sensors can be used as an option.

- 4) *Theoretical pressure model application*: An empirical relationship derived in the Chapter 7 can be used to predict the interfacial pressure of stocking fabrics with different structures as a function of strain. The studies on effect of fabric structures including thread density, filament linear density, and memory stress can be carried out. This would help in designing the stocking with optimized structure with desirable pressure profile required for an efficient compression therapy.
- 5) *Designing the multi-functional stocking*: The body-temperature MP should be optimized in such a way that, the baseline or rest condition pressure (20 mmHg) can be achieved by just body-temperature. The massage or dynamic pressure profile can be further achieved if there is an option for flexible heating device which could trigger the stored memory stress nearly temperature around 50 °C. This type of embodiment could unify both static and dynamic pressure therapy in a simple way.

Memory polymers can also be used in other form such as foam. Exploration of stress-memory behavior in the memory foam could be a new research direction for compression applications as well, such as massage devices for eye, neck, shoulder, waist to treat the orthopedic related health issues. The potential of memory polymers could be implemented with scientific approach and practical expertise into multi-disciplinary applications, where the stimuli responsive forces are needed such as sensors, actuators, and artificial muscles.

REFERENCES

- [1] M. Behl, M.Y. Razzaq, A. Lendlein, Multifunctional Shape-Memory Polymers, *Adv Mater* 22(31) (2010) 3388-3410.
- [2] M. Behl, K. Kratz, J. Zotzmann, U. Nochel, A. Lendlein, Reversible Bidirectional Shape-Memory Polymers, *Adv Mater* 25(32) (2013) 4466-4469.
- [3] S. Felton, M. Tolley, E. Demaine, D. Rus, R. Wood, A method for building self-folding machines, *Science* 345(6197) (2014) 644-646.
- [4] C.S. Haines, M.D. Lima, N. Li, G.M. Spinks, J. Foroughi, J.D.W. Madden, S.H. Kim, S.L. Fang, M.J. de Andrade, F. Goktepe, O. Goktepe, S.M. Mirvakili, S. Naficy, X. Lepro, J.Y. Oh, M.E. Kozlov, S.J. Kim, X.R. Xu, B.J. Swedlove, G.G. Wallace, R.H. Baughman, Artificial Muscles from Fishing Line and Sewing Thread, *Science* 343(6173) (2014) 868-872.
- [5] A. Lendlein, H.Y. Jiang, O. Junger, R. Langer, Light-induced shape-memory polymers, *Nature* 434(7035) (2005) 879-882.
- [6] P. Miaudet, A. Derre, M. Maugey, C. Zakri, P.M. Piccione, R. Inoubli, P. Poulin, Shape and temperature memory of nanocomposites with broadened glass transition, *Science* 318(5854) (2007) 1294-1296.
- [7] H. Qu, O. Semenikhin, M. Skorobogatiy, Flexible fiber batteries for applications in smart textiles, *Smart Mater Struct* 24(2) (2015).
- [8] H. Yang, W.R. Leow, T. Wang, J. Wang, J.C. Yu, K. He, D.P. Qi, C.J. Wan, X.D. Chen, 3D Printed Photoresponsive Devices Based on Shape Memory Composites, *Adv Mater* 29(33) (2017).
- [9] C. Wischke, A. Lendlein, Shape-Memory Polymers as Drug Carriers-A Multifunctional System, *Pharm Res-Dordr* 27(4) (2010) 527-529.

- [10] Q. Zhao, H.J. Qi, T. Xie, Recent progress in shape memory polymer: New behavior, enabling materials, and mechanistic understanding, *Prog Polym Sci* (2015).
- [11] J.S. Leng, X. Lan, Y.J. Liu, S.Y. Du, Shape-memory polymers and their composites: Stimulus methods and applications, *Prog Mater Sci* 56(7) (2011) 1077-1135.
- [12] L. Sun, W.M. Huang, Z. Ding, Y. Zhao, C.C. Wang, H. Purnawali, C. Tang, Stimulus-responsive shape memory materials: A review, *Mater Design* 33 (2012) 577-640.
- [13] A. Lendlein, R. Langer, Biodegradable, elastic shape-memory polymers for potential biomedical applications, *Science* 296(5573) (2002) 1673-1676.
- [14] J.L. Hu, Y. Zhu, H.H. Huang, J. Lu, Recent advances in shape-memory polymers: Structure, mechanism, functionality, modeling and applications, *Prog Polym Sci* 37(12) (2012) 1720-1763.
- [15] J.L. HU, Tao, X., Smart Fibers and Fibrous Assembly Structures, in: X. Tao (Ed.), *Handbook of smart textiles*, Singapore : Springer Reference, 20152015, pp. 1-225.
- [16] D. Ratna, J. Karger-Kocsis, Recent advances in shape memory polymers and composites: a review, *J Mater Sci* 43(1) (2008) 254-269.
- [17] M. Behl, A. Lendlein, Actively moving polymers, *Soft Matter* 3(1) (2007) 58-67.
- [18] R.R. Kohlmeyer, P.R. Buskohl, J.R. Deneault, M.F. Durstock, R.A. Vaia, J. Chen, Shape-Reprogrammable Polymers: Encoding, Erasing, and Re-Encoding, *Adv Mater* 26(48) (2014) 8114-8119.
- [19] W. Choi, I. Lahiri, R. Seelaboyina, Y.S. Kang, Synthesis of Graphene and Its Applications: A Review, *Crit Rev Solid State* 35(1) (2010) 52-71.
- [20] H. Kim, A.A. Abdala, C.W. Macosko, Graphene/Polymer Nanocomposites, *Macromolecules* 43(16) (2010) 6515-6530.

- [21] H. Koerner, G. Price, N.A. Pearce, M. Alexander, R.A. Vaia, Remotely actuated polymer nanocomposites - stress-recovery of carbon-nanotube-filled thermoplastic elastomers, *Nat Mater* 3(2) (2004) 115-120.
- [22] T. Weigel, R. Mohr, A. Lendlein, Investigation of parameters to achieve temperatures required to initiate the shape-memory effect of magnetic nanocomposites by inductive heating, *Smart Mater Struct* 18(2) (2009).
- [23] Y. Zhao, Light-Responsive Block Copolymer Micelles, *Macromolecules* 45(9) (2012) 3647-3657.
- [24] J.L. Hu, F.L. Ji, Y.W. Wong, Dependency of the shape memory properties of a polyurethane upon thermomechanical cyclic conditions, *Polym Int* 54(3) (2005) 600-605.
- [25] J.L. Hu, Z.H. Yang, L.Y. Yeung, F.L. Ji, Y.Q. Liu, Crosslinked polyurethanes with shape memory properties, *Polym Int* 54(5) (2005) 854-859.
- [26] F.L. Ji, J.L. Hu, H.J. Fan, W. Yu, Effects of hard-segment content on the shape memory properties of segmented polyurethanes, *Proceedings of 2005 International Conference on Advanced Fibers and Polymer Materials (ICAFPM 2005)*, Vol 1 and 2 (2005) 64-67.
- [27] J.L. Hu, S.J. Chen, A review of actively moving polymers in textile applications, *J Mater Chem* 20(17) (2010) 3346-3355.
- [28] Y. Liu, J. Lu, J.L. Hu, A.G. Chung, Study on the bagging behavior of knitted fabrics by shape memory polyurethane fiber, *J Text I* 104(11) (2013) 1230-1236.
- [29] K. Takashima, J. Rossiter, T. Mukai, McKibben artificial muscle using shape-memory polymer, *Sensor Actuat a-Phys* 164(1-2) (2010) 116-124.

- [30] H.M. Wache, D.J. Tartakowska, A. Hentrich, M.H. Wagner, Development of a polymer stent with shape memory effect as a drug delivery system, *J Mater Sci-Mater M* 14(2) (2003) 109-112.
- [31] S. Thakur, S. Barua, N. Karak, Self-healable castor oil based tough smart hyperbranched polyurethane nanocomposite with antimicrobial attributes, *RSC Adv* 5(3) (2015) 2167-2176.
- [32] J.B. Jorcin, G. Scheltjens, Y. Van Ingelgem, E. Tourwe, G. Van Assche, I. De Graeve, B. Van Mele, H. Terryn, A. Hubin, Investigation of the self-healing properties of shape memory polyurethane coatings with the 'odd random phase multisine' electrochemical impedance spectroscopy, *Electrochim Acta* 55(21) (2010) 6195-6203.
- [33] Y. Gonzalez-Garcia, J.M.C. Mol, T. Muselle, I. De Graeve, G. Van Assche, G. Scheltjens, B. Van Mele, H. Terryn, SECM study of defect repair in self-healing polymer coatings on metals, *Electrochem Commun* 13(2) (2011) 169-173.
- [34] W. Small, P.R. Buckley, T.S. Wilson, W.J. Benett, J. Hartman, D. Saloner, D.J. Maitland, Shape memory polymer stent with expandable foam: A new concept for endovascular embolization of fusiform aneurysms, *IEEE T Bio-Med Eng* 54(6) (2007) 1157-1160.
- [35] M.C. Chen, H.W. Tsai, Y. Chang, W.Y. Lai, F.L. Mi, C.T. Liu, H.S. Wong, H.W. Sung, Rapidly self-expandable polymeric Stents with a shape-memory property, *Biomacromolecules* 8(9) (2007) 2774-2780.
- [36] I.A. Rousseau, E.J. Berger, J.N. Owens, H.G. Kia, Shape memory polymer medical cast, US Patent: US20100249682 A1, 2010.
- [37] Y.C. Jung, J.W. Cho, Application of shape memory polyurethane in orthodontic, *J Mater Sci-Mater M* 21(10) (2010) 2881-2886.

- [38] J. Fan, G. Li, High performance and tunable artificial muscle based on two-way shape memory polymer, *RSC Adv* 7(2) (2017) 1127-1136.
- [39] A. Lendlein, S. Kelch, Shape-memory polymers, *Angew Chem Int Edit* 41(12) (2002) 2034-2057.
- [40] J.L. Hu, B. Kumar, H. Narayana, Stress memory polymers, *J Polym Sci Pol Phys* 53(13) (2015) 893-898.
- [41] Y. Wu, J.L. Hu, H.H. Huang, J. Li, Y. Zhu, B.Z. Tang, J.P. Han, L.B. Li, Memory Chromic Polyurethane with Tetraphenylethylene, *J Polym Sci Pol Phys* 52(2) (2014) 104-110.
- [42] T. Xie, Tunable polymer multi-shape memory effect, *Nature* 464(7286) (2010) 267-270.
- [43] Y.P. Liu, K. Gall, M.L. Dunn, A.R. Greenberg, J. Diani, Thermomechanics of shape memory polymers: Uniaxial experiments and constitutive modeling, *Int J Plast* 22(2) (2006) 279-313.
- [44] A.Q. Wang, G.Q. Li, Stress memory of a thermoset shape memory polymer, *J Appl Polym Sci* 132(24) (2015).
- [45] J.L. Hu, S.S. Zhu, R.J. Young, Z.Q. Cai, L.B. Li, J.P. Han, N. Pan, Stress memory materials and their fundamental platform, *J Mater Chem A* 5(2) (2017) 503-511.
- [46] J.R. Lin, L.W. Chen, Shape-memorized crosslinked ester-type polyurethane and its mechanical viscoelastic model, *J Appl Polym Sci* 73(7) (1999) 1305-1319.
- [47] J. Ivens, M. Urbanus, C. De Smet, Shape recovery in a thermoset shape memory polymer and its fabric-reinforced composites, *Express Polym Lett* 5(3) (2011) 254-261.
- [48] K. Gall, M.L. Dunn, Y.P. Liu, G. Stefanic, D. Balzar, Internal stress storage in shape memory polymer nanocomposites, *Appl Phys Lett* 85(2) (2004) 290-292.

- [49] K. Yu, T. Xie, J.S. Leng, Y.F. Ding, H.J. Qi, Mechanisms of multi-shape memory effects and associated energy release in shape memory polymers, *Soft Matter* 8(20) (2012) 5687-5695.
- [50] M. Ahmad, J.K. Luo, M. Mirafteb, Feasibility study of polyurethane shape-memory polymer actuators for pressure bandage application, *Sci Technol Adv Mat* 13(1) (2012).
- [51] H. Narayana, Hu, J.L., Kumar, B., Shang, S., Constituent Analysis of Stress Memory in Semi-crystalline Polyurethane, *J Polym Sci Pol Phys* (2015).
- [52] A. Firouzeh, M. Salerno, J. Paik, Stiffness Control With Shape Memory Polymer in Underactuated Robotic Origamis, *IEEE T Robot* 33(4) (2017) 765-777.
- [53] M.C. Yip, G. Niemeyer, On the Control and Properties of Supercoiled Polymer Artificial Muscles, *IEEE T Robot* 33(3) (2017) 689-699.
- [54] B. Kumar, J.L. Hu, N. Pan, Smart medical stocking using memory polymer for chronic venous disorders, *Biomaterials* (2015).
- [55] A.A. Ramelet, Compression therapy, *Dermatol Surg* 28(1) (2002) 6-10.
- [56] H. Partsch, Compression for the management of venous leg ulcers: which material do we have?, *Phlebology* 29 (2014) 140-145.
- [57] S. O'Meara, N. Cullum, E.A. Nelson, J.C. Dumville, Compression for venous leg ulcers, *Cochrane Db Syst Rev* (11) (2012).
- [58] J.L. Feldman, N.L. Stout, A. Wanchai, B.R. Stewart, J.N. Cormier, J.M. Armer, Intermittent Pneumatic Compression Therapy: A Systematic Review, *Lymphology* 45(1) (2012) 13-25.
- [59] B. Carolyn Robinson, RN, CVN, and Steven M. Santilli, Warm-Up Active Wound Therapy: A novel approach to the management of chronic venous stasis ulcers, *Journal of Vascular Nursing* 16(2) (1998) 38-42.

- [60] B. Kumar, A. Das, R. Alagirusamy, *Science of Compression Bandages*, Elsevier Science Limited, ISBN: 978-1-78242-268-6, 2013.
- [61] B. Kumar, A. Das, R. Alagirusamy, An Approach to Determine Pressure Profile Generated by Compression Bandage Using Quasi-Linear Viscoelastic Model, *J Biomech Eng-T Asme* 134(9) (2012).
- [62] B. Kumar, A. Das, R. Alagirusamy, Prediction of internal pressure profile of compression bandages using stress relaxation parameters, *Biorheology* 49(1) (2011) 1-13.
- [63] B. Kumar, A. Das, R. Alagirusamy, An approach to examine dynamic behavior of medical compression bandage, *J Text I* 104(5) (2013) 521-529.
- [64] B. Kumar, A. Das, R. Alagirusamy, Analysis of sub-bandage pressure of compression bandages during exercise, *Journal of Tissue Viability* 21(4) (2012) 115-124.
- [65] B. Kumar, A. Das, R. Alagirusamy, Effect of material and structure of compression bandage on interface pressure variation over time, *Phlebology* 29(6) (2014) 376-385.
- [66] B. Kumar, A. Das, R. Alagirusamy, Study of the effect of composition and construction of material on sub-bandage pressure during dynamic loading of a limb in vitro, *Biorheology* 50(1-2) (2012) 83-94.
- [67] B. Kumar, J. Singh, A. Das, R. Alagirusamy, Comfort and compressional characteristics of padding bandages, *Mater Sci Eng: C* 57 (2015) 215-221.
- [68] B. Kumar, A. Das, N. Pan, R. Alagirusamy, R. Gupta, J. Singh, Liquid transmission characteristics of padding bandages under pressure, *J Biomater appl* (2015) 0885328215597589.
- [69] J. Munch-Fals, M.Y. Benslimane, P. Gravesen, T. Stenstroem, Electro active elastic compression bandage, US Patent: US7868221 B2, 2011.

- [70] S. Pourazadi, S. Ahmadi, C. Menon, Towards the development of active compression bandages using dielectric elastomer actuators, *Smart Mater Struct* 23(6) (2014).
- [71] H. Moein, C. Menon, An active compression bandage based on shape memory alloys: a preliminary investigation, *Biomed Eng Online* 13 (2014).
- [72] H.B. Bauerfeind, Shape memory element for medical aids, US Patent: US20130303957 A1, 2013.
- [73] M. Taylor, Bandage Pressure Sensor, US Patent: US20080306407 A1, 2008.
- [74] L. Pascarella, C.K. Shortell, Medical management of venous ulcers, *Semin. Vasc. Surg.* 28(1) (2015) 21-28.
- [75] K. Protz, K. Heyer, I. Verheyen-Cronau, M. Augustin, Loss of Interface Pressure in Various Compression Bandage Systems over Seven Days, *Dermatology* 229(4) (2014) 343-352.
- [76] M. Dennis, P.A. Sandercock, J. Reid, C. Graham, G. Murray, G. Venables, A. Rudd, G. Bowler, Effectiveness of thigh-length graduated compression stockings to reduce the risk of deep vein thrombosis after stroke (CLOTS trial 1): a multicentre, randomised controlled trial, *Lancet* 373(9679) (2009) 1958-65.
- [77] V.B. Lester B, Vernon HM, Process of manufacturing articles of thermoplastic synthetic resins, US Patent: US2234993 A, 1941.
- [78] J. Hu, J. Lu, Q. Meng, Y. Zhu, H. Zhuo, Shape memory fibers prepared via wet, reaction, dry, melt, and electro spinning, US Patent: US20090093606 A1, 2007.
- [79] Z.G. Wei, R. Sandstrom, S. Miyazaki, Shape-memory materials and hybrid composites for smart systems - Part I Shape-memory materials, *J Mater Sci* 33(15) (1998) 3743-3762.

- [80] Z.G. Wei, R. Sandstrom, S. Miyazaki, Shape memory materials and hybrid composites for smart systems - Part II Shape-memory hybrid composites, *J Mater Sci* 33(15) (1998) 3763-3783.
- [81] W.C.R. Rainer, E.M.; Hitov, J.J.; Sloan, A.W.; Stewart, W.D., Polyethylene product and process., US Patent: 3144398, 1964.
- [82] B.K. Kim, S.Y. Lee, M. Xu, Polyurethanes having shape memory effects, *Polymer* 37(26) (1996) 5781-5793.
- [83] C.D. Liu, S.B. Chun, P.T. Mather, L. Zheng, E.H. Haley, E.B. Coughlin, Chemically cross-linked polycyclooctene: Synthesis, characterization, and shape memory behavior, *Macromolecules* 35(27) (2002) 9868-9874.
- [84] W. Voit, T. Ware, R.R. Dasari, P. Smith, L. Danz, D. Simon, S. Barlow, S.R. Marder, K. Gall, High-Strain Shape-Memory Polymers, *Adv Funct Mater* 20(1) (2010) 162-171.
- [85] H. Tobushi, H. Hara, E. Yamada, S. Hayashi, Thermomechanical properties in a thin film of shape memory polymer of polyurethane series, *Smart Mater Struct* 5(4) (1996) 483-491.
- [86] T. Takahashi, N. Hayashi, S. Hayashi, Structure and properties of shape-memory polyurethane block copolymers, *J Appl Polym Sci* 60(7) (1996) 1061-1069.
- [87] A. Lendlein, S. Kelch, Shape-Memory Polymers, *Angew Chem Int Ed* 41(12) (2002) 2034-2057.
- [88] M. Anthamatten, S. Roddecha, J.H. Li, Energy Storage Capacity of Shape-Memory Polymers, *Macromolecules* 46(10) (2013) 4230-4234.
- [89] K.K. Westbrook, P.T. Mather, V. Parakh, M.L. Dunn, Q. Ge, B.M. Lee, H.J. Qi, Two-way reversible shape memory effects in a free-standing polymer composite, *Smart Mater Struct* 20(6) (2011).

- [90] K. Kratz, S.A. Madbouly, W. Wagermaier, A. Lendlein, Temperature-Memory Polymer Networks with Crystallizable Controlling Units, *Adv Mater* 23(35) (2011) 4058-+.
- [91] J.K. Yuan, C. Zakri, F. Grillard, W. Neri, P. Poulin, Temperature and Electrical Memory of Polymer Fibers, *Aip Conf Proc* 1599 (2014) 198-201.
- [92] J.L. Hu, J. han, J. Lu, Q. Meng, Y. Zhu, Y. Liu, Q. Ling, F. Ji, Items of clothing having shape memory, US Patent: 20120000251 A1, 2010.
- [93] Q.H. Meng, J.L. Hu, Study on poly(epsilon-caprolactone)-based shape memory copolymer fiber prepared by bulk polymerization and melt spinning, *Polym Advan Technol* 19(2) (2008) 131-136.
- [94] Z.M. Zhijian Zhang, Shixiang Xie, Zhe Zheng, Xuqiong Xiao, Wei Wei, Wei Huang, Synthesis of luminescent polyurethane with π -conjugated segment in main chain, *J Mater Sci* 41(10) (2006) pp 3159-3162
- [95] Q.H. Meng, J.L. Hu, Y. Zhu, J. Lu, Y. Liu, Morphology, phase separation, thermal and mechanical property differences of shape memory fibres prepared by different spinning methods, *Smart Mater Struct* 16(4) (2007) 1192-1197.
- [96] Q.H. Meng, J.L. Hu, L.Y. Yeung, Y. Hu, The Influence of Heat Treatment on the Properties of Shape Memory Fibers. II. Tensile Properties, Dimensional Stability, Recovery Force Relaxation, and Thermomechanical Cyclic Properties, *J Appl Polym Sci* 111(3) (2009) 1156-1164.
- [97] Q.H. Meng, J.L. Hu, Y. Zhu, J. Lu, Y. Liu, Polycaprolactone-based shape memory segmented polyurethane fiber, *J Appl Polym Sci* 106(4) (2007) 2515-2523.
- [98] M. Bao, X.X. Lou, Q.H. Zhou, W. Dong, H.H. Yuan, Y.Z. Zhang, Electrospun Biomimetic Fibrous Scaffold from Shape Memory Polymer of PDLA-co-TMC for Bone Tissue Engineering, *ACS Appl Mater Inter* 6(4) (2014) 2611-2621.

- [99] J.E. Deng, Y. Zhang, Y. Zhao, P.N. Chen, X.L. Cheng, H.S. Peng, A Shape-Memory Supercapacitor Fiber, *Angew Chem Int Ed* 54(51) (2015) 15419-15423.
- [100] J. Zhong, J. Meng, Z.Y. Yang, P. Poulin, N. Koratkar, Shape memory fiber supercapacitors, *Nano Energy* 17 (2015) 330-338.
- [101] Q.X. Yang, G.Q. Li, Spider-silk-like shape memory polymer fiber for vibration damping, *Smart Mater Struct* 23(10) (2014).
- [102] S. Sharafi, G.Q. Li, Multiscale modeling of vibration damping response of shape memory polymer fibers, *Compos Part B-Eng* 91 (2016) 306-314.
- [103] Q.X. Yang, J.Z. Fan, G.Q. Li, Artificial muscles made of chiral two-way shape memory polymer fibers, *Appl Phys Lett* 109(18) (2016).
- [104] J.L. Hu, H.P. Meng, G.Q. Li, S.I. Ibekwe, A review of stimuli-responsive polymers for smart textile applications, *Smart Mater. Struct.* 21(5) (2012).
- [105] G.K. Stylios, T.Y. Wan, Shape memory training for smart fabrics, *T I Meas Control* 29(3-4) (2007) 321-336.
- [106] Y. Liu, A. Chung, J.L. Hu, J. Lv, Shape memory behavior of SMPU knitted fabric, *Journal of Zhejiang University-Science A* 8(5) (2007) 830-834.
- [107] Q.H. Meng, J.L. Hu, Y. Zhu, J. Lu, B.H. Liu, Biological Evaluations of a Smart Shape Memory Fabric, *Text Res J* 79(16) (2009) 1522-1533.
- [108] Q.X. Yang, G.Q. Li, Investigation into Stress Recovery Behavior of Shape Memory Polyurethane Fiber, *J Polym Sci Pol Phys* 52(21) (2014) 1429-1440.
- [109] K. Yu, Q. Ge, H.J. Qi, Reduced time as a unified parameter determining fixity and free recovery of shape memory polymers, *Nat Commun* 5 (2014).
- [110] R. Tonndorf, M. Kirsten, R.D. Hund, C. Cherif, Designing UV/VIS/NIR-sensitive shape memory filament yarns, *Text Res J* 85(12) (2015) 1305-1316.

- [111] W. Small, T.S. Wilson, P.R. Buckley, W.J. Benett, J.A. Loge, J. Hartman, D.J. Maitland, Prototype fabrication and preliminary in vitro testing of a shape memory endovascular thrombectomy device, *IEEE T Bio-Med Eng* 54(9) (2007) 1657-1666.
- [112] Z.H. Yang, J.L. Hu, Y.Q. Liu, L.Y. Yeung, The study of crosslinked shape memory polyurethanes, *Mater Chem Phys* 98(2-3) (2006) 368-372.
- [113] T. Defize, R. Riva, J.M. Raquez, P. Dubois, C. Jerome, M. Alexandre, Thermoreversibly Crosslinked Poly(epsilon-caprolactone) as Recyclable Shape-Memory Polymer Network, *Macromol Rapid Comm* 32(16) (2011) 1264-1269.
- [114] X.F. Luo, P.T. Mather, Preparation and Characterization of Shape Memory Elastomeric Composites, *Macromolecules* 42(19) (2009) 7251-7253.
- [115] J. Diani, Y.P. Liu, K. Gall, Finite strain 3D thermoviscoelastic constitutive model for shape memory polymers, *Polym Eng Sci* 46(4) (2006) 486-492.
- [116] P.P. Simon, H.J. Ploehn, Molecular-level modeling of the viscoelasticity of crosslinked polymers: Effect of time and temperature, *J Rheol* 41(3) (1997) 641-670.
- [117] A.Y. Mousa, B.K. Richmond, A.F. AbuRahma, Review and Update on New Horizon in the Management of Venous Ulcers, *Vascular and Endovascular Surgery* 48(2) (2014) 93-98.
- [118] J.C. McDaniel, S. Roy, T.A. Wilgus, Neutrophil activity in chronic venous leg ulcers-A target for therapy?, *Wound Repair Regen* 21(3) (2013) 339-351.
- [119] R. Serra, L. Gallelli, G. Buffone, V. Molinari, D.M. Stillitano, C. Palmieri, S. de Franciscis, Doxycycline speeds up healing of chronic venous ulcers, *Int Wound J* 12(2) (2015) 179-184.
- [120] H. Partsch, Compression therapy in leg ulcers, *Reviews in Vascular Medicine* 1(1) (2013) 9-14.

- [121] S. Vazquez, M.T. Rondina, Review: Graduated compression stockings reduce deep venous thrombosis in hospitalized patients, *Ann Intern Med* 153(12) (2010).
- [122] A. Sachdeva, M. Dalton, S.V. Amaragiri, T. Lees, Graduated compression stockings for prevention of deep vein thrombosis, *Cochrane Db Syst Rev* (12) (2014).
- [123] E.A. Nelson, A. Hillman, K. Thomas, Intermittent pneumatic compression for treating venous leg ulcers, *Cochrane Db Syst Rev* (5) (2014).
- [124] I.J.M. Carl L. Reiber A Review of the “Open” and “Closed” Circulatory Systems: New Terminology for Complex Invertebrate Circulatory Systems in Light of Current Findings, *Int J Zool* 2009 (2009) 8.
- [125] E. Strandén, Edema in venous insufficiency, *Phlebology* 18(1) (2011) 3-14.
- [126] H. Partsch, Understanding compression therapy, *MEDICAL EDUCATION PARTNERSHIP LTD, 53 Hargrave Road, London N19 5SH, UK, 2003.*
- [127] M. Clarke-Moloney, A. Godfrey, V. O'Connor, H. Meagher, P.E. Burke, E.G. Kavanagh, P.A. Grace, G.M. Lyons, Mobility in patients with venous leg ulceration, *Eur J Vasc Endovasc* 33(4) (2007) 488-493.
- [128] M.I. Shiman, B. Pieper, T.N. Templin, T.J. Birk, A.R. Patel, R.S. Kirsner, Venous ulcers: A reappraisal analyzing the effects of neuropathy, muscle involvement, and range of motion upon gait and calf muscle function, *Wound Repair Regen* 17(2) (2009) 147-152.
- [129] P.J. Franks, Posnett, J., Cost-effectiveness of compression therapy, *MEDICAL EDUCATION PARTNERSHIP LTD, 53 Hargrave Road, London N19 5SH, UK, 2003.*
- [130] S.M. Adeyemi Adeyi, Indrajit Gupta, Leg Ulcers in Older People: A Review of Management, *Br J Med Pract* 2(3) (2009) 21-28.

- [131] R. Haram, Ribu, E., Rustøen, T., The views of district nurses on their level of knowledge about the treatment of leg and foot ulcers., *J Wound Ostomy Continence Nurs* 30(1) (2003) 25-32.
- [132] M.J. Callam, Harper, D.R., Dale, J.R., Ruckley, C.V., Arterial disease in chronic leg ulceration: an underestimated hazard? Lothian and Forth Valley leg ulcer study, *Br Med J* 294 (1987) 929-931.
- [133] S. Dean, Leg ulcers - causes and management, *Australian Family Physician* 35(7) (2006) 480-484.
- [134] P. Delmas, Assessment of oedema, *Revue de l'infirmiere* 181 (2012) 35-37.
- [135] L. Naude, Chronic venous ulcers: compression therapy treating the underlying disease-a case study, *Professional Nursing Today* 12 (2008) 25-28.
- [136] B. Eklof, R.B. Rutherford, J.J. Bergan, P.H. Carpentier, P. Gloviczki, R.L. Kistner, M.H. Meissner, G.L. Moneta, K. Myers, F.T. Padberg, M. Perrin, C.V. Ruckley, P.C. Smith, T.W. Wakefield, A.V.F.I.A. Hoc, Revision of the CEAP classification for chronic venous disorders: Consensus statement, *J Vasc Surg* 40(6) (2004) 1248-1252.
- [137] F.T. Padberg, CEAP classification for chronic venous disease, *Dm-Dis Mon* 51(2-3) (2005) 176-182.
- [138] J.M. Porter, G.L. Moneta, H.G. Beebe, J.J. Bergan, D. Bergqvist, B. Eklof, I. Eriksson, M.P. Goldman, L.J. Greenfield, R.W. Hobson, C. Juhan, R.L. Kistner, N. Labropoulos, G.M. Malouf, J.O. Menzoian, K.A. Myers, P. Neglen, A.N. Nicolaides, T.F. Odonnell, H. Partsch, M. Perrin, S. Raju, N.M. Rich, G. Richardson, H. Schanzer, P.C. Smith, D.E. Strandness, D.S. Sumner, Reporting Standards in Venous Disease - an Update, *J Vasc Surg* 21(4) (1995) 635-645.
- [139] E.A. Nelson, R. Mani, K. Thomas, K. Vowden, Intermittent pneumatic compression for treating venous leg ulcers, *Cochrane Db Syst Rev* (2) (2011).

- [140] J.A. Caprini, Commentary on 'Adjustable Velcro Compression Devices are More Effective than Inelastic Bandages in Reducing Venous Edema in the Initial Treatment Phase: A Randomized Controlled Trial', *Eur J Vasc Endovasc* 50(3) (2015) 375-375.
- [141] G. Mosti, A. Cavezzi, H. Partsch, S. Ursa, F. Campana, Adjustable Velcro (R) Compression Devices are More Effective than Inelastic Bandages in Reducing Venous Edema in the Initial Treatment Phase: A Randomized Controlled Trial, *Eur J Vasc Endovasc* 50(3) (2015) 368-374.
- [142] R.S. Farah, M.D.P. Davis, Venous Leg Ulcerations: A Treatment Update, *Current Treatment Options in Cardiovascular Medicine* 12 (2010) 101-116.
- [143] T.J. Phillips, Successful methods for treating leg ulcers, *Postgraduate Medicine* 105 (1999) 159-179.
- [144] W.L. J. Hafner, H. Hanssle, G. Kammerlander, and G. Burg, Instruction of compression therapy by means of interface pressure measurement, *Dermatol Surg* 26 (2000) 481-487.
- [145] H.A.M. Neumann, Compression therapy with medical elastic stockings for venous diseases, *Dermatol Surg* 24(7) (1998) 765-770.
- [146] J. Sue, Compression hosiery in the prevention and treatment of venous leg ulcers, *Journal of Tissue Viability* 12(2) (2002) 67-74.
- [147] M.S. Hegarty, E. Grant, L. Reid, An Overview of Technologies Related to Care for Venous Leg Ulcers, *IEEE Trans Inf Technol Biomed* 14(2) (2010) 387-393.
- [148] A.J. van Geest, J.C.J.M. Veraart, P. Nelemans, H.A.M. Neumann, The effect of medical elastic compression stockings with different slope values on edema - Measurements underneath three different types of stockings, *Dermatol Surg* 26(3) (2000) 244-247.

- [149] M. Junger, H.M. Hafner, Interface pressure under a ready made compression stocking developed for the treatment of venous ulcers over a period of six weeks, *Vasa- J Vascular Dis* 32(2) (2003) 87-90.
- [150] S.J. Palfreyman, , Lochiel, R., Michaels, J.A., A systematic review of compression therapy for venous leg ulcers, *Vascular Medicine* 3(4) (1998) 301-13.
- [151] P.C. Smith, S. Sarin, J. Hasty, J.H. Scurr, Sequential Gradient Pneumatic Compression Enhances Venous Ulcer Healing - a Randomized Trial, *Surgery* 108(5) (1990) 871-875.
- [152] J. Rowland, Intermittent pump versus compression bandages in the treatment of venous leg ulcers, *Aust Nz J Surg* 70(2) (2000) 110-113.
- [153] S.K. Kakkos, M. Griffin, G. Geroulakos, A.N. Nicolaides, The efficacy of a new portable sequential compression device (SCD Express) in preventing venous stasis, *J Vasc Surg* 42(2) (2005) 296-303.
- [154] M. Hegarty, E. Grant, L. Reid, T. Henderson, A Dynamic Compression System for Improving Ulcer Healing: Design of a Sensing Garment, 2008 IEEE International Conference on Multisensor Fusion and Integration for Intelligent Systems, Vols 1 and 2 (2008) 287-292.
- [155] B. Kumar, J. HU, Development Of Smart Compression Stocking For Management Of Venous Leg Ulcers, Autex 2014 World Textile Conference, Bursa - Turkey 2014.
- [156] B.H. Kumar, J.L, and Pan, N., Development of Shape-Memory Stocking for Smart Compression Management Fiber Society's 2014 Fall Meeting and Technical Conference, Chemical Heritage Foundation and Drexel University, Philadelphia, Pennsylvania, USA, 2014.
- [157] L. Macintyre, Designing pressure garments capable of exerting specific pressures on limbs, *Burns* 33(5) (2007) 579-586.

- [158] S. Thomas, The production and measurement of sub-bandage pressure: Laplace's Law revisited, *Journal of Wound Care* 23(5) (2014) 234-246.
- [159] W. Vanscheidt, A. Ukat, H. Partsch, Dose-response of compression therapy for chronic venous edema—higher pressures are associated with greater volume reduction: Two randomized clinical studies, *J Vasc Surg* 49(2) (2009) 395-402. e1.
- [160] M. Zaleska, W.L. Olszewski, P. Jain, S. Gogia, A. Rekha, S. Mishra, M. Durlik, Pressures and timing of intermittent pneumatic compression devices for efficient tissue fluid and lymph flow in limbs with lymphedema, *Lymphatic research and biology* 11(4) (2013) 227-232.
- [161] R. Liu, Y.-L. Kwok, Y. Li, T.-T. Lao, X. Zhang, Effects of material properties and fabric structure characteristics of graduated compression stockings (GCS) on the skin pressure distributions, *Fibers Polym* 6(4) (2005) 322-331.
- [162] S. Ghosh, A. Mukhopadhyay, M. Sikka, K. Nagla, Pressure mapping and performance of the compression bandage/garment for venous leg ulcer treatment, *Journal of Tissue Viability* 17(3) (2008) 82-94.
- [163] P. Onkaraiah, Design and Fabrication of Shape Memory Filaments into Knee high Compression Stockings, Institute of Textiles and Clothing, The Hong Kong Polytechnic University, Hong Kong, 2010, p. 220.
- [164] R. Chattopadhyay, D. Gupta, M. Bera, Effect of input tension of inlay yarn on the characteristics of knitted circular stretch fabrics and pressure generation, *J Text I* 103(6) (2012) 636-642.
- [165] M. Bera, R. Chattopadhyay, D. Gupta, Effect of linear density of inlay yarns on the structural characteristics of knitted fabric tube and pressure generation on cylinder, *J Text I* 106(1) (2015) 39-46.

- [166] T. Dias, W. Cooke, A. Fernando, D. Jayawarna, N.H. Chaudhury, Pressure garment, US Patent: US20050049741 A1, 2005.
- [167] B. Kumar, Hu, J.L., Pan, N., Smart Medical Stocking using Memory Polymer for Chronic Venous Disorders, *Biomaterials* (2015).
- [168] H. Narayana, J.L. Hu, B. Kumar, S.M. Shang, Constituent Analysis of Stress Memory in Semicrystalline Polyurethane, *J Polym Sci Pol Phys* 54(10) (2016) 941-947.
- [169] H. Narayana, J. Hu, B. Kumar, S. Shang, J. Han, P. Liu, T. Lin, F. Ji, Y. Zhu, Stress-memory polymeric filaments for advanced compression therapy, *J Mater Chem B* 5(10) (2017) 1905-1916.
- [170] D.J. Spencer, *Knitting Technology: A Comprehensive Handbook and Practical Guide*, Third ed., CRC Press, Woodhead Publishing Limited, Abington Hall, Abington, Cambridge CB1 6AH, England, 2001.
- [171] G.Q. Li, W. Xu, Thermomechanical behavior of thermoset shape memory polymer programmed by cold-compression: Testing and constitutive modeling, *J Mech Phys Solids* 59(6) (2011) 1231-1250.
- [172] T. Aida, E.W. Meijer, S.I. Stupp, Functional Supramolecular Polymers, *Science* 335(6070) (2012) 813-817.
- [173] W.T.S.H. Martien A. Cohen Stuart, Jan Genzer, Marcus Müller, Christopher Ober, Manfred Stamm, Gleb B. Sukhorukov, Igal Szleifer, Vladimir V. Tsukruk, Marek Urban, Françoise Winnik, Stefan Zauscher, Igor Luzinov & Sergiy Minko, Emerging applications of stimuli-responsive polymer materials, *Nat Mater* 9 (2010) 101–113.
- [174] A. Lendlein, V.P. Shastri, Stimuli-Sensitive Polymers, *Adv Mater* 22(31) (2010) 3344-3347.

- [175] M.M. Ma, L. Guo, D.G. Anderson, R. Langer, Bio-Inspired Polymer Composite Actuator and Generator Driven by Water Gradients, *Science* 339(6116) (2013) 186-189.
- [176] R. Langer, D.A. Tirrell, Designing materials for biology and medicine, *Nature* 428(6982) (2004) 487-492.
- [177] C. Liu, H. Qin, P.T. Mather, Review of progress in shape-memory polymers, *J Mater Chem* 17(16) (2007) 1543-1558.
- [178] W. Small, P. Singhal, T.S. Wilson, D.J. Maitland, Biomedical applications of thermally activated shape memory polymers, *J Mater Chem* 20(17) (2010) 3356-3366.
- [179] R.M. Erb, J.S. Sander, R. Grisch, A.R. Studart, Self-shaping composites with programmable bioinspired microstructures, *Nat Commun* 4 (2013).
- [180] T. Chung, A. Rorno-Urbe, P.T. Mather, Two-way reversible shape memory in a semicrystalline network, *Macromolecules* 41(1) (2008) 184-192.
- [181] J.L. Hu, *Shape Memory Polymers: Fundamentals, Advances and Applications*, Shrewsbury, Shropshire, UK : Smithers Rapra, 2014, SY4 4NR, United Kingdom, ISBN 10: 1909030325, 2014.
- [182] D. Quitmann, N. Gushterov, G. Sadowski, F. Katzenberg, J.C. Tiller, Solvent-Sensitive Reversible Stress-Response of Shape Memory Natural Rubber, *Acs Appl Mater Inter* 5(9) (2013) 3504-3507.
- [183] D. Quitmann, N. Gushterov, G. Sadowski, F. Katzenberg, J.C. Tiller, Environmental Memory of Polymer Networks under Stress, *Adv Mater* 26(21) (2014) 3441-3444.
- [184] N. Labropoulos, A.P. Gasparis, J.A. Caprini, H. Partsch, Compression stockings to prevent post-thrombotic syndrome, *Lancet* 384(9938) (2014) 129-130.
- [185] T. Steve, The use of the Laplace equation in the calculation of sub-bandage pressure, *EWMA Journal* 3(1) (2003) 21-23.

- [186] S.C.B. Mannsfeld, B.C.K. Tee, R.M. Stoltenberg, C.V.H.H. Chen, S. Barman, B.V.O. Muir, A.N. Sokolov, C. Reese, Z.N. Bao, Highly sensitive flexible pressure sensors with microstructured rubber dielectric layers, *Nat Mater* 9(10) (2010) 859-864.
- [187] A. Sachdeva, M. Dalton, S.V. Amaragiri, T. Lees, Elastic compression stockings for prevention of deep vein thrombosis, *Cochrane Db Syst Rev* (7) (2010).
- [188] M. Schulz, Speeding Up Artificial Muscles, *Science* 338(6109) (2012) 893-894.
- [189] C. Wang, D. Hwang, Z.B. Yu, K. Takei, J. Park, T. Chen, B.W. Ma, A. Javey, User-interactive electronic skin for instantaneous pressure visualization, *Nat Mater* 12(10) (2013) 899-904.
- [190] H. Meng, J.L. Hu, A Brief Review of Stimulus-active Polymers Responsive to Thermal, Light, Magnetic, Electric, and Water/Solvent Stimuli, *J Intell Mater Syst Struct* 21(9) (2010) 859-885.
- [191] A. Wang, G. Li, Stress memory of a thermoset shape memory polymer, *J Appl Polym Sci* 132(24) (2015).
- [192] M. Ahmad, J. Luo, M. MirafTAB, Feasibility study of polyurethane shape-memory polymer actuators for pressure bandage application, *Sci Technol Adv Mat* 13(1) (2012) 015006.
- [193] F.L. Ji, J.L. Hu, T.C. Li, Y.W. Wong, Morphology and shape memory effect of segmented polyurethanes. Part I: With crystalline reversible phase, *Polymer* 48(17) (2007) 5133-5145.
- [194] J.H. Kim, T.J. Kang, W.-R. Yu, Thermo-mechanical constitutive modeling of shape memory polyurethanes using a phenomenological approach, *Int J Plast* 26(2) (2010) 204-218.
- [195] H. Partsch, Compression therapy for deep vein thrombosis, *Vasa-European Journal of Vascular Medicine* 43(5) (2014) 305-307.

- [196] B. Kumar, A. Das, R. Alagirusamy, Effect of material and structure of compression bandage on interface pressure variation over time, *Phlebology* 29(6) (2013) 376-385.
- [197] B. Kumar, A. Das, R. Alagirusamy, Prediction of internal pressure profile of compression bandages using stress relaxation parameters, *Biorheology* 49(1) (2012) 1-13.
- [198] J.R. Basford, The Law of Laplace and its relevance to contemporary medicine and rehabilitation, *Arch Phys Med Rehab* 83(8) (2002) 1165-1170.
- [199] J. Al Khaburi, E.A. Nelson, J. Hutchinson, A.A. Dehghani-Sani, Impact of multilayered compression bandages on sub-bandage interface pressure: a model, *Phlebology* 26(2) (2011) 75-83.
- [200] K. Takashima, K. Sugitani, N. Morimoto, S. Sakaguchi, T. Noritsugu, T. Mukai, Pneumatic artificial rubber muscle using shape-memory polymer sheet with embedded electrical heating wire, *Smart Mater Struct* 23(12) (2014).
- [201] D. Wang, J. Guo, H. Zhang, B.C. Cheng, H. Shen, N. Zhao, J. Xu, Intelligent rubber with tailored properties for self-healing and shape memory, *J Mater Chem A* 3(24) (2015) 12864-12872.
- [202] Y.K. Bai, X.R. Zhang, Q.H. Wang, T.M. Wang, A tough shape memory polymer with triple-shape memory and two-way shape memory properties, *J Mater Chem A* 2(13) (2014) 4771-4778.
- [203] D. Kai, M.P. Prabhakaran, B.Q.Y. Chan, S.S. Liow, S. Ramakrishna, F.J. Xu, X.J. Loh, Elastic poly(epsilon-caprolactone)-polydimethylsiloxane copolymer fibers with shape memory effect for bone tissue engineering, *Biomed Mater* 11(1) (2016).
- [204] P.F. Zhang, G.Q. Li, Structural relaxation behavior of strain hardened shape memory polymer fibers for self-healing applications, *J Polym Sci Pol Phys* 51(12) (2013) 966-977.

- [205] G.Q. Li, H. Meng, J.L. Hu, Healable thermoset polymer composite embedded with stimuli-responsive fibres, *J Royal Soc Interface* 9(77) (2012) 3279-3287.
- [206] J. Kaursoin, A.K. Agrawal, Melt spun thermoresponsive shape memory fibers based on polyurethanes: Effect of drawing and heat-setting on fiber morphology and properties, *J Appl Polym Sci* 103(4) (2007) 2172-2182.
- [207] Y. Zhu, J.L. Hu, L.Y. Yeung, Y. Liu, F.L. Ji, K.W. Yeung, Development of shape memory polyurethane fiber with complete shape recoverability, *Smart Mater Struct* 15(5) (2006) 1385-1394.
- [208] Q.H. Meng, J.L. Liu, L.M. Shen, Y. Hu, J.P. Han, A Smart Hollow Filament with Thermal Sensitive Internal Diameter, *J Appl Polym Sci* 113(4) (2009) 2440-2449.
- [209] H.T. Zhuo, J.L. Hu, S.J. Chen, Electrospun polyurethane nanofibres having shape memory effect, *Mater Lett* 62(14) (2008) 2074-2076.
- [210] H.T. Zhuo, J.L. Hu, S.J. Chen, Coaxial electrospun polyurethane core-shell nanofibers for shape memory and antibacterial nanomaterials, *Express Polym Lett* 5(2) (2011) 182-187.
- [211] H.T. Zhuo, J.L. Hu, S.J. Chen, Study of water vapor permeability of shape memory polyurethane nanofibrous nonwovens, *Text Res J* 81(9) (2011) 883-891.
- [212] B. Kumar, J.L. Hu, N. Pan, H. Narayana, A smart orthopedic compression device based on a polymeric stress memory actuator, *Mater Design* 97 (2016) 222-229.
- [213] S.J. Chen, J.L. Hu, C.W.M. Yuen, L.K. Chan, Fourier transform infrared study of supramolecular polyurethane networks containing pyridine moieties for shape memory materials, *Polym Int* 59(4) (2010) 529-538.
- [214] Y. Zhu, J.L. Hu, H.S. Luo, R.J. Young, L.B. Deng, S. Zhang, Y. Fan, G.D. Ye, Rapidly switchable water-sensitive shape-memory cellulose/elastomer nanocomposites, *Soft Matter* 8(8) (2012) 2509-2517.

- [215] F.L. Ji, Y. Zhu, J.L. Hu, Y. Liu, L.Y. Yeung, G.D. Ye, Smart polymer fibers with shape memory effect, *Smart Mater Struct* 15(6) (2006) 1547-1554.
- [216] S. Toki, I. Sics, B.S. Hsiao, M. Tosaka, S. Poompradub, Y. Ikeda, S. Kohjiya, Probing the nature of strain-induced crystallization in polyisoprene rubber by combined thermomechanical and in situ X-ray diffraction techniques, *Macromolecules* 38(16) (2005) 7064-7073.
- [217] S. Çalamak, C. Erdoğan, M. Özalp, K. Ulubayram, Silk fibroin based antibacterial bionanotextiles as wound dressing materials, *Mater Sci Eng: C* 43(Supplement C) (2014) 11-20.
- [218] M.B. Dreifke, A.A. Jayasuriya, A.C. Jayasuriya, Current wound healing procedures and potential care, *Mater Sci Eng: C* 48(Supplement C) (2015) 651-662.
- [219] B. Kumar, J. Singh, A. Das, R. Alagirusamy, Comfort and compressional characteristics of padding bandages, *Mater Sci Eng: C* 57(Supplement C) (2015) 215-221.
- [220] M. Patchan, J.L. Graham, Z. Xia, J.P. Maranchi, R. McCally, O. Schein, J.H. Elisseeff, M.M. Trexler, Synthesis and properties of regenerated cellulose-based hydrogels with high strength and transparency for potential use as an ocular bandage, *Mater Sci Eng: C* 33(5) (2013) 3069-3076.
- [221] N. Vojackova, J. Fialova, J. Hercogova, Management of lymphedema, *Dermatol Ther* 25(4) (2012) 352-357.
- [222] A. Chant, The biomechanics of leg ulceration, *Ann Roy Coll Surg* 81(2) (1999) 80-85.
- [223] J. Green, R. Jester, R. McKinley, A. Pooler, The impact of chronic venous leg ulcers: a systematic review, *J Wound Care* 23(12) (2014) 601-+.

- [224] J.F. Uhl, C. Gillot, Anatomy of the veno-muscular pumps of the lower limb, *Phlebology* 30(3) (2015) 180-193.
- [225] B. Kumar, A. Das, R. Alagirusamy, Study on interface pressure generated by a bandage using in vitro pressure measurement system, *J Text I* 104(12) (2013) 1374-1383.
- [226] D. Sajn, J. Gersak, R. Flajs, Prediction of stress relaxation of fabrics with increased elasticity, *Text Res J* 76(10) (2006) 742-750.
- [227] M. Bera, R. Chattopadhyay, D. Gupta, Effect of linear density of inlay yarns on the structural characteristics of knitted fabric tube and pressure generation on cylinder, *J Text I* 106(1) (2015) 39-46.
- [228] T. Bias, G.B. Delkumburewatte, Changing porosity of knitted structures by changing tightness, *Fiber Polym* 9(1) (2008) 76-79.
- [229] R. Liu, T.T. Lao, S.X. Wang, Impact of Weft Laid-in Structural Knitting Design on Fabric Tension Behavior and Interfacial Pressure Performance of Circular Knits, *J Eng Fiber Fabr* 8(4) (2013) 96-107.
- [230] Y.R. Wang, P.H. Zhang, Y.P. Zhang, Experimental investigation the dynamic pressure attenuation of elastic fabric for compression garment, *Text Res J* 84(6) (2014) 572-582.
- [231] B. Kumar, J.L. Hu, N. Pan, Smart medical stocking using memory polymer for chronic venous disorders, *Biomaterials* 75 (2016) 174-181.
- [232] B. Kumar, A. Das, R. Alagirusamy, Study of the effect of composition and construction of material on sub-bandage pressure during dynamic loading of a limb in vitro, *Biorheology* 50(1-2) (2013) 83-94.